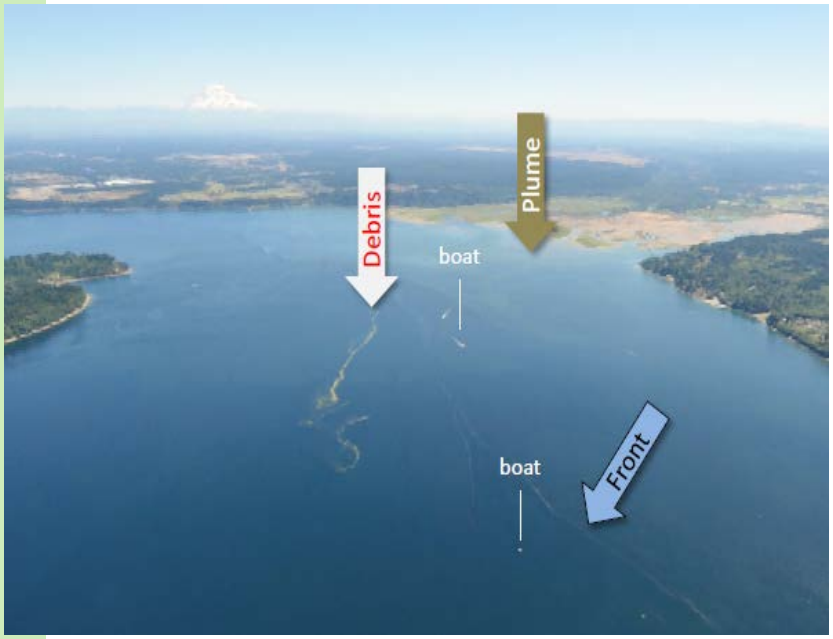


# South Puget Sound Dissolved Oxygen Study

## South and Central Puget Sound Water Circulation Model Development and Calibration

DEPARTMENT OF ECOLOGY
State of Washington

April 2014

Publication No. 14-03-015

## Publication Information

This report is available on the Department of Ecology's website at
https://fortress.wa.gov/ecy/publications/SummaryPages/1403015.html

Data for this project are available at Ecology's Environmental Information Management (EIM) website www.ecy.wa.gov/eim/index.htm. Search Study ID SPSMEM.

Ecology's Activity Tracker Code for this study is 06-509-02.

## Contact Information

For more information contact:

Publications Coordinator
Environmental Assessment Program
P.O. Box 47600, Olympia, WA 98504-7600
Phone: (360) 407-6764

Washington State Department of Ecology - www.ecy.wa.gov

| | | |
|---|---|---|
| o | Headquarters, Olympia | (360) 407-6000 |
| o | Northwest Regional Office, Bellevue | (425) 649-7000 |
| o | Southwest Regional Office, Olympia | (360) 407-6300 |
| o | Central Regional Office, Yakima | (509) 575-2490 |
| o | Eastern Regional Office, Spokane | (509) 329-3400 |

**Cover photo**: Department of Ecology's Marine Monitory Unit, Eyes Over Puget Sound (www.ecy.wa.gov/programs/eap/mar_wat/eops/EOPS_2013_07_15.pdf).
Large debris rafts (algal mats) following water movement, Nisqually Reach, South Puget Sound, July 15, 2013 at 1:41 pm.

# South Puget Sound Dissolved Oxygen Study

# South and Central Puget Sound Water Circulation Model Development and Calibration

by

Mindy Roberts, Skip Albertson,
Anise Ahmed, and Greg Pelletier

Environmental Assessment Program
Washington State Department of Ecology
Olympia, Washington 98504-7710

Water Resource Inventory Area (WRIA) and 8-digit Hydrologic Unit Code (HUC) numbers for the study area

WRIAs
- 8 through 15

HUC numbers
- 17110012 through 17110016, 17110019

*This page is purposely left blank*

# Table of Contents

# List of Figures

# List of Tables

# Abstract

Portions of South Puget Sound do not meet Washington State water quality standards for dissolved oxygen. To determine whether humans are contributing to these low oxygen levels, the Washington State Department of Ecology will collect and analyze data, develop circulation and water quality models, and assess alternative management scenarios.

This report, part of the *South Puget Sound Dissolved Oxygen Study*, summarizes the calibration of the South and Central Puget Sound water circulation model.

The model's purpose is to describe how water moves around, and the model performs well. The model reproduces both water surface elevations and tidal constituents throughout the model domain. Root mean square errors (RMSEs) are <16 cm, or <5% of the tidal range, in all but Oakland Bay and Totten Inlet where the error was approximately 9% of the tidal range. The model simulates salinity with an overall mean RMSE of 0.75 ppt at all stations and depths. Temperature simulation likewise has mean RMSEs of 0.8°C. Current velocity measurements, both transects across inlets and time series in key locations, were also used to check the model.

We estimated flushing time in various inlets of South Puget Sound for late-summer conditions. We also simulated dye tracers from rivers and wastewater treatment plants in both Central and South Puget Sound as an initial indication of areas influenced by either. Some of the tracer from Central Puget Sound sources travels south through the Tacoma Narrows. Therefore, we cannot rule out the influence of Central Puget Sound sources on South Puget Sound water quality. However, the results are not sufficient to rule in an influence, given the complexity of nutrient transport and transformation. A separate water quality model report addresses nutrient and oxygen patterns.

# Acknowledgements

The authors of this report thank the following people and organizations for their contribution to this study:

- The South Puget Sound Dissolved Oxygen Study Advisory Committee members provided feedback on interim model products and interpretations. In particular, Mitsuhiro Kawase (University of Washington) and Bruce Nairn (King County) provided key input and perspectives on initial calibration products.

| | |
|---|---|
| Dave Adams | Citizens for a Healthy Bay |
| John Bolender | Mason Conservation District |
| Seth Book | Mason County Department of Health Services |
| Kevin Buckley | Snoqualmie Tribe |
| Roma Call | Puget Sound Partnership |
| Ben Cope | EPA Region 10 |
| Joe Gibbens | Fort Lewis Public Works |
| Bill Dewey | Taylor Shellfish Co. |
| Larry Ekstrom | Pierce County Public Works and Utilities |
| John Eliasson | Washington State Dept. of Health |
| Duane Fagergren | Puget Sound Partnership |
| Bill Fox | Cosmopolitan Engineering Group |
| Cheryl Greengrove | University of Washington - Tacoma |
| Keith Grellener | Kitsap |
| Mitsuhiro Kawase | University of Washington |
| Bill Kingman | City of DuPont |
| Andrew Kolosseus | Department of Ecology |
| Scott Steltzner | Squaxin Island Tribe |
| Dave Lenning | Washington State Dept. of Health |
| Lincoln Loehr | Stoel Rives |
| Tom Moore | Mason County Department of Utilities and Waste Management |
| Bruce Nairn | King County WTD |
| Greg Narum | Simpson Tacoma Kraft |
| Anthony Paulson, Ph. D. | U.S. Geological Survey |
| Dave Ragsdale | EPA Region 10 |
| Debbie Riley | Mason County Environmental Health |
| Wayne Robinson | LOTT Alliance |
| Lynn Schneider | WA State Dept of Health |
| Dan Thompson | Tacoma Wastewater Treatment Plant |
| Dave Peeler | People for Puget Sound |
| Bruce Wishart | People for Puget Sound |
| Dan Wrye | Pierce County Public Works and Utilities |
| Tyle Zuchowski | LOTT Alliance |
| Char Naylor | Puyallup Tribe |
| Dave Clark | HDR |

- Curt Ebbesmeyer (Evans-Hamilton Inc.), Hal Mofjeld (NOAA), and Bill Lavelle (NOAA) provided important historical insight to circulation and tidal processes in Puget Sound.
- Venkat Kolluru and other staff with Environmental Resources Management (ERM) provided technical assistance and software development for the GEMSS model.
- Chuck Hoffman (Washington State Department of Ecology) provided the mixing zone modeling analysis that guided the setup of model inputs for wastewater treatment plants.

This project has been funded wholly or in part by the United States Environmental Protection Agency (EPA) under assistance agreement X-96028501 to the Department of Ecology. The contents of this document do not necessarily reflect the views and policies of the EPA, nor does mention of trade names or commercial products constitute endorsement or recommendation for use.

# Executive Summary

## Introduction

Portions of South Puget Sound do not meet Washington State water quality standards for dissolved oxygen. To determine whether humans are contributing to these low oxygen levels, the Washington State Department of Ecology will collect and analyze data, develop circulation and water quality models, and assess alternative management scenarios. This report summarizes the calibration of the South and Central Puget Sound water circulation model.

The primary area of interest is the region southwest of the Tacoma Narrows. However, one of the project questions is whether the larger rivers and population centers northeast of the Tacoma Narrows contribute to water quality problems within South Puget Sound. Therefore, the model domain includes both South and Central Puget Sound.

To describe water circulation in South and Central Puget Sound (Figure ES-1), we apply a three-dimensional model that simulates tides, water velocity, temperature, and salinity within each grid cell. The model grid cells are arranged to represent the complex morphology and bathymetry of the region, including such features as the shallow entrance sill within the Tacoma Narrows, inlets in South Puget Sound, and deeper basins in Carr Inlet and Central Puget Sound. The selected grid cell resolution (nominally 500 meters by 500 meters) optimizes tradeoffs between the precision required to describe circulation and the amount of time required to run the model.


Figure ES-1. South and Central Puget Sound study area.

Circulation strongly influences dissolved oxygen levels, which will be evaluated in the subsequent water quality modeling efforts. Factors influencing circulation include the tides at the northern boundary, the physical shape of Puget Sound, meteorology including wind and air temperature, and freshwater inflows. Data collected during the first phase of the project are used as both input to the model and as output for comparison with model predictions.

## Hydrodynamic Model Setup and Calibration

The model was calibrated using water surface elevations, tidal constituents, surface temperature and salinity spatial patterns, temperature and salinity profiles, and current velocities. Calibration refers to the iterative process of comparing model output to data and adjusting appropriate factors. The model was calibrated using data from July 2006 through October 2007.

Overall the model performs well. The model predicts water surface elevations with a root-mean-square error (RMSE) of <10 cm throughout most of the water domain. Somewhat higher but still acceptable errors exist for Hammersley Inlet and Oakland Bay due to shape complexities that the model grid could not describe without significantly decreasing the model grid cell size, which would require greater computer runtime. The RMSEs are generally within 5% of the tidal range, which ranges from 2 m at the northern boundary to 5 m in Budd Inlet and Hammersley Inlet/Oakland Bay. Figure ES-2 presents examples from near the boundary, a typical South Sound station, and Hammersley Inlet. The RMSE for Hammersley Inlet is high because the model does not represent the two 90-degree bends in Hammersley Inlet.

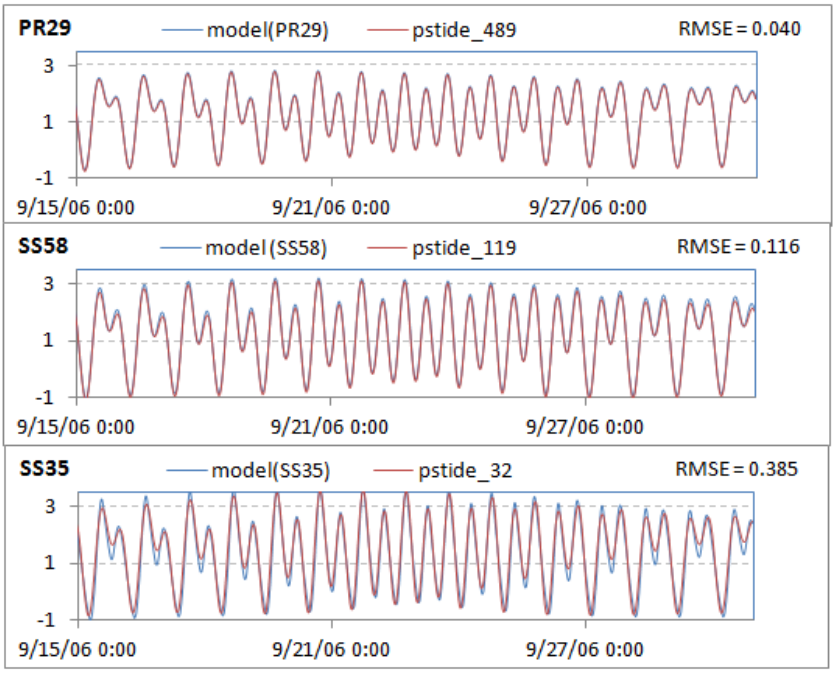


Figure ES-2. Predicted water surface elevations (meters) compared with PSTides for (a) PR29, a typical Central Puget Sound location; (b) SS58, a typical South Puget Sound location; and (c) SS35, Oakland Bay.

The complex shape and circulation patterns produce highly variable temperature and salinity patterns in Puget Sound, particularly in the surface layers that are influenced by both the meteorology and rivers. The model reproduces the spatial temperature and salinity patterns as shown in Figure ES-3.

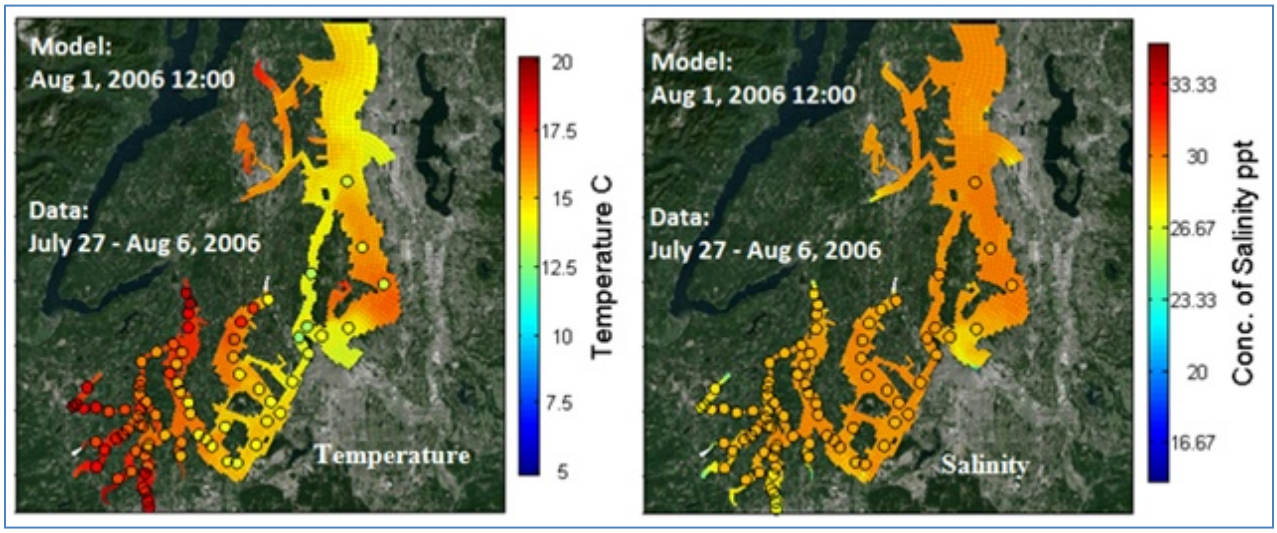


Figure ES-3. Observed and predicted domain-wide temperature and salinity patterns in surface layer.

Time-depth temperature and salinity patterns are shown in Figure ES-4. Temperature and salinity calibration produced seasonal and temporal patterns with best RMSEs in stations near the Edmonds open boundary and worsening RMSEs at stations farthest from the open boundary. For example, mean RMSEs for station PR29 were 0.3 ppt and 0.4 °C for salinity and temperature, respectively. However, for a station in Oakland Bay, the mean RMSEs for salinity and temperature were 0.9 ppt and 2 °C, respectively.

Model-predicted current velocity phasing and magnitudes were compared with field data. Model predictions of cross-sectional averaged velocity magnitude across inlets and direction matched observed data in South Puget Sound. These comparisons focused on complex flow areas in South Puget Sound where the flood and ebb tides split around Harstine Island. The model predicts the phasing correctly based on velocities recorded over two-week periods in 2007 (Figure ES-5), as well as the magnitude of the northerly and easterly components of the velocity. The surface currents predicted by the model are reasonable and match large-scale patterns (Figure ES-6).

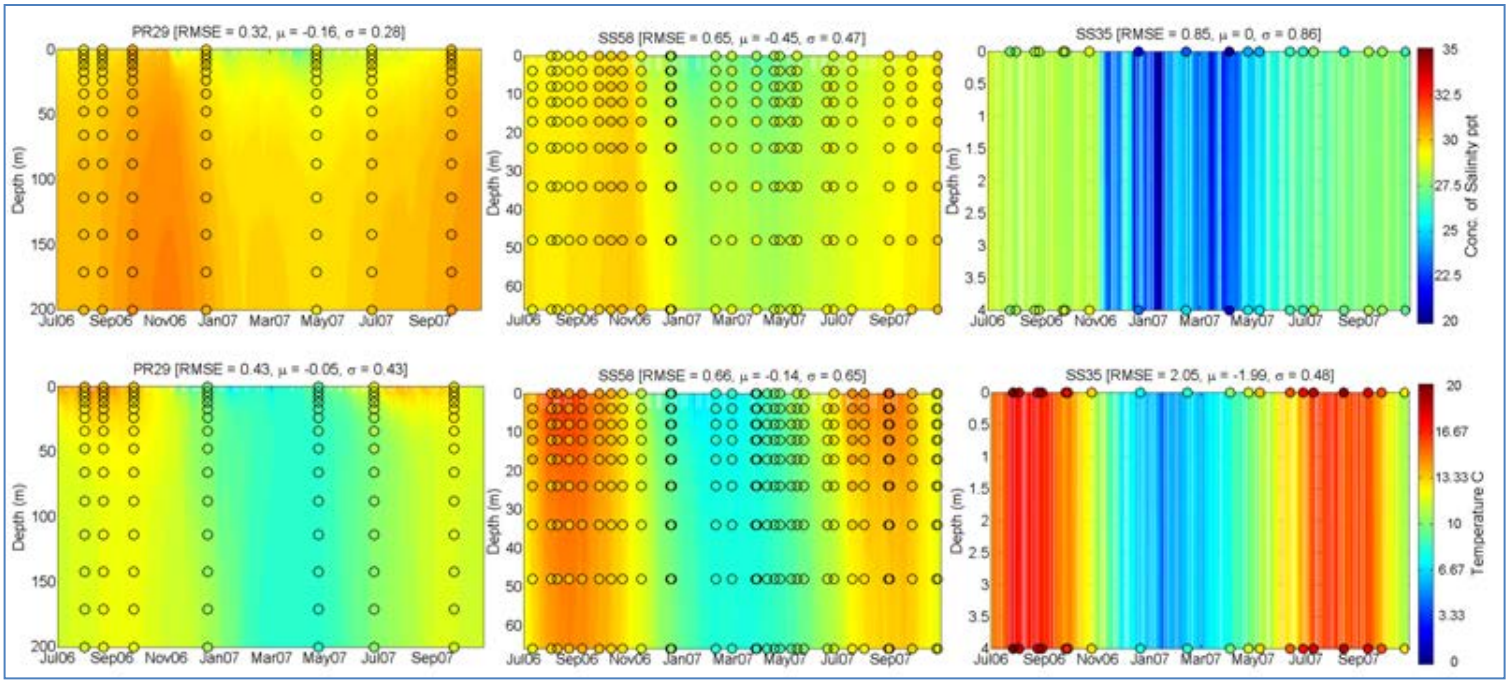


Figure ES-4. Salinity and temperature time-depth predictions compared with field data for PR29, a typical Central Puget Sound location; SS58, a typical South Puget Sound location; and SS35, Oakland Bay.

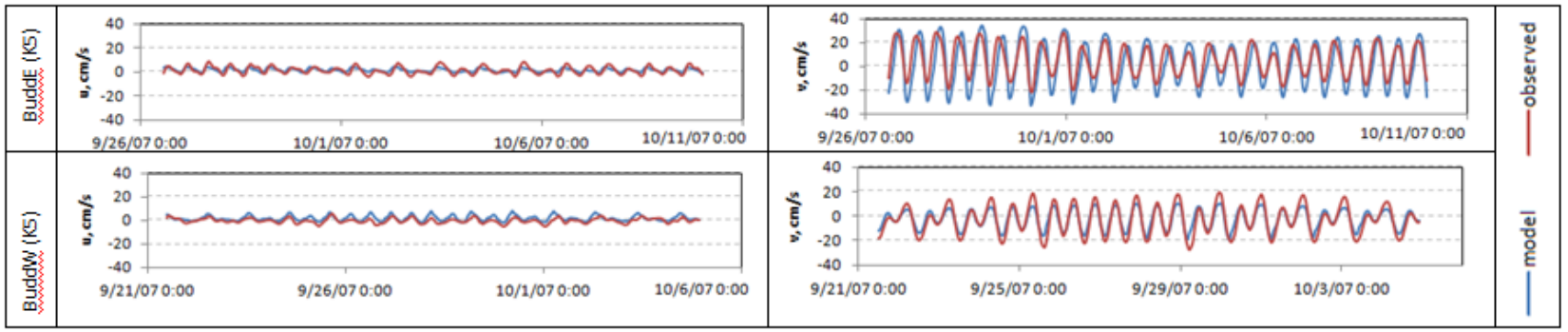


Figure ES-5. Velocity comparison between model and observed data for northerly (v) and easterly (u) velocities for layer K5 in Budd Inlet.

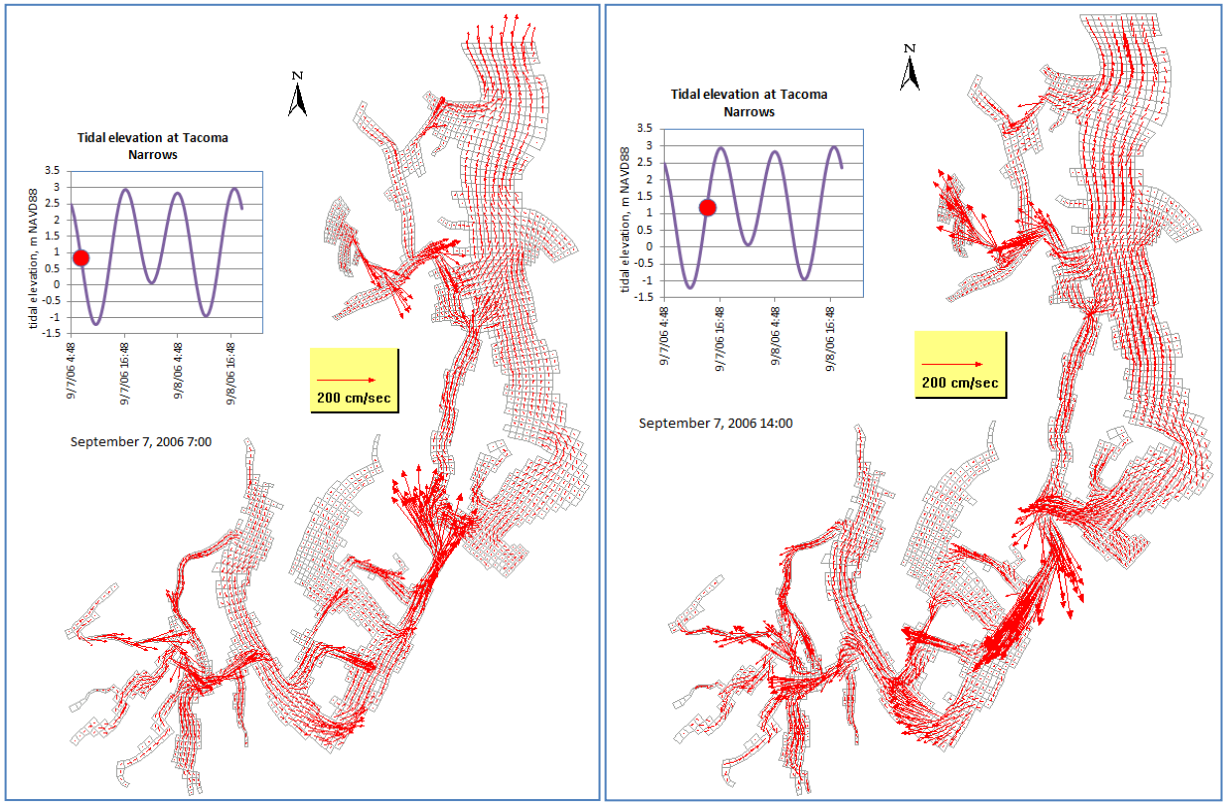


Figure ES-6. Surface current velocities predicted by the model during strongly ebbing and flooding tidal conditions.

## South Puget Sound Flushing Times and Areas of Influence

Using the calibrated circulation model, we added virtual dye to various waters to evaluate (1) the flushing time for South Puget Sound inlets as well as (2) the areas influenced by marine point sources and watershed inflows.

Numerous methods have been used in Puget Sound and elsewhere, and the numeric value for the flushing time strongly depends on the method used. We added a dye tracer to areas of South Puget Sound and quantified the time required to reduce the dye concentration to 37% of the initial value, known as the e-folding time, within each grid cell. Portions of South Puget Sound flush in 3 to 108 days. The flushing time is lowest near the Tacoma Narrows and is significantly higher toward the heads of each inlet. Flushing time varies seasonally. Oakland Bay flushes the fastest and Eld Inlet flushes the slowest of the smaller inlets.

We also simulated dye released from all river inflows and wastewater discharges in four separate model runs, two each for South Puget Sound and Central Puget Sound. This was done to identify areas influenced by rivers and wastewater treatment plants. All rivers and wastewater discharges released the same concentration of dye. The dye releases began in July 2006 and slowly accumulated within the model domain through 2007.

We quantified the maximum dye concentrations that occurred anywhere in the water column towards the end of the dye simulation period (July 2006 – October 2007). As the tide floods and ebbs, we recorded the maximum concentration at the end of September 2007. The dilution factor for each grid cell is the ratio of the maximum concentration to the initial concentration; a dilution factor of 100 corresponds to a maximum tracer concentration of $1/100^{th}$ or 1% of the initial value.

Based on predicted dilution levels derived from water-column maximum dye concentrations at the end of September 2007, dye from South and Central Puget Sound exchanges through the Tacoma Narrows (Figure ES-7). Therefore, we cannot rule out the influence of Central Puget Sound sources on South Puget Sound water quality. However, the results are not sufficient to rule in an influence either, given the complexity of nutrient transport and transformation within marine environments. The water quality model is needed to quantify the link between sources and water quality impairments.

## Conclusions and Recommendations

The South and Central Puget Sound circulation model was calibrated and verified using water surface elevations, temperature and salinity data, and current velocities from 2006 and 2007. The model reproduces water surface elevations and tidal constituents well. Oakland Bay had the largest errors in phase because the model could not reproduce the two 90-degree bends without inducing instabilities. The model also reproduced temperature and salinity patterns without significant bias. Current profiles and surface currents matched values from available literature. We recommend that future model assessments consider additional monitoring programs.

Ahmed et al. (2014) describes the corollary water quality model development. We recommend additional model development focused on sediment-water exchanges.

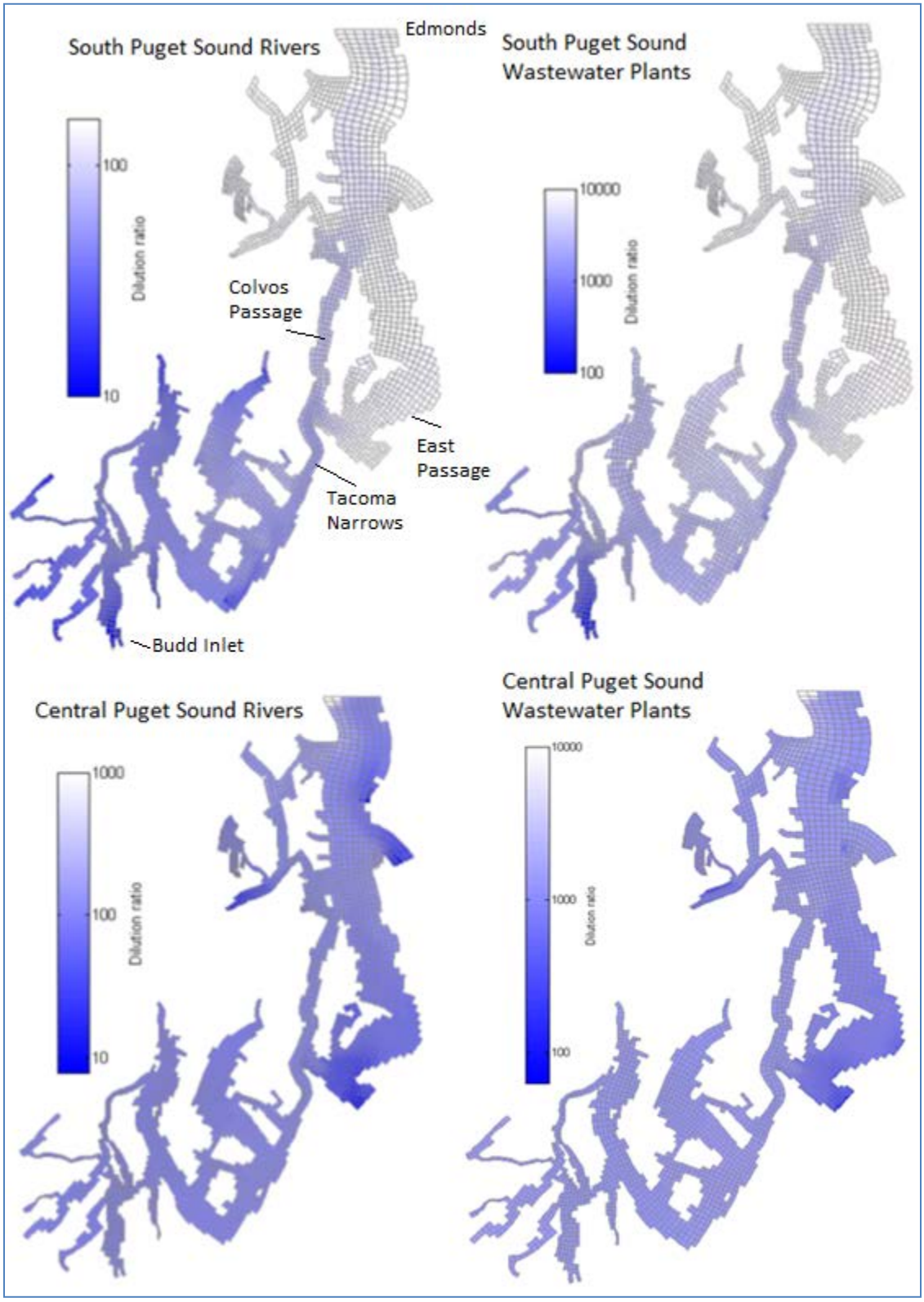


Figure ES-7. Dilution factors calculated from maximum water-column dye concentrations for South and Central Puget Sound rivers and wastewater treatment plants for September 2007.

*This page is purposely left blank*

# Introduction

Portions of South Puget Sound do not meet Washington State water quality standards for dissolved oxygen. The purpose of this study is to determine whether humans are contributing to low levels of dissolved oxygen in South Puget Sound. Because sources outside of South Sound could contribute to low dissolved oxygen levels within South Sound, we evaluated both South and Central Puget Sound (Figure 1).

Table 1 presents the waterbodies classified as Category 5 under the federal Clean Water Act Section 303(d) list of impaired waters. Category 5 indicates that water quality violates standards and a Total Maximum Daily Load (TMDL) study is required.


Figure 1. South and Central Puget Sound study area.

Table 1. Category 5 dissolved oxygen listings in South and Central Puget Sound.

| Listing Number | Name |
|---|---|
| **South Puget Sound (south and west of Tacoma Narrows)** | |
| 3770 | Squaxin, Peale, and Pickering Passages |
| 5852 | Budd Inlet (Inner) |
| 5853 | |
| 5863 | |
| 5864 | |
| 3769 | Budd Inlet (Outer) |
| 5862 | |
| 7582 | |
| 7583 | |
| 7584 | |
| 7585 | |
| 7586 | |
| 7587 | |
| 10188 | |
| 66263 | Little Skookum Inlet |
| 10241 | Henderson Bay |
| 43004 | |
| 10192 | Henderson Inlet |
| 66164 | |
| 10233 | Case Inlet and Dana Passage |
| 10244 | |
| 42985 | |
| 42986 | |
| 42987 | |
| 42988 | |
| 42989 | |
| 42990 | |
| 43020 | |
| 43022 | |
| 66082 | |
| 66084 | |
| 66085 | |
| 66086 | |
| 66088 | |

| Listing Number | Name |
|---|---|
| **South Puget Sound (south and west of Tacoma Narrows)** | |
| 10222 | Balch and Cormorant Passages |
| 42998 | |
| 43006 | |
| 10229 | Carr Inlet |
| 42999 | |
| 43000 | |
| 43001 | |
| 43002 | |
| 43003 | |
| 66075 | |
| 42993 | Nisqually Reach/Drayton Passage |
| 42994 | |
| 42995 | |
| 66307 | |
| 66309 | |
| 66312 | |
| 66318 | |
| 43007 | Tacoma Narrows |
| 43008 | |
| **Central Puget Sound (north and east of Tacoma Narrows and south of** | |
| 10175 | Commencement Bay |
| 43009 | Colvos Passage |
| 66090 | |
| 10178 | Quartermaster Harbor |
| 12702 | Duwamish Waterway |
| 12703 | |
| 38840 | Puget Sound (S-Central) and East Passage |
| 38939 | |
| 52995 | |
| 52996 | |
| 52997 | |
| 52998 | |

| Listing Number | Name |
|---|---|
| **Central Puget Sound (north and east of Tacoma Narrows and south of Edmonds)** | |
| 38463 | Port Orchard, Agate Passage, and Rich Passage |
| 38547 | |
| 38847 | |
| 52999 | |
| 53000 | |
| 53002 | |
| 10268 | Liberty Bay |
| 23537 | |
| 23540 | |
| 23541 | |
| 38682 | |
| 38710 | Port Madison |
| 38714 | |

The study includes collecting and analyzing data, developing circulation and water quality models, and assessing alternative management scenarios. Roberts et al. (2008) summarized the data collected from June 2006 through October 2007. This report summarizes the development and calibration of the water circulation model of South and Central Puget Sound. Ahmed et al. (2014) presents the water quality model development.

The water circulation model describes how the marine waters of South and Central Puget Sound move around. To simulate circulation, we represent South and Central Puget Sound as a series of model grid cells of varying length, width, and depth to define the complex shape of the inlets and

passages. The computer model simulates water velocities, salinity, and temperature within each grid cell that result from the complex interaction of tides, bathymetry, meteorology, and freshwater inflows. The circulation model is the basis of the water quality model.

## Physical Description

South and Central Puget Sound include a complex and interconnected system of straits and open waters in Washington State.

The northern border of South Puget Sound is defined traditionally by the Tacoma Narrows and an entrance sill located just to the south of the Tacoma Narrows. The sill is a shallow reach formed during the glacial epochs tens of thousands of years ago, with typical depths around 50 m. Deeper regions to the west and landward of the sill are greater than 150 m.

Central Puget Sound, also called the main basin, extends from the Tacoma Narrows to the north or seaward. Commencement Bay, Colvos Passage, Quartermaster Harbor, Sinclair and Dyes Inlets, Elliott Bay, and Liberty Bay are all distinct areas within Central Puget Sound. The Puget Sound Partnership divides Central Puget Sound, which extends north to Whidbey Island, into north and south components. Due to the complex circulation patterns near Whidbey Island, the northern model boundary for this study was located further south, near Edmonds. This location balances the need to include Central Puget Sound water quality contributions against the circulation difficulties near Whidbey Island.

Several previous studies evaluated South and Central Puget Sound circulation and physical oceanography. Albertson et al. (2007a) described general circulation patterns and how stratification increases residence time. Previous complex and simple modeling efforts improved understanding of how water moves around in South Puget Sound, but these efforts were limited by available information (Albertson et al., 2002a and 2002b) and by coarse model scales (URS Company, 1986). Thomson (1981) and Collias et al. (1974) provided detailed summaries of the physical oceanography and chemistry of South Puget Sound inferred from data collection efforts. Seim and Gregg (1997) described the physical processes at Tacoma Narrows. Babson et al. (2006) described seasonal and annual patterns using a two-layer box model of Puget Sound. Edwards et al. (2007) simulated circulation within Carr Inlet using a three-dimensional model.

## Potential Factors Contributing to Low Dissolved Oxygen

Multiple physical, chemical, and biological processes contribute to seasonally low dissolved oxygen levels in late summer. All will be considered by the circulation and water quality models. Sunlight and nutrients may lead to algae growth. Excessive algae growth, or a bloom, produces high organic matter levels. When the algae die and sink to the bottom, bacteria decompose the organic matter and consume oxygen in the process. Lower dissolved oxygen levels occur where water stagnates, when water columns stratify, and where ample nutrients and warm temperatures occur. In addition, there are low seasonal winds and lower tidal energy near the fall equinox in September that could inhibit flushing. Typically, late summer and fall produce conditions conducive to algae growth, as noted in Bos et al. (2001) for South Puget Sound.

## Factors Influencing Circulation and Flushing Time

South and Central Puget Sound experience two high and two low tides each day. The difference between high tide and low tide, or the tidal range, varies from 2 m at the northern model boundary to as much as 5 m in Olympia and Shelton. Large water surface elevation differences produce strong tidal currents (~1 m/s). Density differences produce weaker estuarine circulation currents (~0.1 m/s) that vary with depth, freshwater input, stratification, and wind. Tidal and estuarine circulation result in a net outflow of buoyant fresher water at the surface and a compensating inflow of denser saltwater from North and Central Puget Sound at depth that ultimately draws from the Pacific Ocean. Despite being much smaller in magnitude, this weaker estuarine flow can greatly influence water quality because the tidal exchanges (ebbs and floods) largely cancel each other out.

*Residence time* describes how long water masses persist within a particular volume. The related term *flushing time* refers to how quickly or slowly water flushes out of a given volume of water, such as flushing time for a specific inlet. The net circulation of water influences biological productivity because nutrients that enter Puget Sound from one watershed can affect another area at some distance. Residence time or flushing time depends on the overall volume of water of interest and the shape of the waterbody. Because they also vary with freshwater inflows and tidal exchanges, residence time or flushing time vary by season and tidal cycle.

## Report Organization

Circulation model development, calibration, and initial applications are described in five sections:

- *Model Setup* describes the capabilities of the computer software selected for the South and Central Puget Sound circulation model, how the model grid was developed, the boundary conditions used to force the model, and the initial conditions used at the start.

- *Model Calibration* describes the detailed process used to calibrate the model, including what data were used to check against the model output and what parameters were varied to achieve calibration.

- *South Puget Sound Flushing Times* presents residence time estimates for various inlets.

- *Areas Influenced by Marine Point Sources and Watershed Inflows* summarizes results of a virtual dye study, where the model was used to track how water from both rivers and wastewater treatment plant discharges in South and Central Puget Sound moves around.

- *Conclusions* and *Recommendations* summarize the overall performance of the circulation model and basic capabilities. The section also documents why the northern boundary was established at Edmonds as well as recommendations for any ongoing work.

# Hydrodynamic Model Setup

Model selection criteria were detailed in Albertson et al. (2007b). In summary, the circulation and associated water quality models must simulate 3-dimensional processes appropriate to estuarine areas with both tidal circulation and density-driven circulation. For potential use as a regulatory tool, the model must be peer reviewed, available in the public domain, and have thorough documentation of the theory and source code. In addition, we evaluated models with past applications within Puget Sound and emphasized the quality of the graphical user interface to facilitate scenario generation. While several model frameworks provided the minimum capabilities, the Generalized Environmental Modeling System for Surface Waters (GEMSS) framework was selected (Edinger and Buchak, 1995).

This section presents the capabilities of GEMSS as well as the development of the model grid. Boundary conditions are described for the northern boundary, meteorology, and river and point source inflows. The final subsection describes how we established initial conditions within the model domain to begin the simulation.

## Model Description

The GEMSS application to South and Central Puget Sound uses a curvilinear (curved) grid to represent the complex shapes. Below the intertidal zone in areas always covered with water, the layers in the model grid have fixed thicknesses that are thinner near the surface. The top three surface layers span the intertidal range, and the top layer varies in thickness as water surface elevations change. The model simulates the wetting and drying of mud flats, an important process for nearshore areas. Model time steps are small enough that high gradients like acceleration through the Tacoma Narrows do not cause instabilities. GEMSS allows a variable time step. In addition, the model simulates both rivers and wastewater treatment plant outfalls.

The software was used for the Lacey Olympia Tumwater Thurston (LOTT) wastewater treatment plant certification study (Aura Nova et al., 1998) as well as the more recent *Deschutes River, Capitol Lake, and Budd Inlet Total Maximum Daily Load* study (Roberts et al., 2012). GEMSS has a fully integrated hydrodynamic, water quality and sediment flux model embedded in a geographic information system (GIS) with environmental data tools. The graphical user interface (GUI) facilitates running scenarios.

The hydrodynamic model in GEMSS is the three-dimensional Generalized, Longitudinal-Lateral-Vertical Hydrodynamic and Transport (GLLVHT) model (Edinger and Buchak, 1980). The hydrodynamic routines extend the well known, two-dimensional transport model CE-QUAL-W2 (Cole and Buchak, 1995). Kolluru et al. (1998) modified the transport scheme, added water quality modules, and incorporated supporting software, GIS, visualization tools, post-processors, and a graphical user interface. Albertson et al. (2007b) details the water quality model capabilities of the GEMSS framework.

## Computational Grid Development

The current model grid was developed based on a previous model grid of South Puget Sound through Alki Point (Albertson et al., 2002b). Given the potential for Central Puget Sound sources to impact South Puget Sound water quality, the model grid was extended northward to Edmonds by Environmental Resource Management (ERM) using a grid generation module "GridGen" within the GEMSS modeling framework. Each of the 2623 grid cells has a slightly different shape and surface area, but the nominal grid cell size is about 500 m x 500 m (Figure 2). We considered using finer grids near Hope Island and in Hammersley Inlet. However, these were not desirable since it would increase model runtimes.

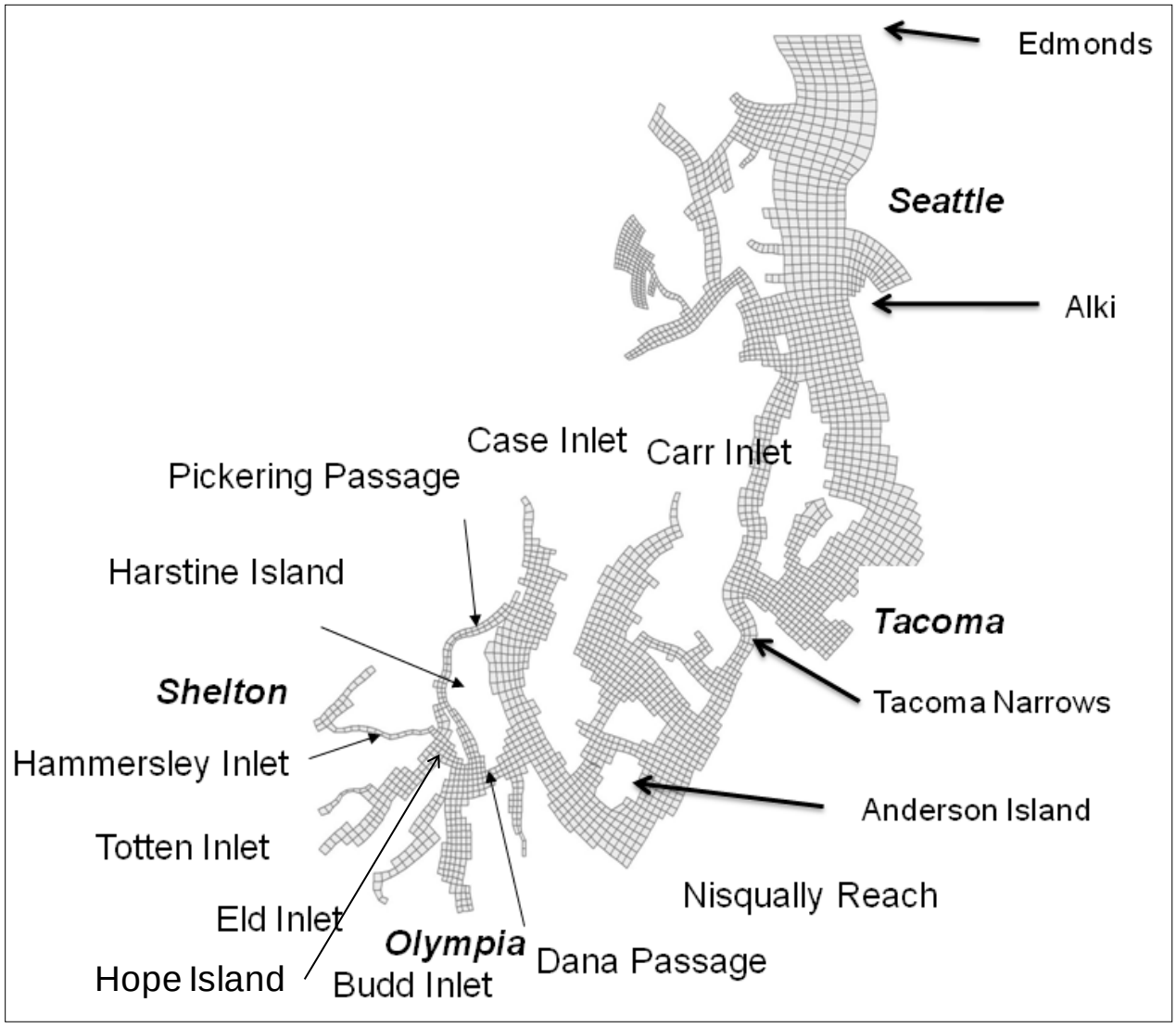


Figure 2. South and Central Puget Sound model grid.

## Bathymetry

Depths for each model grid cell were determined by sampling the Finlayson (2005) digital elevation model. We re-projected the data from Washington State Plane North (feet) NAD83 to Washington State Plane South (feet) NAD83 HARN. We preserved the NAVD88 vertical datum from the original data. Using GIS, we used the model grid cell layer to define the spatial extent and averaged depth values within the 30-ft raster grid cells from the Finlayson (2003) combined bathymetry. These initial bottom elevations were smoothed once using the GEMSS Bathymetry tool. Appendix A presents the details.

Figure 3 presents the bathymetry used to simulate circulation in South and Central Puget Sound. The complex patterns are evident in a profile view along the deepest part (thalweg) of the channel from the northern boundary into Budd Inlet. While much of Central Puget Sound includes depths as great as 200 to 250 m, depths decrease substantially at the Tacoma Narrows sill (50 m). Water depths are as much as 150 m east of McNeil and Anderson Islands before decreasing to 50 m around the Nisqually Reach. Depths as great as 100 m occur south of the Key Peninsula but are much lower through Dana Passage and into Budd Inlet. The quickly changing water depths produce localized bottom friction and upwelling that affect circulation and water quality.

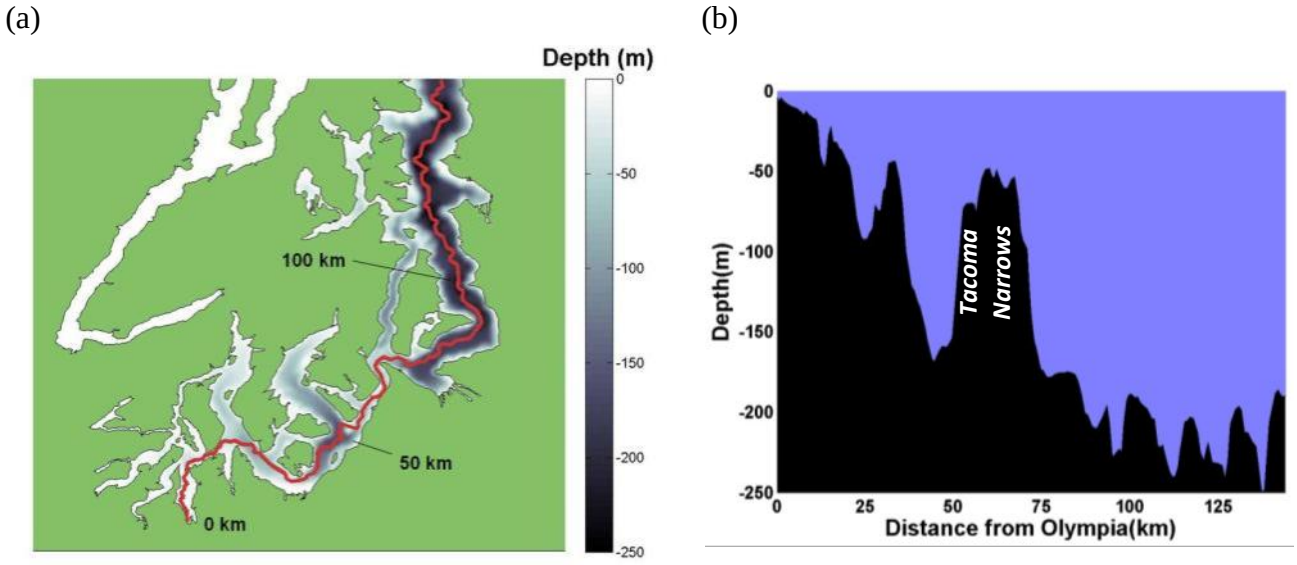


Figure 3. Bathymetry used for South and Central Puget Sound in (a) plan view, where dark colors depict deeper water, and (b) as a vertical section, showing depth along the thalweg with an origin in Olympia, WA.

## Model Layering

After the bottom elevations were determined, layers were assigned to fixed elevations relative to zero NAVD88. We evaluated multiple vertical layering thicknesses during the calibration process. Initially we developed a 35-layer model. However, even with a powerful computer[1], the 35-layer run required 9 days to simulate 17 months compared to 2.6 days for the 17-layer model. Initial runs with the 35-layer model produced slightly lower RMSEs in water surface elevations compared with the selected 17-layer model. Because the water quality model will need to evaluate multiple scenarios in a reasonable time period, the disadvantages of a slow run time far outweighed the slight improvement in water surface elevations. The 17-layer version was a reasonable compromise between providing good vertical structure in density stratification and available computational speed.

We also evaluated increased spatial detail near the surface in case that is needed to describe the complex biogeochemical processes and spatial scales in the upcoming water quality model. Layer thicknesses of 3 m or less led to model instabilities and could not be used. Maintaining 4-m layer thicknesses near the surface proved feasible. However, any additional layering beyond 17 layers increased model run times substantially. The increased layering did not significantly improve temperature and salinity profiles, described below. If the detail is warranted during water quality model development, we will investigate detailed surface layering further. However, the current layering (17 layers with a surface layer of 4 m) reproduces vertical profiles and is sufficient for calibration.

Figure 4 shows the thickness and elevations of the 17 layers that represent the maximum water column depth. Fewer layers are used in shallower locations. Time-varying water surface elevations show up in layers 2, 3, and 4 to define the intertidal zone.

[1] 2.66-GHz CPU with 8 GB of RAM under a Windows server 64-bit operating system.

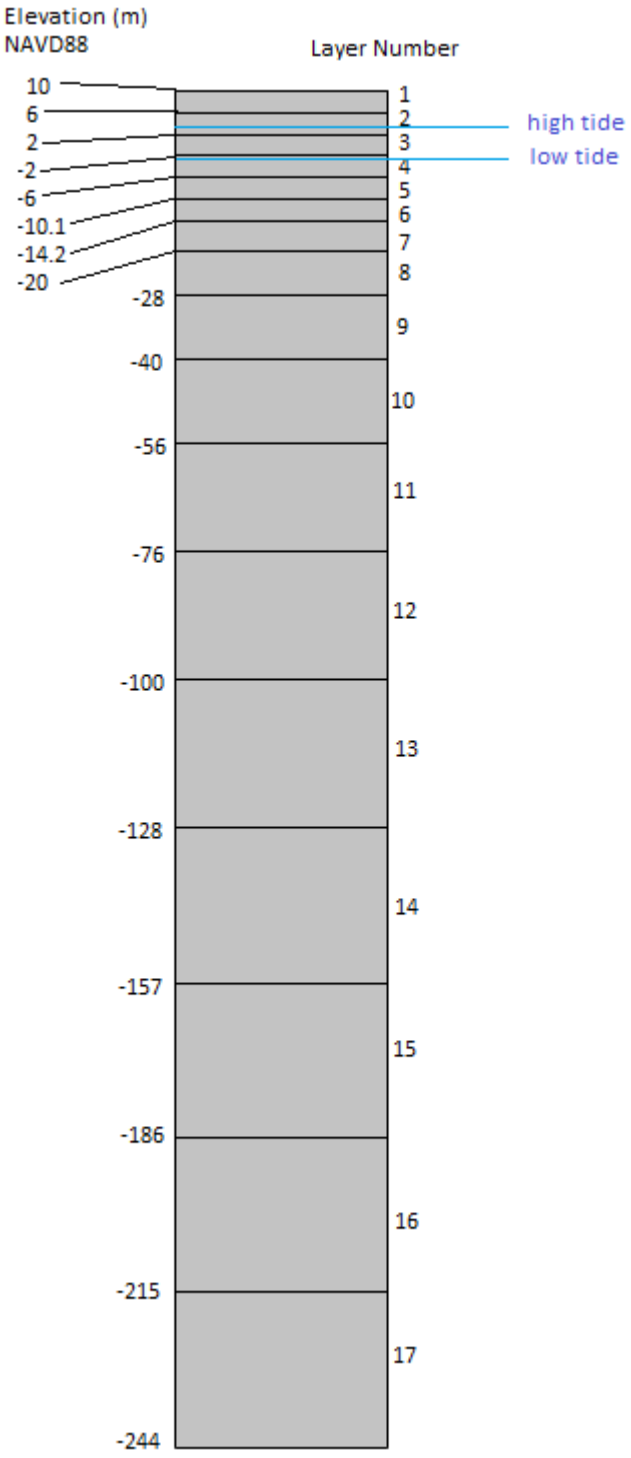


Figure 4. Elevations (meters) at the top and bottom of each of the 17 model layers used in the model grid relative to the NAVD88 vertical datum.

# Boundary Conditions

## Water Surface Elevations

Water surface elevations result from the complex interaction of tidal forces from the moon and sun, the shape of marine waterbodies, wind, and freshwater inputs. Correctly predicting water surface elevations is a key indicator that circulation models are calibrated correctly. Within the model domain, NOAA records and publishes water surface elevations at only two stations. However, both stations, in Elliott Bay and Commencement Bay, were too far from the Edmonds boundary to describe conditions there. To supplement these data, well established tools are available that provide detailed estimates of water surface elevations throughout the model domain.

The Puget Sound Tide Channel Model (PSTCM) predicts water surface elevations throughout Puget Sound based on the amplitude and phase of the full suite of tidal constituents (Lavelle et al., 1988; Mofjeld et al., 2002). Finlayson (2004) developed a stand-alone version of the updated PSTCM called PSTides.

We used PSTides to generate tidal elevation predictions at Edmonds. We converted PSTides tidal elevations, expressed relative to mean lower low water (MLLW), to NAVD88 using NOAA's VDatum program (nauticalcharts.noaa.gov/csdl/vdatum.htm). All vertical elevations are expressed as NAVD88, Ecology's standard datum, unless otherwise specified. Positive elevations indicate locations above the datum and negative elevations below it. The water surface elevation time series at PSTides segment 388 (see *Model Calibration* for location) was used as the northern boundary condition. In addition, we used PSTides to obtain water surface elevation for nearly every bay and channel in Puget Sound to compare with model output during model calibration.

## Temperature and Salinity Profiles

In addition to the time series of tidal elevation, the open northern boundary also requires vertical profiles of temperature and salinity gathered from monthly cruises to describe density-driven flow. Albertson et al. (2007b) describes the boundary station cruise sampling design, and Roberts et al. (2008) presents the data collected by King County Department of Natural Resources under contract to Ecology. The Edmonds east and Edmonds west vertical profiles were used as boundary conditions for the model. Table 2 lists the dates for both these boundary cruises as well as data collection at interior stations by program and vessel.

Temperature and salinity boundary conditions are shown in Figure 5. The model implements linear interpolation between monthly cruise dates. Monthly intervals were selected to capture seasonal variability and to optimize resources available for data collection. Because monthly data could induce errors if sub-monthly phenomena are missed, we evaluated two supplemental sources of information for continuous temperature and salinity for northern boundary conditions: (1) the existing Princeton Ocean Model (POM) application for Puget Sound and (2) data from the nearest ORCA (Oceanic Remote Chemical Analyzer) buoy near Hood Canal.

Table 2. Data collection cruise schedule by vessel for Ecology's *R/V Skookum* (S), University of Washington's *R/V Barnes* (B), and King County Department of Natural Resources' *R/V Liberty* (L); and cruises sponsored by University of Washington's Puget Sound Regional Synthesis Model (PRISM (P)) initiative.

| Cruise | Program | Dates |
|---|---|---|
| P1 | PRISM | 6/26/06 - 6/28/06 |
| L1 | Liberty | 7/26/06 |
| B1 | Barnes | 7/31/06 - 8/3/06 |
| L2 | Liberty | 8/16/06 |
| S1 | Skookum | 8/21/06 - 8/24/06 |
| L3 | Liberty | 9/20/06 |
| B2 | Barnes | 9/25/06 - 9/29/06 |
| L4 | Liberty | 10/18/06 |
| S2 | Skookum | 10/23/06 - 10/24/06 |
| L5 | Liberty | 11/8/06 |
| S3 | Skookum | 11/14/06 - 11/16/06 |
| L6 | Liberty | 12/6/06 |
| B3 | Barnes | 12/18/06 - 12/21/06 |
| L7 | Liberty | 1/10/07 |
| L8 | Liberty | 2/14/07 |
| S4 | Skookum | 2/26/07 - 2/27/07 |
| L9 | Liberty | 3/15/07 |
| S5 | Skookum | 3/26/07 - 3/27/07 |
| S6 | Skookum | 4/9/07 - 4/11/07 |
| L10 | Liberty | 4/11/07 |
| B4 | Barnes | 4/23/07 - 4/26/07 |
| L11 | Liberty | 5/9/07 |
| S7 | Skookum | 5/21/07 - 5/23/07 |
| L12 | Liberty | 6/13/07 |
| B5 | Barnes | 6/25/07 - 6/29/07 |
| L13 | Liberty | 7/11/07 |
| S8 | Skookum | 7/31/07 - 8/2/07 |
| L14 | Liberty | 8/8/07 |
| S9 | Skookum | 8/28/07 - 8/30/07 |
| L15 | Liberty | 9/5/07 |
| B6 | Barnes | 9/24/07 - 9/27/07 |
| L16 | Liberty | 10/3/07 |
| S10 | Skookum | 10/23/07 - 10/25/07 |

(a) Temperature at Edmonds West

(b) Temperature at Edmonds East

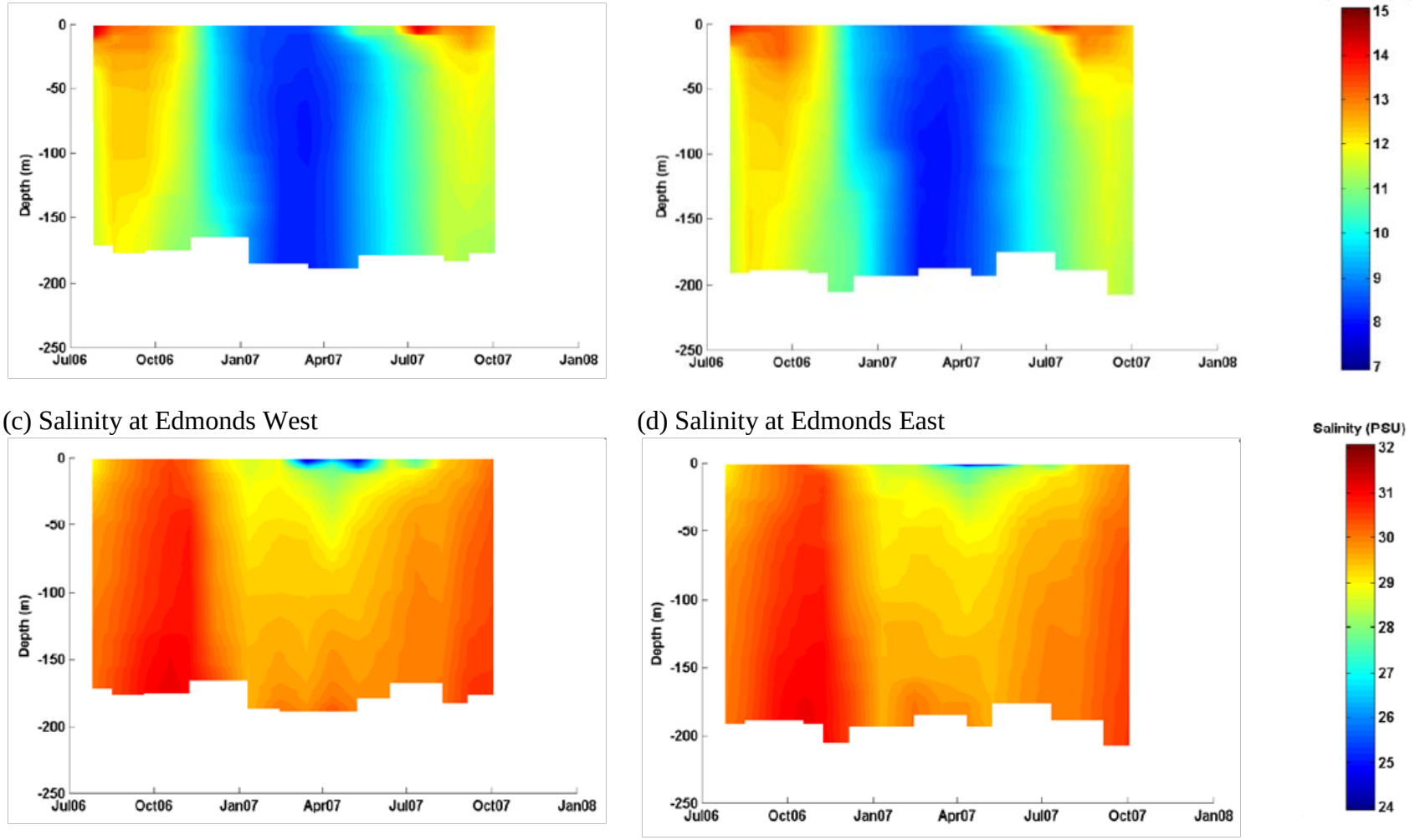


(c) Salinity at Edmonds West

(d) Salinity at Edmonds East




Figure 5. Temperature (a and b) and salinity (c and d) at Edmonds east and Edmonds west used as the northern boundary condition.

First, we evaluated using results from POM. POM uses monthly data from a transect in the Strait of Juan de Fuca as a boundary condition. We compared POM salinity output to monthly cruise data at both the Edmonds and Alki locations for several months, including June 2007. POM surface salinity was over-predicted, and near-bottom salinity was under-predicted, by 0.5 to 1.5 ppt by the model at the Edmonds and Alki stations compared with our measured data. POM predicts small sub-daily salinity variations at Edmonds and Alki, even though the monthly boundary condition does not include sub-monthly forcing. POM does not simulate the heat balance or water temperature, so the model could not provide temperature profiles. For these reasons and because output was not available for the entire simulation period, we determined that POM output was not a viable substitute to describe the northern boundary condition.

Second, we investigated using data collected more frequently using the nearest ORCA profiling buoy, which is near Admiralty Inlet but slightly within Hood Canal (Ruef and Devol, Hood Canal Dissolved Oxygen Program, personal communication). Comparing the monthly *R/V Liberty* data in Figure 5 with the buoy data confirms that monthly data do describe the overall seasonal variation well. Both time series show high-salinity water throughout the water column in October 2006 and similar conditions that are less salty in October 2007. The water column freshens in the winter with salinity decreasing to 27 ppt near the surface. The ORCA buoy data show two episodes of near-bottom salinity increasing 2 ppt between January and April 2007. The monthly data capture the earlier event but not the later event. However, the event was short-lived and not coincident with the September-October critical period.

The ORCA buoy provides high-resolution data useful for many purposes. For example, the salinity and temperature records do not show strong diel (24-hour) variations. However, the ORCA buoy is 90 km from the northern boundary, and several large data gaps disrupt the time series when the equipment was either inoperable or out of calibration.

Because the monthly boundary data do appropriately capture the seasonal variability and because the other two potential sources of information were incomplete, the monthly boundary cruise data provided a better alternative for this modeling project.

## Freshwater Inputs

Freshwater inflows from 66 rivers were compiled as described in Roberts et al. (2008) and Mohamedali et al. (2011). Figure 6 presents the watershed definitions. Discharges were based on several USGS gaging stations within the model domain (Figure 7). Daily flows were estimated based on the ratios of watershed area and mean precipitation. Freshwater inflows, including the shoreline areas not tributary to a major river or stream, were mapped to the surface layer of the grid cell nearest the discharge location, with the exception of Sinclair and Dyes Inlets. Mohamedali et al. (2011) summarizes the inflow rate development.

Sinclair and Dyes Inlets are not in the primary area of interest for this modeling application. Because the waterbodies received distributed freshwater inflow from numerous small streams, watershed contributions were simplified as one composite input. All inflows are added to the western extent of Sinclair Inlet, and detailed predictions within this region will be affected. If the area influenced by this simplification extends to the primary area of interest, freshwater inflows to Sinclair and Dyes Inlets will be reevaluated.

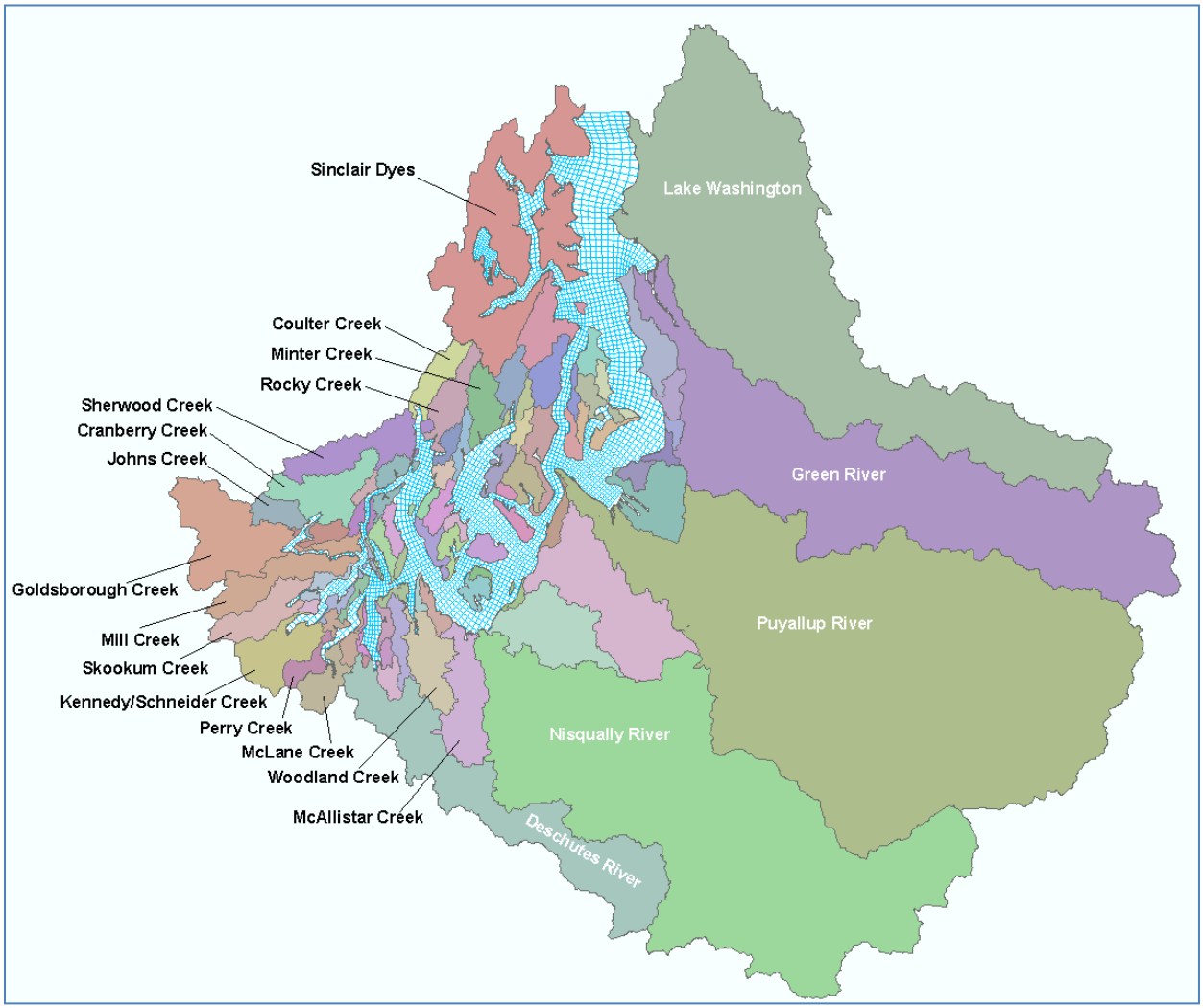


Figure 6. Watershed definitions for freshwater inflows.

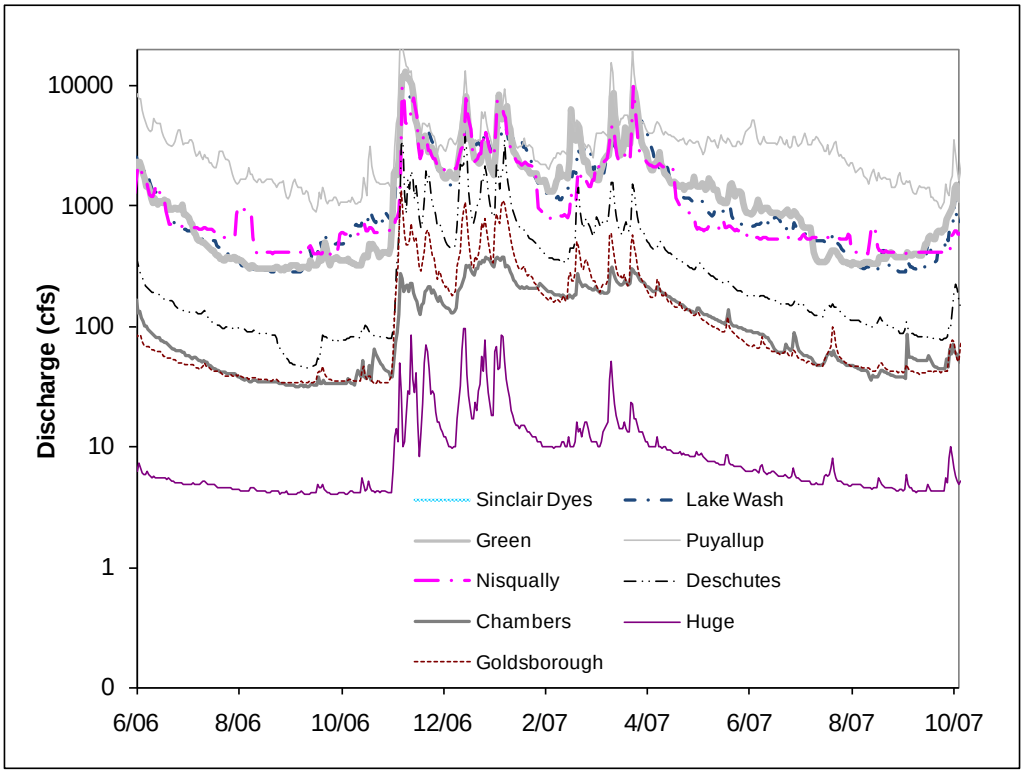


Figure 7. River, creek, and tributary discharge (cfs).

Wastewater treatment plants also discharge freshwater to South and Central Puget Sound, although they represent <5% of the total freshwater inflows. Figure 8 shows the locations of all wastewater treatment plants discharging directly to marine waters within the model domain. These point sources discharge below the water surface and, being less dense, rise in the water column, entraining denser ambient water. This rising plume either reaches the surface if there is sufficient vertical momentum or gets trapped below the surface where plume and ambient densities equilibrate. If upon reaching the surface or at trapping level, the plume diameter is smaller than or equal to the thickness of the surface layer or of the layer in which it traps, then all the flow from the wastewater plant is assigned to that layer. However, if the size of the trapped plume crosses several grid layers, the flow is distributed over these layers in proportion to the layer thickness.

These point source discharges to marine waters are dynamic in nature with seasonal high and low flows. The ambient density profile also changes with seasons. Due to these factors, the trapping level and the size of the trapped plume will also vary dynamically with seasons. To address this issue, monthly average flows and ambient densities were used to assess seasonal plume characteristics (i.e., plume diameter and trapping level). Plume trapping levels were estimated externally using Visual Plumes model (www.epa.gov/ceampubl/swater/vplume/). A summary of the procedure in establishing trapping levels for most marine point source discharges are included in Appendix B. These were provided by the Water Quality Section at Ecology's Southwest Regional Office (Charles Hoffman, 2010). Trapping levels for West Point and South King County wastewater plants were provided by Bruce Nairn (2009).

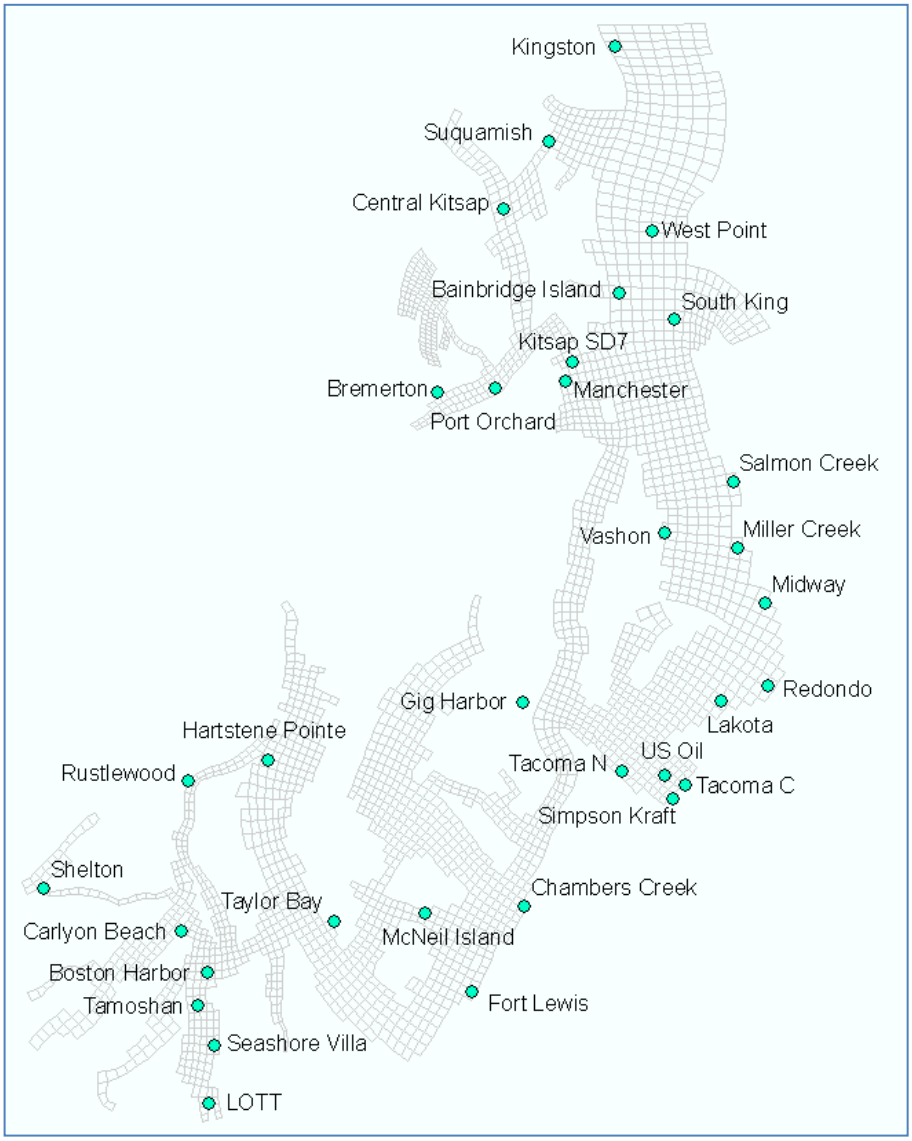


Figure 8. Locations of municipal wastewater treatment plants with direct discharge to marine waters.

The final source of freshwater is precipitation falling directly on the surface of South and Central Puget Sound. Figure 9 presents the precipitation volumes measured at the Shelton Airport for South Puget Sound and at SeaTac Airport for Central Puget Sound. *Meteorological Forcing* describes the meteorological boundary conditions in more detail.

Continuous water temperature data are available year-round only for the Cedar River at Renton (USGS gage 12119000) (Figure 10). Continuous summer temperatures recorded at Ecology's ambient monitoring stations in the Nisqually River and Deschutes River for 2001-2006 were close to Cedar River temperatures with a mean error of +0.4 and -0.5°C, respectively. These mean errors in temperature translate to <0.1 ppt density differences, which are negligible. Therefore, the water temperatures for the Cedar River were applied to all freshwater inflows. Rivers have no measurable salinity.

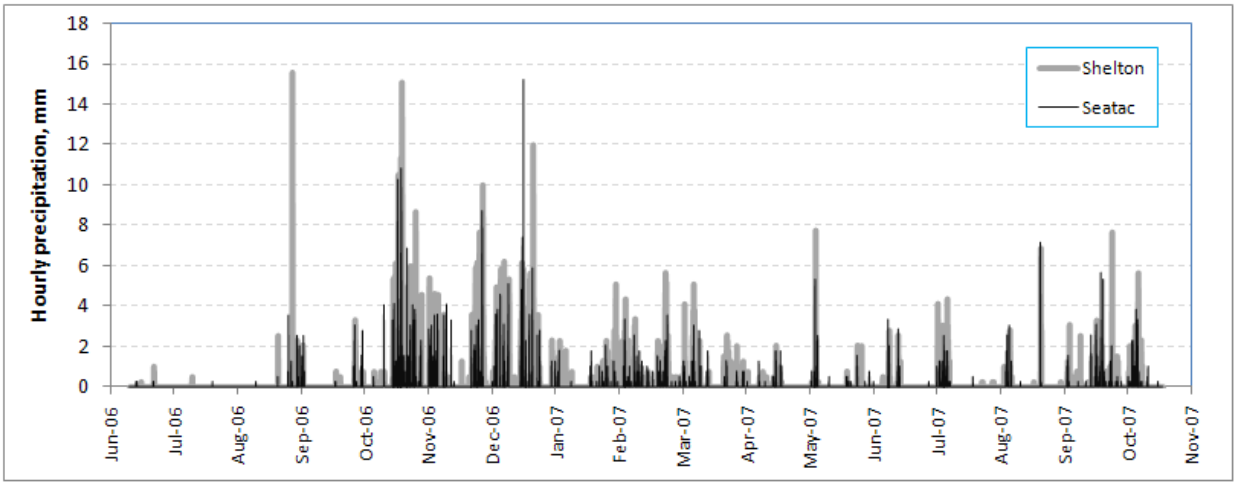


Figure 9. Precipitation measured at Shelton and SeaTac Airports for the study period.

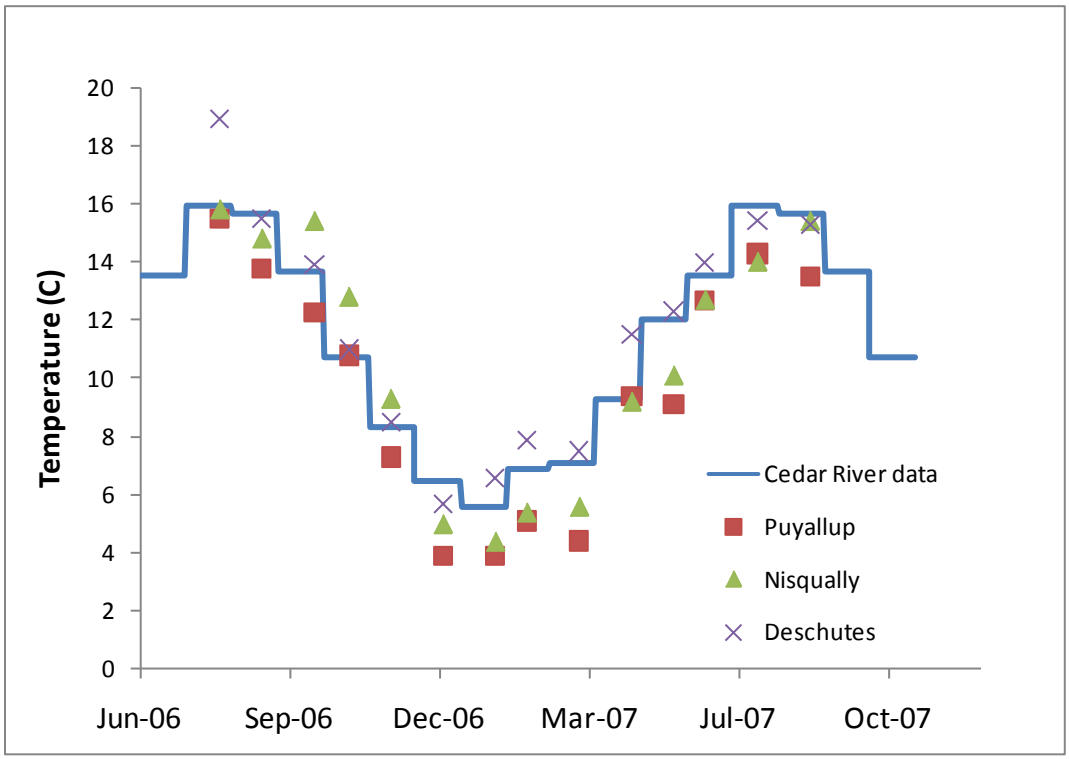


Figure 10. Cedar River mean monthly temperature (°C) compared with instantaneous monthly values recorded by Ecology's ambient monitoring programs.

## Meteorological Forcing

In addition to precipitation, meteorology forcing functions included air and dew point temperatures, wind speed and direction, cloud cover, atmospheric pressure, relative humidity, and solar radiation. Meteorological stations considered in this model are depicted in Figure 11.

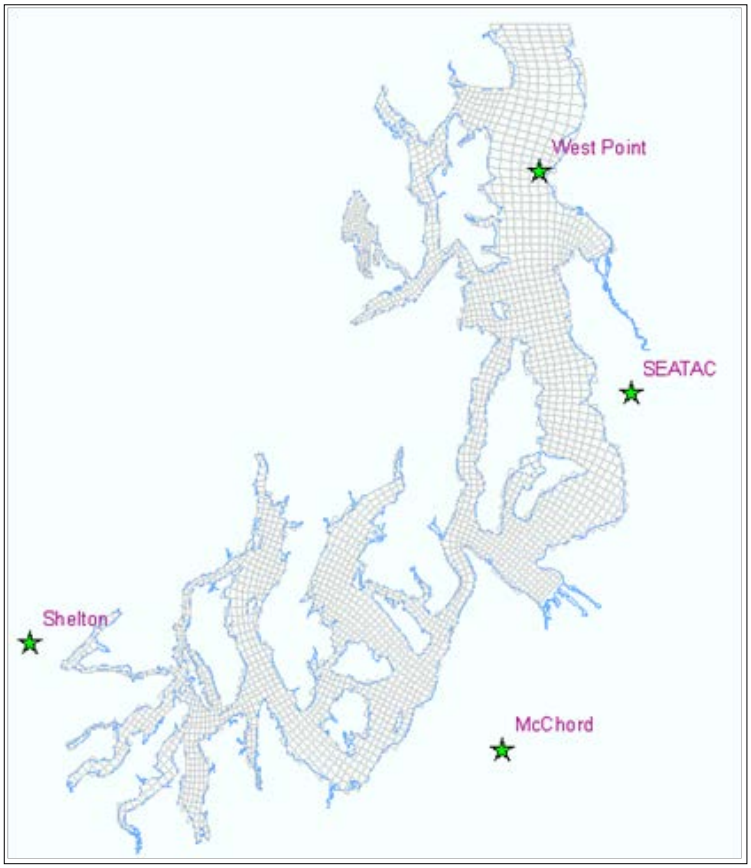


Figure 11. Location of meteorological stations considered for the model domain.

GEMSS couples Puget Sound with the atmosphere through surface shear stress and heat flux. The program converts wind speed and direction, barometric pressure, precipitation, relative humidity, air temperature, cloud cover, and solar radiation into these air-sea surface terms. The solar radiation term is further split between incoming solar shortwave radiation and net outgoing longwave radiation (see Appendix C for meteorological rates and constants).

Initially, meteorology data from the McChord station were used for the model domain, primarily because of its central location. During model calibration, we determined that the McChord data did not represent region-wide meteorology. The SeaTac Airport data were then used north of the Tacoma Narrows in combination with McChord data for south of Tacoma Narrows. However, McChord's warm air temperature and low cloud cover produced surface water temperatures that were too warm in southern Puget Sound. The cooler air temperatures and higher cloud cover from the Shelton Airport near Oakland Bay were more representative of marine systems. This improved model calibration.

The Olympic and Cascade Mountain ranges profoundly influence wind speed and direction in Puget Sound. In South Puget Sound winds tend to be southwesterly, while in Central Puget Sound they are more southerly. Figure 12 presents the wind roses from these airport locations. Predominant wind direction at McChord was from the south and did not represent the southwesterly winds in the southern part of the model domain near Shelton. Therefore, we selected two meteorological stations, one in the south (Shelton) and the other in the north (SeaTac). The regional divide between these two stations was set immediately north of Tacoma Narrows.

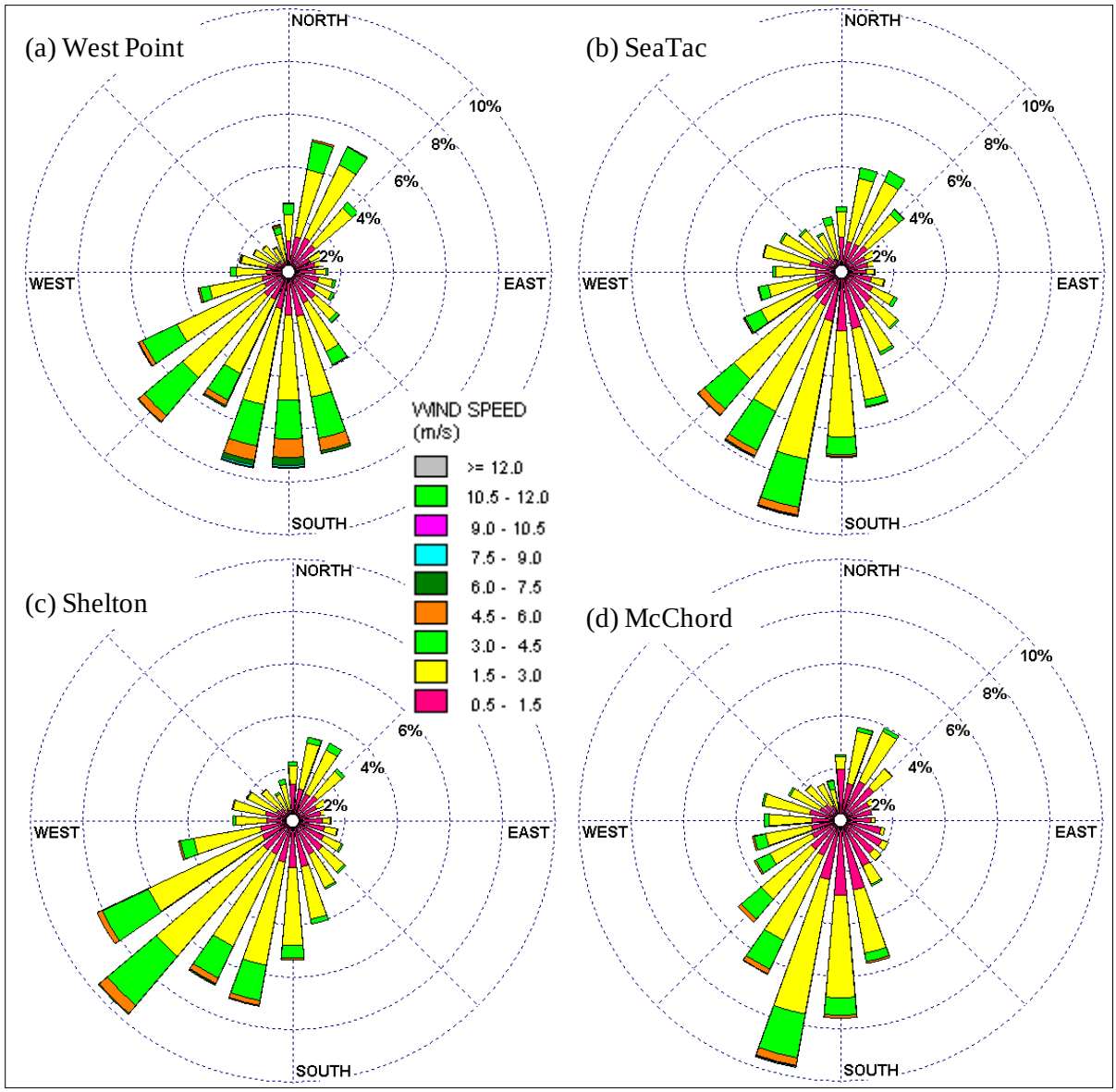


Figure 12. Wind speed, direction, and frequency plotted as wind roses at four meteorology stations in the model domain.

*Direction refers to where the winds originate.*

Because both SeaTac and Shelton are still somewhat inland, we evaluated data from the West Point station, operated by the National Data Buoy Center (www.ndbc.noaa.gov/station_page.php?station=wpow1). Air temperatures at West Point were cooler than those at Shelton and SeaTac and reflected a marine influence. However, wind at West Point was still significantly different compared to Shelton although somewhat similar to SeaTac. Therefore a hybrid approach was used for meteorological forcing.

For the entire model domain, West Point station data were used for air temperature, dewpoint temperature, relative humidity, and atmospheric pressure. South of Tacoma Narrows, the Shelton station was used for wind, wind direction, cloud cover, and precipitation. North of Tacoma Narrows, the SeaTac station was used for cloud cover and precipitation, but the West Point station was used for wind and wind direction. A summary of these decisions is included in Table 3.

Table 3. Summary of sources of meteorological data for different regions of model domain.

| Met_station | Model_Region | Parameter |
|---|---|---|
| Shelton | South of Tacoma Narrows | precipitation, cloud cover, wind, wind direction |
| West Point | North of Tacoma Narrows | wind, wind direction |
| Seatac | North of Tacoma Narrows | precipitation, cloud cover |
| West Point | Region Wide | air temperature, dewpoint temperature, relative humidity, atmospheric pressure |

Cloud-free solar radiation was estimated at Shelton and SeaTac with Ecology's *SolRad* spreadsheet (www.ecy.wa.gov/programs/eap/models.html). We selected the Ryan/Stolzenbach solar radiation model.

## Simulation Period

Data were collected between June 2006 and October 2007, as described in Roberts et al. (2008), to provide both input to the model and output with which to compare model predictions. Although 2007 had more detailed data available, the unusually cold and wet summer did not produce typical low dissolved oxygen concentrations. Year 2006 represented more typical summer conditions.

# Initial Conditions

The model was initialized with profiles of temperature and salinity throughout the model domain at the beginning of the simulation (July 1, 2006) using data collected during a late-June 2006 cruise. Several approaches were evaluated, including simulating an entire year and using the predicted July 2007 conditions as the initial July 2006 conditions. However, because 2006 and 2007 were so different in terms of meteorological boundary conditions and measured dissolved oxygen levels, we used the June 2006 cruise data as initial conditions. We divided the model domain into three zones, as shown in Figure 13, and averaged available cruise data within each zone.

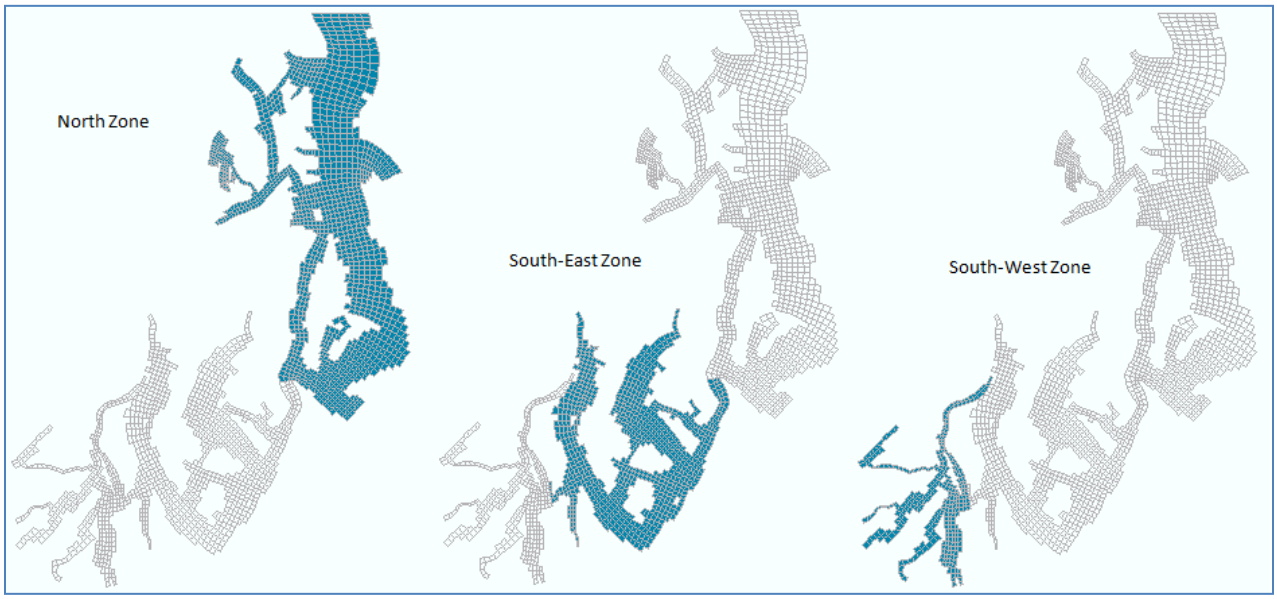


Figure 13. Three zones used to establish initial conditions for June 2006.

## Bottom Friction

In addition to varying the bathymetry to achieve calibration, we adjusted the bottom friction to enhance or reduce tidal exchanges. We varied bottom friction within a typical range of 20 to 50 (unitless Chezy friction coefficient) in multiple model runs, but the effect on water surface elevations was much lower than refining the model bathymetry. Overall, a bottom friction of 40 for the main basins in Central and South Puget Sound provided the best fit between water surface elevations predicted between the model and both PSTides and the measured tide stations. For the finger inlets (Budd, Eld, Totten, and Henderson Inlets and Oakland Bay), a Chezy friction factor of 20 was used. These friction factors were kept constant throughout the simulation period.

## Numerical Solutions, Time Steps, and Turbulence Closure Schemes

The three transport schemes (Upwind, QUICKEST[2], and QUICKEST with ULTIMATE[3]) within GEMSS were evaluated, but the best result with respect to model stability was obtained using the higher-order transport scheme QUICKEST with ULTIMATE. Upwind scheme assumes that the concentration at the face of a grid cells equals the concentration of the grid upstream of the face. QUICKEST employs a three-point, upstream-biased interpolation scheme to calculate face concentrations. QUICKEST with ULTIMATE applies a limiter to each cell face to prevent any overshoot or undershoot. Other details of the transport scheme are present in the GEMSS user's manual available from Environmental Resources Management (ERM).

A dynamic time-stepping scheme was used with an initial time step of 10 seconds and a maximum allowable time step of 120 seconds during the simulation period. The exception was the last week of January 2007, when the maximum time step was reduced to 10 seconds due to model instability. These time steps were derived following sensitivity runs to obtain the best combination of stability and computational time.

GEMSS solves the turbulent time-averaged Reynolds momentum equations in three dimensions. While GEMSS includes several options to parameterize turbulence, we used an option characterizing Von Karman's mixing length based on model stability and optimum computational time steps. Additional details are in the GEMSS user's manual available from ERM. These and other parameters used in the hydrodynamic and transport model are summarized in Appendix C.

[2] Quadratic Upstream Interpolation for Convective Kinematics with Estimated Streaming Terms
[3] Universal Limiter for Transient Interpolation Modeling for Advective Transport Equation

# Model Calibration

*Calibration* refers to the iterative process of comparing model output to observed data and adjusting appropriate factors. The ability to model circulation accurately includes well-described processes such as tidal exchanges and highly variable processes such as wind.

Marine circulation model calibration begins with comparing predicted and measured water surface elevations. Modelers adjust the grid shape, primarily depth, and the bottom friction to optimize fit. PSTides-based water surface elevations within the model domain were used to check the GEMSS model predictions. In addition, two continuous recording tide gages were used to check model predictions of water surface elevations in Commencement Bay and in Elliott Bay.

The second set of information consists of water *temperature* and *salinity* values recorded during monthly cruises. To verify the model-predicted spatial patterns appropriately, we compared the measured and predicted surface and near-bottom temperature and salinity time series for the simulation time period. In addition, we compared the detailed observed profiles with model output.

The third set of information used to calibrate water circulation models is measured *velocities*. For South Puget Sound, we measured current velocities both as transects across inlets and from the bottom of several inlets. We compared both depth-averaged values between the model and the observed data as well as the tide phase (ebb and flood timing) and current velocity.

The model was calibrated using data collected from July 2006 through October 2007. Table 4 summarizes information sources used in the calibration process.

Table 4. Information used to calibrate and confirm the circulation model.

| Parameter | Information source | Stations |
|---|---|---|
| Water surface elevations | PSTides | 23 segments throughout model domain. |
| | NOAA tide gages | Elliott Bay (Seattle) and Commencement Bay (Tacoma). |
| Tidal constituent frequency and amplitude | NOAA tide gages and historical NOS stations | Elliott Bay, Commencement Bay, Budd Inlet/Boston Harbor (Olympia), and Oakland Bay (Shelton). |
| Surface temperature and salinity spatial patterns | Six quarterly detailed cruise data | All available stations (>70) throughout model domain. |
| Surface and near-bottom temperature and salinity time series | All project cruise data | 22 stations throughout model domain. |
| Salinity and temperature profiles | All project cruise data | 11 stations throughout model domain. |
| Current velocities | Project current velocity data | Carr Inlet, Case Inlet, Budd Inlet, Dana Passage, and Pickering Passage. |

NOS: National Ocean Survey

## Water Surface Elevations

Water surface elevations predicted by the hydrodynamic model were compared with those predicted by PSTides elevations. Comparison locations spanned the model domain, ranging from near Alki Point within Central Puget Sound to Oakland Bay in the western model domain (Figure 13). Other interim stations were used to verify circulation around complex geometry.

A station within Sinclair Inlet (SIN01) provided a check on the circulation around Bainbridge Island. Several stations within the Tacoma Narrows were compared, since the amount of water passing over the sill influences circulation in South Puget Sound. A station in southern Budd Inlet (SS08) was used because circulation influences Budd Inlet water quality (Roberts et al., 2012). Several stations were compared near Hope Island (SS21), Hammersley Inlet (SS35), and Pickering Passage (SS43) because of the complex flow patterns.

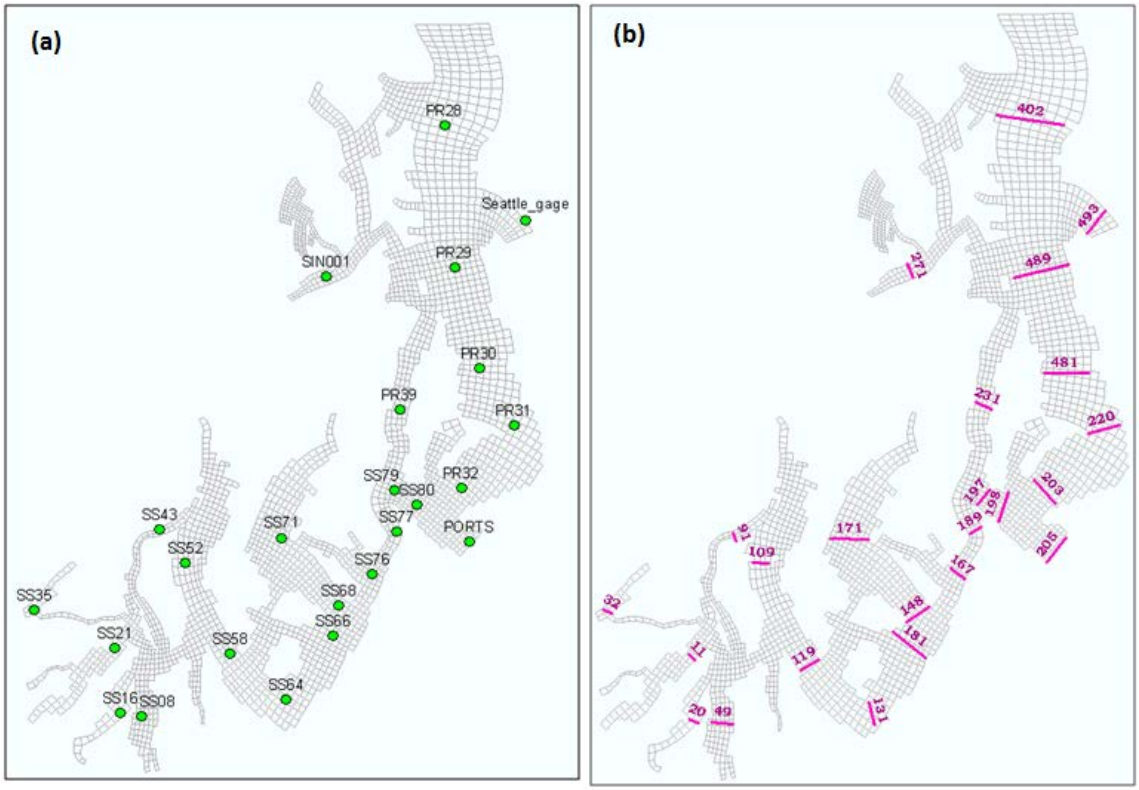


Figure 14. Station locations (a) and PSTide segments (b) used to calibrate water surface elevation.

To calibrate water surface elevations within South Puget Sound, the bathymetry in the Tacoma Narrows area was evaluated carefully. Initially, the grid development from the source data and smoothing steps underestimated the model grid cell depths through the Tacoma Narrows. The model grid cell widths and depths were scaled so that the grid volume within about 3 km of the Tacoma Narrows Bridge matched the volume estimated from the Finlayson (2003) digital elevation model (DEM) below MLLW. Grid cells within the Tacoma Narrows were further deepened to optimize water surface elevation predictions. The final Puget Sound grid cells are within 5% of the Finlayson values.

The original grid development and smoothing produced model grid depths that were much shallower than the deeper areas of Budd Inlet, even though the total volume error for Budd Inlet was low (3.3%). Grid cell depths in southern Budd Inlet were increased to match the Finlayson volumes for this region. Because deeper areas of Budd Inlet lie within channels, smoothing for the nominal 500-m wide grid cells averages these depths with shallower values.

Similar to Budd Inlet, the grid development and smoothing process produced model grids for Oakland Bay, Hammersley Inlet, Pickering Passage, and Hope Island that missed key bathymetric elements. In Hammersley Inlet, the abrupt bend in the east-west arm could not be represented in the horizontal plane without causing model instabilities. Because the grid passed over land surfaces, the averaged grid cell depths were artificially shallow. The narrow channel also produced vertical constrictions that incorrectly impeded water flow into Oakland Bay and underestimated tidal exchanges. The volumes of the east-west Hammersley Inlet arm were adjusted to match the Finlayson (2003) volumes.

Pickering Passage initially was represented by shallow depths. The cross section is somewhat triangular in shape, with much deeper depths in the center of the channel than at the margins. Using two grid cells across the passage produces correct average depths but does not match the deepest depths. Therefore, widths and depths were adjusted to closer represent the shape of Pickering Passage. (See *Current Velocities* section for implications.) Peak tidal velocities through Pickering Passage, described below under *Current Velocities*, were close to those predicted by PSTides. Hope Island influences exchanges into Hammersley and Totten Inlets. Shallow water depths both northeast and southwest of the island produce high local friction that impedes flow south of Harstine and Squaxin Islands and produces extensive tidal eddies and boils. The number of grid cells used to represent the island and the surrounding model grid cell depths were varied. Small bathymetric adjustments were made, and two inactivated model grid cells represent Hope Island.

## Calibration to NOAA Stations

The hydrodynamic model-predicted tidal elevations (with wind turned ON) were compared with those recorded at the NOAA continuously recording tide stations in Elliott Bay (Seattle_gage) and Commencement Bay (PORTS).

The hydrodynamic model predicts Commencement Bay and Elliott Bay water surface elevations well, with RMSEs of 13 cm and 11.8 cm, respectively, for September 2006 (Figure 15). Model predictions versus PSTide elevations at these locations show better RMSE of 3.8 cm and 2.9 cm, respectively.

The hydrodynamic model predictions are closer to PSTides-generated water surface elevations, partly because PSTides data were used to force the model and partly because the comparison was conducted with the wind turned off. Variability in wind magnitude and direction over the water likely contributes to the differences, but model predictions are still appropriate and acceptable. Strong wind events, as occurred later in December 2006, may produce bigger differences in water surface elevations (>50 cm) over those predicted by PSTides, but these events generally do not occur during critical conditions for low dissolved oxygen (e.g., late summer). These wind events may affect circulation during less critical times of year.

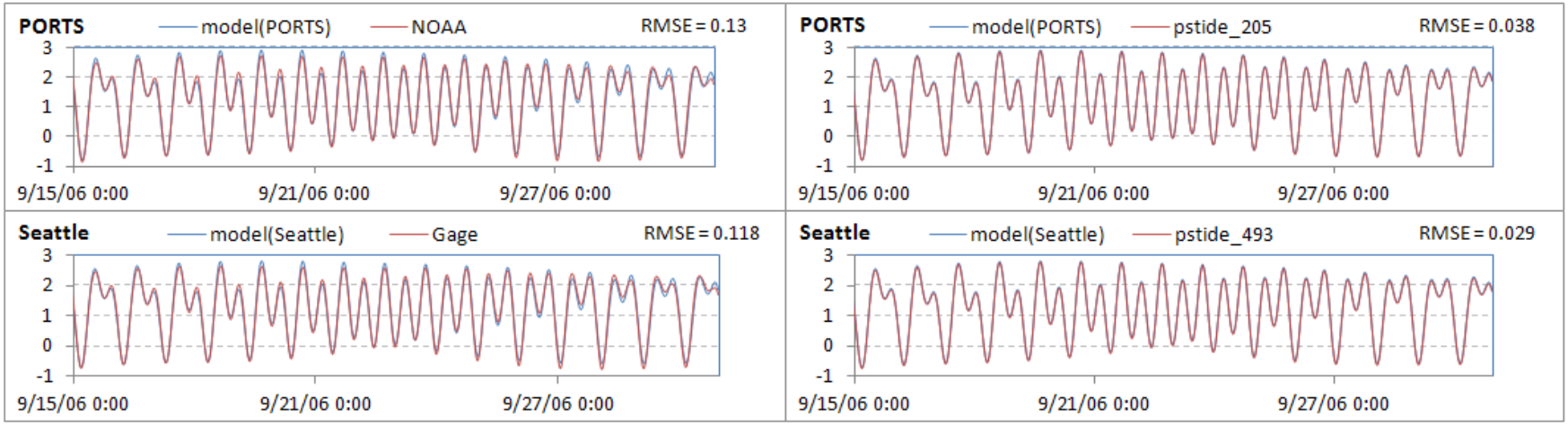


Figure 15. Predicted water surface elevations (meters) compared with NOAA recording stations (left) and PSTides (right) in Commencement Bay (top) and Elliot Bay (bottom) for September 2006.

## Calibration to PSTides

Overall the model represents the time series of water surface elevations well, including both the phasing and amplitude of the tide.

Water surface elevation predictions in the northern part of the model domain (Figure 16), including Colvos Passage and stations east of Vashon Island, were very close to those predicted by PSTides. Sites nearest the northern boundary have the lowest RMSE (2.2 cm) due to proximity to the northern boundary and relatively low bathymetric complexity. The Sinclair Inlet RMSE in water surface elevation predictions (4.4 cm) is also low, and no adjustments to the local bathymetry were needed in Central Puget Sound. Figures 17 and 18 compare water surface elevations in the central model domain (Commencement Bay through the Tacoma Narrows) and southern model domain, respectively.

The tuning of southern Budd Inlet bathymetry (as discussed earlier) produced a RMSE of 15.6 cm between the model and PSTides for Budd Inlet (station SS08).

With adjustments to Hammersley Inlet, Pickering Passage, and Hope Island, the water surface elevations predicted for South Puget Sound ranged from 9.1 cm near Nisqually Reach to 15.7 cm in Eld Inlet. However, Oakland Bay near Shelton still produced a RMSE of 40 cm when compared with PSTides. We evaluated several nearby segments in Pickering Passage and in Totten Inlet, but no other station produced such high errors as calculated for Oakland Bay. The amplitudes are reasonable, but the lack of the sharp bend in the east-west arm of Hammersley Inlet affects the phasing of tides within Oakland Bay. Bathymetry smoothing during grid development likely made the inlets shallower than they really are. Adjustments to depths were made, but slight errors in volumes remain when compared with Finlayson's volumes. Compared with Oakland Bay, the amplitudes in Totten Inlet were more in sync with PSTides. However, the high and low tides occur about 20 minutes later compared with PSTides. We accepted this model performance because the process did not influence water surface predictions in adjacent segments nor did it affect the overall amplitude of the tide calibration to NOAA Recording Tide Stations.

For 2007 (Figures19 and 20), compared with PSTides or the NOAA recording tide stations described above, the model produced water surface elevation RMSEs ranging from 2.1 cm (station PR28) near the northern model boundary to 7.8 cm in Case Inlet (station SS52). Oakland Bay (station SS35) and Totten Inlet (station SS21) continued to have the highest errors (36.8 and 40.9 cm, respectively) due to the phase advance in the model. Figures 18 through 20 compare water surface elevations in the north, central, and southern model domain areas, respectively, during September 2007. Overall the circulation model performs well and matches the water surface elevations throughout the model domain for 2007.

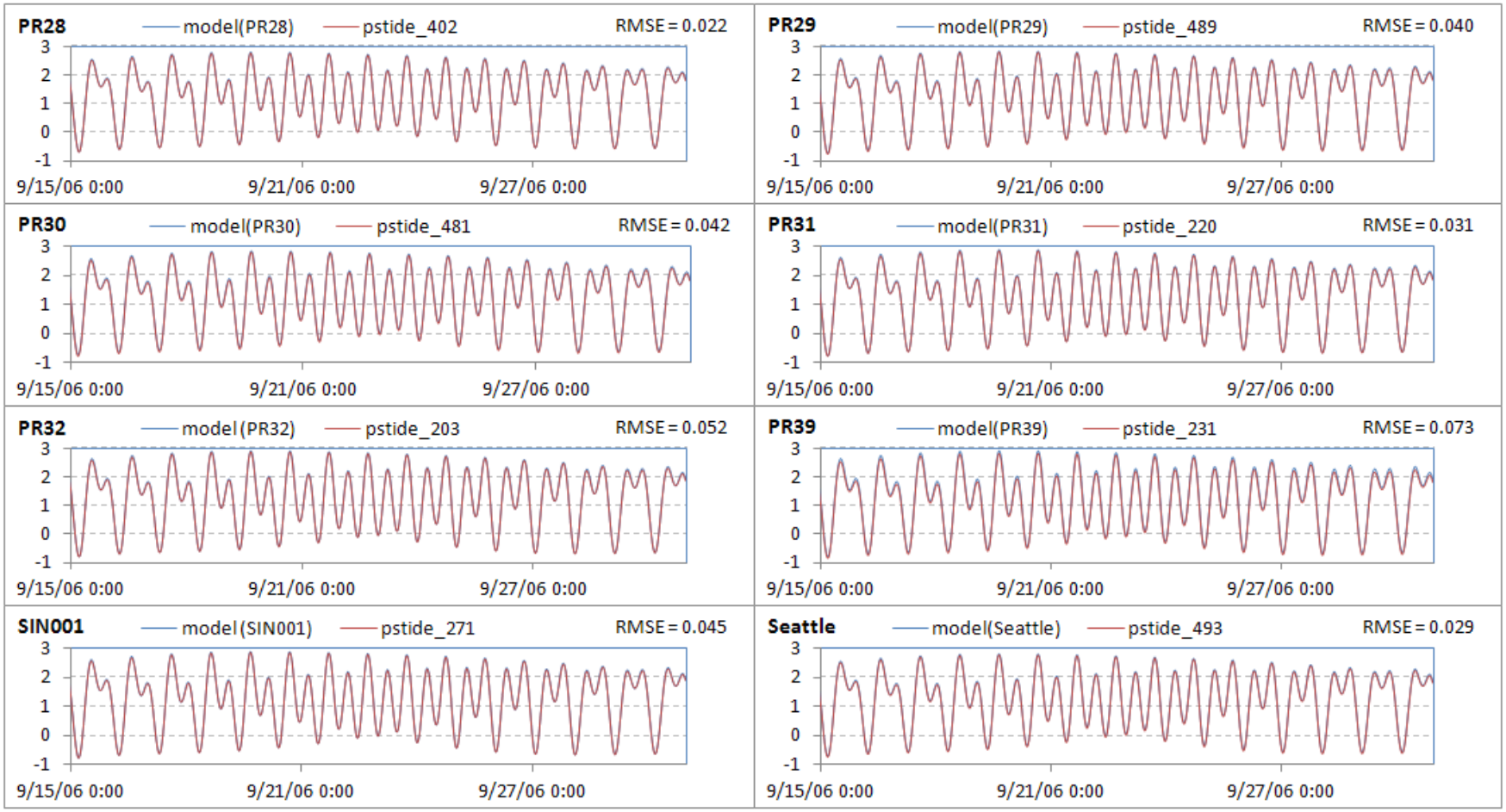


Figure 16. Predicted water surface elevations (meters) compared with PSTides for the northern model domain (south to Vashon Island) for September 2006.

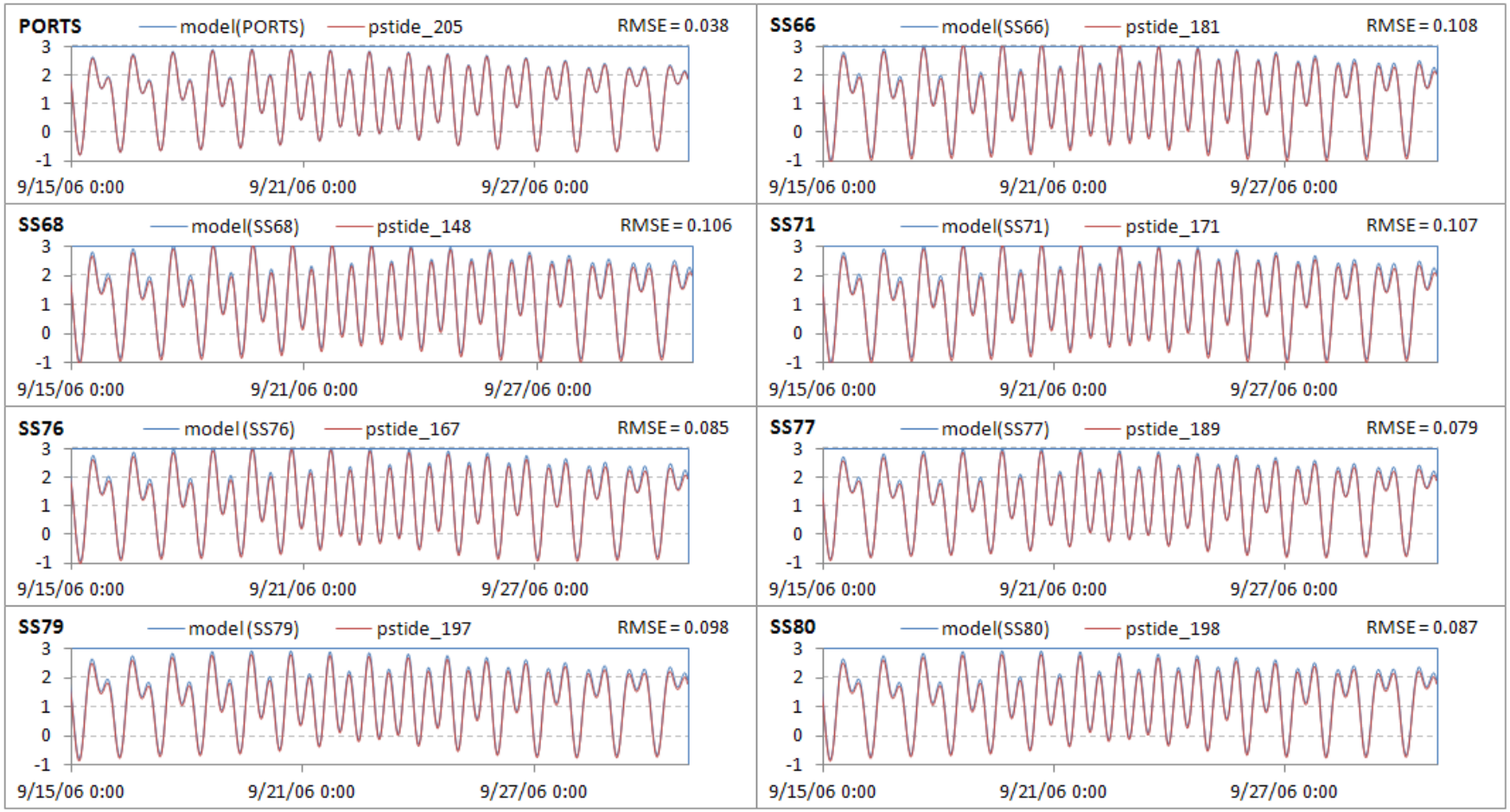


Figure 17. Predicted water surface elevations (meters) compared with PSTides for the central model domain (Commencement Bay and Tacoma Narrows) for September 2006.

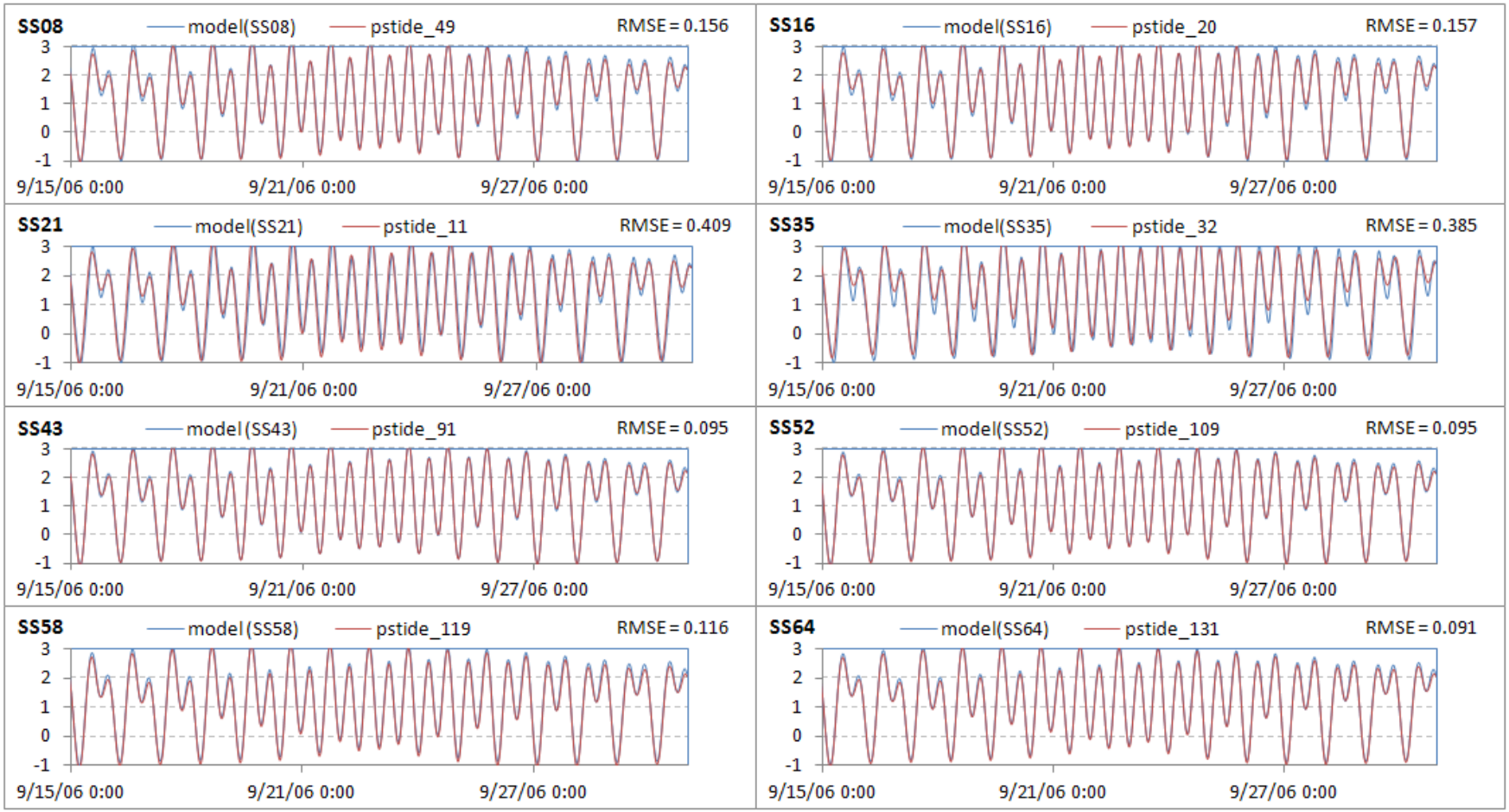


Figure 18. Predicted water surface elevations (meters) compared with PSTides for the southern model domain (west of Tacoma Narrows) for September 2006.

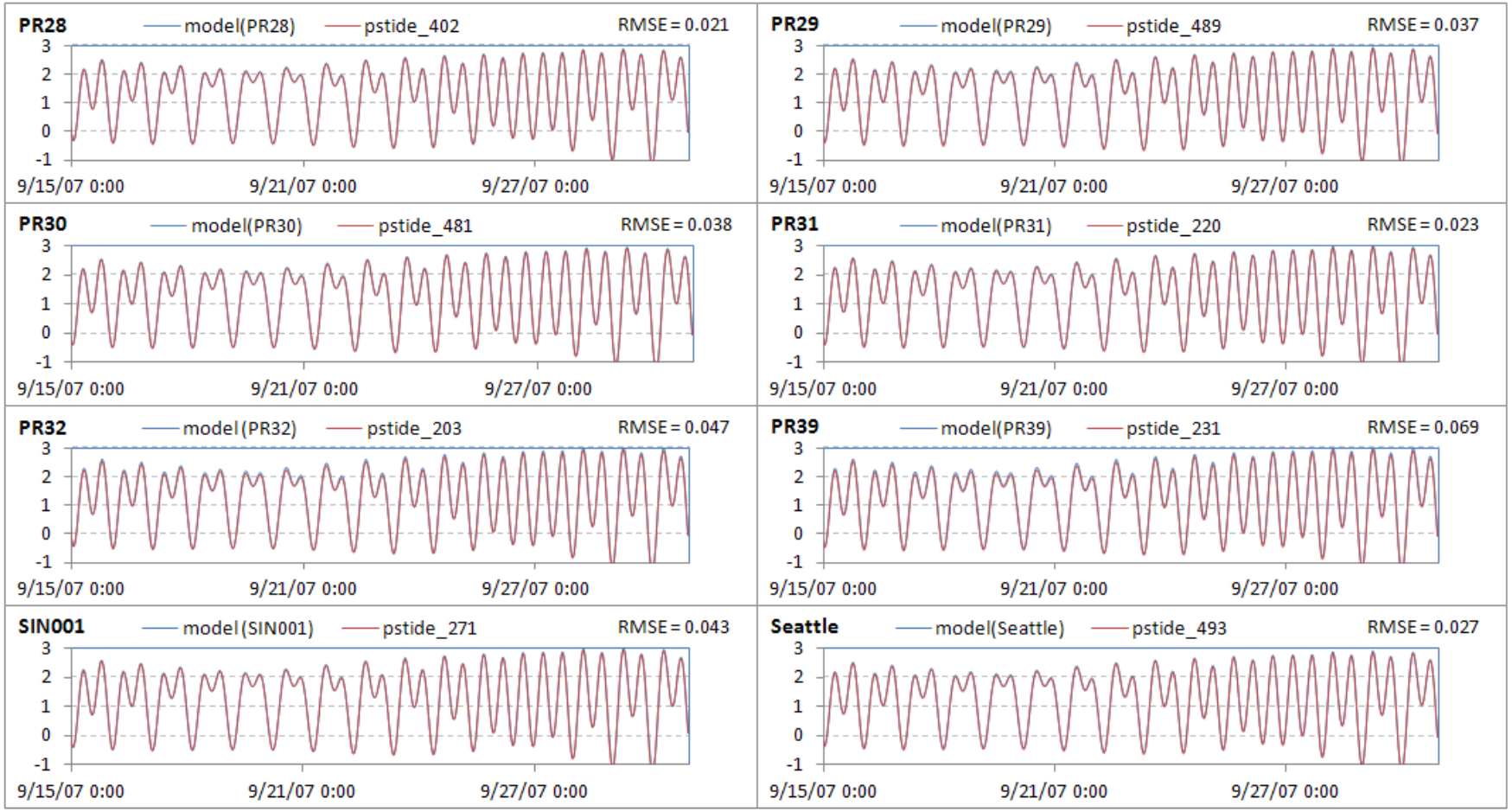


Figure 19. Predicted water surface elevations (meters) compared with PSTides for the northern model domain (south to Vashon Island) for September 2007.

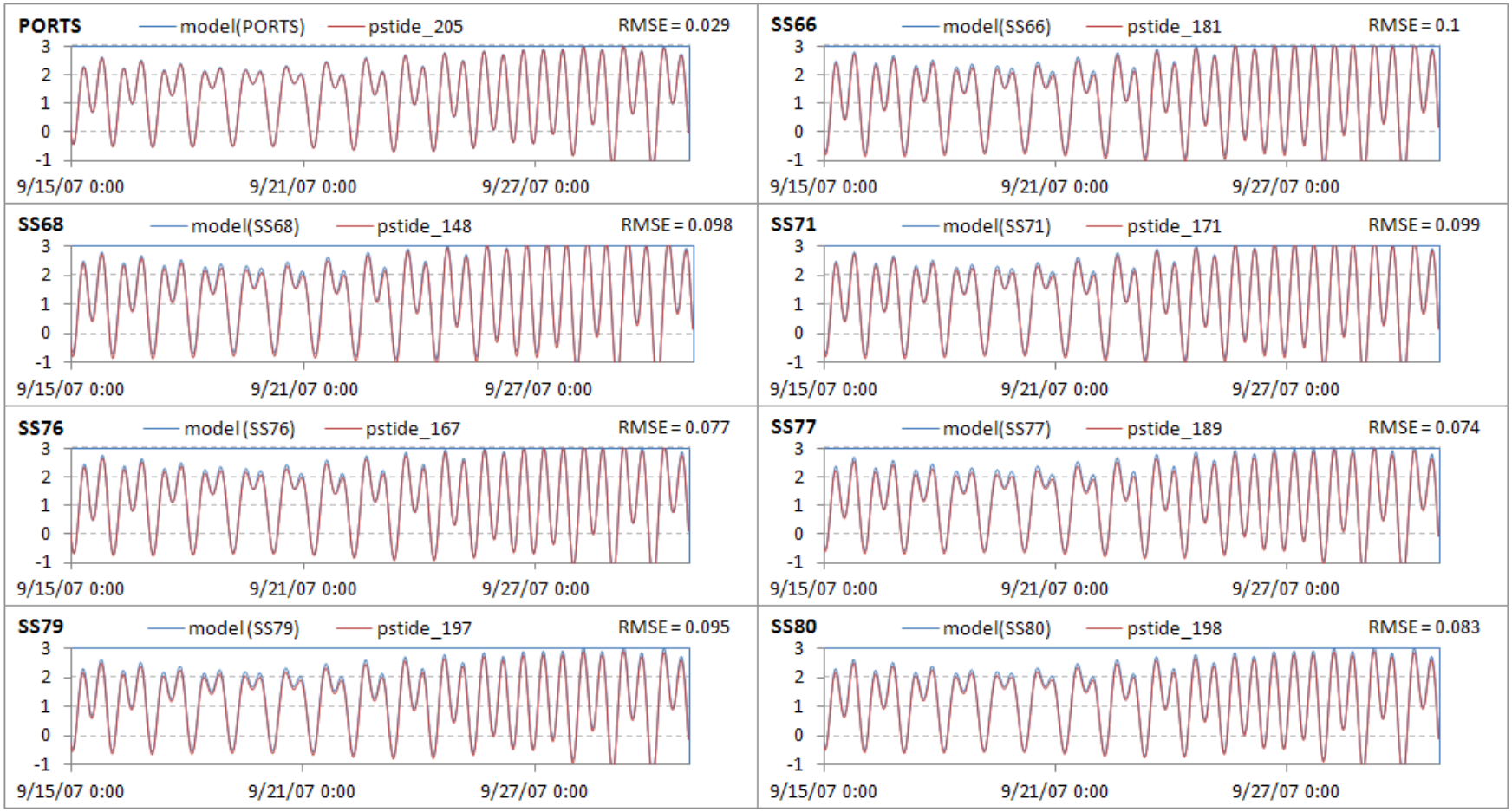


Figure 20. Predicted water surface elevations (meters) compared with PSTides for the central model domain (Commencement Bay and Tacoma Narrows) for September 2007.

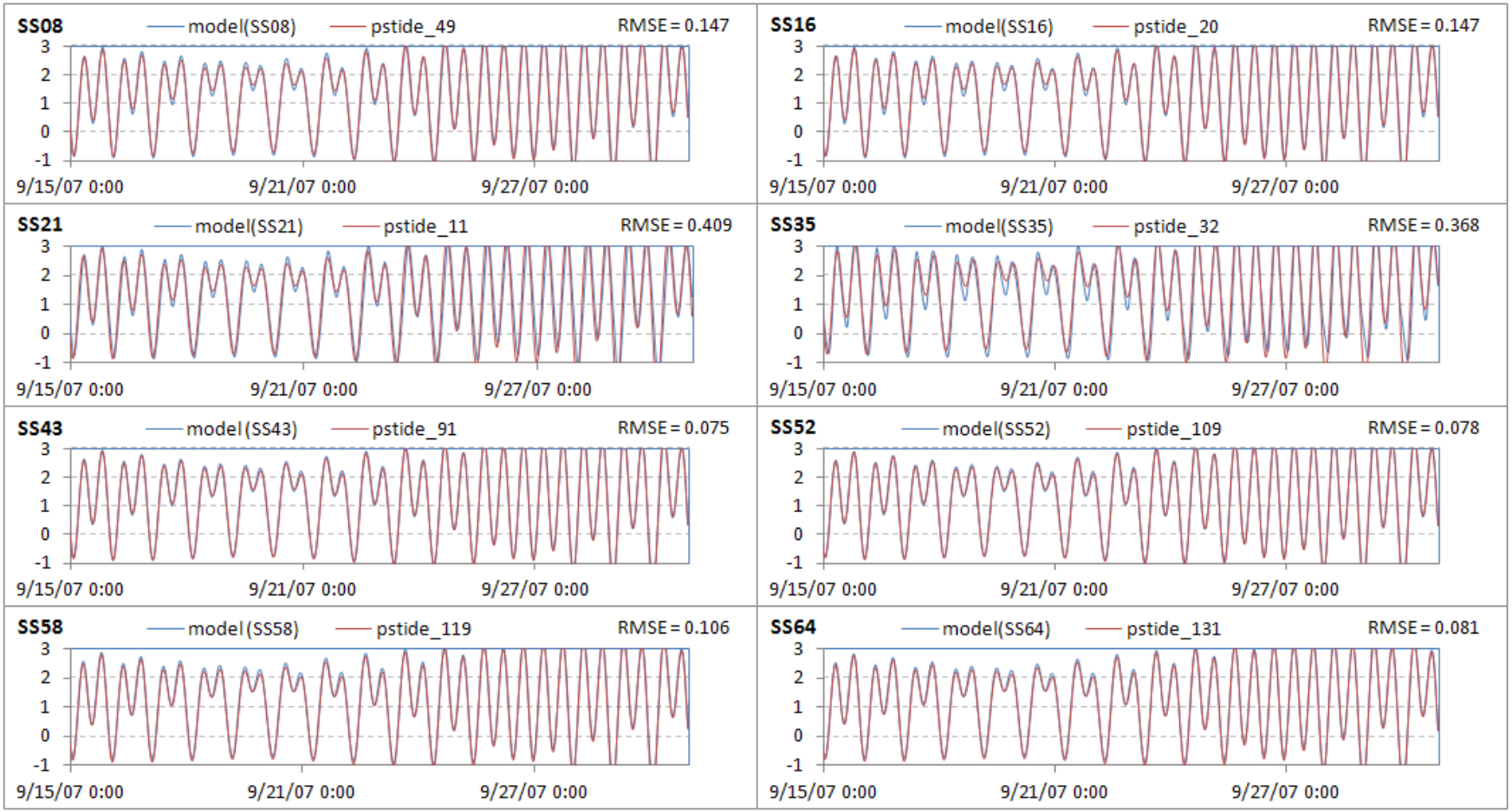


Figure 21. Predicted water surface elevations (meters) compared with PSTides for the southern model domain (west of Tacoma Narrows) for September 2007.

## Tidal Constituents Comparison

In addition to the time-series plots above, where we compared the amplitude and timing of the predicted and PSTides-generated water surface elevations, we compared predictions in the frequency domain. Water surface elevations result from the superposition of multiple tidal constituents, or harmonics (Hicks, 2006), each represented with an amplitude in meters and phase in degrees relative to Greenwich Mean Time. These constituents represent the separate effects of solar and lunar gravitational pull, the tilt of Earth, and the orbits of the moon around Earth and Earth around the sun.

We compared the five dominant harmonics, including M2, K1, S2, N2, and O1 (see Appendix E). The principal component is the M2 tide, or the half lunar day. Fourier transforms were used to calculate the harmonic phase and amplitude for the predicted model water surface elevations to compare with values from the two measured tide gages and other historical monitoring stations for which the tidal constituents are available. Table 5 summarizes the (1) amplitude (H) and phase ($\Omega$) for the model run, literature values, and PSTides for the four comparison locations, and (2) measured data for the two available sites for September 2006 during the calibration period.

The model describes the amplitudes and phases of the various tidal constituents well, compared with literature values (Lavelle et al., 1988), PSTides, and measured data. GEMSS predictions are within an amplitude of 2 cm and a phase shift of approximately 2.4 degrees (142 minutes) of each tidal constituent in the measured data (NOAA) in Elliott Bay and Commencement Bay for September 2006.

GEMSS tidal constituent predictions for amplitudes are within 5.6 cm of the published literature values for all four stations, including Oakland Bay. Phases are generally within about 9 degrees (540 minutes) of the published literature values.

GEMSS predictions also compare well with PSTides. All amplitudes are within 6 cm, including Oakland Bay. However, Oakland Bay phases are off compared with PSTides.

Budd Inlet reflects the accumulation of constituent amplitude and phase errors through South Sound and generally exhibits greater errors than the two Central Puget Sound stations compared with either PSTides or literature values. As described above, the model cannot simulate the lag associated with the sharp bend in the east-west arm, and Oakland Bay predictions have the largest error due to the geometry. The effect is limited to Hammersley Inlet and Oakland Bay.

In addition, we compared tidal constituents for 2007 for both March (Table 6) and September (Table 7). We found that the September 2007 tidal constituents were comparable to September 2006. The March 2007 comparison shows somewhat higher differences compared with the measured data. The model was run without wind for these comparisons, and the differences in this spring period could be due in part to the effect of wind. However, the GEMSS predictions compared well with the literature, PSTides, and measured data throughout 2007.

Table 5. Tidal harmonics (amplitude and phase, relative to Greenwich Mean Time) predicted by GEMSS for September 2006.

| | GEMSS | | Lavelle et al. (1988) | | GEMSS vs. literature | | | PSTides | | GEMSS vs. PSTides | | | NOAA | | GEMSS vs. NOAA | | |
|---|---|---|---|---|---|---|---|---|---|---|---|---|---|---|---|---|---|
| Tidal Constituent | amplitude H (m) | Phase, Ω (deg) | amplitude H (m) | Phase, Ω (deg) | H (%) | dH (cm) | dΩ (deg) | amplitude H (m) | Phase, Ω (deg) | H (%) | dH (cm) | dΩ (deg) | amplitude H (m) | Phase, Ω (deg) | H (%) | dH (cm) | dΩ (deg) |
| **Elliott Bay (Seattle), Pstide_493, (I,J = 81,149)** | | | | | | | | | | | | | | | | | |
| O1 | 0.47 | 255 | 0.46 | 255.4 | 103% | 1.53 | -0.27 | 0.47 | 255 | 100% | 0.10 | 0.00 | 0.48 | 254 | 99% | -0.40 | 0.95 |
| K1 | 0.84 | 281 | 0.83 | 277.3 | 101% | 0.96 | 3.23 | 0.84 | 281 | 100% | 0.11 | 0.01 | 0.84 | 280 | 100% | 0.34 | 0.96 |
| N2 | 0.25 | 344 | 0.21 | 340.3 | 116% | 3.31 | 4.08 | 0.24 | 344 | 101% | 0.17 | 0.47 | 0.26 | 342 | 93% | -1.85 | 1.93 |
| M2 | 1.06 | 12 | 1.07 | 11.5 | 99% | -0.76 | 0.43 | 1.05 | 12 | 101% | 0.83 | 0.32 | 1.06 | 11 | 100% | 0.11 | 0.97 |
| S2 | 0.26 | 29 | 0.26 | 37.9 | 102% | 0.63 | -8.66 | 0.26 | 29 | 100% | 0.11 | 0.45 | 0.28 | 28 | 95% | -1.44 | 0.75 |
| **Commencement Bay (Tacoma PORTS), pstide_205, (I,J = 82, 95)** | | | | | | | | | | | | | | | | | |
| O1 | 0.48 | 256 | 0.47 | 255 | 103% | 1.32 | 0.7 | 0.48 | 255 | 100% | -0.03 | 0.14 | 0.48 | 255 | 100% | 0.18 | 0.81 |
| K1 | 0.85 | 281 | 0.83 | 278 | 102% | 1.85 | 2.97 | 0.85 | 281 | 100% | 0.05 | 0.17 | 0.84 | 281 | 101% | 1.05 | 0.36 |
| N2 | 0.26 | 346 | 0.24 | 343 | 111% | 2.56 | 2.95 | 0.26 | 345 | 101% | 0.38 | 1.00 | 0.27 | 344 | 96% | -1.15 | 2.37 |
| M2 | 1.14 | 13 | 1.13 | 13 | 101% | 0.77 | 0.39 | 1.12 | 13 | 102% | 2.02 | 0.66 | 1.13 | 12 | 101% | 1.25 | 1.33 |
| S2 | 0.28 | 31 | 0.27 | 39 | 104% | 1.14 | -7.65 | 0.28 | 30 | 101% | 0.38 | 0.92 | 0.29 | 29 | 97% | -0.79 | 1.67 |
| **Budd Inlet/Boston Harbor (SS13), pstide_53, (I,J = 49,28)** | | | | | | | | | | | | | | | | | |
| O1 | 0.51 | 265 | 0.48 | 259 | 105% | 2.56 | 6.15 | 0.51 | 262 | 100% | 0.10 | 2.98 | | | | | |
| K1 | 0.91 | 292 | 0.95 | 288 | 97% | -3.24 | 4.41 | 0.91 | 289 | 100% | -0.16 | 3.60 | | | | | |
| N2 | 0.32 | 9 | 0.26 | 1 | 121% | 5.60 | 8.08 | 0.33 | 2 | 95% | -1.51 | 7.23 | | | | | |
| M2 | 1.44 | 35 | 1.44 | 32 | 100% | -0.20 | 2.36 | 1.46 | 30 | 99% | -2.11 | 4.86 | | | | | |
| S2 | 0.35 | 56 | 0.35 | 62 | 100% | -0.07 | -5.26 | 0.37 | 48 | 95% | -1.94 | 8.27 | | | | | |
| **Oakland Bay (SS35), pstide_35, (I,J = 54, 14)** | | | | | | | | | | | | | | | | | |
| O1 | 0.46 | 282 | | | | | | 0.51 | 276 | 91% | -4.85 | 6.36 | | | | | |
| K1 | 0.86 | 310 | | | | | | 0.92 | 303 | 94% | -5.93 | 6.57 | | | | | |
| N2 | 0.29 | 38 | | | | | | 0.34 | 32 | 86% | -4.74 | 5.86 | | | | | |
| M2 | 1.44 | 66 | 1.49 | 58 | 97% | -4.69 | 7.74 | 1.50 | 58 | 96% | -5.77 | 7.77 | | | | | |
| S2 | 0.36 | 88 | | | | | | 0.39 | 78 | 93% | -2.79 | 10.55 | | | | | |

H% = predicted amplitude as percent of observed (literature, PSTides, or NOAA) values.
dH = amplitude difference in centimeters (cm).
dΩ = phase difference in degrees.

Table 6. Tidal harmonics (amplitude and phase, relative to Greenwich Mean Time) predicted by GEMSS for March 2007.

| | GEMSS | | Lavelle et al. (1988) | | GEMSS vs. literature | | | PSTides | | GEMSS vs. PSTides | | | NOAA | | GEMSS vs. NOAA | | |
|---|---|---|---|---|---|---|---|---|---|---|---|---|---|---|---|---|---|
| Tidal Constituent | amplitude H (m) | Phase, Ω (deg) | amplitude H (m) | Phase, Ω (deg) | H (%) | dH (cm) | dΩ (deg) | amplitude H (m) | Phase, Ω (deg) | H (%) | dH (cm) | dΩ (deg) | amplitude H (m) | Phase, Ω (deg) | H (%) | dH (cm) | dΩ (deg) |
| **Elliott Bay (Seattle), Pstide_493, (I,J = 81,149)** | | | | | | | | | | | | | | | | | |
| O1 | 0.46 | 253 | 0.46 | 255 | 100% | -0.01 | -2.23 | 0.46 | 254 | 100% | 0.05 | -0.60 | 0.46 | 254 | 99% | -0.27 | -0.95 |
| K1 | 0.89 | 281 | 0.83 | 277 | 107% | 5.65 | 3.46 | 0.89 | 281 | 100% | 0.15 | -0.02 | 0.87 | 279 | 102% | 1.84 | 1.53 |
| N2 | 0.23 | 351 | 0.21 | 340 | 109% | 1.95 | 10.58 | 0.23 | 350 | 101% | 0.12 | 0.65 | 0.25 | 350 | 93% | -1.68 | 1.37 |
| M2 | 1.07 | 12 | 1.07 | 12 | 100% | -0.29 | 0.52 | 1.06 | 12 | 101% | 0.63 | 0.39 | 1.07 | 11 | 100% | -0.50 | 1.37 |
| S2 | 0.27 | 35 | 0.26 | 38 | 104% | 1.10 | -3.12 | 0.27 | 34 | 100% | 0.10 | 0.55 | 0.28 | 34 | 95% | -1.48 | 0.93 |
| **Commencement Bay (Tacoma PORTS), pstide_205, (I,J = 82, 95)** | | | | | | | | | | | | | | | | | |
| O1 | 0.46 | 254 | 0.47 | 255 | 99% | -0.45 | -0.40 | 0.46 | 254 | 99% | -0.29 | 0.40 | 0.46 | 255 | 100% | 0.21 | -0.14 |
| K1 | 0.90 | 282 | 0.83 | 278 | 108% | 6.27 | 3.73 | 0.90 | 281 | 100% | -0.18 | 0.69 | 0.88 | 280 | 101% | 1.21 | 1.69 |
| N2 | 0.24 | 353 | 0.24 | 343 | 103% | 0.61 | 9.79 | 0.24 | 351 | 99% | -0.16 | 1.51 | 0.26 | 350 | 95% | -1.37 | 2.88 |
| M2 | 1.14 | 13 | 1.13 | 13 | 100% | 0.23 | 0.34 | 1.13 | 13 | 101% | 0.76 | 0.60 | 1.14 | 12 | 100% | -0.42 | 1.39 |
| S2 | 0.29 | 37 | 0.27 | 39 | 105% | 1.46 | -1.95 | 0.29 | 35 | 101% | 0.18 | 1.20 | 0.30 | 35 | 97% | -1.00 | 1.65 |
| **Budd Inlet/Boston Harbor (SS13), pstide_53, (I,J = 49,28)** | | | | | | | | | | | | | | | | | |
| O1 | 0.49 | 263 | 0.48 | 259 | 102% | 1.07 | 3.84 | 0.49 | 261 | 100% | 0.18 | 2.05 | | | | | |
| K1 | 0.97 | 292 | 0.95 | 288 | 102% | 2.11 | 4.34 | 0.96 | 288 | 101% | 0.52 | 3.64 | | | | | |
| N2 | 0.30 | 18 | 0.26 | 1 | 116% | 4.17 | 16.89 | 0.31 | 8 | 97% | -1.10 | 9.84 | | | | | |
| M2 | 1.44 | 35 | 1.44 | 32 | 100% | -0.40 | 2.81 | 1.47 | 30 | 98% | -3.23 | 5.24 | | | | | |
| S2 | 0.36 | 62 | 0.35 | 62 | 102% | 0.73 | 0.76 | 0.38 | 53 | 95% | -1.91 | 8.97 | | | | | |
| **Oakland Bay (SS35), pstide_35, (I,J = 54, 14)** | | | | | | | | | | | | | | | | | |
| O1 | 0.45 | 277 | | | | | | 0.50 | 274 | 91% | -4.33 | 3.06 | | | | | |
| K1 | 0.92 | 310 | | | | | | 0.97 | 302 | 95% | -4.38 | 7.33 | | | | | |
| N2 | 0.29 | 50 | | | | | | 0.31 | 37 | 92% | -2.41 | 13.51 | | | | | |
| M2 | 1.46 | 65 | 1.49 | 58 | 98% | -2.67 | 7.13 | 1.52 | 58 | 96% | -5.34 | 7.06 | | | | | |
| S2 | 0.36 | 93 | | | | | | 0.39 | 82 | 92% | -3.22 | 10.28 | | | | | |

H% = predicted amplitude as percent of observed (literature, PSTides, or NOAA) values.
dH = amplitude difference in centimeters (cm).
dΩ = phase difference in degrees.

Table 7. Tidal harmonics (amplitude and phase, relative to Greenwich Mean Time) predicted by GEMSS for September 2007.

| | GEMSS | | Lavelle et al. (1988) | | GEMSS vs. literature | | | PSTides | | GEMSS vs. PSTides | | | NOAA | | GEMSS vs. NOAA | | |
|---|---|---|---|---|---|---|---|---|---|---|---|---|---|---|---|---|---|
| Tidal Constituent | amplitude H (m) | Phase, Ω (deg) | amplitude H (m) | Phase, Ω (deg) | H (%) | dH (cm) | dΩ (deg) | amplitude H (m) | Phase, Ω (deg) | H (%) | dH (cm) | dΩ (deg) | amplitude H (m) | Phase, Ω (deg) | H (%) | dH (cm) | dΩ (deg) |
| **Elliott Bay (Seattle), Pstide_493, (I,J = 81,149)** | | | | | | | | | | | | | | | | | |
| O1 | 0.45 | 256 | 0.46 | 255 | 99% | -0.37 | 0.87 | 0.46 | 256 | 99% | -0.30 | 0.24 | 0.46 | 255 | 98% | -0.90 | 1.15 |
| K1 | 0.84 | 280 | 0.83 | 277 | 101% | 0.84 | 3.16 | 0.84 | 280 | 100% | 0.25 | -0.01 | 0.84 | 280 | 100% | 0.10 | 0.92 |
| N2 | 0.20 | 351 | 0.21 | 340 | 96% | -0.82 | 10.61 | 0.20 | 350 | 101% | 0.29 | 1.31 | 0.21 | 351 | 96% | -0.89 | 0.08 |
| M2 | 1.07 | 11 | 1.07 | 12 | 100% | 0.19 | -0.86 | 1.06 | 10 | 101% | 0.92 | 0.38 | 1.07 | 10 | 100% | 0.11 | 0.98 |
| S2 | 0.26 | 30 | 0.26 | 38 | 100% | 0.11 | -7.66 | 0.26 | 30 | 100% | 0.01 | 0.51 | 0.28 | 29 | 94% | -1.68 | 0.96 |
| **Commencement Bay (Tacoma PORTS), pstide_205, (I,J = 82, 95)** | | | | | | | | | | | | | | | | | |
| O1 | 0.46 | 257 | 0.47 | 255 | 99% | -0.66 | 1.79 | 0.46 | 256 | 99% | -0.49 | 0.33 | 0.46 | 256 | 100% | -0.19 | 0.96 |
| K1 | 0.85 | 281 | 0.83 | 278 | 102% | 1.77 | 2.88 | 0.85 | 281 | 100% | 0.23 | 0.14 | 0.84 | 281 | 101% | 0.92 | 0.29 |
| N2 | 0.22 | 353 | 0.24 | 343 | 92% | -1.81 | 9.73 | 0.21 | 351 | 102% | 0.53 | 2.06 | 0.22 | 351 | 100% | 0.09 | 1.95 |
| M2 | 1.15 | 12 | 1.13 | 13 | 102% | 1.80 | -0.89 | 1.13 | 11 | 102% | 2.13 | 0.73 | 1.14 | 11 | 101% | 1.39 | 1.24 |
| S2 | 0.28 | 32 | 0.27 | 39 | 102% | 0.59 | -6.54 | 0.28 | 31 | 101% | 0.28 | 1.10 | 0.29 | 30 | 97% | -1.01 | 1.81 |
| **Budd Inlet/Boston Harbor (SS13), pstide_53, (I,J = 49,28)** | | | | | | | | | | | | | | | | | |
| O1 | 0.49 | 266 | 0.48 | 259 | 101% | 0.55 | 6.60 | 0.49 | 263 | 99% | -0.27 | 2.54 | | | | | |
| K1 | 0.92 | 292 | 0.95 | 288 | 97% | -2.80 | 3.82 | 0.91 | 288 | 101% | 0.60 | 3.06 | | | | | |
| N2 | 0.27 | 18 | 0.26 | 1 | 102% | 0.42 | 17.51 | 0.27 | 7 | 97% | -0.86 | 11.05 | | | | | |
| M2 | 1.45 | 33 | 1.44 | 32 | 101% | 0.85 | 0.89 | 1.47 | 28 | 98% | -2.29 | 4.69 | | | | | |
| S2 | 0.35 | 58 | 0.35 | 62 | 99% | -0.24 | -3.77 | 0.37 | 49 | 96% | -1.51 | 8.87 | | | | | |
| **Oakland Bay (SS35), pstide_35, (I,J = 54, 14)** | | | | | | | | | | | | | | | | | |
| O1 | 0.45 | 281 | | | | | | 0.50 | 276 | 91% | -4.25 | 4.84 | | | | | |
| K1 | 0.88 | 310 | | | | | | 0.92 | 303 | 96% | -3.73 | 6.44 | | | | | |
| N2 | 0.26 | 56 | | | | | | 0.28 | 34 | 93% | -1.98 | 22.21 | | | | | |
| M2 | 1.47 | 64 | 1.49 | 58 | 99% | -1.96 | 5.58 | 1.52 | 57 | 97% | -4.67 | 6.68 | | | | | |
| S2 | 0.36 | 90 | | | | | | 0.38 | 78 | 96% | -1.38 | 11.19 | | | | | |

H% = predicted amplitude as percent of observed (literature, PSTides, or NOAA) values.
dH = amplitude difference in centimeters (cm).
dΩ = phase difference in degrees.

## Temperature and Salinity Time-Depth Plots

The hydrodynamic model output was compared with cruise data to confirm the spatial and temporal patterns in temperature and salinity at 24 stations spread throughout the model domain (Figure 22). Cruise data were collected over multiple days and at different times of day. However, differences in cloud cover, tidal phase, and diel variations contribute to variability during the multi-day data collection period.

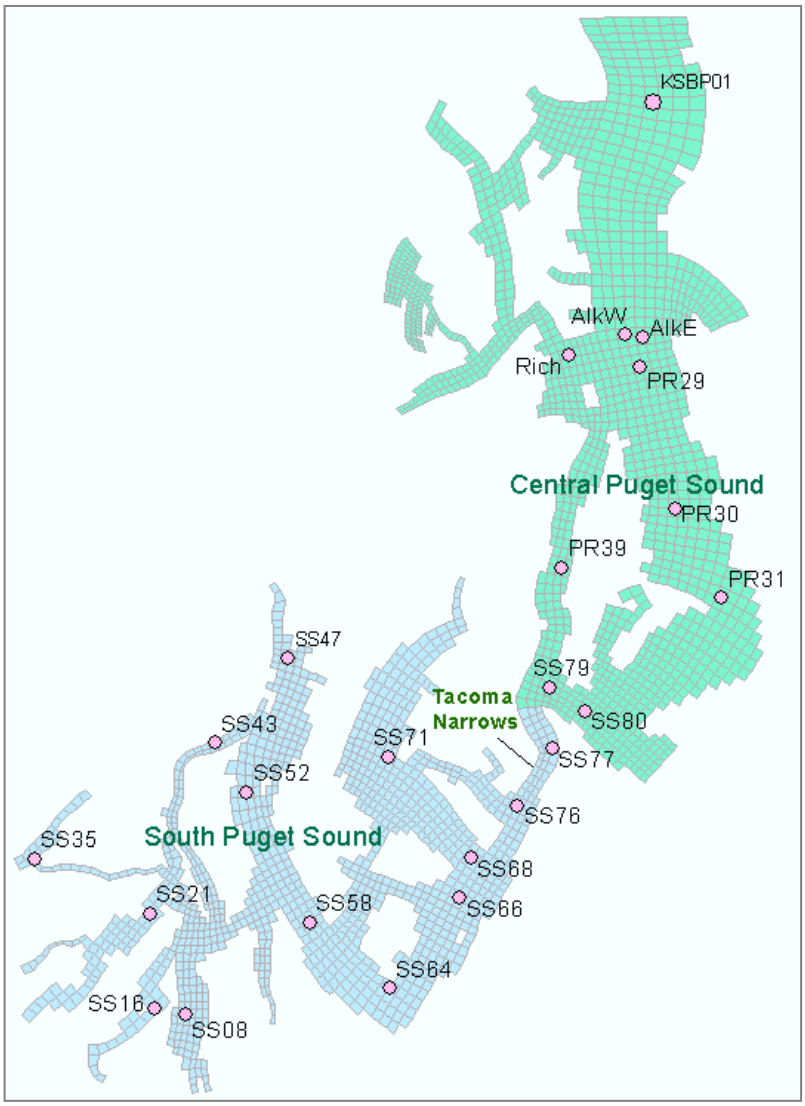


Figure 22. Stations used to compare salinity and temperature between the model and measured data.

The model reproduces the seasonal variation in measured temperature at all stations (Figures 23, 24, and 25). Vertical stratification is well represented in deeper regions where surface layers exhibit warmer temperatures during summer and cooler in the winter. In shallow areas stratification is not well represented likely due to fewer layers that promote mixing. However, measured data do not suggest strong stratification in shallow areas. The RMSE is between 0.4°C to 0.8°C in Central Puget Sound north of Tacoma Narrows. The RMSE is between 0.5°C and 0.7°C at stations in Tacoma Narrows, Carr Inlet, and stations along McNeil and Anderson Islands. Moving south to the finger inlets, the RMSE becomes larger between 0.7 (at station SS58 near Key Peninsula) to 2 (at station SS35 in Oakland Bay). The RMSE of 1.3 for Budd Inlet station (SS08) is comparable to previous studies (Roberts et al., 2012).

Seasonal variation in salinity is tied to freshwater coming into Puget Sound during the fall/winter rainy season. The magnitude of reduced salinity increases as we move from deeper stratified waters in the north to shallow and relatively vertically mixed waters in the finger inlets (Figures 26, 27, and 28). This is as expected since the volume of water in the finger inlets relative to the freshwater inputs is much less in shallow waters than in deeper waters. Overall, the model captures the seasonality relatively well. The RMSE statistic for predicted and observed salinity varies from 0.2 ppt to 1.9 ppt with low RMSE in deeper waters and higher RMSE in the finger inlets. Again, it is likely that fewer vertical layers in the shallows inlets caused more vertical mixing, causing lowered salinity in the bottom layers and higher salinity in the top layers.

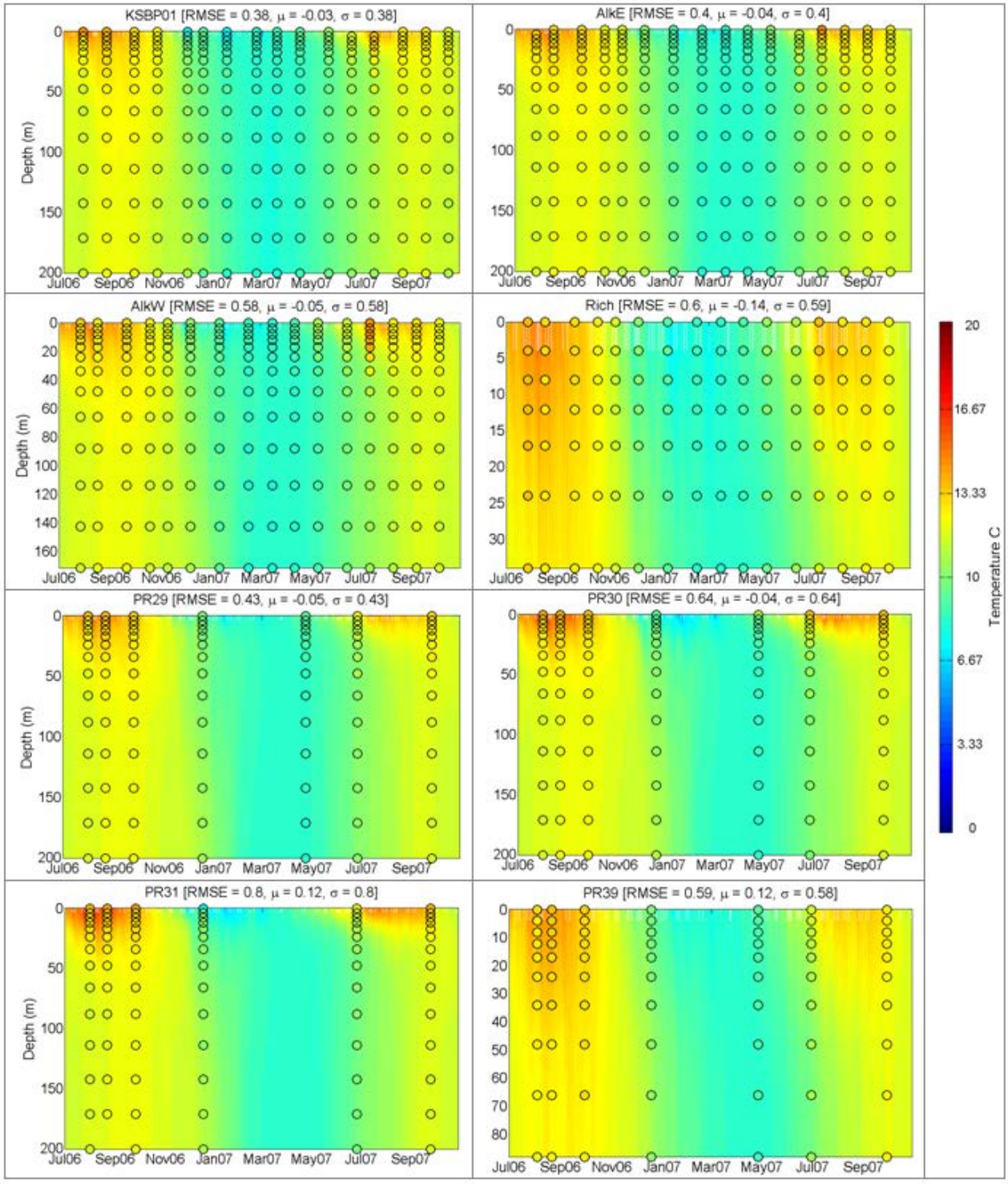


Figure 23. Temperature time-depth plots at stations north of Tacoma Narrows.

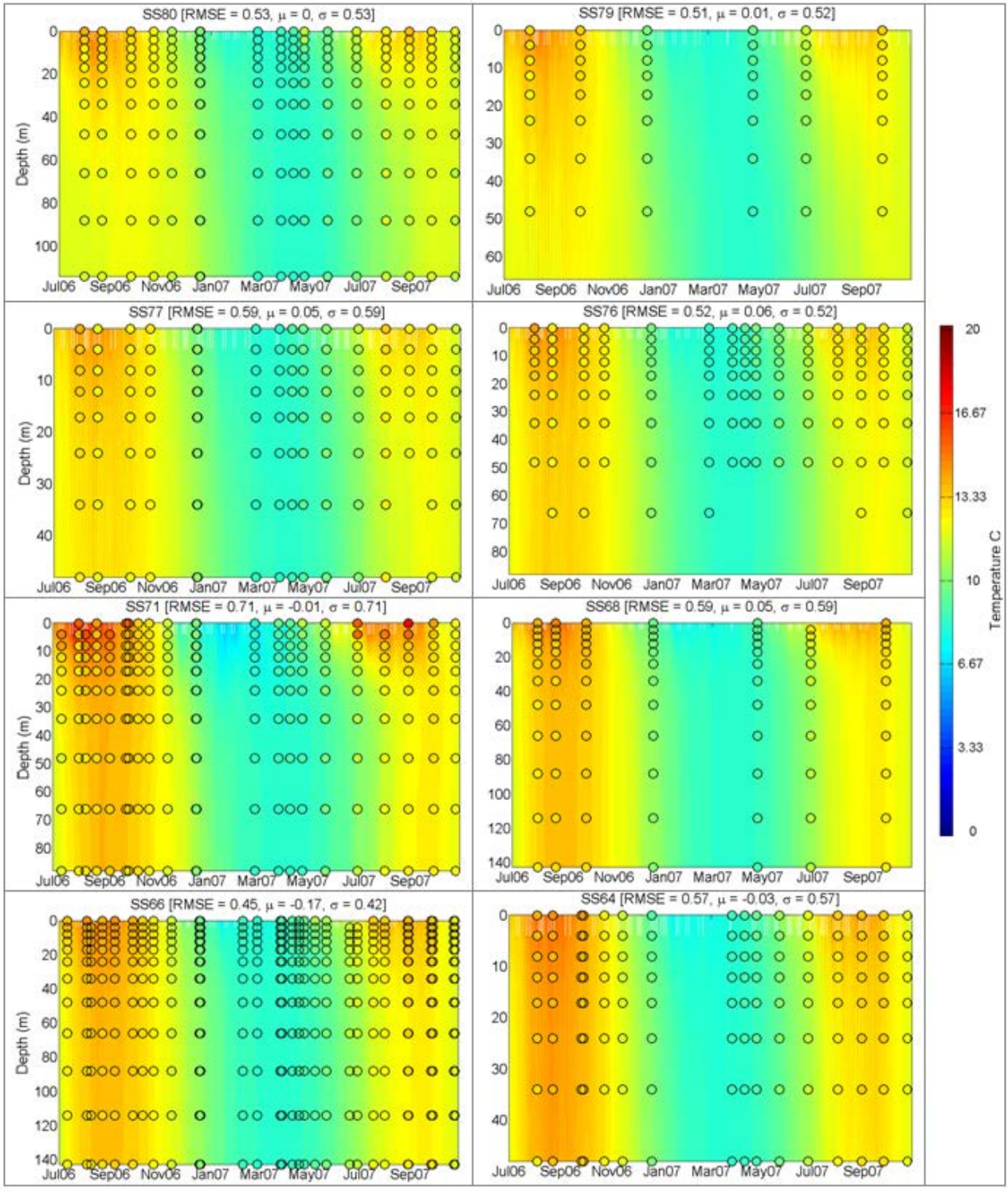


Figure 24. Temperature time-depth plots at stations between Tacoma Narrows and Nisqually Reach.

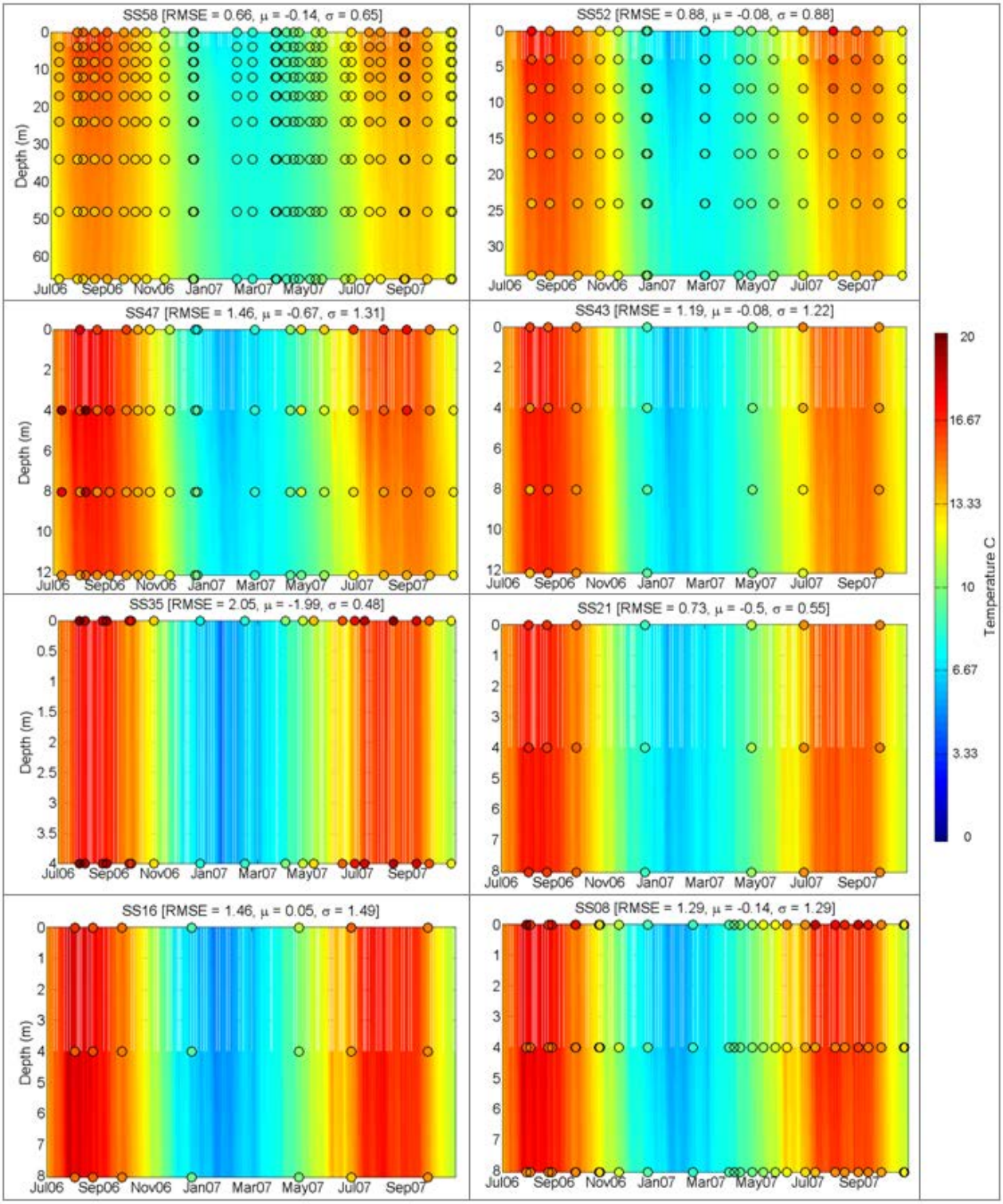


Figure 25. Temperature time-depth plots at stations south and west of Nisqually Reach.

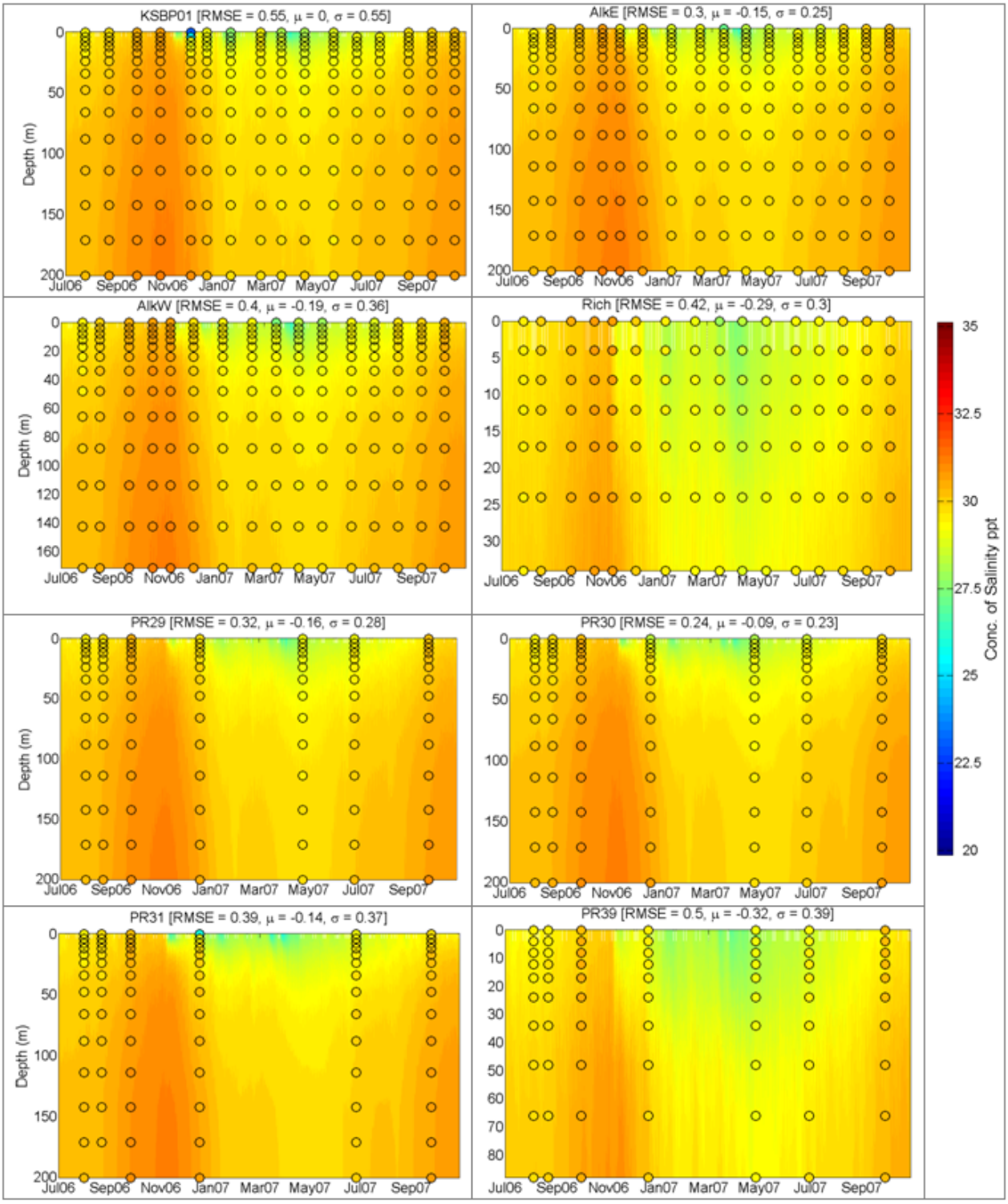


Figure 26. Salinity time-depth plots at stations north of Tacoma Narrows.

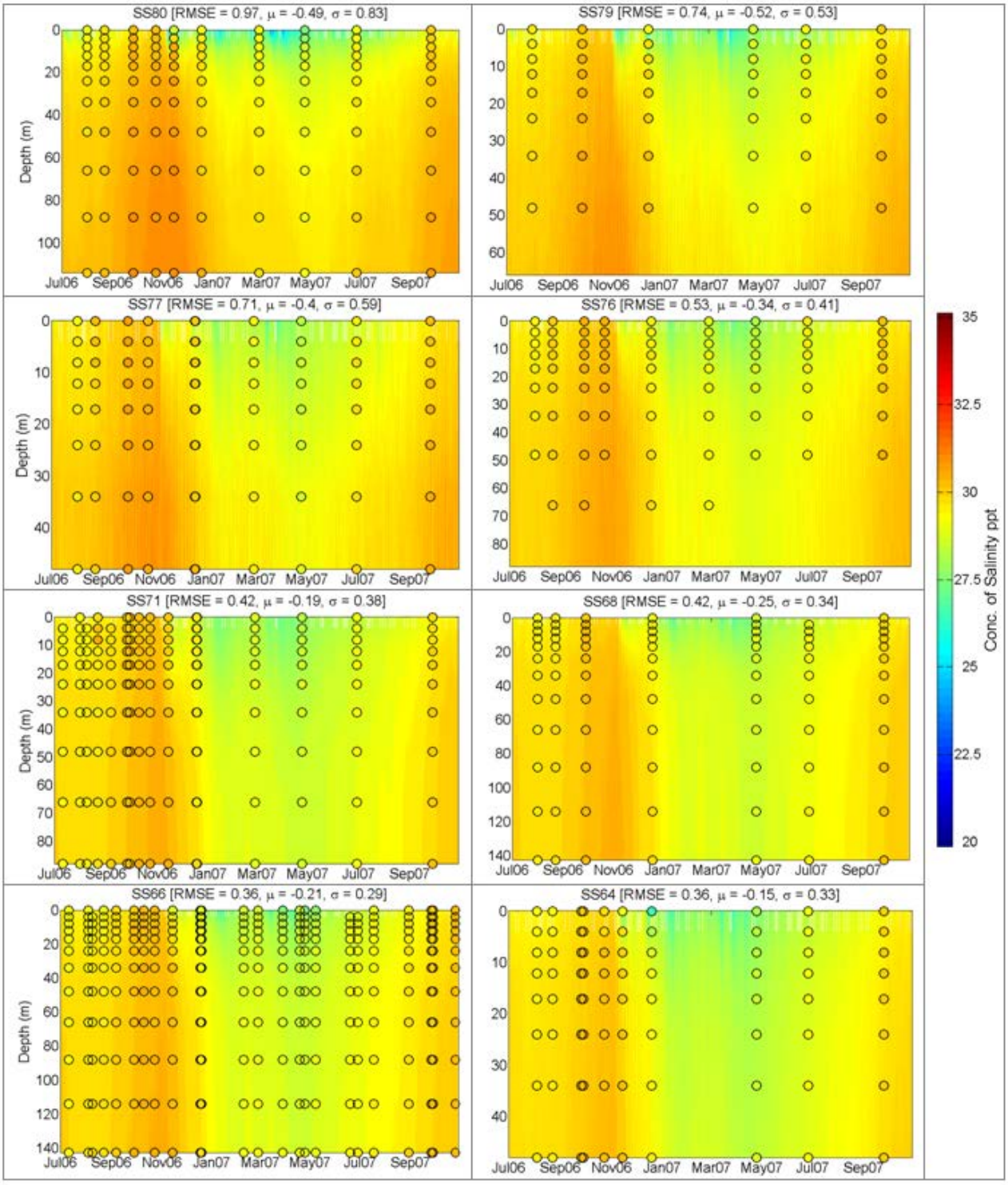


Figure 27. Salinity time-depth plots at stations between Tacoma Narrows and Nisqually Reach.

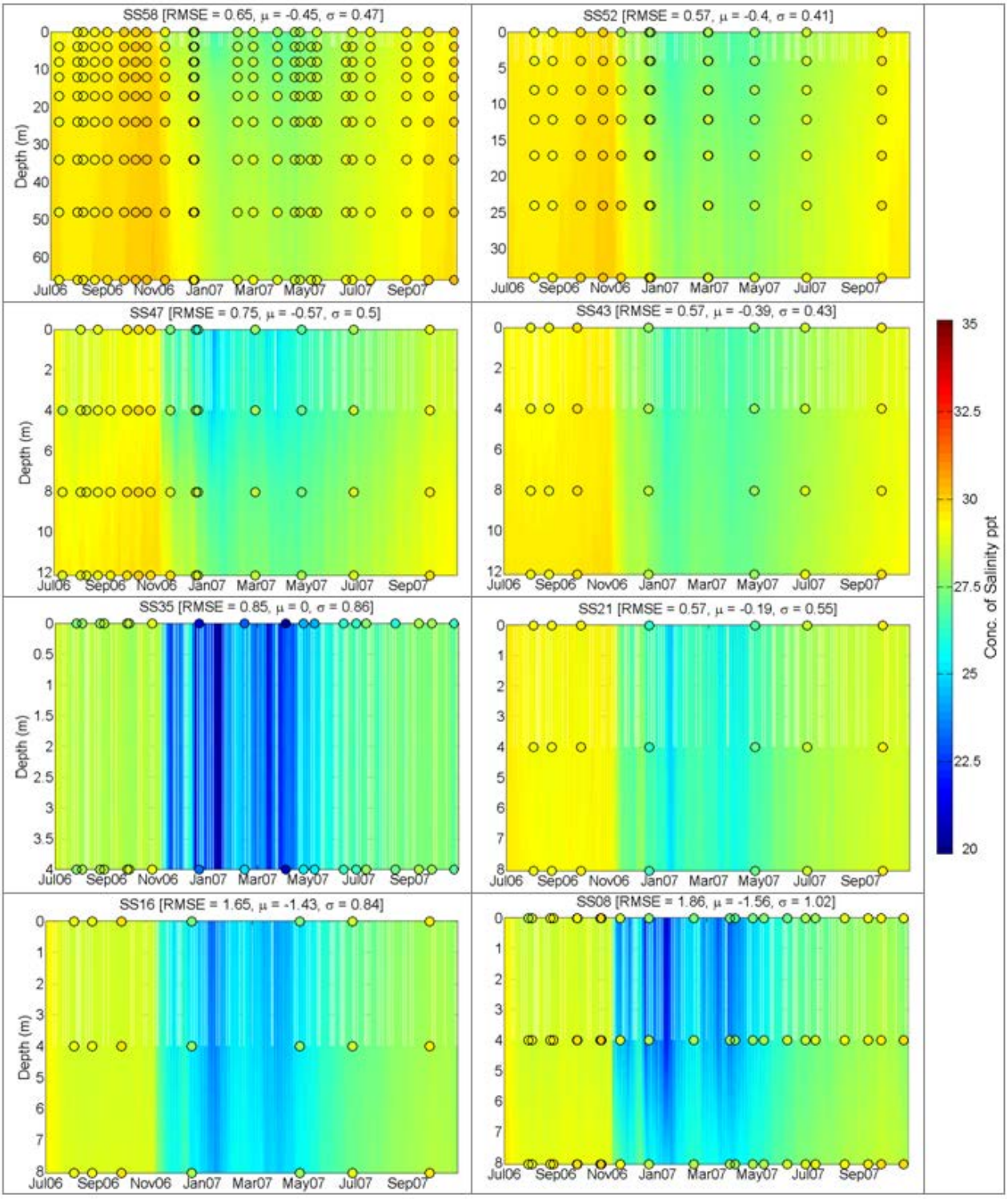


Figure 28. Salinity time-depth plots at stations south and west of Nisqually Reach.

## Temperature and Salinity Time-Series Plots

To confirm that the model captures temporal patterns in both water temperature and salinity, we compared model predictions to measured values throughout the calibration period for surface and bottom layers at 24 stations (Figure 22) in South and Central Puget Sound. The surface values exhibit much greater variability than the near-bottom values, but both are important to describing the density structure.

Temperatures predicted at the calibration stations exhibit the seasonal patterns of warming through summer and cooling into the winter months (Figures 29 and 30). The near-bottom conditions do not vary as much as the surface waters. Surface temperature RMSEs range from 0.5°C to 1.4°C at stations north of Tacoma Narrows and from 0.6°C to 2.3°C at stations south of Tacoma Narrows. Bottom temperature RMSE ranged from 0.2°C to 0.6°C at stations north of Tacoma Narrows and from 0.4°C to 2°C at stations south of Tacoma Narrows. The higher RMSE were at the shallow inlets where fewer grid layers allowed for relatively more vertical mixing so that surface layers were predicted to be cooler while bottom layers warmer. The highest RMSE was at the Oakland Bay station (SS35). This is also the station with the highest RMSE for water surface elevations primarily due to inability of the model to represent the horizontal bend in Hammersley Inlet without causing model instability.

The highest temperatures measured at SS71 in central Case Inlet were under-predicted by the model; measured temperatures at nearby stations were not as high. Surface temperatures predicted at stations within the Tacoma Narrows (SS76, SS77, and SS79) exhibit much greater sub-daily variability than at other stations within the model domain and likely reflect lateral and vertical mixing phenomenon within the Narrows.

Salinity values at stations north of Tacoma Narrows generally rise in the summer months before exhibiting episodic freshening of the surface waters with fall and winter storm events (Figure 31). The RMSE varied from 0.8 to 1.5 at these stations (north of SS80, see Figure 22Figure 22). Near-bottom salinity gradually rises through September and gradually declines with fall storms. The model produces salinity RMSEs of <0.2 ppt for bottom layers at these stations. Time-series plot for salinity at stations (SS76 through SS80) near Tacoma Narrows show more response to episodic events in surface layers due to narrow and shallow passage at this location. Puyallup River water decreases surface salinity at stations SS80 and SS79, but other stations also show decreased surface salinity. Due to these effects, the RMSE 0.8 to 2.4) at these stations is higher for surface layers compared to other stations north of Tacoma Narrows. Near-bottom salinity values are more constant than surface values but do reflect seasonal freshening. The RMSE for bottom layers are in the order of 0.2 ppt.

South of Tacoma Narrows (Figure 32), near-bottom salinities had RMSEs <0.6 ppt except Budd (RMSE = 1.5) and Eld (RMSE = 1.6) Inlets. Surface salinities at these stations followed the same trend. Budd and Eld Inlets showed higher RMSE as the model-predicted lower salinity than measured. From previous modeling efforts (Roberts et al., 2012), the plume from the Deschutes River and Capitol Lake travels northward on the east side of the inlet due in part to the Budd Inlet gyre, but surface salinity suggests it spreads out across the inlet in this model. The grid scale may not resolve this feature, and the model predicts that Deschutes River/Capitol Lake influences surface salinity at station SS08. Both Budd and Eld Inlets have a few grid layers. This increases

vertical mixing within the model giving rise to reduced salinity. Station SS35 in Oakland Bay shows higher RMSE (2.2 ppt) in surface layer due to fewer layers and induced vertical mixing, although bottom layer RMSE is low (0.55 ppt). Results at Oakland Bay station is likely also impacted by the deficiency in the model to accurately define the channel bends in Hammersley Inlet, as discussed previously.

In summary, surface and near-bottom temperature and salinity time series are well represented by the model throughout Central Puget Sound and in the major inlets and open waters of South Puget Sound. The western inlets had greater differences between modeled and measured values, but the model appropriately captures the seasonal variation in temperature and salinity in values recorded during data collection.

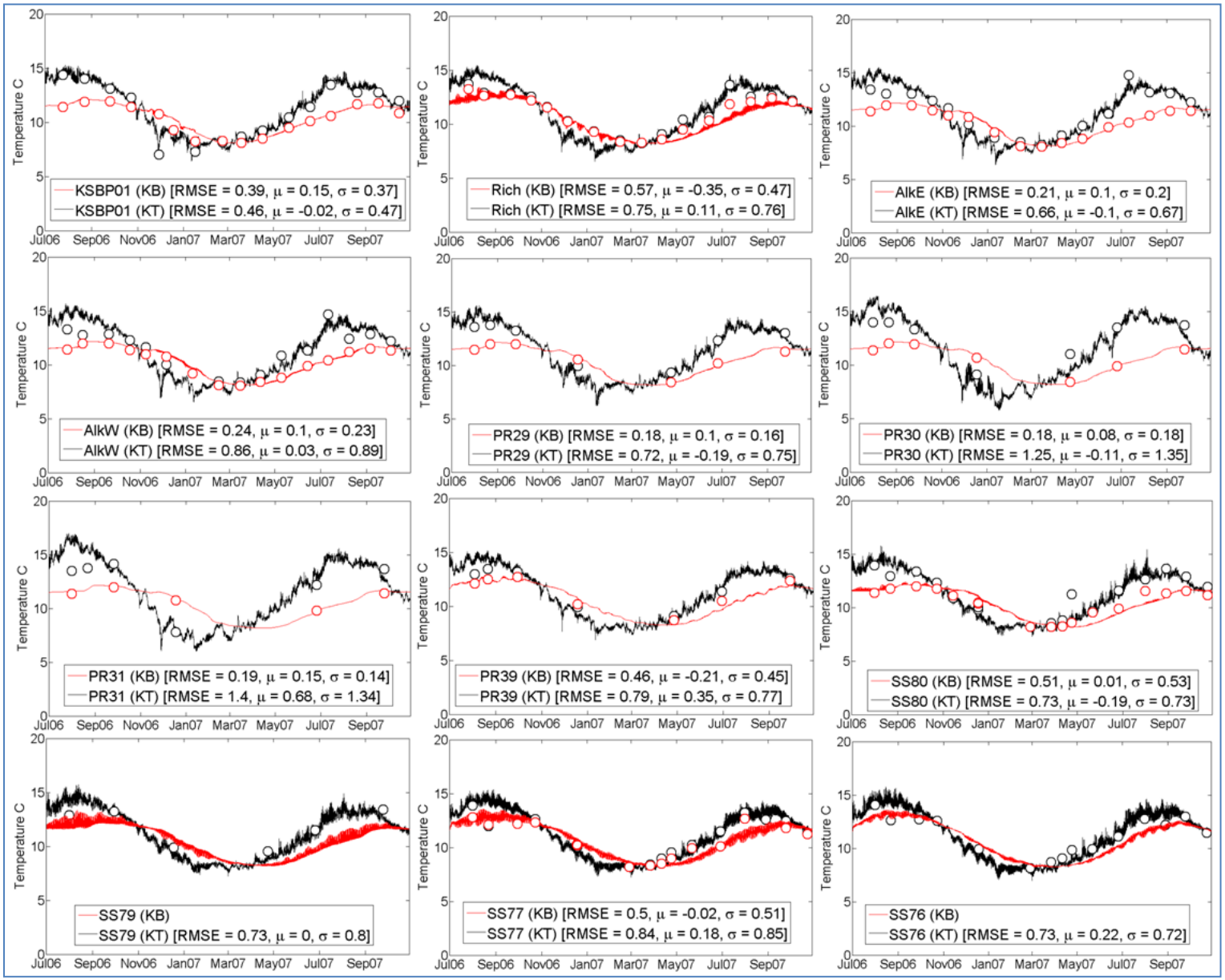


Figure 29. Observed and predicted temperature at surface (KT) and bottom (KB) layers at stations in and north of Tacoma Narrows.

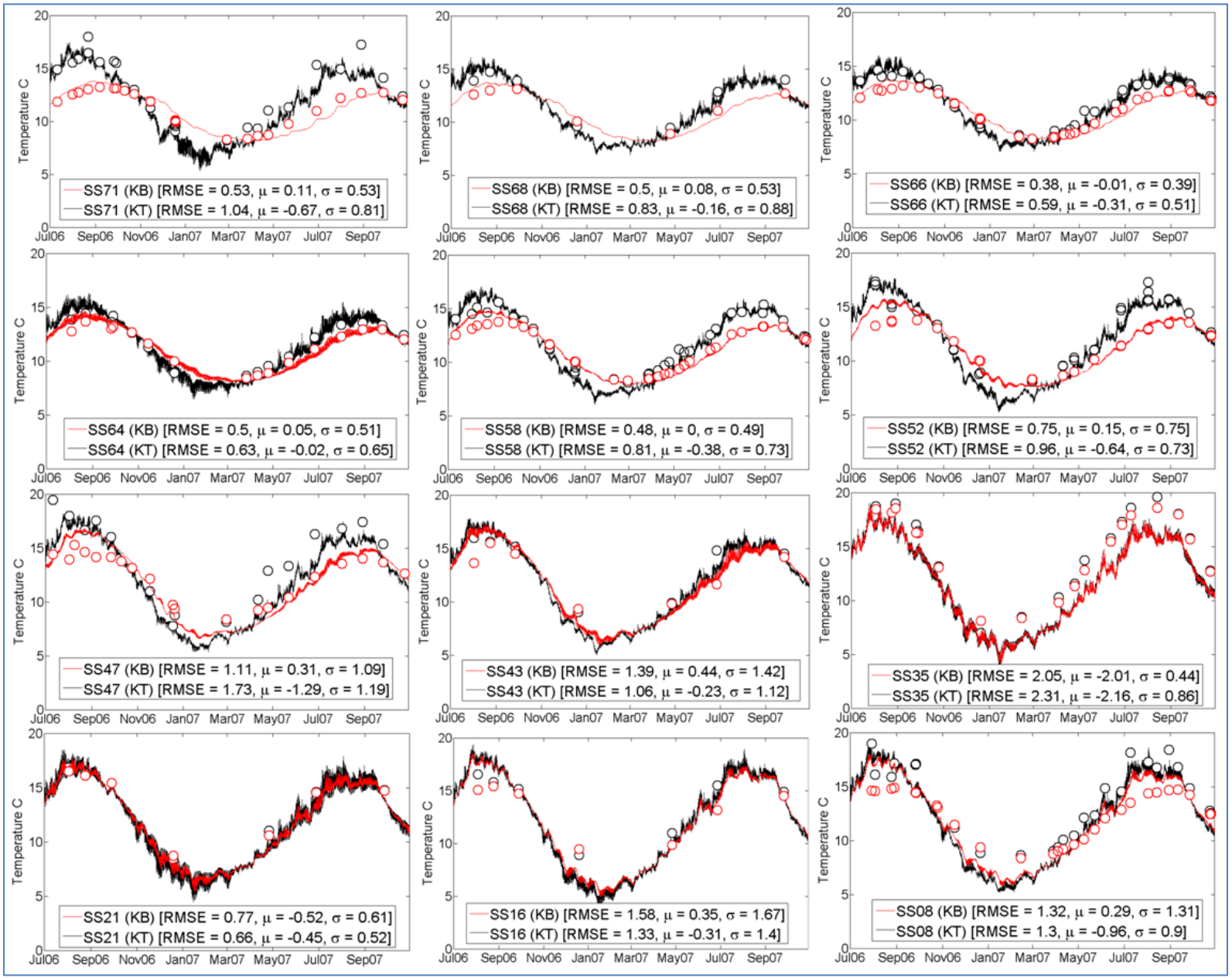


Figure 30. Observed and predicted temperatures at surface (KT) and bottom (KB) layers at stations south of Tacoma Narrows.

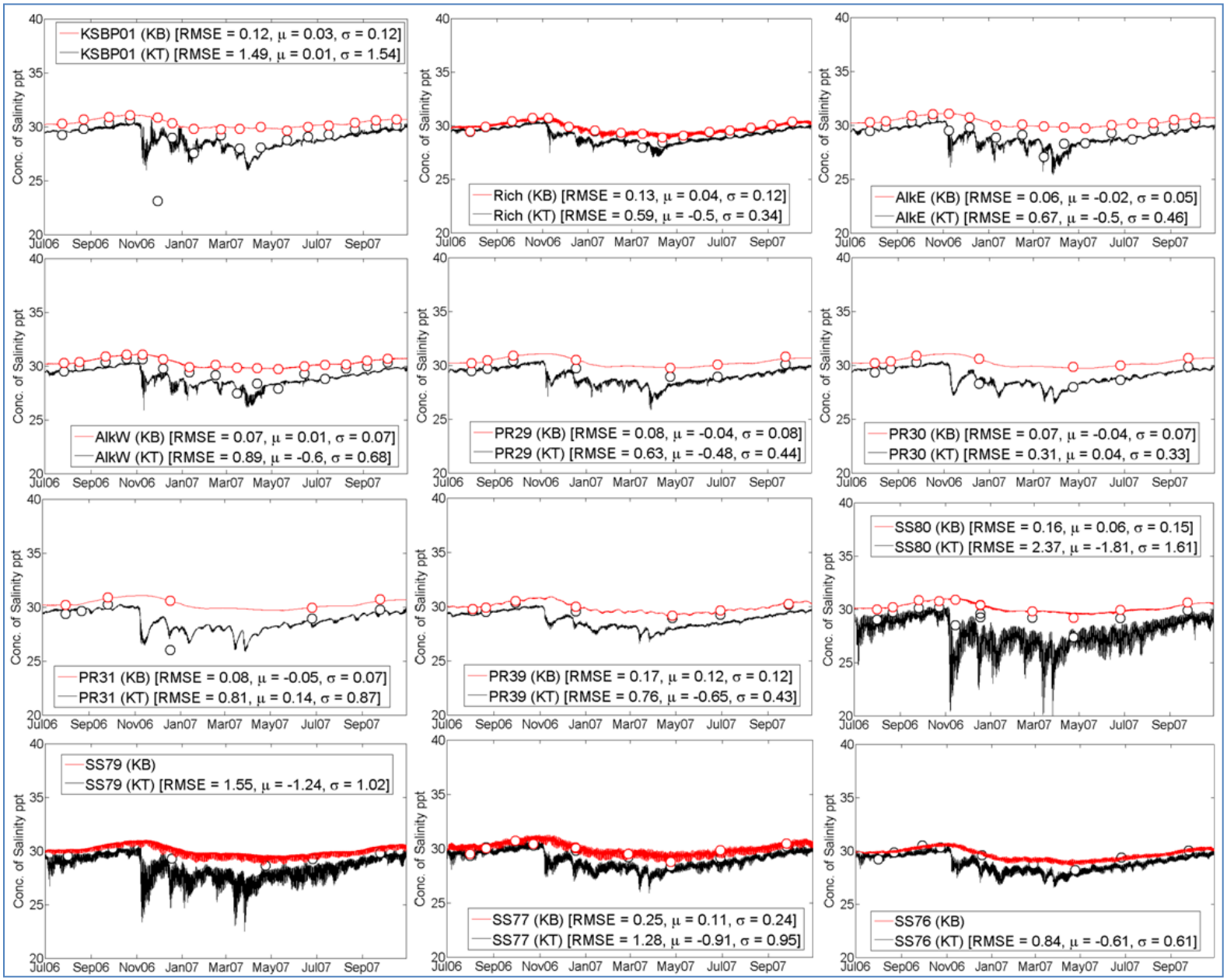


Figure 31. Observed and predicted salinity at top (KT) and bottom (KB) layers at stations in and north of Tacoma Narrows.

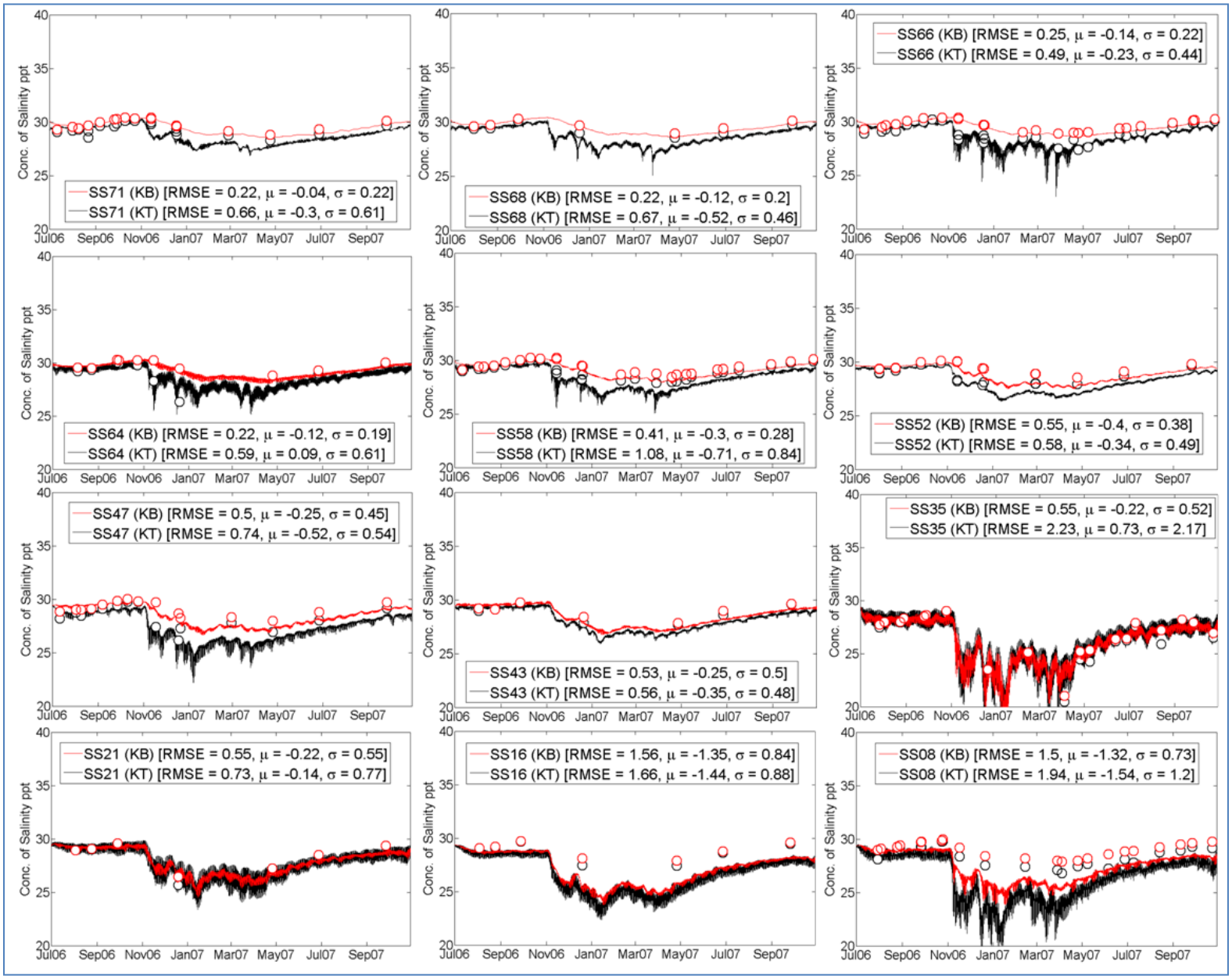


Figure 32. Observed and predicted salinity at top (KT) and bottom (KB) layers at stations south of Tacoma Narrows.

## Salinity and Temperature Profiles

Vertical profiles predicted by the model were compared with data collected during cruises (2006 – 2007). Details in vertical profiles indicate fine-scale stratification structures often difficult to reproduce when modeling estuarine conditions. Figure 33 identifies the profile locations used for calibration.

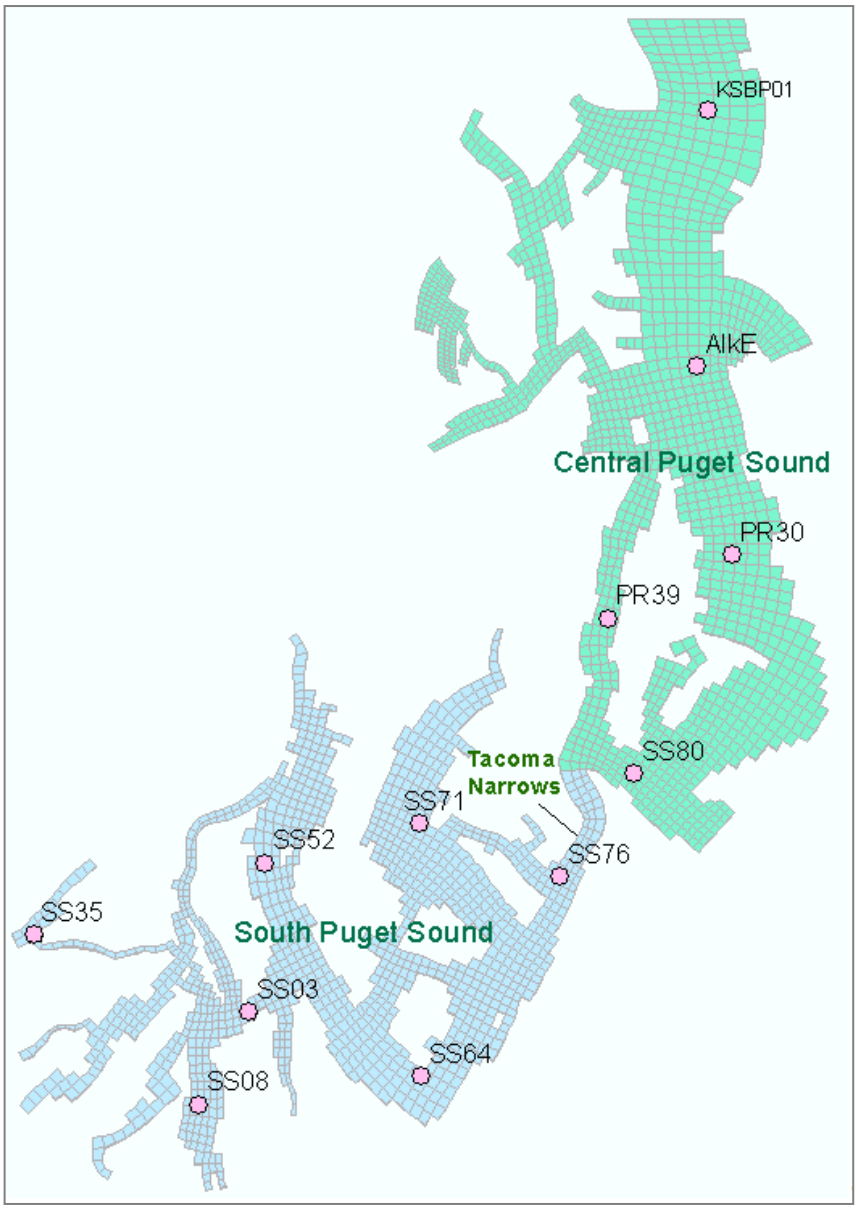


Figure 33. Station locations for temperature and salinity profile comparisons between model predictions and observed data.

Figures 34-37 present temperature profiles at all stations (Figure 33) in the model domain. Each station has a maximum of eight profiles spanning July 2006 through October 2007. Observed data were measured at 0.5 m depth intervals but were averaged for each grid layer depth in order to compare with model predictions. The model-predicted temperature profiles reflect the average data structure including warming of the near-surface layers. Stations north and around Tacoma Narrows exhibit lowest RMSE ($\leq 1$) compared with the finger inlets (RMSE $\leq 2$).

Figures 38 through 41show the salinity profile comparison between model predictions and observed data. Profiles North of Tacoma Narrows (stations KSBP01, AlkE and PR30) show good agreement between predicted and observed salinities. However, at station KSBP01 the model fails to predict a sporadic freshening of near-surface waters on November 29 2006. The spatial extent of a grid cell is much larger than that of the station location. Model-predicted concentrations are an average over the horizontal and vertical extent of the grid cell. Around the Tacoma Narrows, the model predicts more freshening within 20 meters of the surface, whereas the data indicate freshening is limited to nearer the surface (see station SS80 in Figure 39) or little at all. The model predicts limited salinity-induced stratification at SS76 (Figure 39) until fall storms began, but data indicate a nearly uniform profile.

The model predicts surface, water column, and near-bottom patterns and magnitudes well, overall. In the Nisqually Reach, salinity and temperature was well-described through late summer and into the winter months (station SS64). Model-predicted salinity profiles in Case Inlet were good, but temperatures were over-predicted throughout the water column in August (Station SS52). Oakland Bay salinity was reasonable, although temperatures were consistently under-predicted. Budd Inlet temperature profiles differed most between model and data, but salinity profiles were reasonable through late summer. In the winter months, the model under-predicts the salinity, due to the river plume.

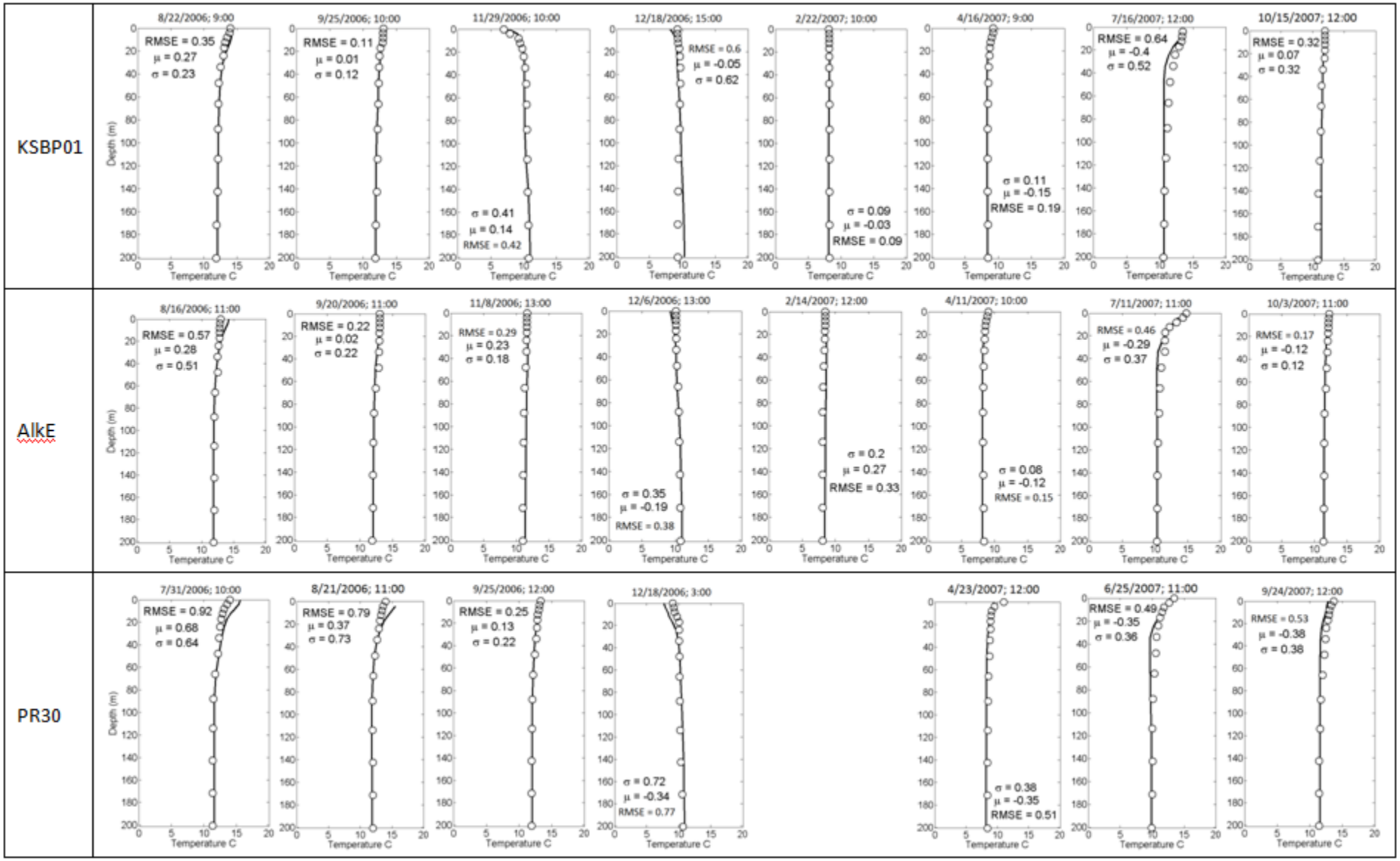


Figure 34. Temperature profile comparison between model prediction (firm line) and observed data (circles) at stations KSBP01, AlkE, and PR30.

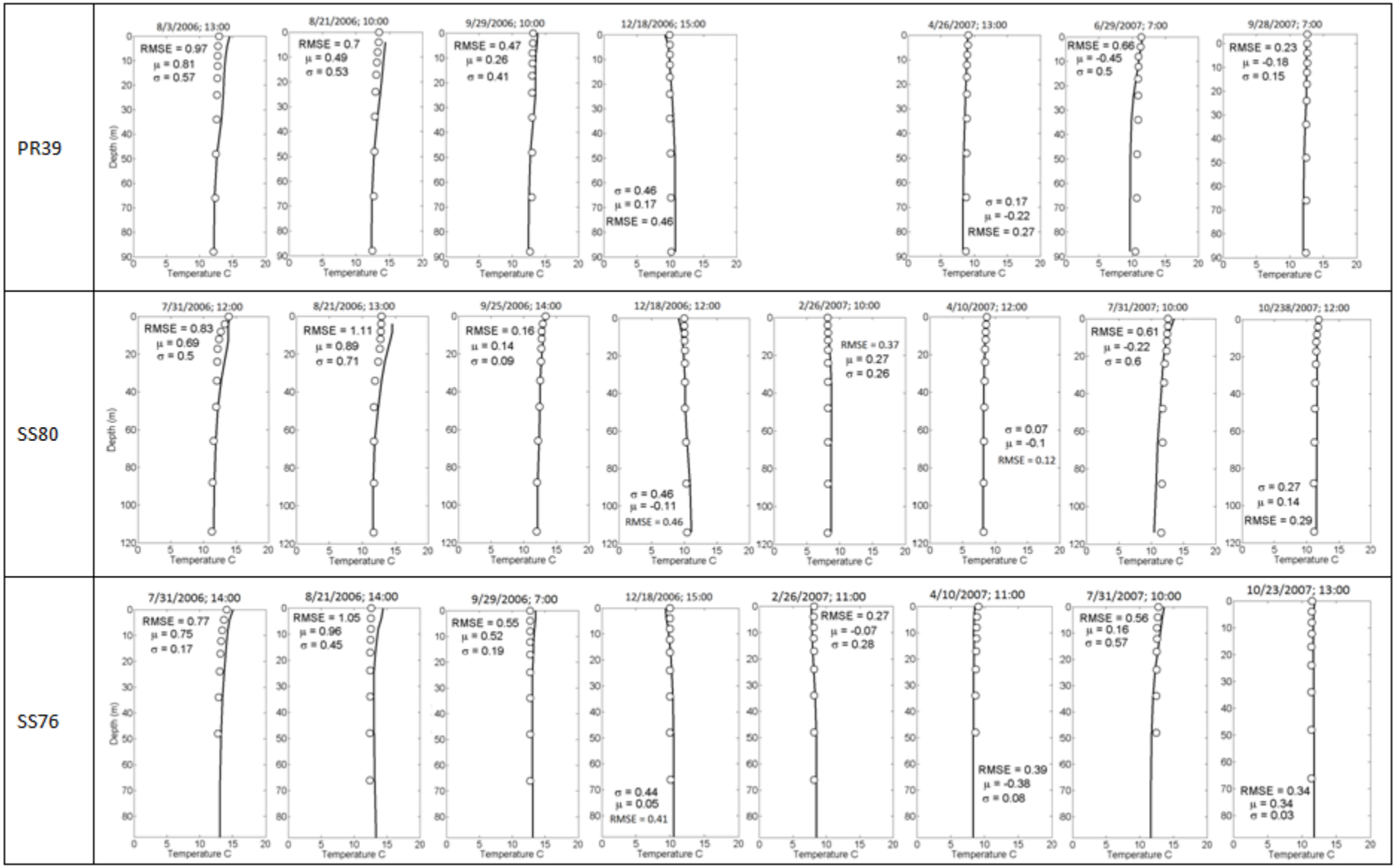


Figure 35. Temperature profile comparison between model prediction (firm line) and observed data (circles) at stations PR39, SS80, and SS76.

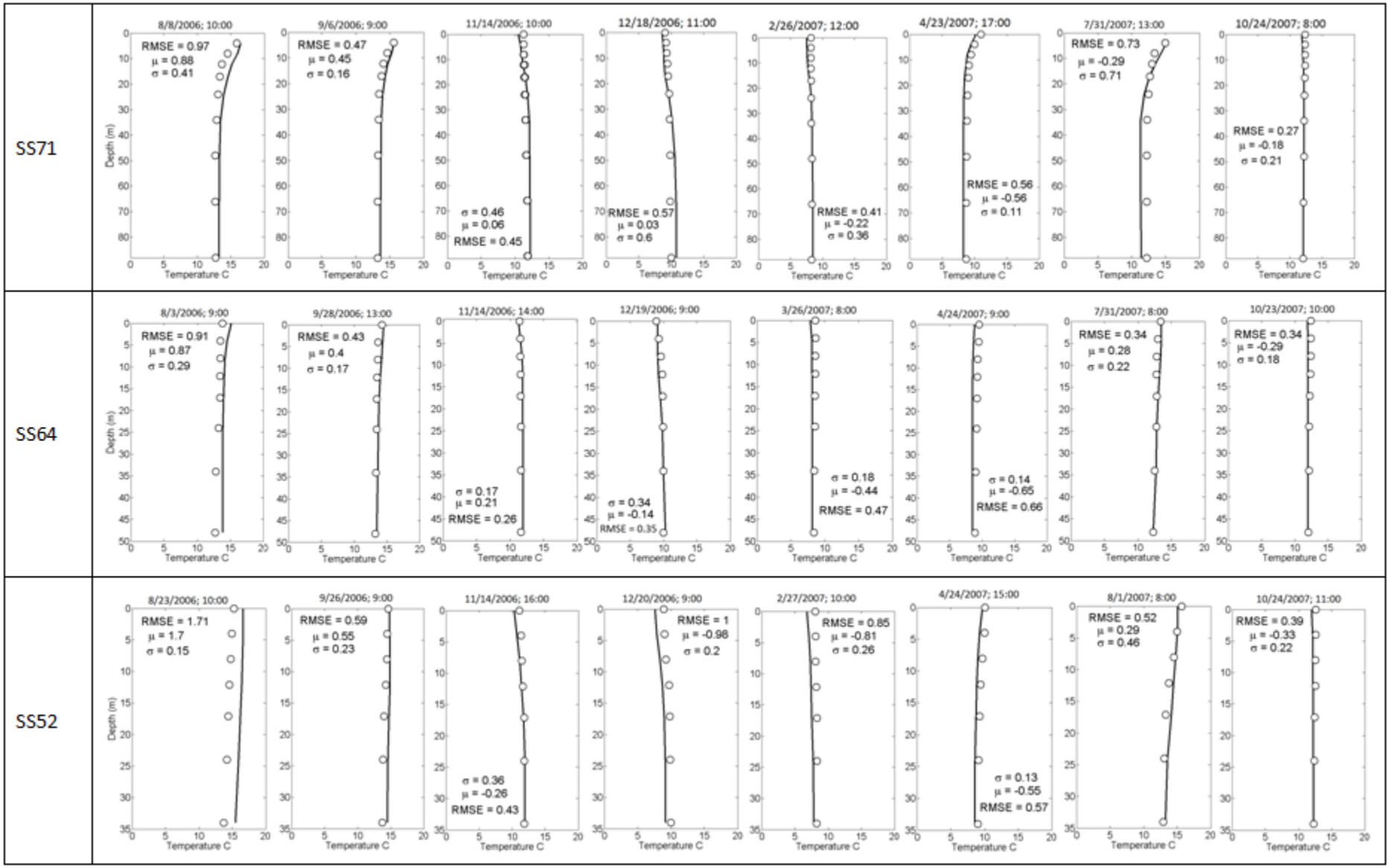


Figure 36. Temperature profile comparison between model prediction (firm line) and observed data (circles) at stations SS71, SS64, and SS52.

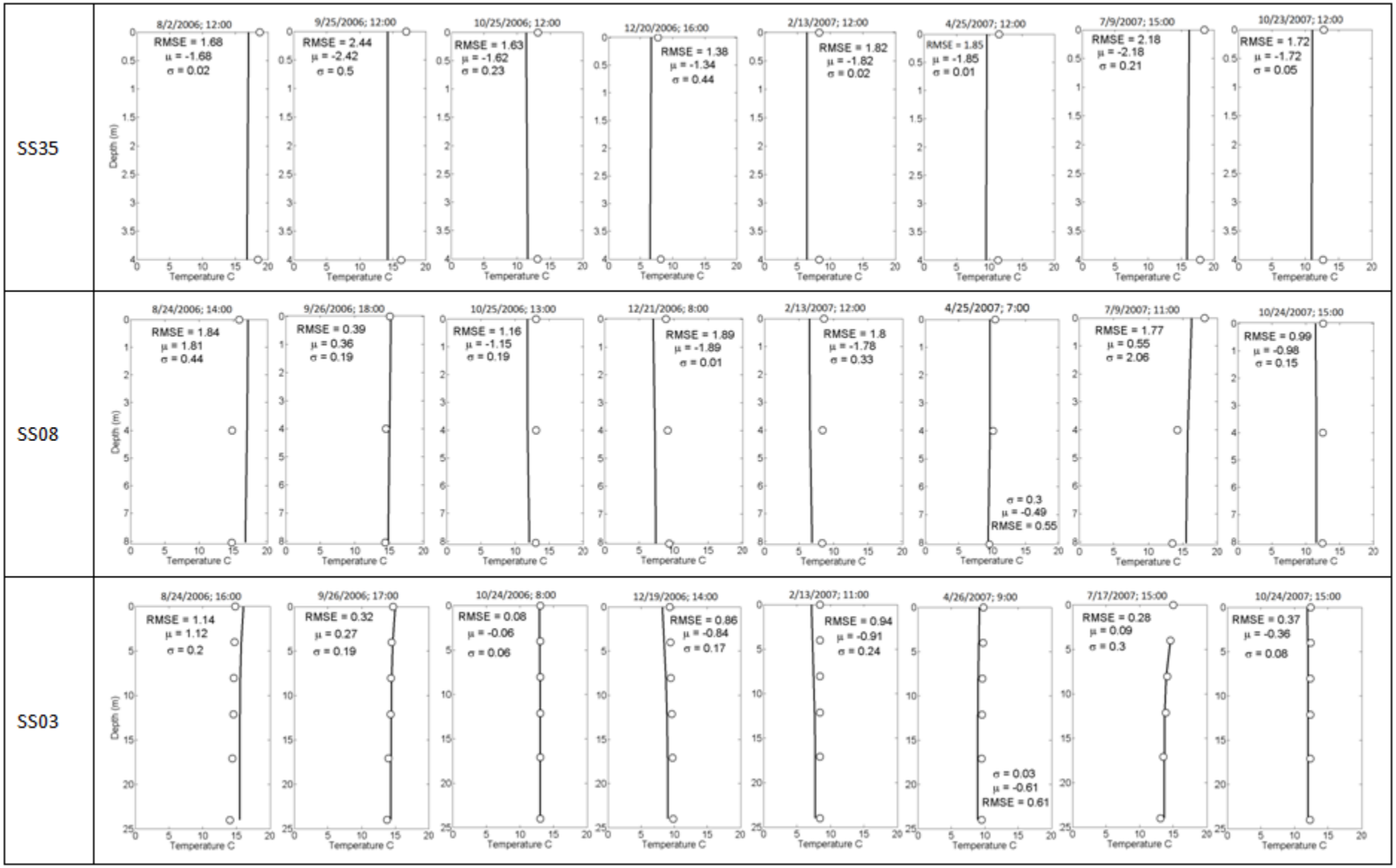


Figure 37. Temperature profile comparison between model prediction (firm line) and observed data (circles) at stations SS35, SS08, and SS03.

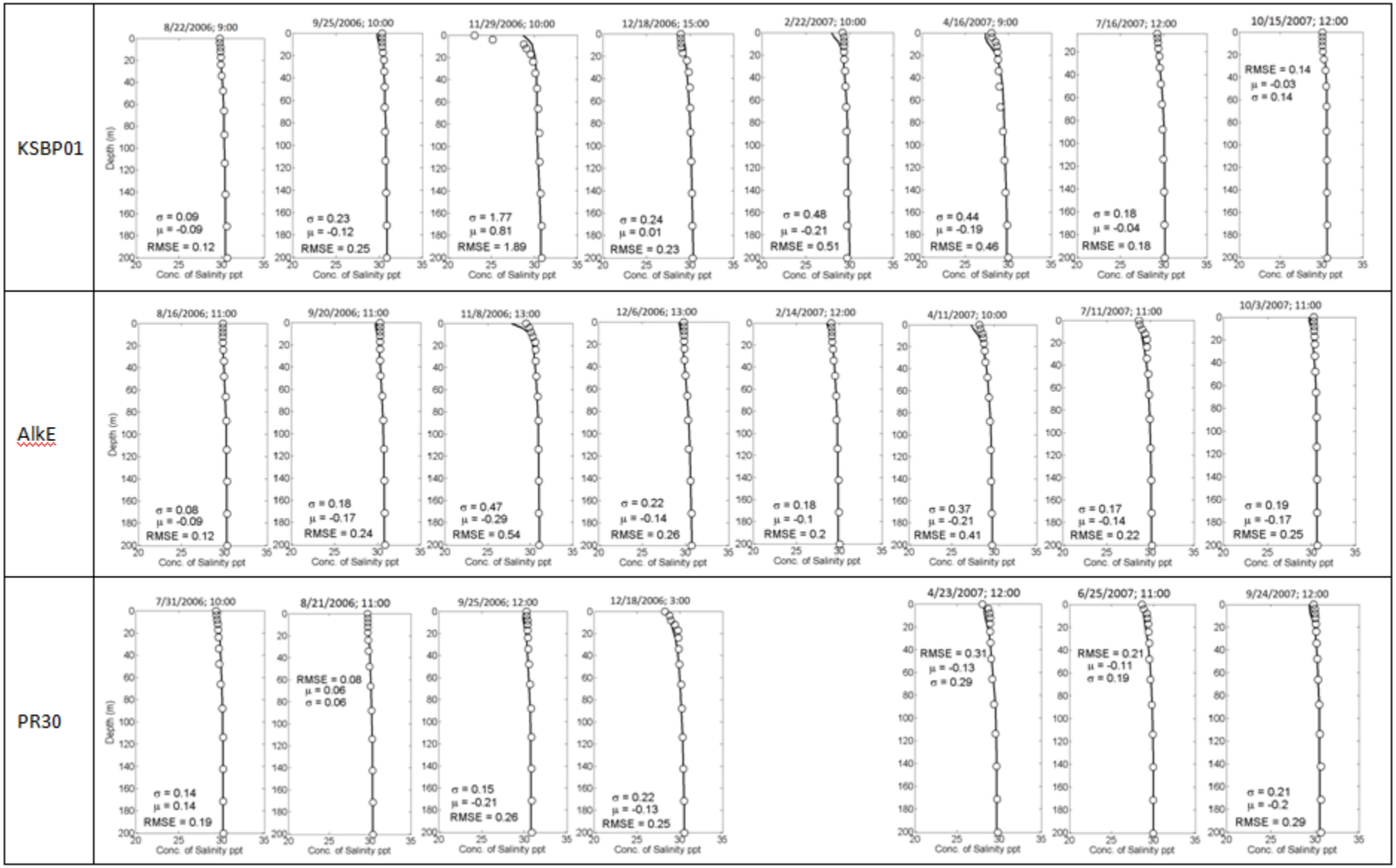


Figure 38. Salinity profile comparison between model prediction (firm line) and observed data (circles) at stations KSPB01, AlkE, and PR30.

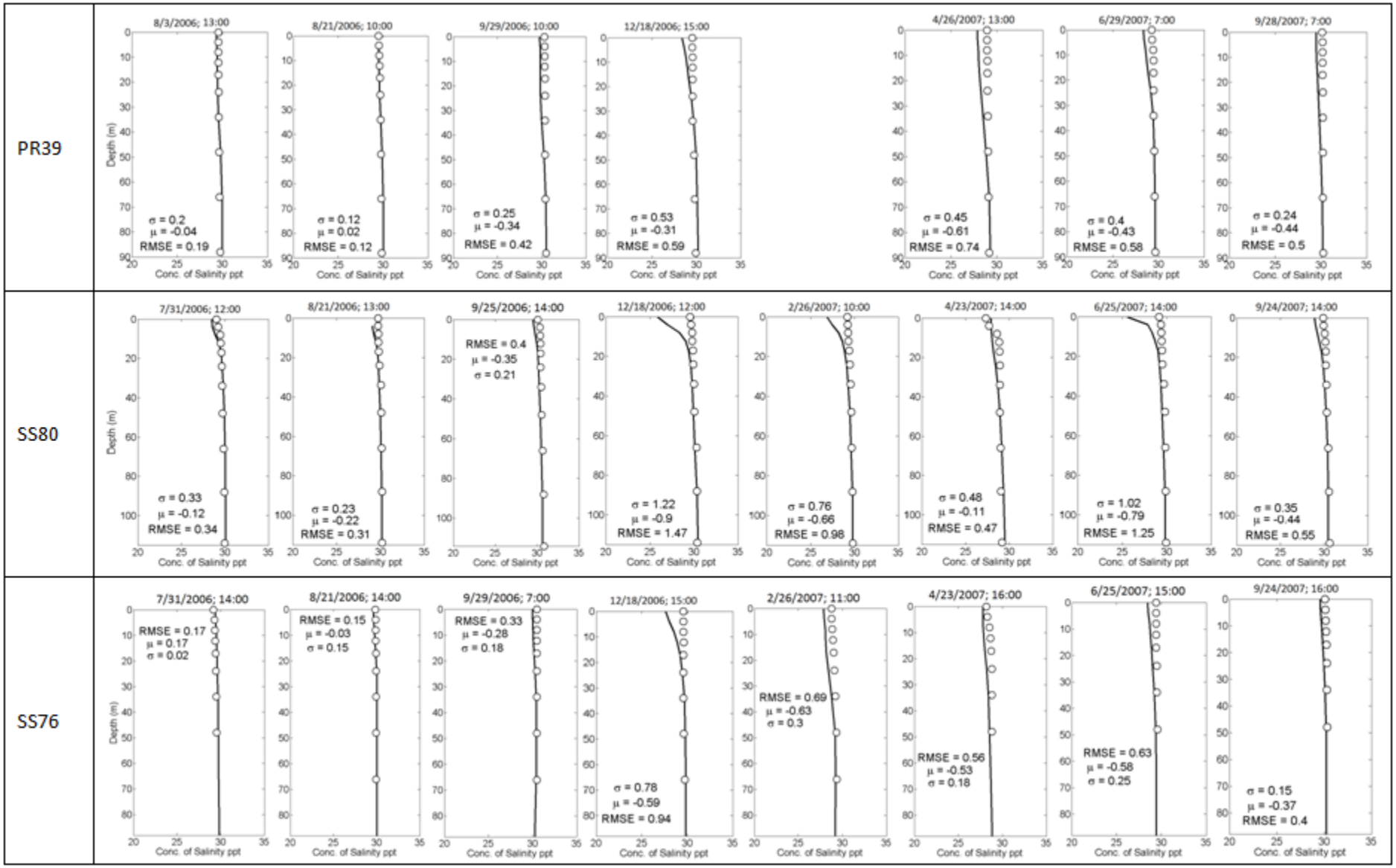


Figure 39. Salinity profile comparison between model prediction (firm line) and observed data (circles) at stations PR39, SS80, and SS76.

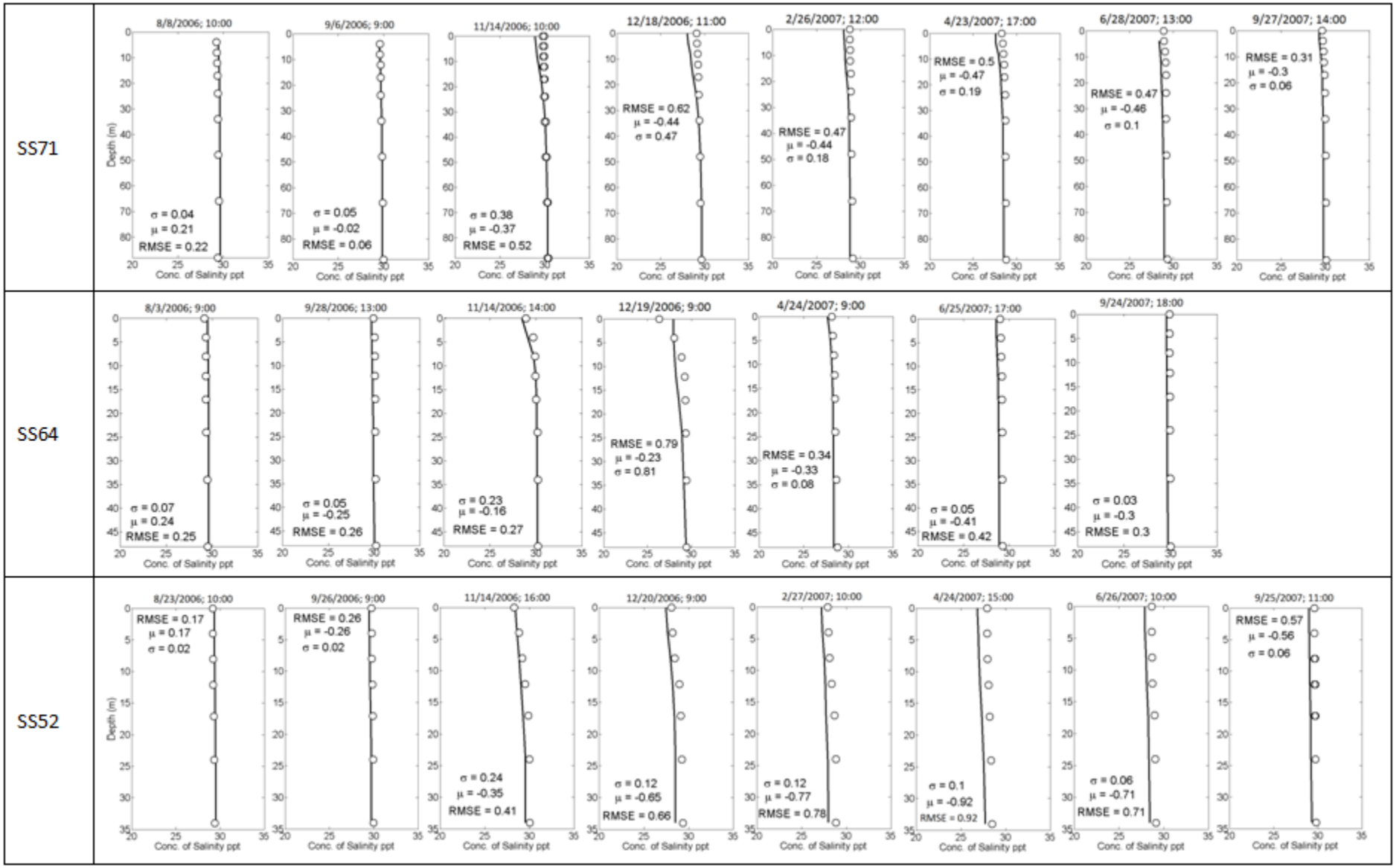


Figure 40. Salinity profile comparison between model prediction (firm line) and observed data (circles) at stations SS71, SS64, and SS52.

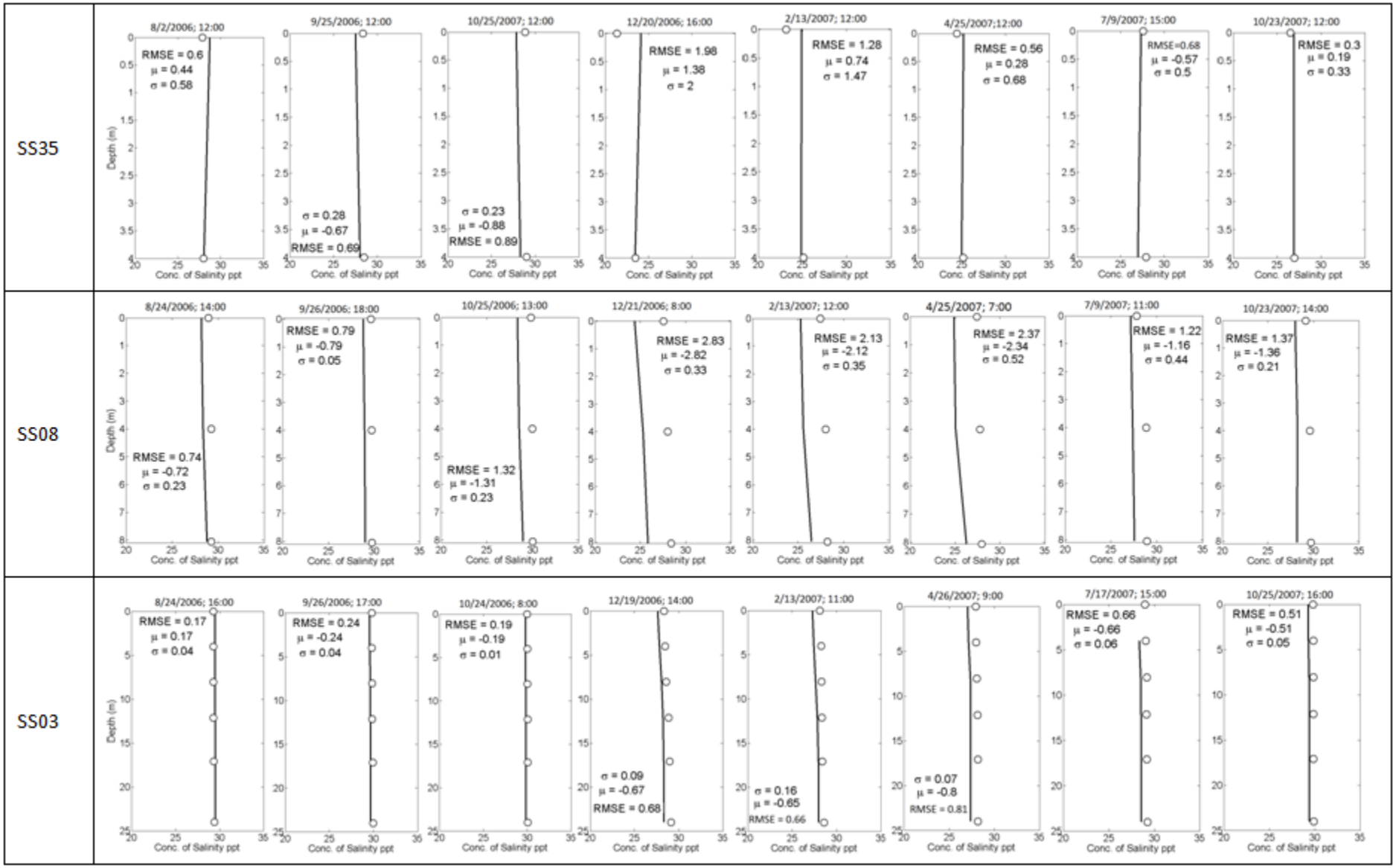


Figure 41. Salinity profile comparison between model prediction (firm line) and observed data (circles) at stations SS35, SS08, and SS03.

## Surface Temperature and Salinity Spatial and Temporal Patterns

Model output was compared with cruise data to confirm spatial patterns in temperature and salinity predicted by the model during the 2006 – 2007 period. We compared near-surface patterns because they are influenced by river and meteorology boundary conditions and generally show more variability than near-bottom conditions. We presented near-bottom results in the *Temperature and Salinity Time-Series Plots* section.

Cruise data were collected over multiple days and at different times of day. However, differences in cloud cover, tidal phase, and diel variations contribute to variability during the multi-day data collection period. We compared model results from noon in the middle of the cruise window as a snapshot of conditions as a synoptic proxy for cruise conditions. The cruise data plotted were over a 5-day window around the model output date. This was necessary to gather sufficient observed data to span the model domain.

Predicted surface temperatures for summer 2006 cruises reflect available data (August 2006 plot in Figure 42). Cruise tracks did not reach the shallow terminus of each inlet to verify these spatial patterns, but the model predicts high temperatures consistent with the shallow water depths. Warm water temperatures within Sinclair and Dyes Inlets, Liberty Bay, and Quartermaster Harbor are reasonable, but no data were collected within these regions of Central Puget Sound. Outside of these shallow bays, Central Puget Sound surface temperatures were cooler than those in South Puget Sound in both the model predictions and measured data, and overall magnitudes and spatial patterns are appropriate. Overall cooler summer temperatures near the Tacoma Narrows reflect intense mixing with cooler bottom waters.

September 2006 surface temperatures show transition from summer warm temperatures to cooler fall temperatures. Winter surface temperatures are more uniform than summer throughout the domain in both the model predictions and data (December 2006 plot in Figure 42), with the coldest temperatures in the shallow waters of western inlets.

April 2007 surface temperatures (Figure 42) remain cool throughout the model domain. The shallow western inlets were warmer than other areas, and the coolest waters were around the Tacoma Narrows and northern boundary. By June 2007, significant heating contributed to warm temperatures in the shallow western inlets in particular. Cool and wet summer conditions decreased surface temperatures by September 2007. The model captures the temperature patterns and magnitudes.

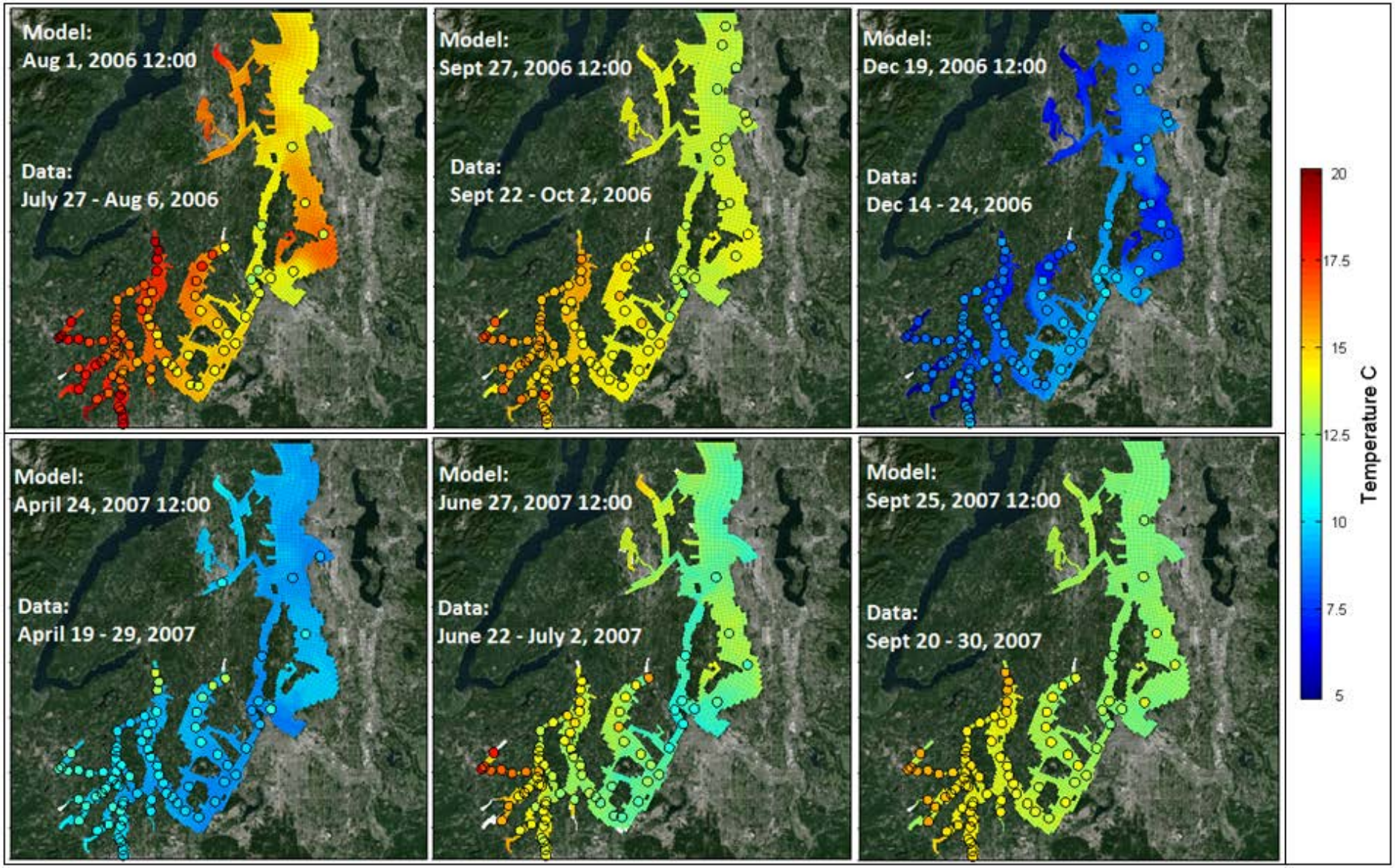


Figure 42. Field observations of near-surface temperatures compared with model output.

The model also predicts surface salinity patterns and magnitudes well. Salinity has a stronger effect on density than does temperature. The summer 2006 model output and cruise data show good agreement throughout the model domain (Figure 43). Lowest surface salinities occur nearest river inputs, but few data were available from these shallow waters to corroborate. The plumes from the Puyallup and Nisqually Rivers are evident, as are smaller river inputs to more quiescent regions in the model.

Surface salinities reached seasonal maxima in September 2006, coincident with low river inputs. The December 2006 cruise data confirm the wide range of surface salinities predicted by the model (from <20 ppt to nearly 30 ppt) due to the increase in river inflows (Figure 26).

The April 2007 predictions and data (Figure 42) show continuing freshened conditions, particularly near freshwater sources. Similarly, the June 2007 cruise data and model predictions both show similar patterns, with surface salinities generally dominated by freshwater inflows with continued high discharge rates.

By September 2007, cruise data and model predictions show higher and more uniform values than in June throughout South and Central Puget Sound except for limited areas near freshwater inflows where no cruise data are available to corroborate. Overall patterns and magnitudes are reasonable. The model predicts 1 to 3 ppt fresher conditions than in the data for the surface layer, partly because the cruises did not include shallow areas nearest the freshwater inflows and partly because the observed data are plotted over a window of 5 days around the model prediction date.

In summary, cruise data corroborate the predicted surface temperatures and salinities within South and Central Puget Sound. The surface values are more difficult to simulate than near-bottom values because surface values reflect meteorology and river inflow boundary conditions that change significantly over time. The seasonal shifts are appropriately represented by the model, and the spatial patterns are well-characterized.

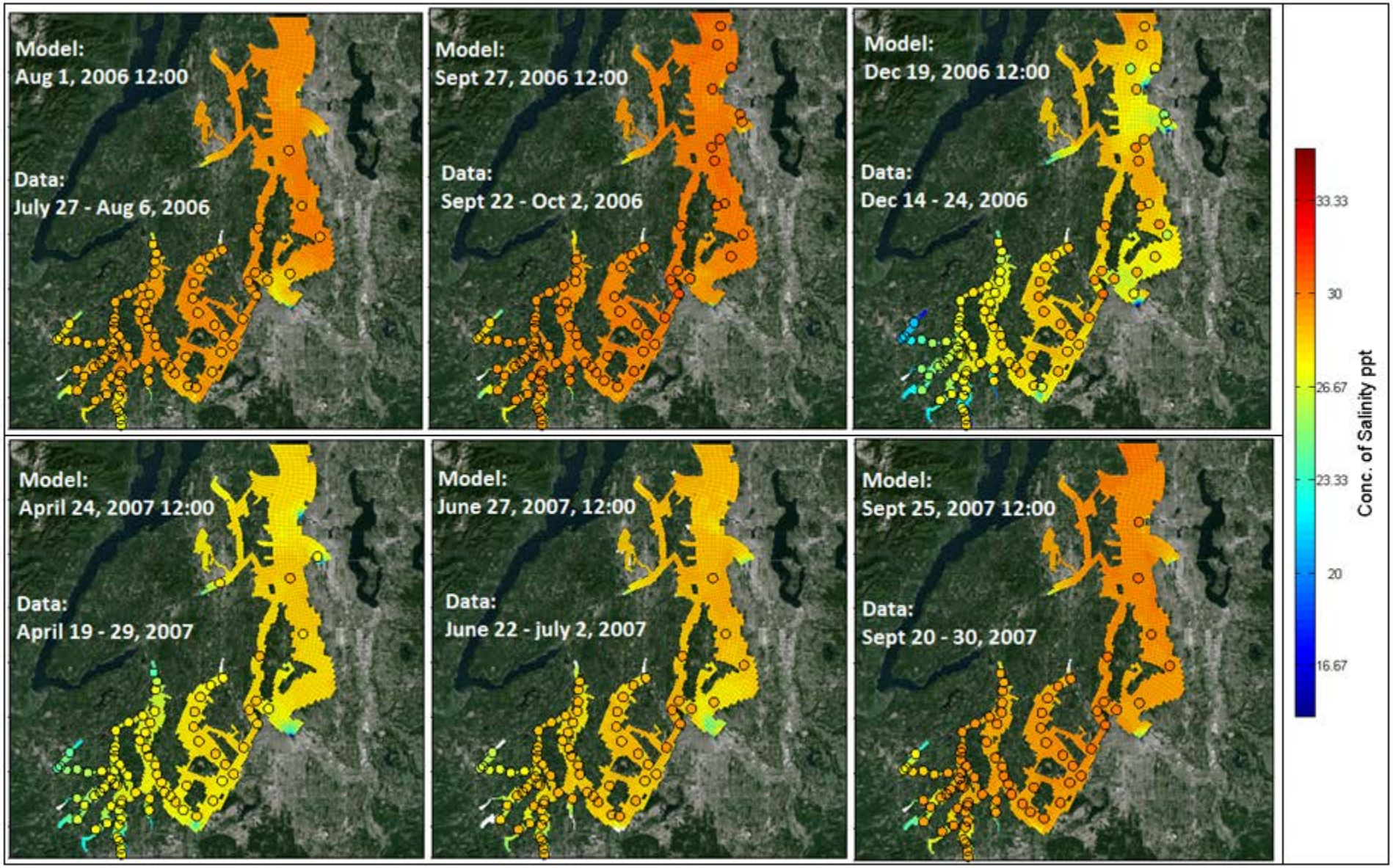


Figure 43. Field observations of near-surface salinity compared with model output.

## Model Uncertainty

The RMSE is an unbiased statistic of how well the model is predicting observed values. It is mathematically defined as the square-root of the average squared difference between paired observed and predicted data, as defined below:

$$RMSE = \sqrt{\frac{\sum \left(X_o - X_p\right)^2}{n}}$$

Where $X_0$ = observed data; $X_p$ = predicted data; n = number of paired data sets

We also evaluated bias, or the tendency to over-predict or under-predict water quality patterns. The mean bias (μ) of the predictions is the average of the differences between predicted and measured values, while σ is the standard deviation of the bias. If the range (μ ± 2 σ) does not contain zero, then model would be biased at the 95% confidence interval.

$$bias = average\left\{\left(X_{pred,1} - X_{obs,1}\right) + \left(X_{pred,2} - X_{obs,2}\right) \ldots + \left(X_{pred,n} - X_{obs,n}\right)\right\}$$

If the range is below zero, then the model under-predicts. If the range is above zero, then the model over-predicts. The model predictions are average values within a given grid-cell layer in the error statistics. The field data were binned to the model layers.

Figure 44 shows the overall goodness of fit of temperature and salinity predictions to observed data from all stations at all depths and times from July 2006 through October 2007. A perfect match would be when all data lie on the 1:1 line, i.e., when predicted and measured values match exactly. The histogram shows the frequency distribution of the residuals (which are the differences between predicted and observed values) with the mean and standard deviation of the bias. The overall RMSE for temperature was 0.78 °C with a mean bias of -0.14 °C. However the bias for temperature is not statistically significant because it lies within 2 standard deviations of zero difference (i.e., at the 95% confidence interval). The overall RMSE for salinity was 0.75 ppt with a mean bias of -0.32 ppt. Again, within the 95% confidence interval, the bias is not statistically significant. These results are comparable to those present in Roberts et al. (2012).

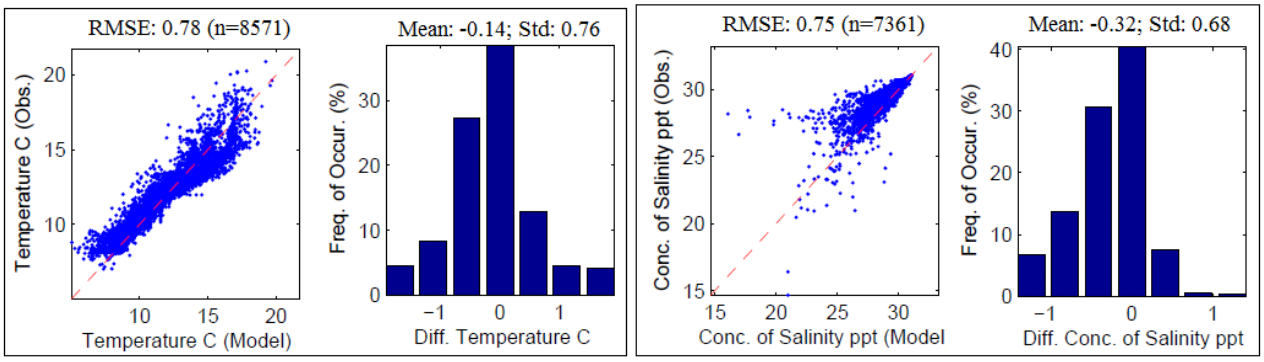


Figure 44. Goodness of fit for temperature and salinity predictions for 2006-2007 across all stations.

## Sensitivity Analyses

While only monthly data are available, the northern marine boundary conditions are sufficient for the purposes of this project. We tested the uncertainty in these boundary conditions by adding and subtracting 2°C and 1 ppt to the monthly profiles and comparing predicted values within both Central and South Puget Sound. The area influenced by these changes in temperature and salinity was limited to the immediate vicinity of the northern boundary and did not influence the primary area of interest in South Puget Sound.

## Brunt-Väisälä Buoyancy Frequency

The Brunt-Väisälä buoyancy frequency is a measure of the stability of the water column or stratification calculated from water density and the rate of change of density with depth. The value includes the effects of both temperature and salinity and provides a numeric corollary to the profile plots presented above. The buoyancy frequency (N) is calculated as

$$N = \sqrt{-\frac{g}{\rho}\frac{\partial \rho}{\partial z}}$$

Where g is gravitational acceleration, ρ is density, and $\partial\rho/\partial z$ is the density gradient, either between adjacent data bins or model layers.

The buoyancy frequency, expressed as Hertz (Hz), increases as the density gradient increases and typically reaches a maximum value at the depth of the pycnocline. The square of the buoyancy frequency was calculated for stations shown in Figure 45 and no other adjustments to the model were made to improve fit. Figure 46 through 49 show the Brunt-Väisälä buoyancy frequency comparisons between model predictions and observed values for July 2006 through Oct 2007.

The buoyancy frequency squared generally decreases with depth in both the data and model predictions. Data and model predictions are of comparable magnitude at most stations and generally higher in the western inlets.

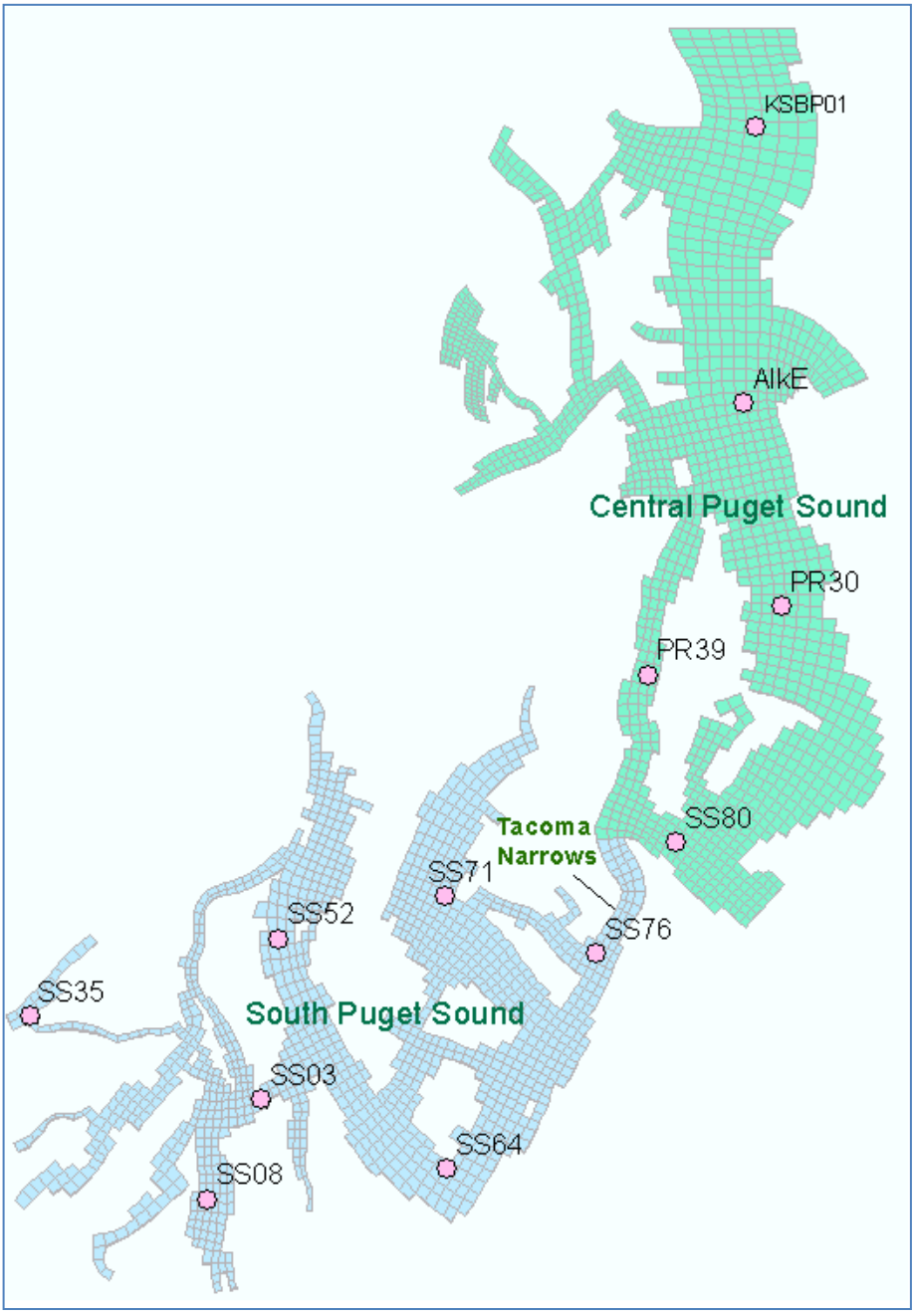


Figure 45. Locations for comparing model and data Brunt-Väisälä buoyancy frequency.

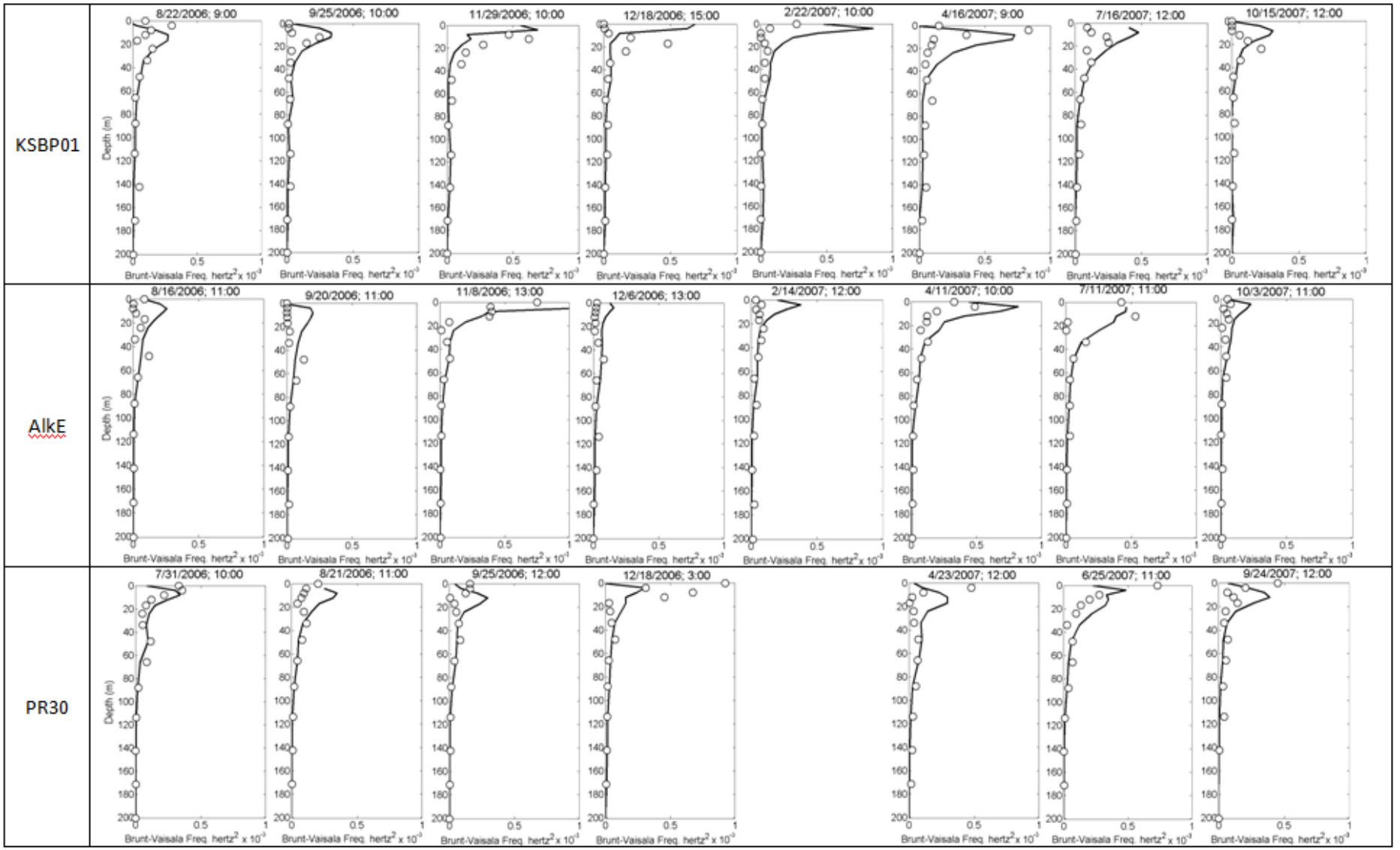


Figure 46. Density buoyancy frequency profile comparison between model prediction (firm line) and observed data (circles) at stations KSBP01, AlkE, and PR30.

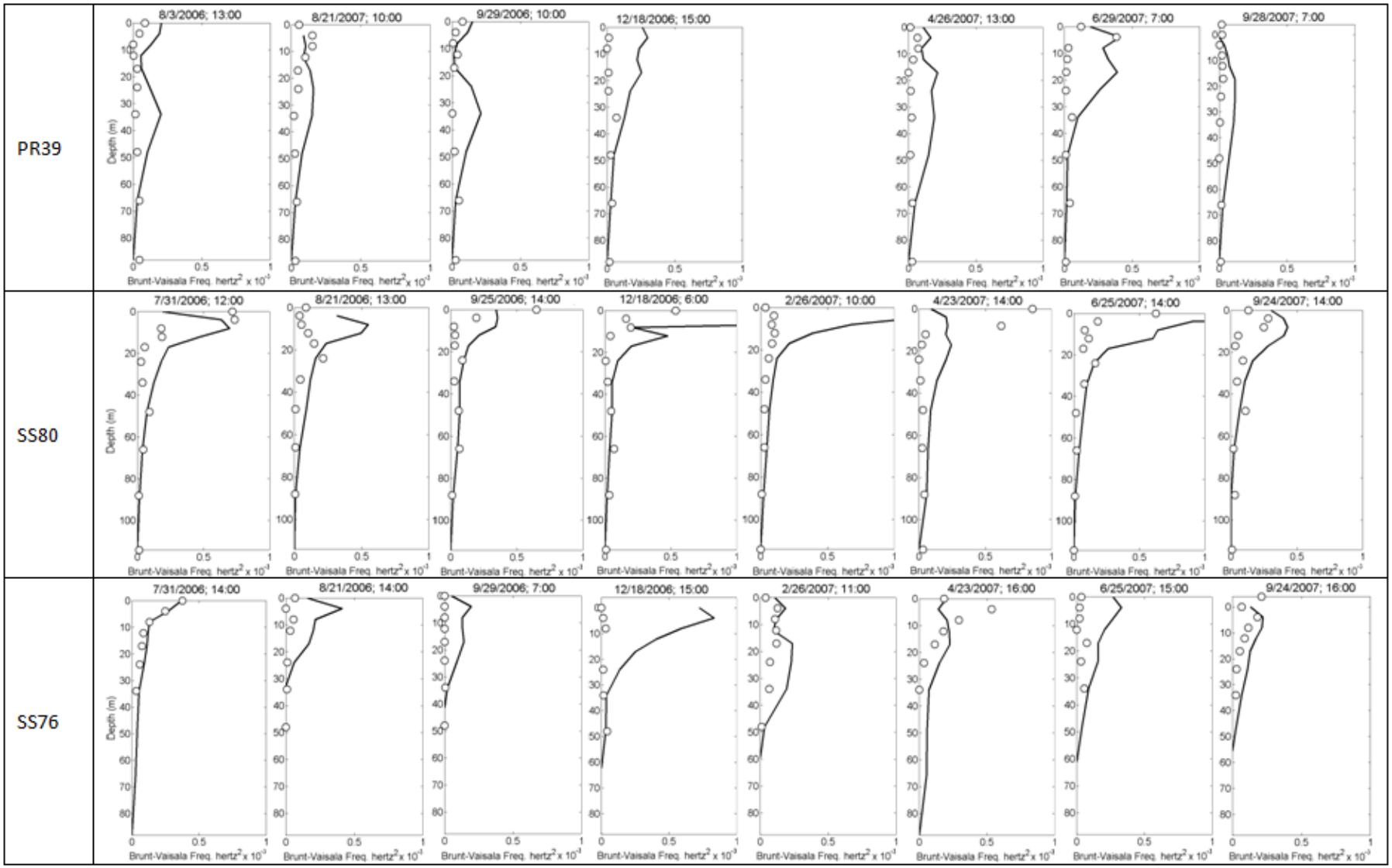


Figure 47. Density buoyancy frequency profile comparison between model prediction (firm line) and observed data (circles) at stations PR39, SS80, and SS76.

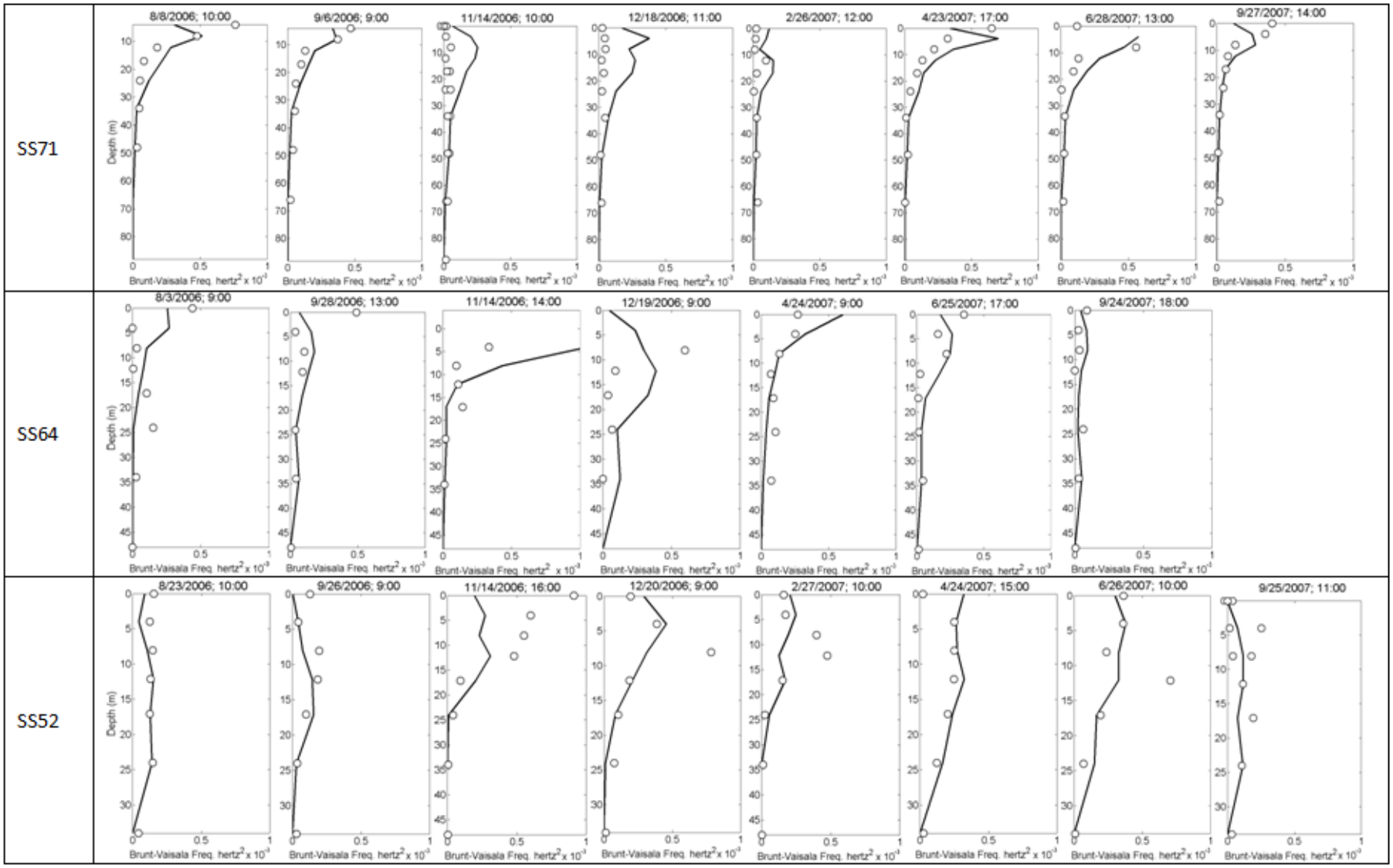


Figure 48. Density buoyancy frequency profile comparison between model prediction (firm line) and observed data (circles) at stations SS71, SS64, and SS52.

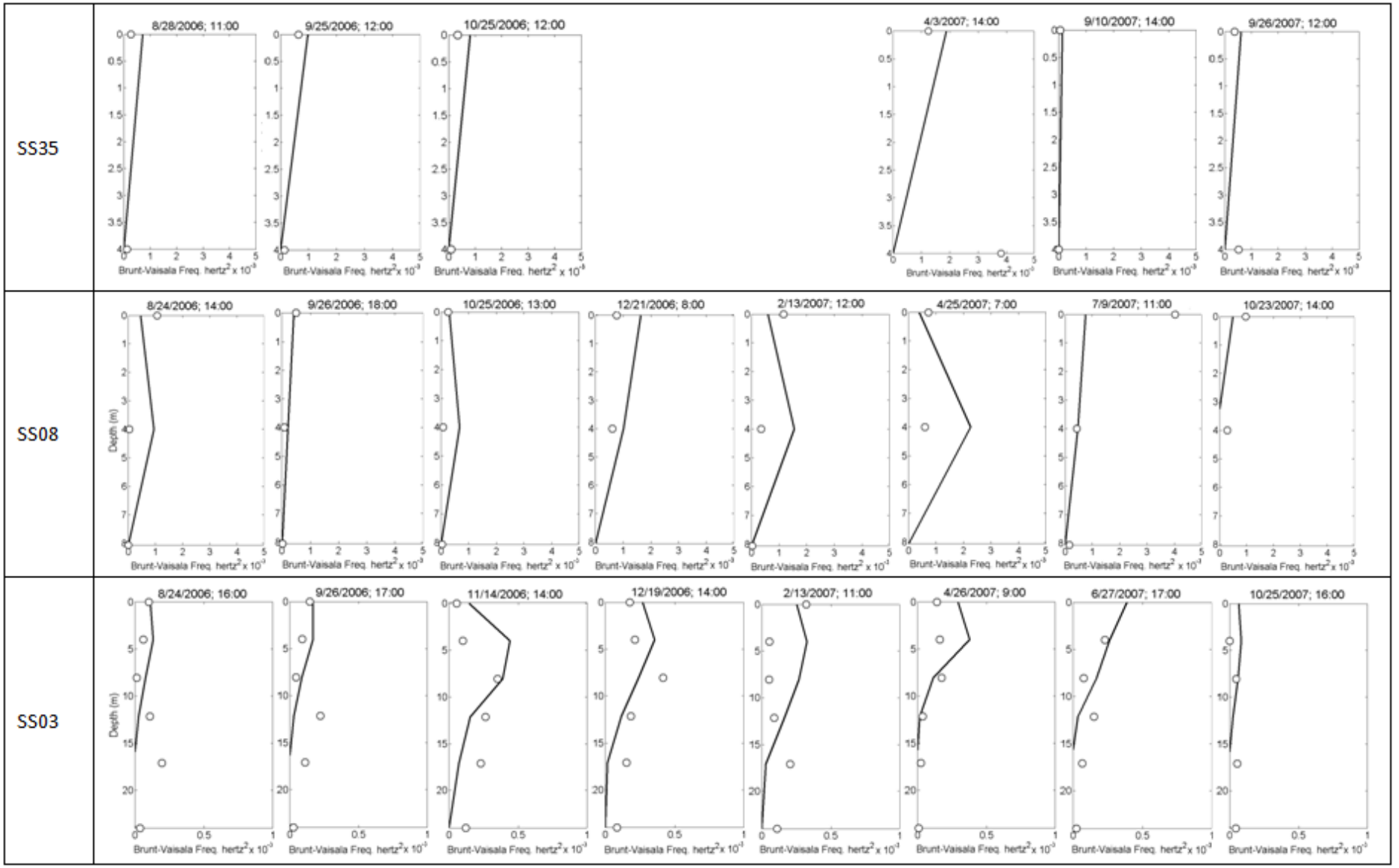


Figure 49. Density buoyancy frequency profile comparison between model prediction (firm line) and observed data (circles) at stations SS35, SS08, and SS03.

# Current Velocities

The current velocity data were used as a general comparison during calibration to verify that the phasing and magnitude are correct. Field programs were developed to investigate current directions within complex passages and inlets and to evaluate inlet-to-inlet differences. Because the model simplifies the vertical structure into layers and averages bathymetry over model grid cells on the order of 500 m, the model does not capture finer-resolution features that may be evident in the observed current data. However, observed current data are useful to confirm large-scale patterns.

Both surface-mounted transects and bottom deployments characterized currents in key locations within South Puget Sound. Roberts et al. (2008) summarizes current data recorded using acoustic Doppler current profilers (ADCPs) during 2007, based on the deployment plan described in Addendum 1 to the Quality Assurance Project Plan (Albertson et al., 2007b). Additional bottom-mounted deployments in Dana and Pickering Passages were part of a separate project that coincided with the 2006 calibration period.

All measurements were recorded with a 300-kHz Workhorse Sentinel ADCP from Teledyne-RD Instruments. The instrument sends a ping and records scattering over a broadband spectrum. The frequency is related to the velocity of the water masses encountered. Due to interference and equipment limitations near the water surface and the sediment surface, data cannot be recorded close to either boundary, typically within a few meters. In addition, the unit cannot record velocities at water depths below 100 m, and no data are returned. While the recorded velocity data are highly precise, field factors (such as boat tracks not perpendicular to shore or lack of data near the surface or bottom) may increase the uncertainty in derived parameters such as water flux and average velocity.

## Surface-Mounted Transects

During July and September 2007, Ecology measured velocity and depth profiles with an ADCP mounted on a boat along various transect (Figures 50 and 51, respectively). The resulting profiles provide both the cross-sectional area and the detailed velocity distribution along transects. Data were recorded in 1-m bins, a finer scale than can be resolved with the layering of the model. The field data were mapped to model layers to facilitate comparisons. The data collection program was designed to estimate instantaneous velocities on flooding and ebbing tides. Detailed results were presented in Appendix E of Roberts et al. (2008). Transects were recorded during different tide stages and were not coincident in time. Boat passes across the inlet required 10 to 20 minutes to complete.

Table 8 compares instantaneous cross-sectional area ($m^2$) and average velocity (m/s) with those predicted by the model. While the model operates on a fine time scale, output data are saved at hourly intervals. These hourly values were linearly interpolated to the time when a transect was navigated. Model cross-sectional areas and velocities are similar to those recorded during the ADCP transects. Differences in transect aspect and model grid cell orientation likely contribute to some differences, particularly at transect T5, but overall the velocities predicted by the model reasonably describe those derived from field data.

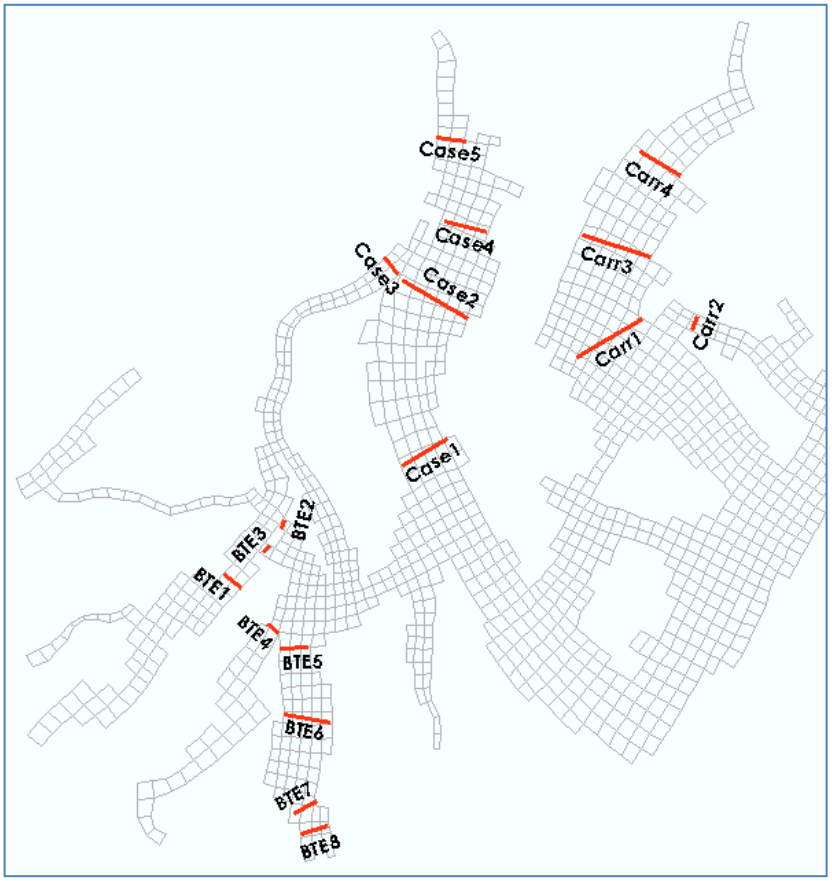


Figure 50. July 2007 surface-mounted ADCP transect locations.

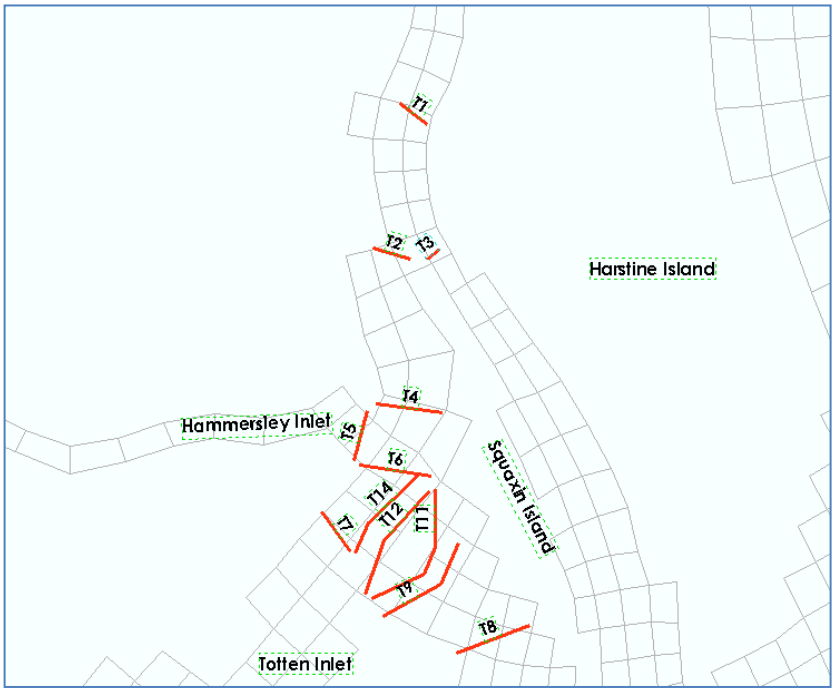


Figure 51. September 2007 surface-mounted ADCP transect locations.

Table 8. Summary of surface-mounted, ADCP-measured tidal fluxes versus model results from July and September 2007. *Positive values are flood tide directions and negative values are ebbs.*

| Transect | Date/Time | Area ($m^2$) | | Mean Velocity (m/s) | |
|---|---|---|---|---|---|
| | | ADCP | Model | ADCP | Model |
| BTE1 - Mouth of Totten | 7/10/07 09:27 | 14,327 | 20,094 | 0.10 | 0.08 |
| BTE4 - Mouth of Eld | 7/10/07 10:05 | 10,300 | 8,254 | 0.26 | 0.16 |
| BTE5 - Mouth of Budd | 7/10/07 10:25 | 22,663 | 22,601 | 0.20 | 0.14 |
| BTE3a - South of Hope Island | 7/10/07 11:01 | 3,452 | 3,650 | 0.91 | 0.86 |
| BTE3b - Replicate | 7/10/07 11:10 | 3,509 | 3,650 | 0.90 | 0.86 |
| BTE6 - Central Budd | 7/10/07 11:57 | 25,869 | 25,141 | 0.13 | 0.06 |
| CARR4 - Allen Point | 7/11/07 13:29 | 44,986 | 62,140 | 0.11 | 0.02 |
| CASE1a - South of McMicken | 7/11/07 14:56 | 96,638 | 100,767 | 0.14 | 0.15 |
| CASE1b - Replicate | 7/11/07 15:28 | 97,170 | 100,767 | 0.12 | 0.15 |
| CASE3 - North of Harstine | 7/12/07 13:20 | 24,672 | 25,928 | 0.31 | 0.22 |
| CASE4 - East of Stretch Island | 7/12/07 13:48 | 44,986 | 51,424 | 0.11 | 0.06 |
| T1 - Harstine bridge (ebb) | 9/26/07 08:00 | 7,258 | 7,158 | -0.55 | -0.29 |
| T3 - North Squaxin Peale (ebb) | 9/26/07 08:43 | 1,458 | 1,506 | -0.36 | -0.76 |
| T5 - Hammersley Inlet (ebb) * | 9/26/07 09:28 | 2,657 | 6,438 | -1.19 | -0.14 |
| T8 - South Squaxin (flood) * | 9/26/07 13:13 | 12,039 | 9,568 | 0.41 | 0.53 |
| T7 - Totten (flood) | 9/26/07 14:46 | 11,538 | 9,696 | 0.64 | 0.27 |
| T6 - Potlatch Point (flood) * | 9/26/07 15:09 | 10,177 | 12,106 | 0.25 | 0.46 |
| T5 - Hammersley Inlet (flood) | 9/26/07 15:31 | 3,316 | 7,081 | 0.93 | 0.13 |
| T1 - Harstine bridge (flood) | 9/26/07 16:37 | 7,609 | 8,280 | 0.72 | 0.37 |

* Indicates transect and model grid cell orientation are very different, and some error may be due to this.

## Bottom-Mounted Deployments

Bottom-mounted ADCPs were deployed at paired locations in South Puget Sound shown in Figure 52 over at least one full neap-spring cycle of the moon (~14 days). The instruments recorded the three components of water velocity (longitudinal, lateral, and vertical) at 90-second intervals that were averaged over 6 minutes in 1-m layers or bins. The data was further averaged over the grid layer bins. We evaluated whether cross-inlet variability was present by comparing results for the two paired instruments.


Figure 52. Locations for comparisons between model output and measured current velocities from bottom-mounted ADCP deployments.

We placed the bottom-mounted ADCPs in the deepest part of any channels present. The model grid cells were assigned depths that represent the average of all actual depths within the horizontal extent of that grid cell. Where the bottom depth changes quickly toward land, such as the channels of Budd Inlet and Pickering Passage, the average depths of the model are shallower than the depth of the ADCP deployment. The water-column velocity structure could be quite different from that determined from field data. Also, the field data did not capture the velocity structure nearest the surface and nearest the bottom. Figure 53 shows the location of the water surface, the grid bottom, ADCP location, and model grid layers. Because each grid has a smoothed cell depth, most of the ADCP depths are below the grid depth. This makes it difficult to choose a grid depth (layer) and ADCP depth to compare velocities.

To circumvent this issue, two approaches were taken. First, a layer that is away from both the surface and the bottom (whether grid or ADCP) was selected for comparison of model prediction and observed data. Secondly, the mean of all water column observed data is compared with the predicted water column mean velocities.

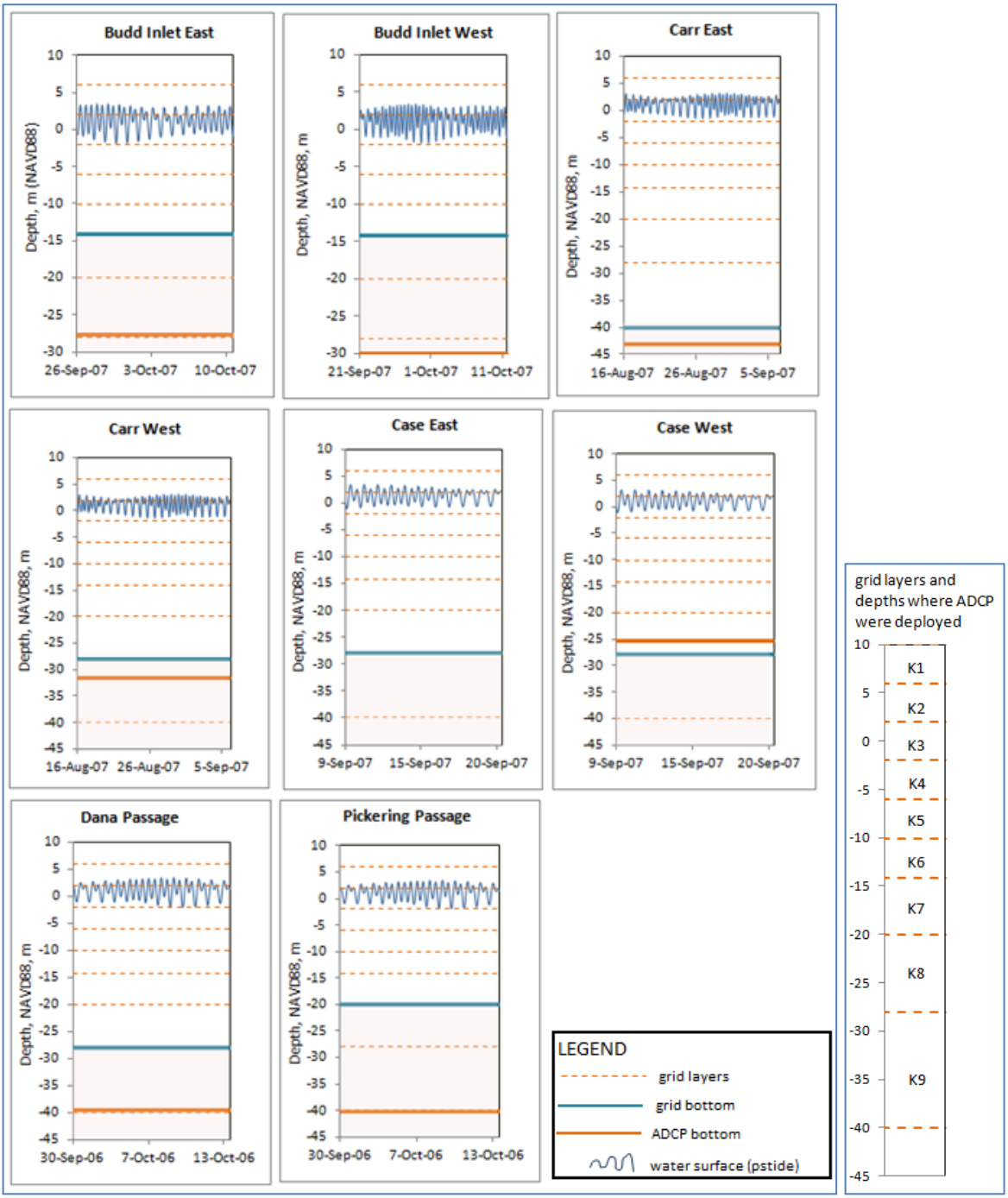


Figure 53. ADCP depths and grid water-column depths.

Figure 54 shows the model-predicted velocities and observed ADCP average velocity within the selected layer for each of the ADCP stations. The layer was selected so that it was away from both the surface and the bottom of the water column. This was done because the ADCP failed to capture the velocities near the surface and because the ADCP and model grid depths did not always match. However, the phases of the tidal velocities match well. In most cases the magnitudes of the velocity component appear to match, except perhaps in Dana Passage where the model over-predicts the observed velocities.

Figures 55 through 58 show the mean (firm black line) minimum and maximum (grey band) water column velocities predicted by the model as well as all water column observed data (with color dots denoting its location in the water column). The RMSEs are based upon model-predicted and observed average water column velocities.

We distinguished between the north-south (v) components and the east-west (u) components of the velocity. Dana Passage (Figure 55) has a stronger east-west (u) component than north-south (v) in both the field data and model predictions, consistent with its physical orientation. Predicted phasing agrees well with field data. The model over-predicts the larger east-west velocity components compared with the observed data. Pickering Passage (Figure 55) velocity predictions have a better RMSE compared to Dana Passage. However, the observed data, particularly at the surface, are highly variable.

Carr Inlet velocities (Figure 56) are low overall. Case Inlet (Figure 57) exhibits a lower east-west component in the field data and model. The model reproduces the overall velocities at both Carr and Case Inlets pretty well.

In Budd Inlet, nearly all of the energy is in the northerly velocity components (Figure 58).

The observed velocities confirm the overall phasing of the tide and relative cross-inlet components. The model cannot resolve the fine-scale complexities captured in the ADCP measurements because each layer is thicker than 1 m and horizontal grid cell dimensions are nominally 500 m. The detailed ADCP data also provide a qualitative sense of the vertical and temporal complexity at the deployment locations.

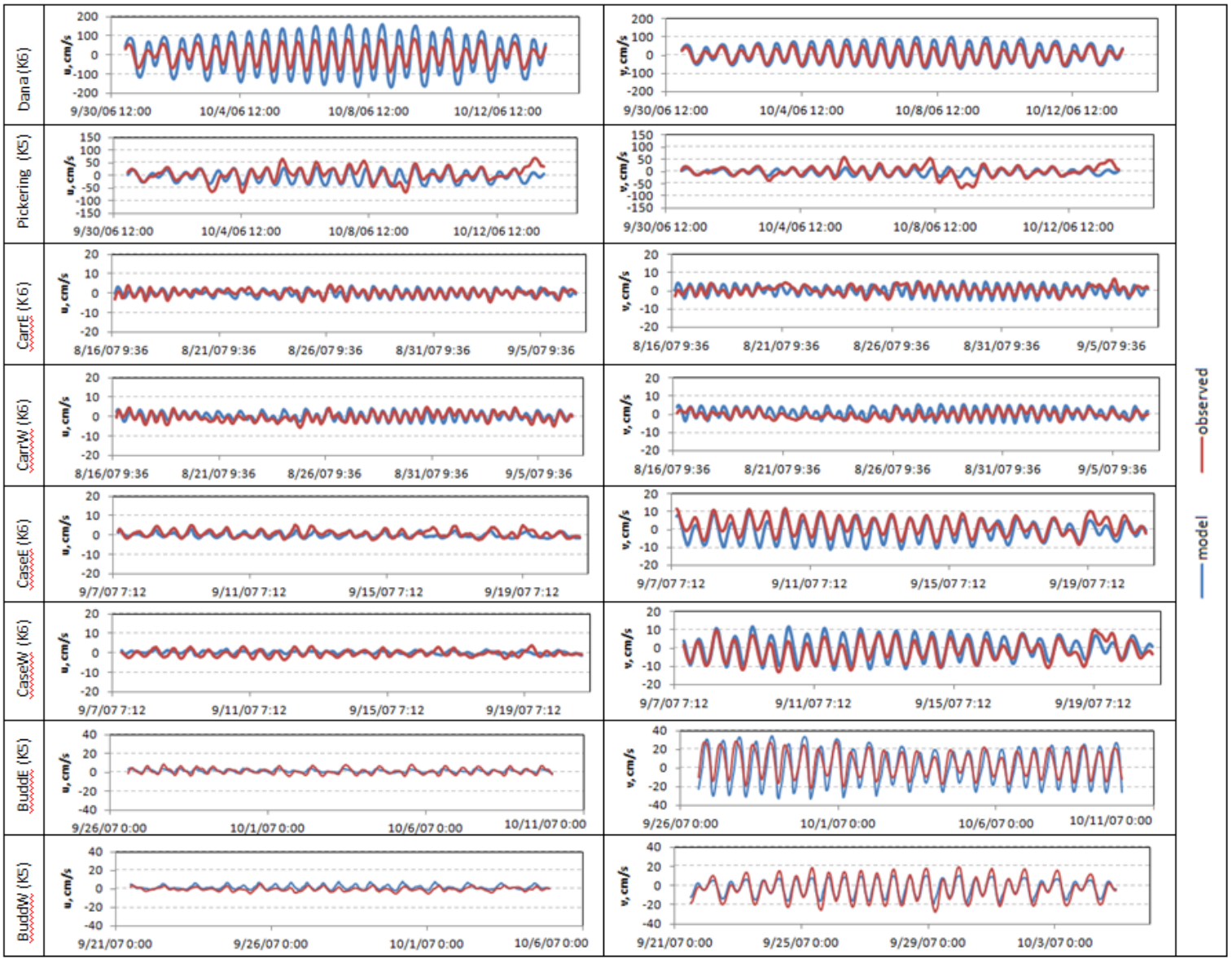


Figure 54. Velocity (u =east-west and v= north south) time series (observed and predicted) at ADCP stations for a given grid layer (K).

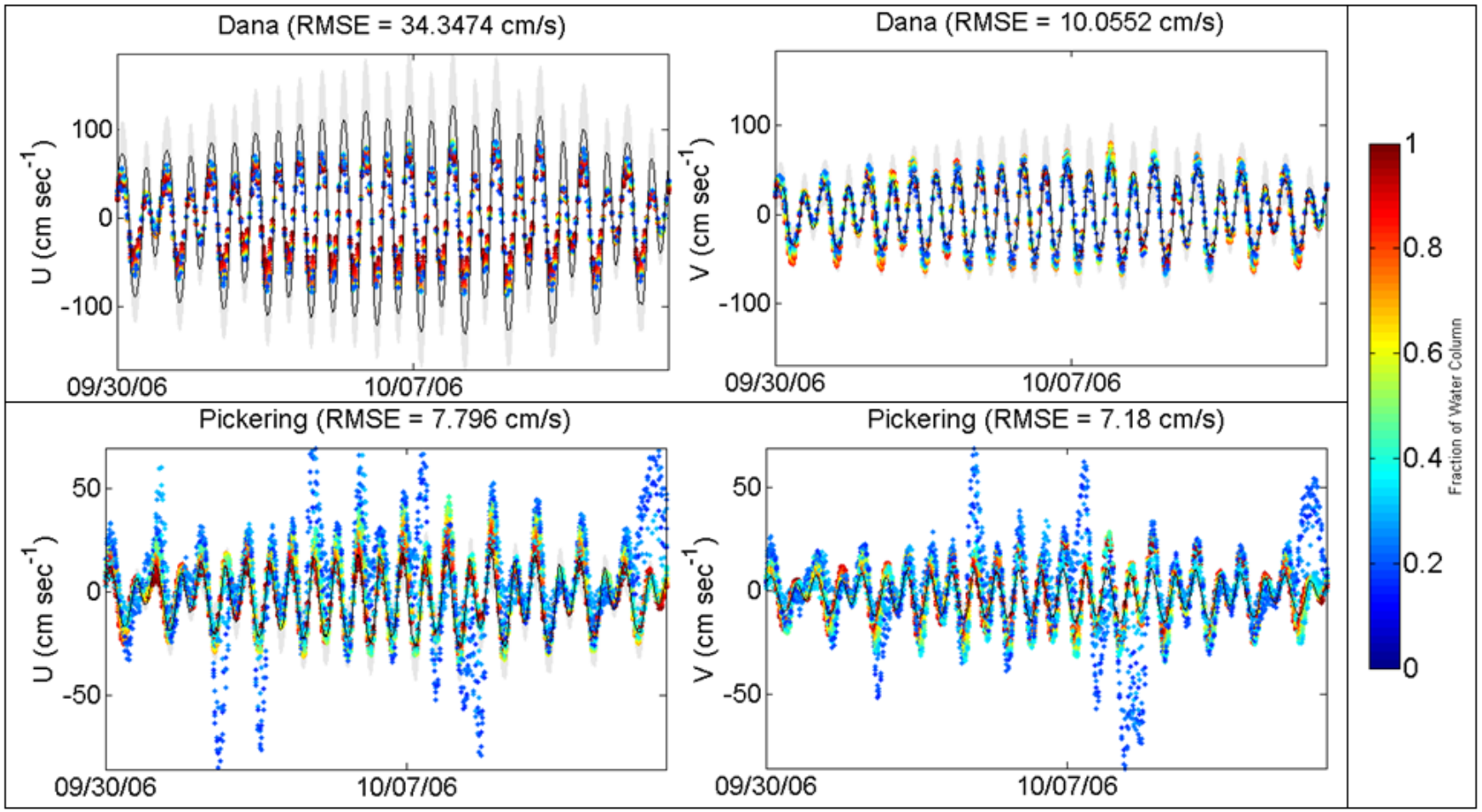


Figure 55. Dana and Pickering Passage velocity comparison between the model and data for the northerly (v) and easterly (u) velocity components.

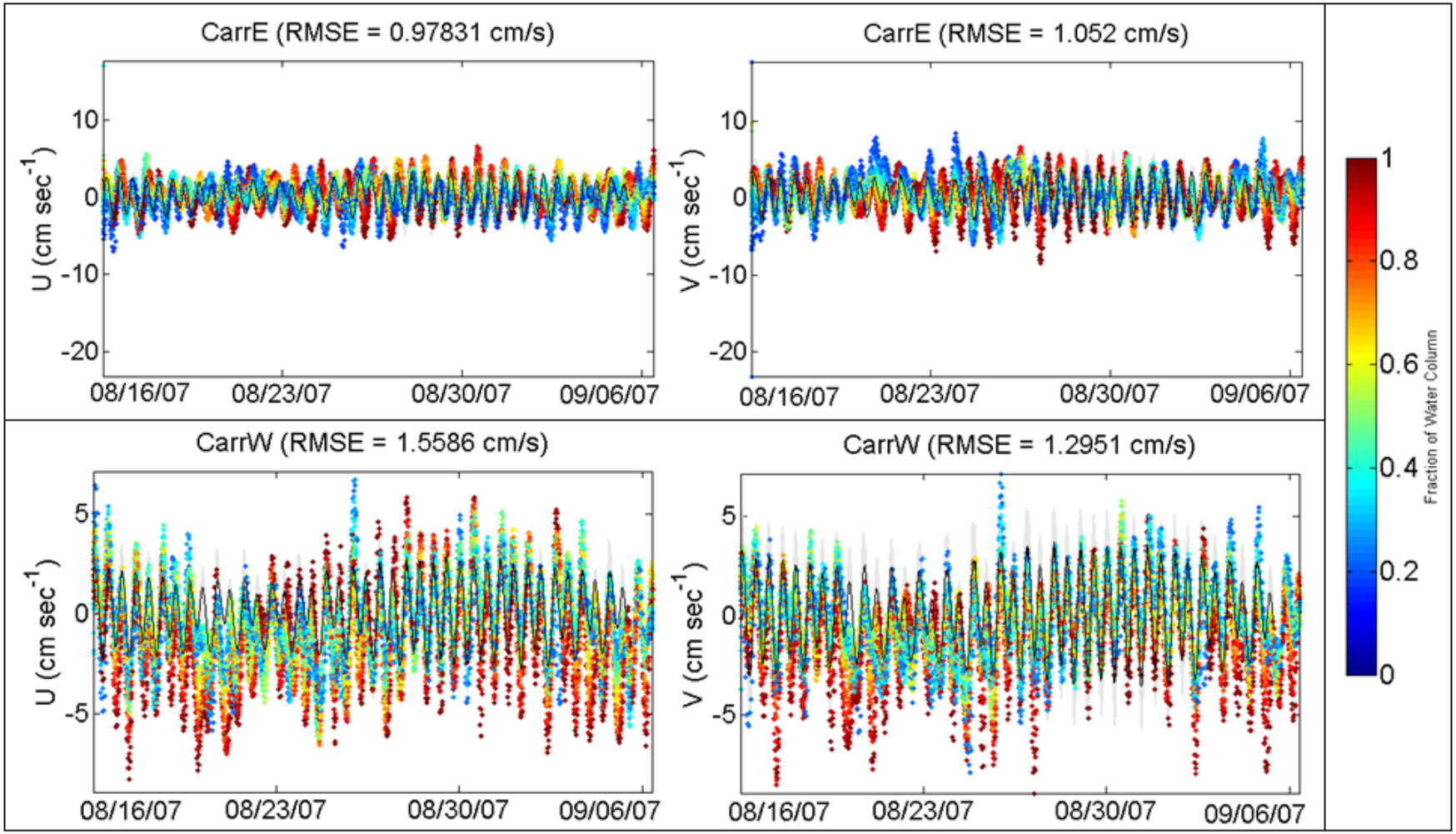


Figure 56. Carr Inlet East and West velocity comparison between the model and data for the northerly (v) and easterly (u) velocity components.

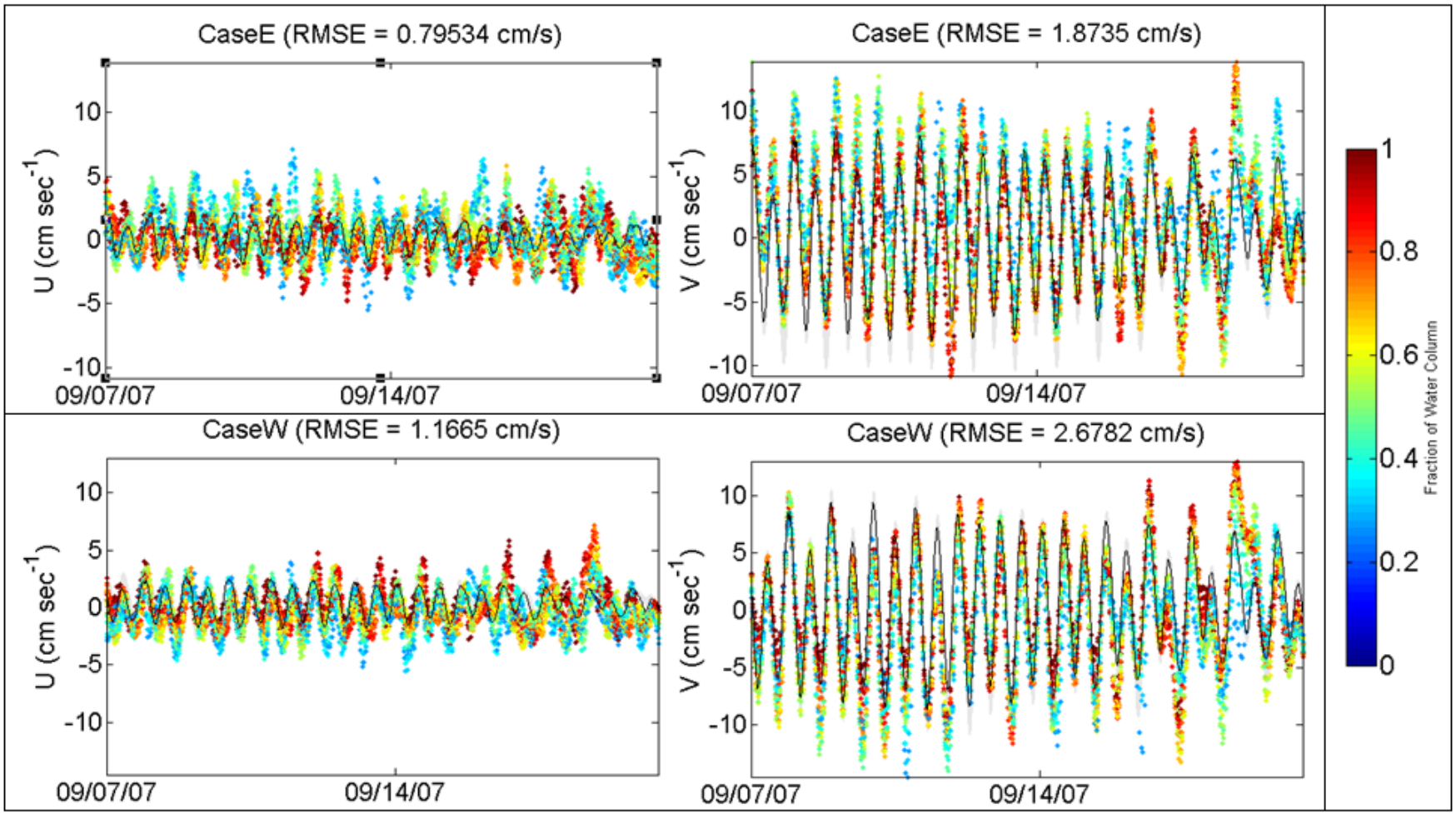


Figure 57. Case Inlet East and West velocity comparison between the model and data for the northerly (v) and easterly (u) velocity components.

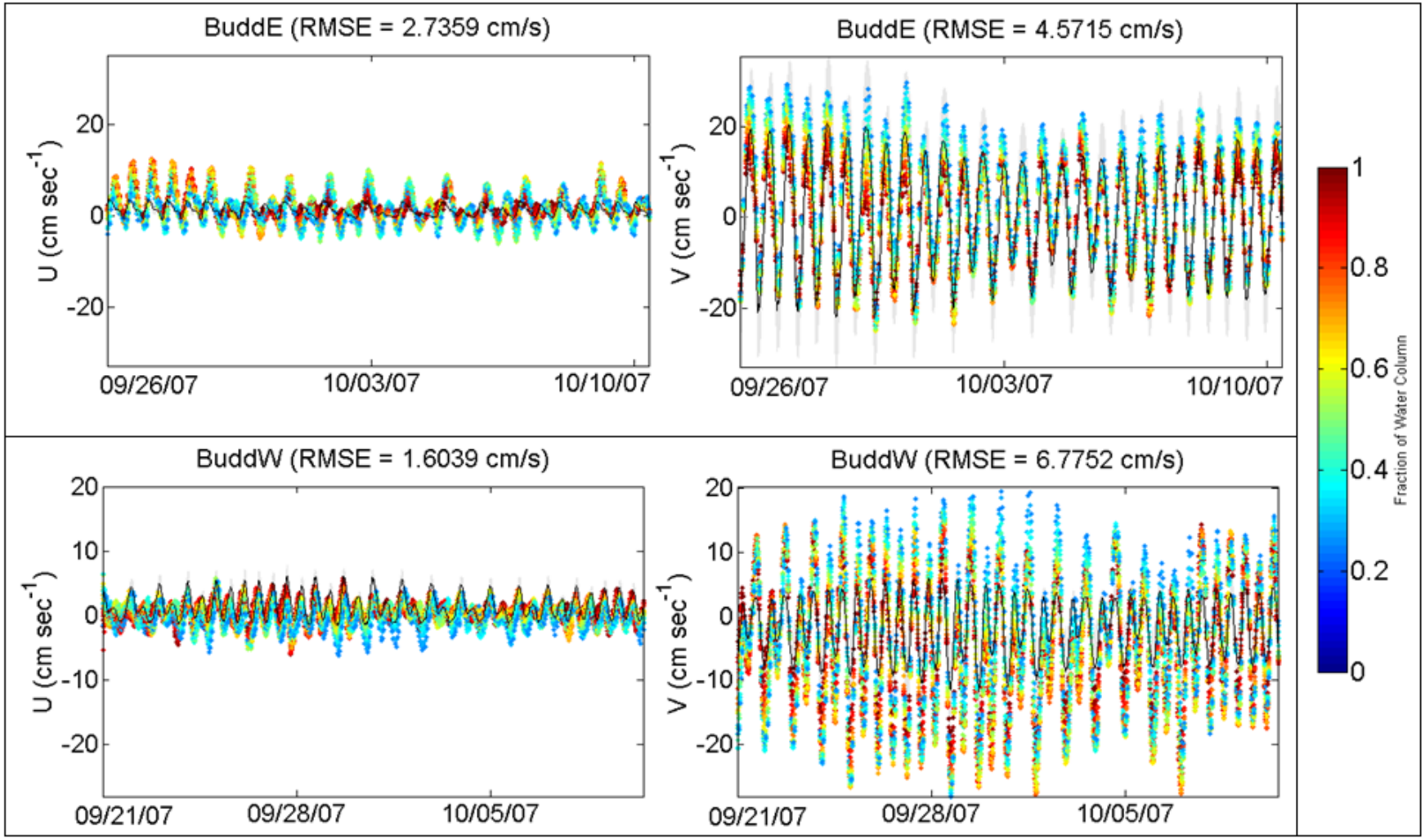


Figure 58. Budd Inlet East and West velocity comparison between the model and data for the northerly (v) and easterly (u) velocity components.

## Surface Currents

After the model was compared with observed velocity data, we evaluated surface currents during strong and weak ebb and flood tides. We compared the results with surface current patterns developed with Tide Prints (McGary and Lincoln, 1977). Appendix D includes tide prints for South Sound and main basin. Tide Prints was developed with the physical Puget Sound model using time-lapse photos of floating beads. The 2-dimensional figures represent typical strong and weak ebb- and flood-tide conditions. We compared model output for a strong and weak ebb- and flood-tide condition in September 2006.

On a strong ebbing tide (Figure 59), Central Puget Sound surface currents in the main basin reflect northerly currents, with more quiescent waters in Elliott Bay, Sinclair and Dyes Inlets, Quartermaster Harbor, and Commencement Bay. Strong surface currents are evident in the narrow passages of the Agate Passage, Port Washington Narrows, Rich Passage, and Colvos Passage. In South Puget Sound, the strong currents in Tacoma Narrows, Hale Passage, north and south of Anderson Island, Dana Passage, Hammersley Inlet, and Pickering Passage are well-represented. The model also reproduces the quiescent waters of northern Carr and Case Inlets, Oakland Bay, and the southern ends of Totten, Eld, and Budd Inlets.

Strong flood tides (Figure 60) produce similar patterns of varying quiescent and strong currents as well as the zones of convergence and divergence from Tide Prints. The model predicts that Colvos Passage floods to the south under this particularly strong event.

Under weak ebb (Figure 61) and flood (Figure 62) tidal exchanges, velocities are much lower in both Tide Prints and as predicted by the model. Quiescent waters extend further from land in the inlets of South Puget Sound. While diminished, surface currents through the narrow inlets are larger than those in the more quiescent bays. Under a weak flood tide, Colvos Passage floods to the north.

The model predicts the overall surface current patterns, including relative magnitude and direction, well.

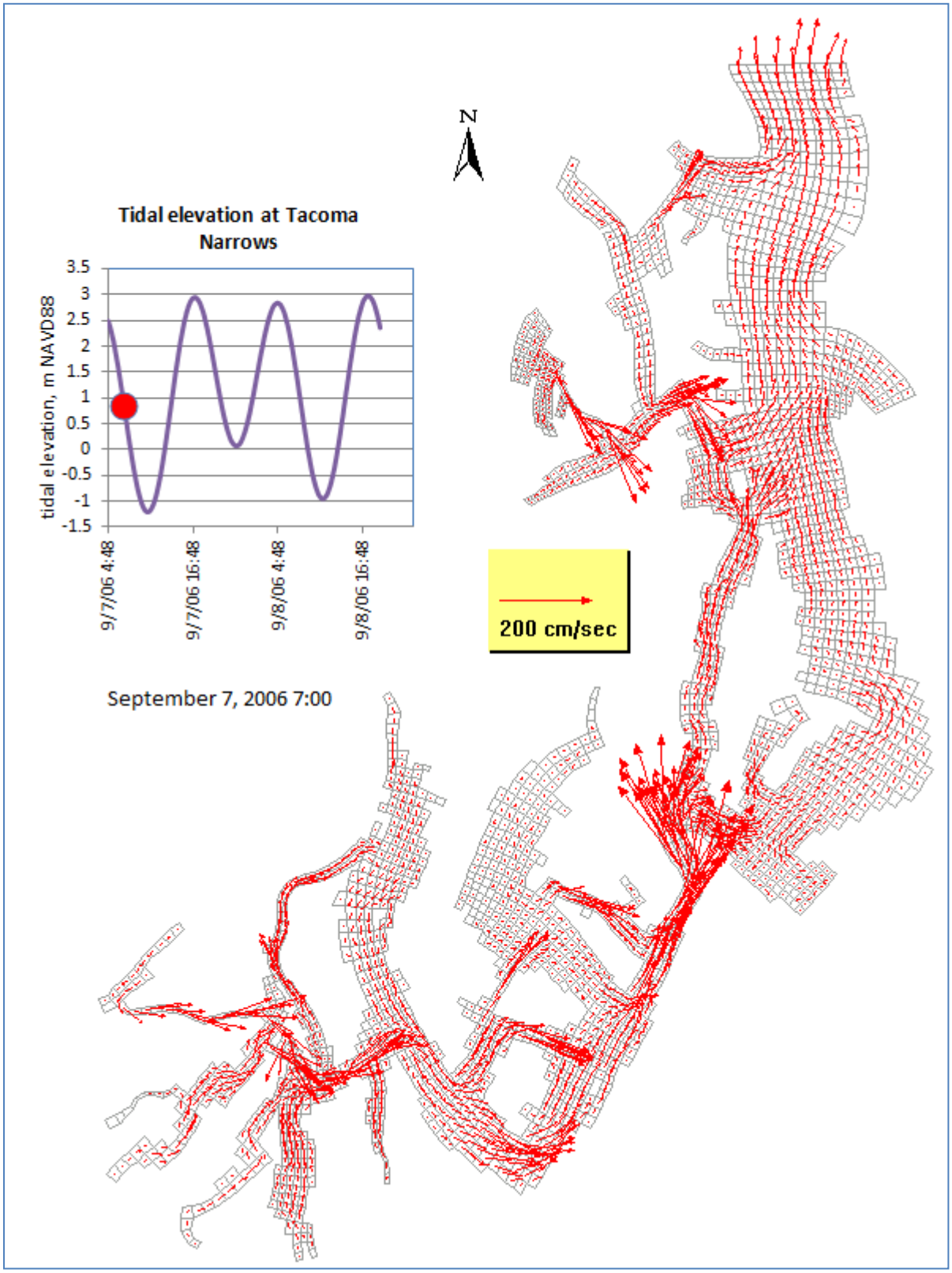


Figure 59. Surface current patterns during a strong ebb tide.

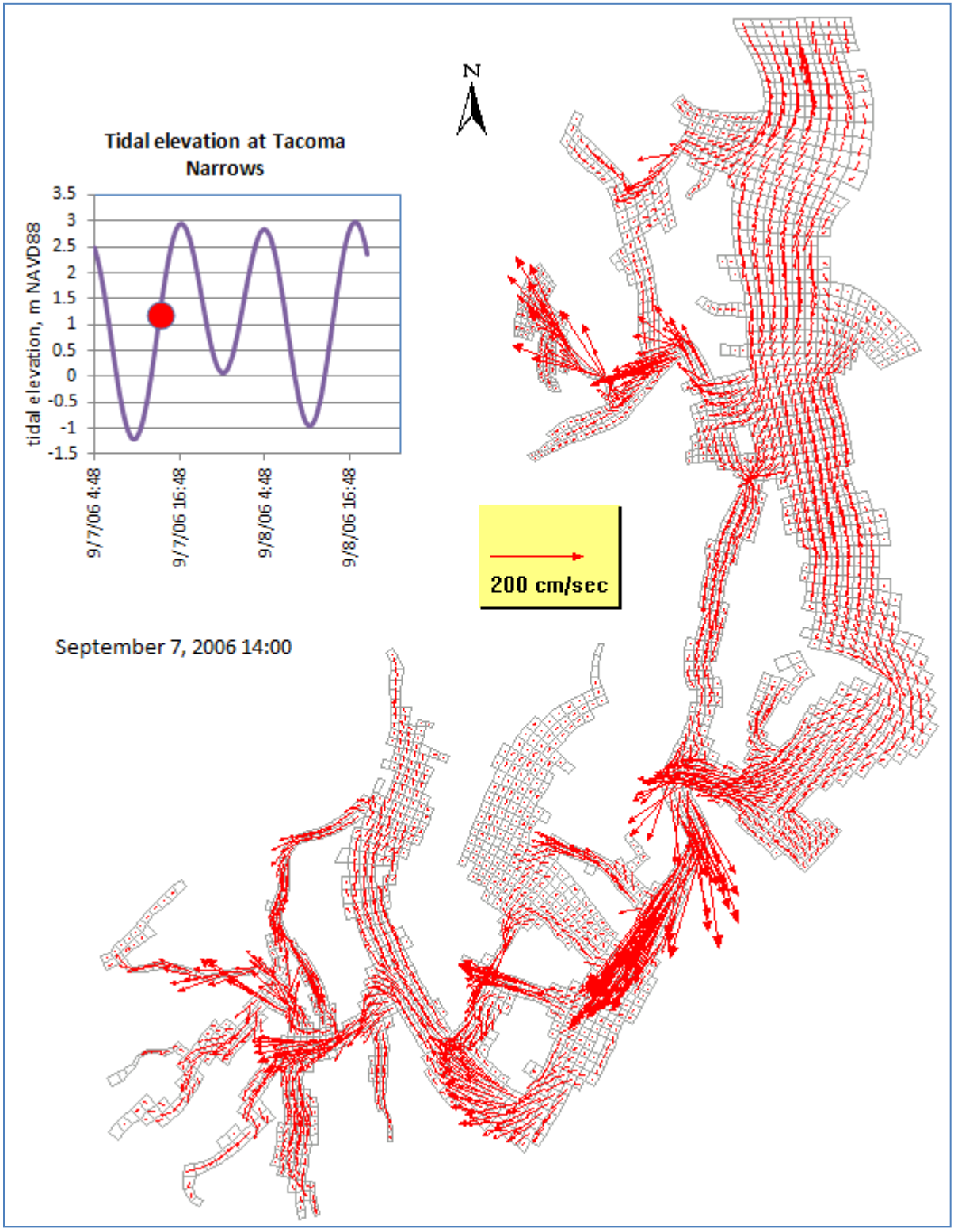


Figure 60. Surface current patterns during a strong flood tide.

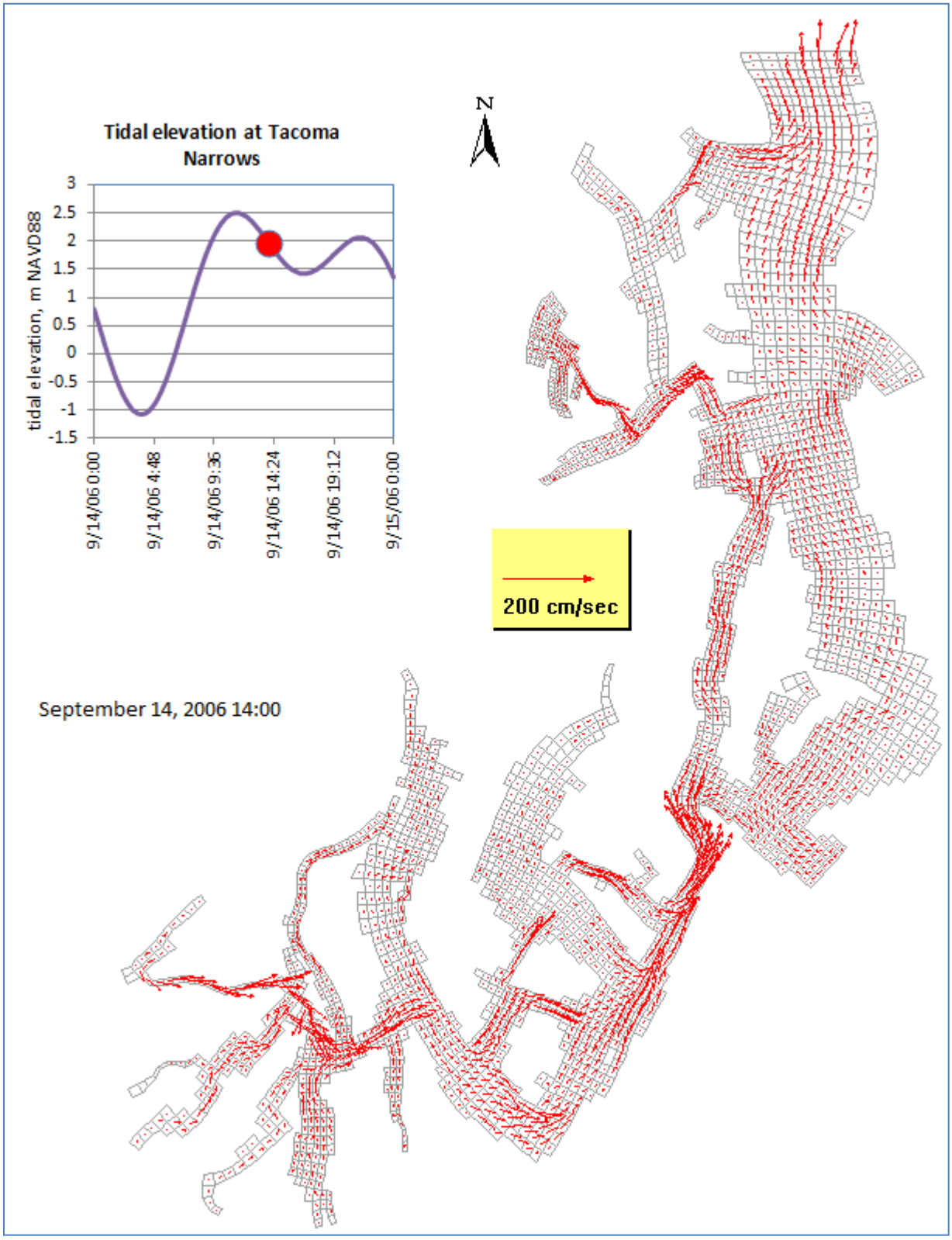


Figure 61. Surface current patterns during a weak ebb tide.

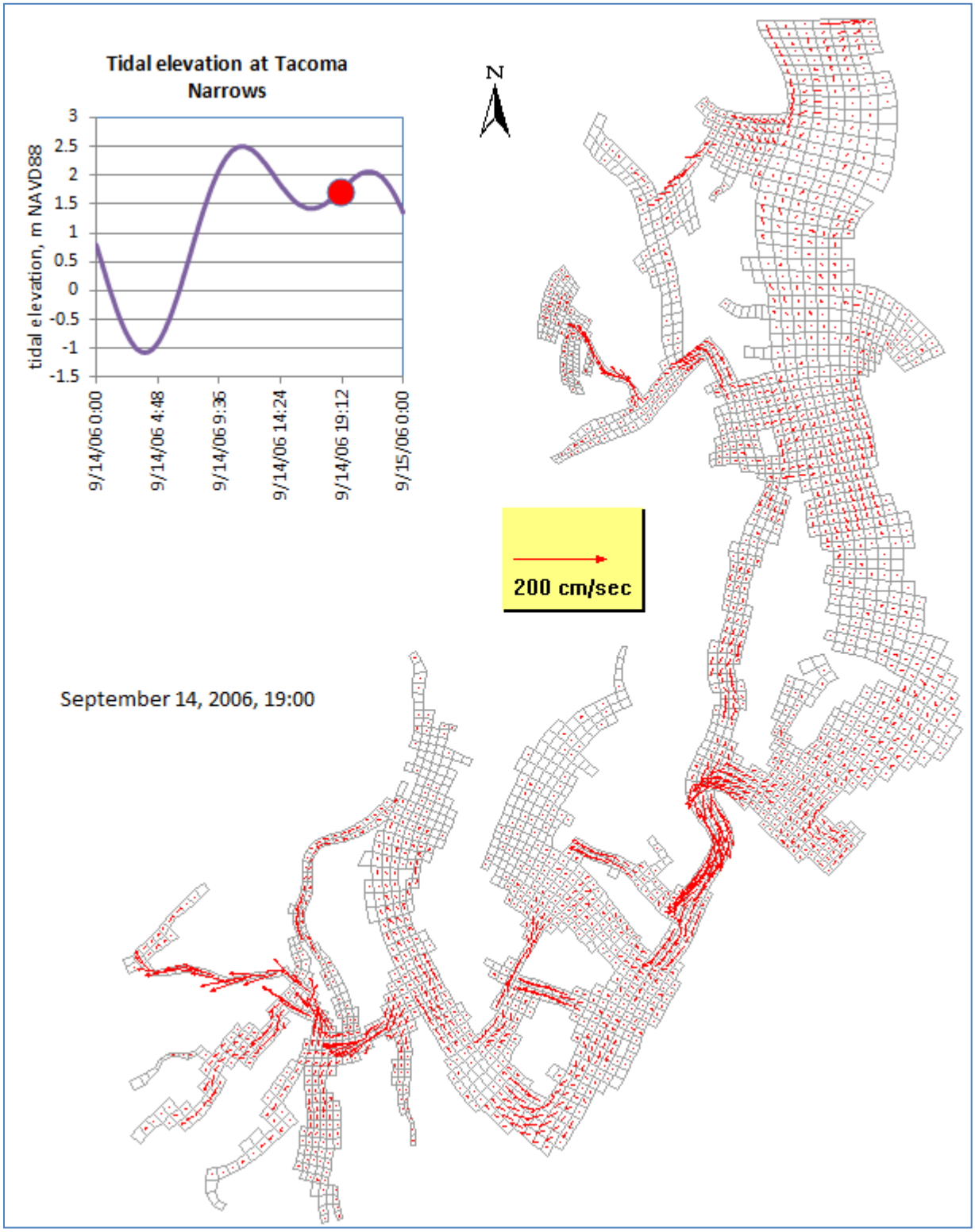


Figure 62. Surface current patterns during a weak flood tide.

## Channel Flows Across Transects

Channel flows were estimated from model at seven transects as shown in Figure 63. These transects were selected based on available literature data on channel flows at these locations.

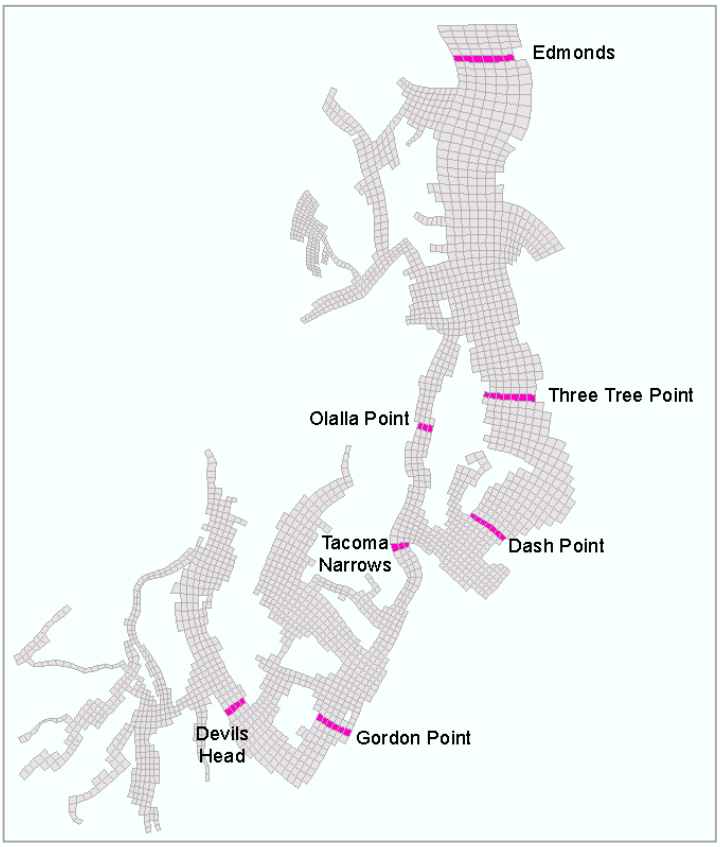


Figure 63. Locations of transects where channel flows were estimated.

Table 9 shows the model-predicted channel flows and the associated literature values. Note the difference in the method used. The model-predicted flows were based on average of all hourly model outputs between April and September 2007 across all cells and layers.

At Edmonds the model-predicted flows (16,520 $m^3/s$) were of the same order of magnitude as the Babson et al. (2006) box-model annual average flow (11,250 $m^3/s$). They are also within the range of flows predicted by Cokelet et al. (1990) (9,000 to 19,000 $m^3/s$) using fresh and salt water distributions. Flows based on month-long, cross-channel and mid-channel mooring data (Ebbesmeyer et al., 1984 and Cannon and Ebbesmeyer, 1978) were much higher (20,000 to 40,000 $m^3/s$) likely due to shorter time-span data.

Flow in East and Colvos Passages predicted by the model was an order of magnitude lower than most literature values except that from Babson et al. (2006) (estimated at 7500 $m^3/s$, which is the average of Tacoma Narrows and Edmonds flows reported by Babson et al., 2006). The model

does show the circulatory flow pattern around Vashon Island as described in the literature (see Table 9).

The model-predicted channel flows at Gordon Point, Devils Head, and Tacoma Narrows were of the same order of magnitude as literature values.

Table 9. Channel flows across various transects as predicted by the model and associated literature values.

| South and Central Puget Sound Model Location | Comparable station in literature | Seaward flow, $m^3/s$ | Landward flow, $m^3/s$ | Reference | Method |
|---|---|---|---|---|---|
| Near Edmonds | | 16520 | 16210 | Current study | time-weighted average (April-September 2007) |
| | Jefferson Point | | 9,000 - 19,000 | Cokelet et al. 1990 | salt and freshwater distribution, annual average (1953-1955) |
| | Jefferson Point | | 42,000 - 43,000 | Cannon and Ebbesmeyer, 1978 | month long single mid-channel current mooring (1972 - 1973) |
| | Jefferson Point | | 20,000 - 22,000 | Ebbesmeyer et al. , 1984 | cross-channel current moorings |
| | Main to Admiralty | | 11250 | Babson et al. 2006 | Box model annual average (1992 - 2001) |
| Upper East Passage | Three Tree Point | 1580 | 10160 | Current study | time-weighted average (April-September 2007) |
| | | | 24,000 - 40,000 | Cokelet et al. 1990 | salt and freshwater distribution, annual average (1953-1955) |
| | | | 38,000 | Cannon, 1983 | mid-channel current mooring |
| | | | 23,000 | Bretschneider et al. 1985 | Cross-channel current moorings (March 18 - April 25, 1983) |
| | | | 7,500 | Babson et al. 2006 | estimated as average of Edmonds and Tacoma Narrows |
| Lower East Passage | Dash Point | 1980 | 10620 | Current study | time-weighted average (April-September 2007) |
| | | | 21,000 | Bretschneider et al. 1985 | Cross-channel current moorings (March 18 - April 25, 1983) |
| Colvos Passage | Olalla Point | 8540 | | Current study | time-weighted average (April-September 2007) |
| | | 24,000 - 40,000 | | Cokelet et al. 1990 | salt and freshwater distribution, annual average (1953-1955) |
| | | 27,000 | | Cannon, 1983 | mid-channel current mooring |
| | | 25,000 | | Barnes and Ebbesmeyer, 1978 | mid-channel current mooring |
| | | 26,000 | | Bretschneider et al. 1985 | mid-channel current mooring |
| Near Ketron Island | Gordon Point | 5500 | 4911 | Current study | time-weighted average (April-September 2007) |
| | | | 8,400 - 21,000 | Cokelet et al. 1990 | salt and freshwater distribution, annual average (1953-1955) |
| Uper Nisqually Reach | Devils Head | 4030 | 4030 | Current study | time-weighted average (April-September 2007) |
| | | | 3,800 - 6,500 | Cokelet et al. 1990 | salt and freshwater distribution, annual average (1953-1955) |
| Upper Tacoma Narrows | Tacoma Narrows | 5870 | 5830 | Current study | time-weighted average (April-September 2007) |
| | South Sound to Narrows | | 3750 | Babson et al. 2006 | Box model annual average (1992 - 2001) |

# South Puget Sound Flushing Times

The amount of time water parcels and constituents in the water remain in a given geographical area is fundamental to understanding water quality. However, there is no single agreed-upon method for doing so (Monsen et al., 2002). Flushing time, age, and residence time have been used synonymously to describe how long a water parcel stays in a waterbody. Different mathematical approaches produce order-of-magnitude differences in the resulting time calculations.

Considering a waterbody or a model grid cell as a continuously stirred tank reactor (CSTR), the concentration of an added conservative tracer (that neither decays nor settles) will be instantly mixed throughout the reactor so that the concentration at the outlet will be the same as that in the tank. If C(t) is the concentration of the tracer in the outlet at any time represented as t, then C(t) is described as a simple exponential equation:

$$C(t) = C_o e^{-t/T_f}$$

Where $C_o$ is the initial concentration and $T_f$ is the flushing time.

When t = $T_f$ , $\frac{C(t)}{C_o} = \frac{1}{e}$ = 0.37, also known as the fraction remaining after one e-folding time or flushing time/residence time. Additional, correlations exist between time to achieving a certain percent reduction and flushing time:

- Time to reach 50% of initial concentration (half-life) = ln(2)*$T_f$ = 0.693*$T_f$
- Time to reach 10% of initial concentration = ln(10)*$T_f$ = 2.3*$T_f$
- Time to reach 1% of initial concentration = ln(100)*$T_f$ = 4.3*$T_f$

However, different formulations/methods exist to estimate $T_f$. These are discussed below.

The simplest flushing time estimate, $T_{f1}$, is simply the volume (V, $m^3$) divided by the net exchanges (Q, cms):

$$T_{f1} = \frac{V}{Q}$$

The equation can be modified to account for just the intertidal volume and the reflux of water at the boundary of the user-defined volume:

$$T_{f2} = \frac{VT}{(1-b)P}$$

Where V is the total volume, P is the volume of the tidal prism between high tide and low tide, T is the tidal period, and b is the reflux factor that varies from 0.0 to 1.0.

The flushing time for South Puget Sound is 4.7 days using a reflux factor of 3% and tidal period of 12.2 hrs (University of Washington, 1971). This approach neglects the freshwater contribution.

However, the effective flushing time of South Puget Sound is longer than the simple $T_{f1}$ or $T_{f2}$ calculations. First, physical processes along the shallow entrance sill just southwest of the Tacoma Narrows impede flow and increase the residence time (Seim and Gregg, 1997). Flood tides transport some of the same water that exited on the previous ebb tide in a process called reflux. Second, estuarine flow leads to two-layer flow that isolates the lower layer and increases flushing time. A third approach to estimate flushing based on a two-layer salt balance (Friebertshauser and Duxbury, 1972) produces flushing times of 28 to 174 days (average annual of 56 days), longer than those derived from simple tidal volume replacement because of estuarine circulation.

Babson et al. (2006) report simple $T_{f1}$ (V/Q) residence times of 19 to 33 days for South Puget Sound. They used a simple two-layer box model to estimate residence time as the ratio of basin volumes to estuarine transport flows.

Another approach is following a tracer concentration that accounts for both advective and dispersive transport. Rearranging the exponential equation for tracer concentration shown previously, a linear equation can be written as follows:

$$\ln C(t) = -\frac{1}{Tf_3}\, t + lnC_0$$

$T_{f3}$ can be estimated as the slope of a best-fit linear regression drawn through a time series of observed tracer concentrations. This approach accounts for not just advection, as per the previous methods, but also dispersion.

We evaluated flushing time by filling portions of South Puget Sound in the model with a simulated dye tracer and then estimated the time to achieve 37% (1/e) dye remaining at specific locations. This method is also called the e-folding time. We first evaluated patterns throughout South Puget Sound by filling the entire region with dye southwest of the Tacoma Narrows and then the entire region south of the Edmonds open boundary (Figure 64).

The time to reach 1/e (37%) of the initial tracer concentration ranges from 3 to 108 days depending upon station location within South Puget Sound (Table 10). This residence time increased, as expected, to 70 to 157 days for the same stations when the whole domain was dyed. Figure 64 presents the time series of maximum water column tracer concentration at the 13 grid cells south of Tacoma Narrows for the two regional dye tracer studies. Figure 65 presents the dye concentration contours at the end of the simulation to illustrate spatial patterns. Longer flushing times when larger domain is considered is evident from all these figures and tables.

We also evaluated flushing time on an inlet-by-inlet basis. To evaluate inlet-specific flushing time and spatial variability within smaller regions, we filled each of five small inlets with simulated dye tracer (Figure 66). The e-folding time for a remote cell in each inlet is also presented in Figure 66. The remote cell in Oakland Bay and Eld Inlet has the shortest and

longest e-folding time, respectively, among the 5 inlets. A plan view map of the inlets showing maximum water column dye concentrations when the remote cell reaches e-folding time are also presented in Figure 66. Higher concentrations remain at the heads of each of the inlets, where exchanges with South Puget Sound are lowest. Given the large variation within an inlet, an inlet-average value must be interpreted carefully.

Because different methods previously used to quantify flushing time produce such highly variable results (4.7 to 174 days), comparing an absolute flushing time for South Puget Sound is not appropriate. However, the model confirms that when estuarine circulation is considered, residence times on the order of several months are reasonable and comparable to the range from previous salt-balance estimates. Also, tracer concentrations at the Tacoma Narrows will be strongly affected by the tidal stage at the beginning of the tracer run. Flushing time will vary seasonally due to changing freshwater contributions that affect net transport and changing tidal prisms.

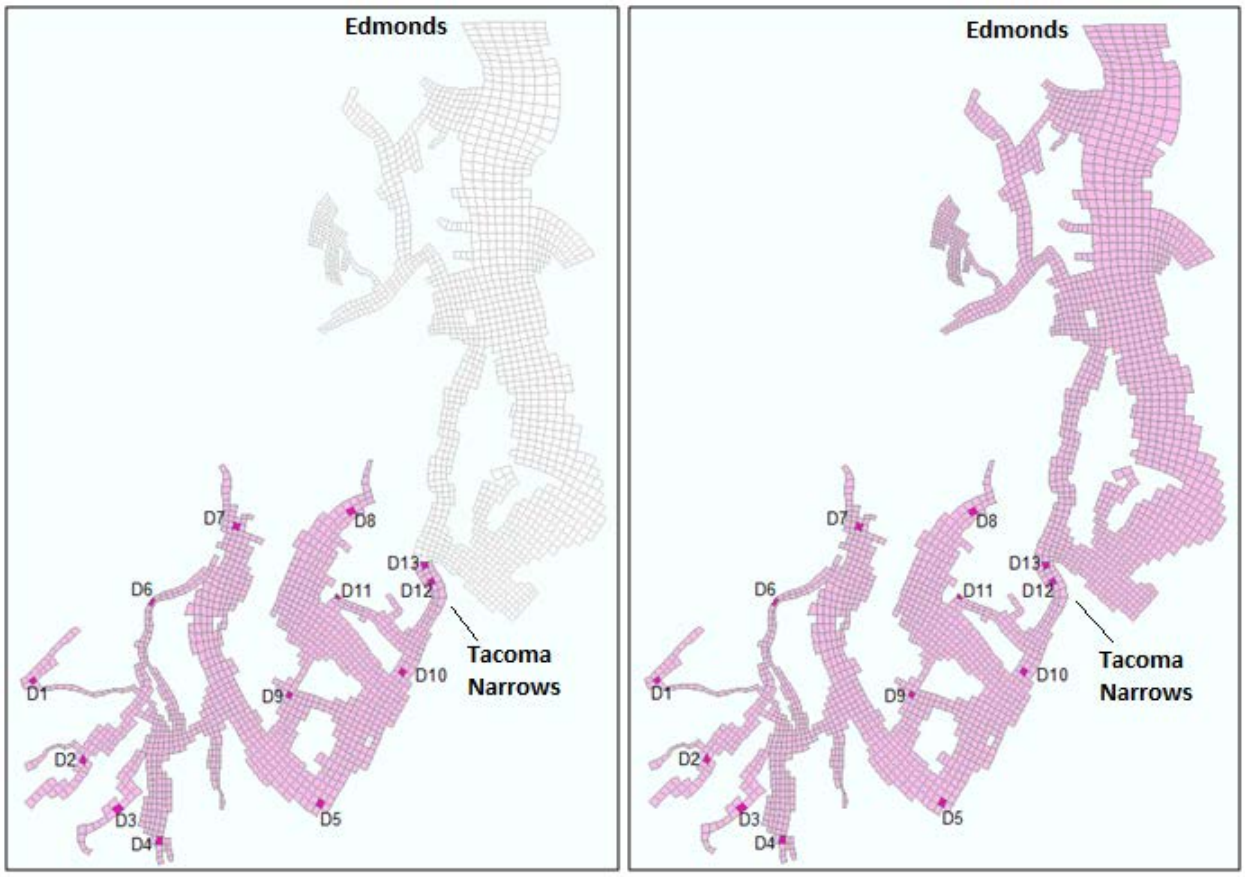


Figure 64. Station locations for flushing times and regional extent where initial simulated dye was added.

Table 10. e-folding times at various stations with South Sound and domain-wide initial dye.

| Station | e-folding time, days | |
|---|---|---|
| | Dye_south of TN | Domain wide dye |
| D13 | 3.1 | 70.4 |
| D12 | 17.6 | 70.4 |
| D11 | 56.4 | 98.3 |
| D10 | 24.3 | 80.2 |
| D9 | 66.1 | 99.6 |
| D8 | 81.8 | 112.3 |
| D7 | 107.7 | 157.1 |
| D6 | 103.8 | 153.7 |
| D5 | 65.2 | 111.5 |
| D4 | 100.8 | 129.6 |
| D3 | 104.5 | 145.0 |
| D2 | 99.1 | 137.2 |
| D1 | 93.6 | 129.4 |

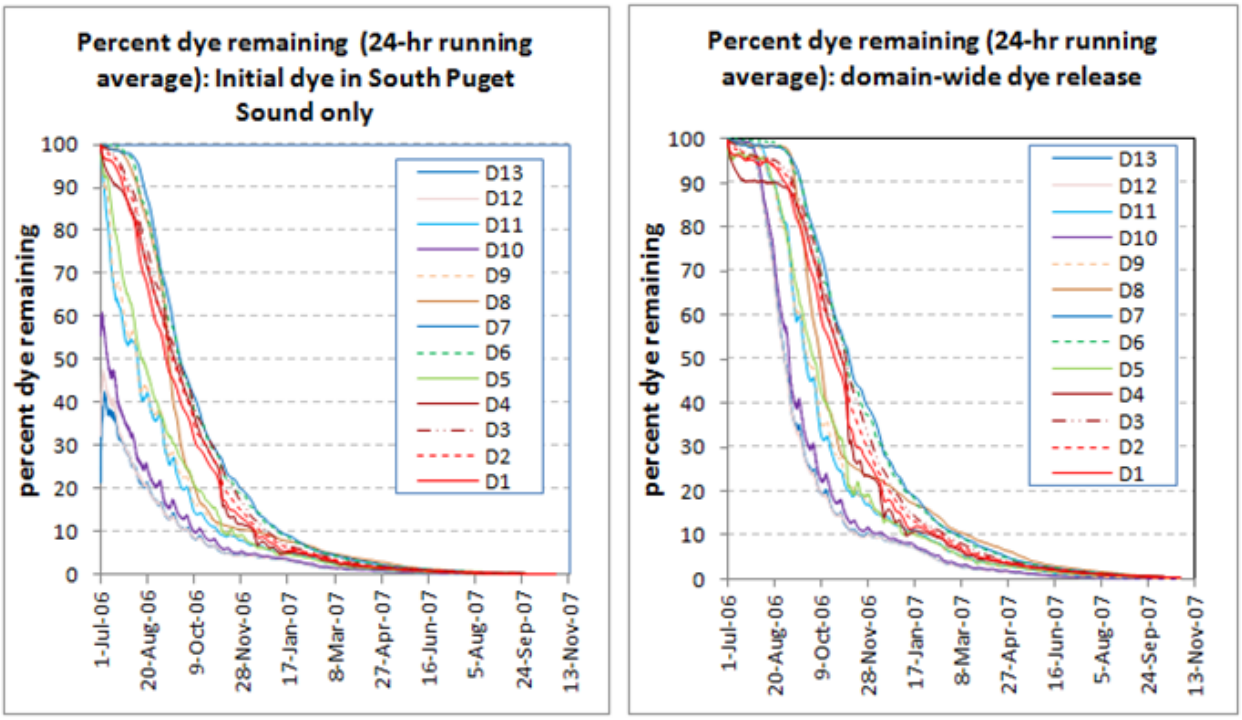


Figure 65. Simulated tracer time-series at different locations (Figure 64) in South Puget Sound.

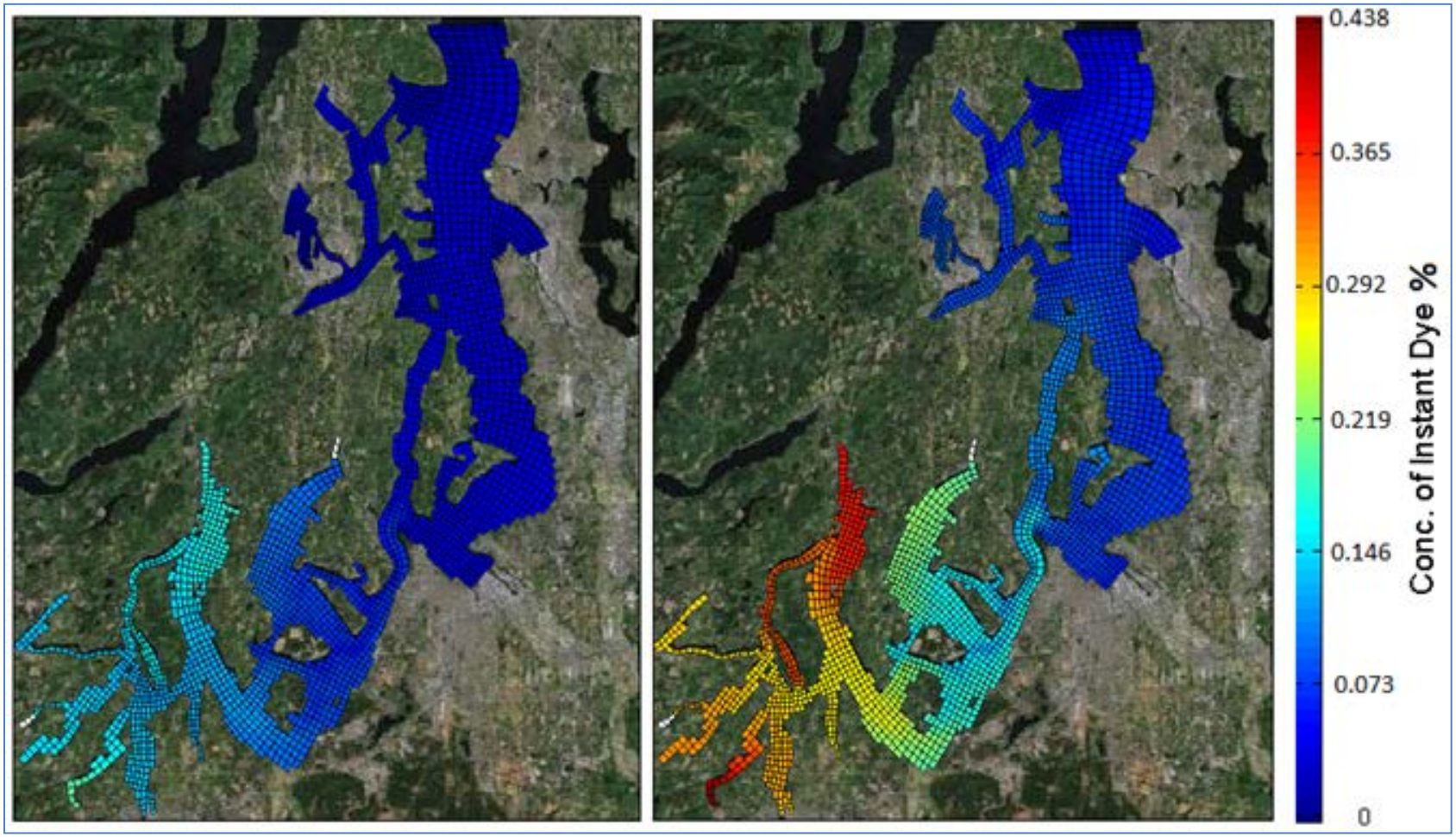


Figure 66. Spatial patterns of simulated dye concentration at the end of the model simulation period (Oct 29, 2007) with initial dye south of Tacoma Narrows (left) and domain wide (right).

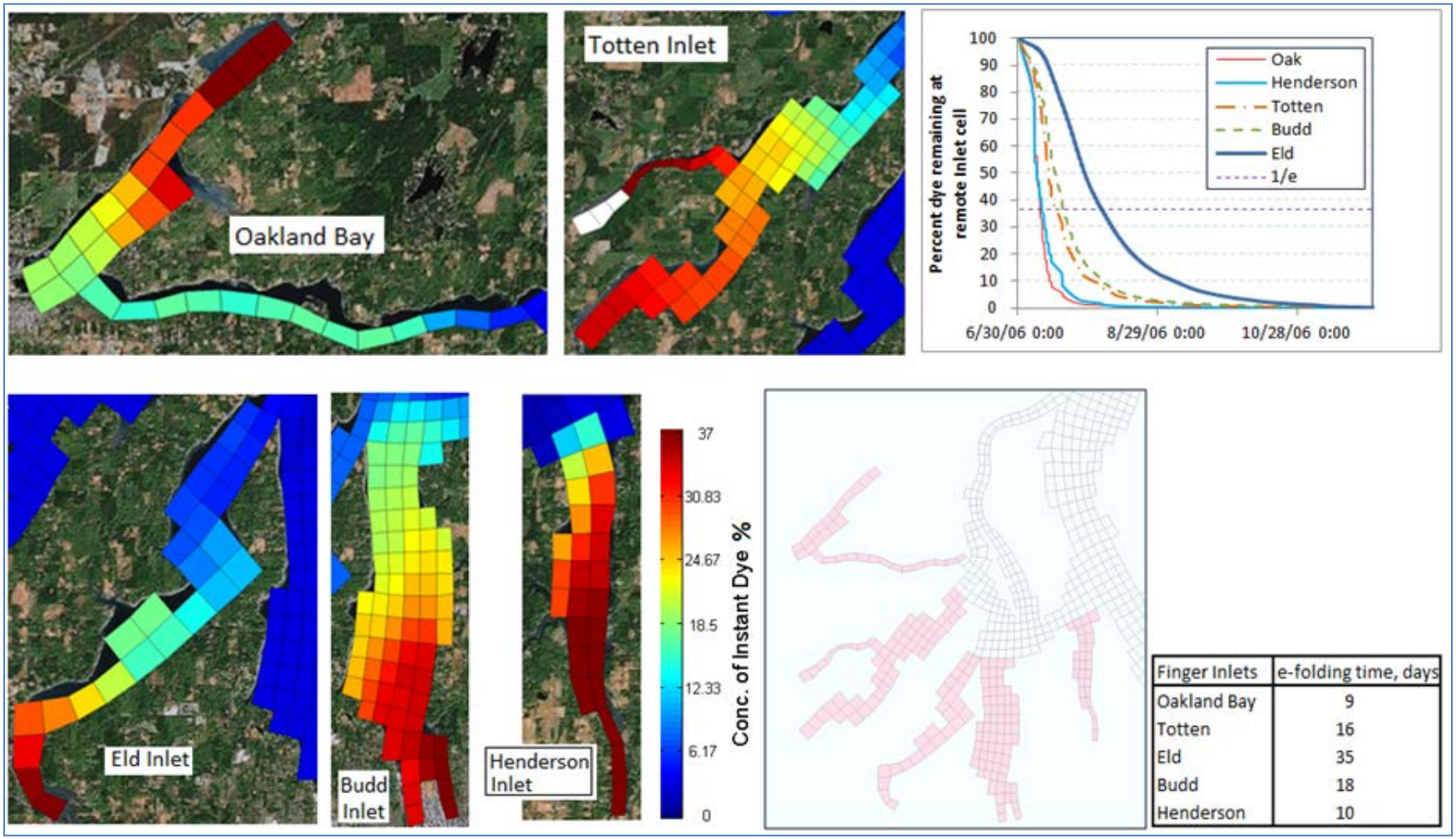


Figure 67. Snapshot of maximum simulated dye concentration at end of e-folding time for remote cell in each inlet.

# Areas Influenced by Marine Point Sources and Watershed Inflows

We simulated dye releases from all river inflows and wastewater facilities to evaluate areas influenced by watershed inflows and wastewater treatment plants. Watershed inflows were added to the surface layer while marine point source discharges were added to the various trapping layers (see Appendix B).

The model simulated continuous virtual dye releases equivalent to 30 mg/L concentration with neutral buoyancy beginning July 1, 2006. The model uses time-varying daily river flows and wastewater facility discharges. Table 11, however, lists the mean September 2006 flows for watershed inflows >10 cfs and marine point sources > 1 mgd to indicate relative discharge rates. Figure 68 and Figure 69 identify the discharge locations for the watershed inflows and marine point sources, respectively.

Table 11. Mean September 2006 discharges for all watershed inflows >10 cfs and marine point source discharges >1 mgd.

| River or Creek | Flow rate (cfs) | | Treatment plant | Flow rate (cfs) |
|---|---|---|---|---|
| Puyallup River | 1272 | | West Point | 136 |
| Nisqually River | 499 | | South King | 86 |
| Lake Washington watershed | 395 | | Simpson Tacoma (process) | 28 |
| Green River | 340 | | Chambers Creek | 25 |
| Sinclair/Dyes watershed | 112 | | Tacoma Central | 22 |
| Deschutes River | 61 | | LOTT | 13 |
| Goldsborough Creek | 42 | | Lakota | 7.4 |
| Chambers Creek | 32 | | Bremerton | 6.4 |
| Burley Creek | 20 | | Midway | 6.0 |
| McAllister Creek | 19 | | Tacoma North | 5.6 |
| Mill Creek | 18 | | Central Kitsap | 5.2 |
| Sherwood Creek | 18 | | Fort Lewis | 4.3 |
| Sequalitchew Creek | 17 | | Miller | 3.9 |
| Cranberry Creek | 17 | | Redondo | 3.3 |
| Kennedy Creek | 14 | | Salmon | 2.8 |
| Curley Creek | 14 | | Port Orchard | 2.1 |
| Rocky Creek | 14 | | Shelton | 2.1 |
| Skookum Creek | 12 | | Gig Harbor | 1.1 |
| Coulter Creek | 12 | | | |
| Minter Creek | 12 | | | |
| Olalla Creek | 11 | | | |
| Hylebos Creek | 11 | | | |

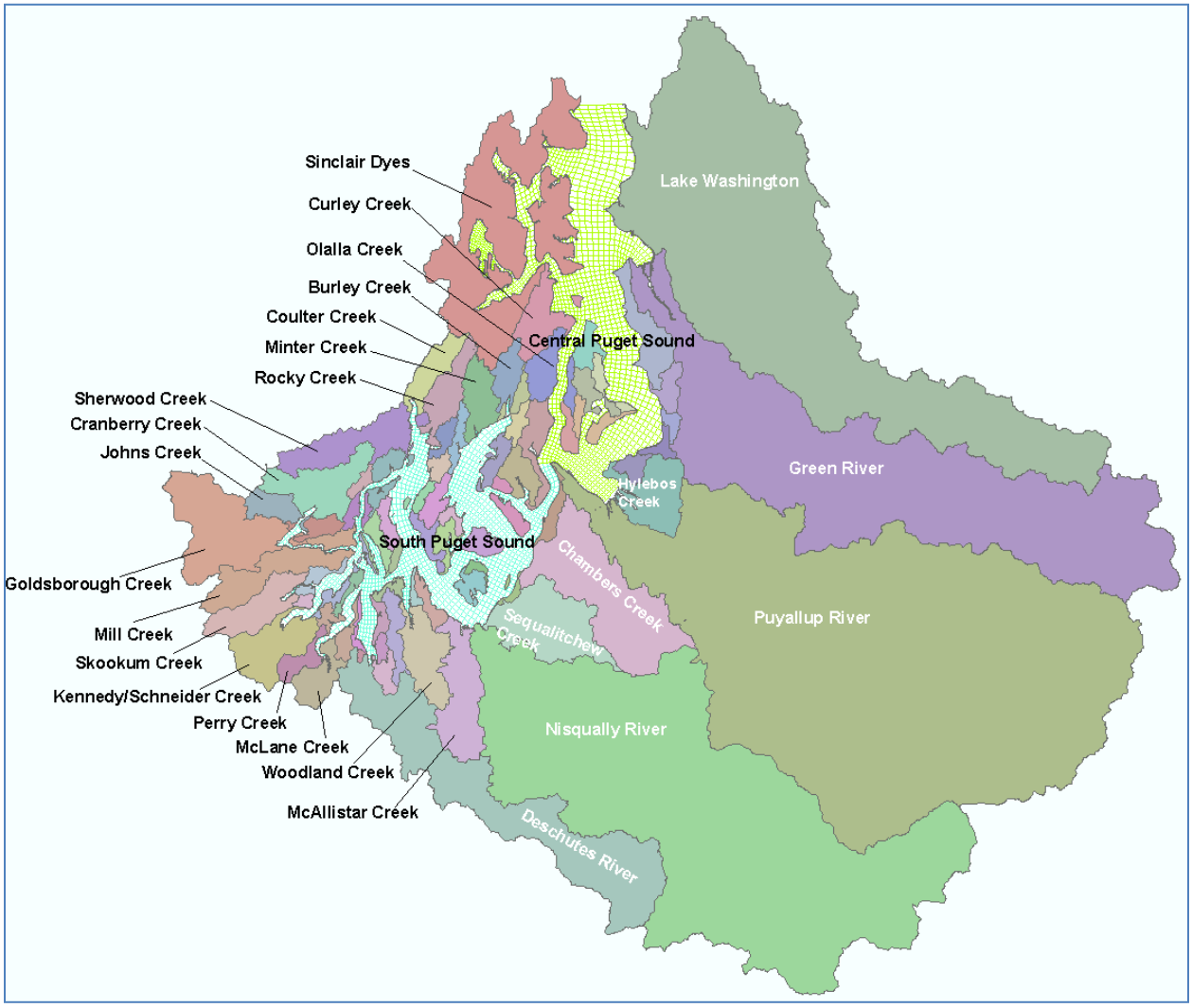


Figure 68. Locations of watersheds in South and Central Puget Sound (only major watersheds labeled).


Figure 69. Marine point source discharges to South and Central Puget Sound.

.

The model simulates virtual tracer concentrations throughout the model domain in four separate runs, one each for watershed inflows and marine point sources in either South or Central Puget Sound, distinguished by the Tacoma Narrows. Maximum dye concentrations can occur near the surface or near the bottom, but results are represented as a water-column maximum value from any model layer. Also, the marine flow trajectory reverses with the flood- or ebb-tide phase and varies with the current velocity.

Because tracer concentrations decrease rapidly away from inflows, the figures in this section summarize model predictions as contours of the minimum dilution factors to illustrate how the freshwater moves through the marine system. Where predicted concentrations are highest, the dilution factor is lowest, and the dilution factor incorporates order of magnitude changes in dye concentration. A dilution factor of 10 means the maximum tracer concentration is $1/10^{th}$ or 10% of the initial inflow tracer and a dilution factor of 100 corresponds to a maximum tracer concentration of $1/100^{th}$ or 1% of the initial value.

We used the Puget Sound box model (Babson et al., 2006; Sackmann, 2009) to evaluate how long dye released into South or Central Puget Sound would continue to build up to a pseudo-steady-state condition. Box model simulations indicated that the dye continues to build up for several months. We selected September 2007 for output comparison to represent a critical condition for two reasons. First, the model run begins July 1, 2006, and the dye would not reach pseudo-steady state by the September 2006 critical period. Second, although the buildup reaches pseudo-steady state in the winter months, this is not a time of year when low dissolved oxygen levels occur. Therefore, we continued the dye releases through October 2007 and investigated the levels in September 2007.

Figure 69 summarizes tracer releases from South Puget Sound watershed inflows. Lowest dilution levels correspond to the highest predicted tracer concentrations nearest to the inflows. Maximum concentrations occur near the water surface close to the watershed inflows, but watershed tracers extend throughout South Puget Sound. At least some tracer exits through Tacoma Narrows with a dilution level on the order of 100:1, and that water tends to travel north up Colvos Passage.

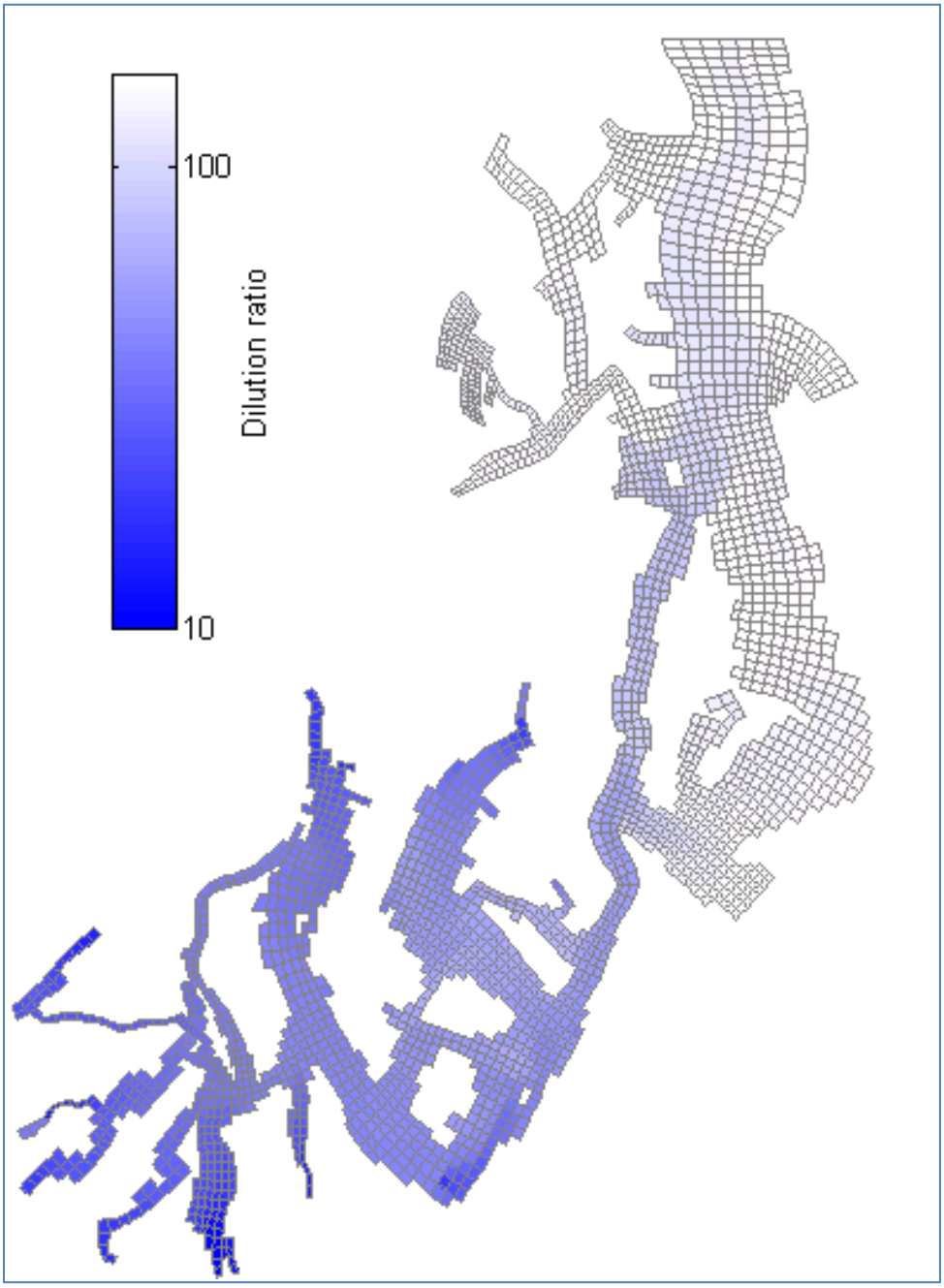


Figure 70. Dilution factors calculated from maximum water-column dye concentrations for South Puget Sound watershed inflow tracer simulations (September 2007).

Tracer from South Puget Sound marine point sources also is highest and the dilution levels are lowest closest to the inflows (Figure 71). Lowest dilution levels, which reflect highest tracer concentrations, occur in Budd Inlet and Hammersley Inlet/Oakland Bay, where marine point sources discharge to quiescent waters. Tracers from the Chambers Creek and Fort Lewis wastewater discharges produce more rapid dilution even though those facilities have higher flow rates, likely due to the higher water exchanges. Beyond the immediate vicinity of the marine point sources, maximum concentration and minimum dilution occur within the top several model layers due in part to the overall shallow water at the discharges and fewer model layers. Wastewater effluent buoyancy may also contribute.

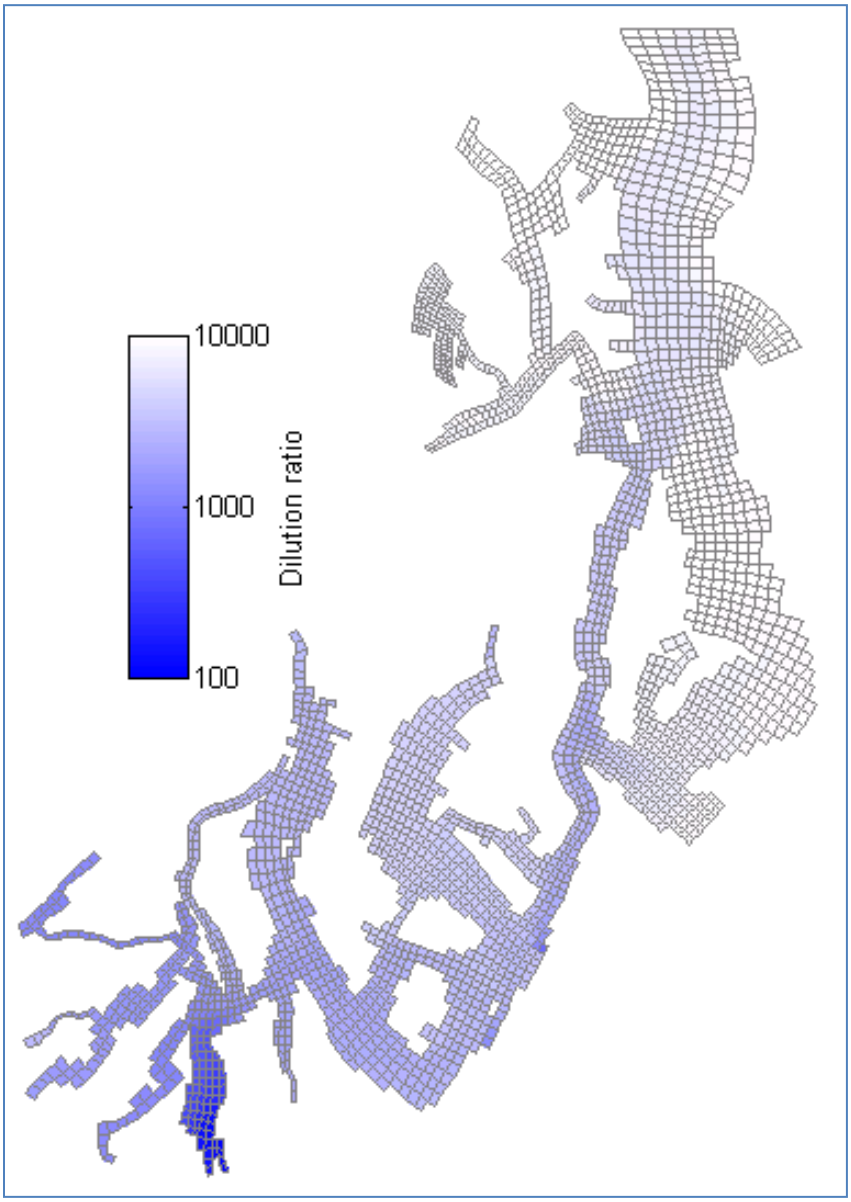


Figure 71. Dilution factors calculated from maximum water-column dye concentrations for South Puget Sound marine point source tracer simulations (September 2007).

Next, virtual tracer was added to watershed inflows discharging to Central Puget Sound (Figure 71). Lowest dilution (highest tracer concentration) occurs in Commencement Bay and Elliott Bay, where the Puyallup River and Lake Washington watersheds produce high inflow volumes. On flood tides, at least some Central Puget Sound watershed inflow tracer enters South Puget Sound. Lowest dilution occurs in the surface waters of Central Puget Sound, and the tracer that enters South Puget Sound tends to remain in the surface layers with uniform dilution levels.

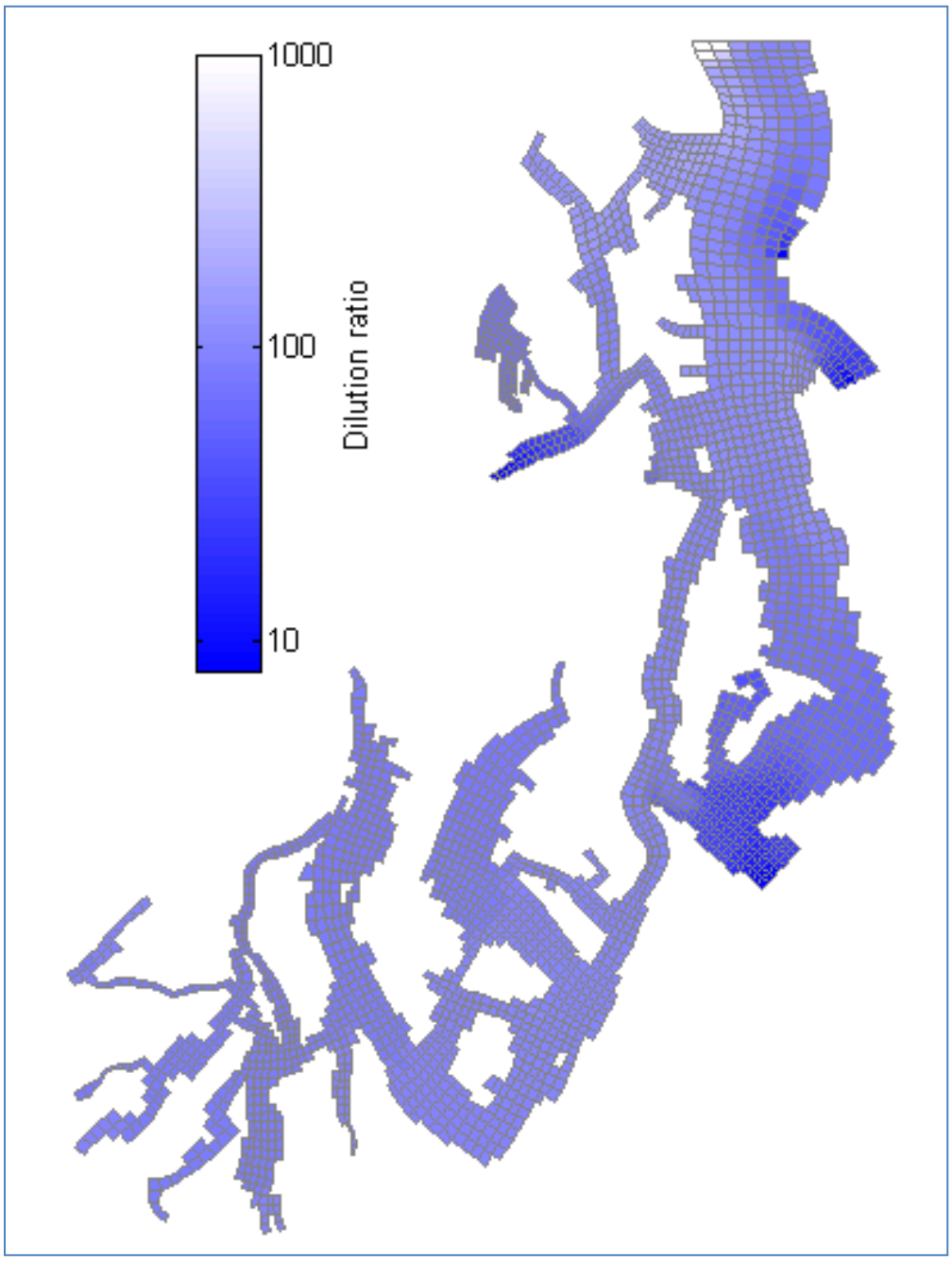


Figure 72. Dilution factors calculated from maximum water-column dye concentrations for Central Puget Sound watershed inflow tracer simulations (September 2007).

Marine point source discharges to Central Puget Sound produce the highest concentrations and lowest dilution nearest the discharges near the population centers of Seattle, Tacoma, and Bremerton (Figure 73). Nearest the marine point source discharges, maximum concentrations and minimum dilution occur in deeper model layers, consistent with near-bottom effluent discharges. However, some dye reaches surface layers within Central Puget Sound. At least some tracer from the Central Puget Sound marine point source discharges enters South Puget Sound on flood tides. Dye concentrations produced in South Puget Sound by Central Puget Sound sources are relatively uniform and reach maximum levels in the lower water column.

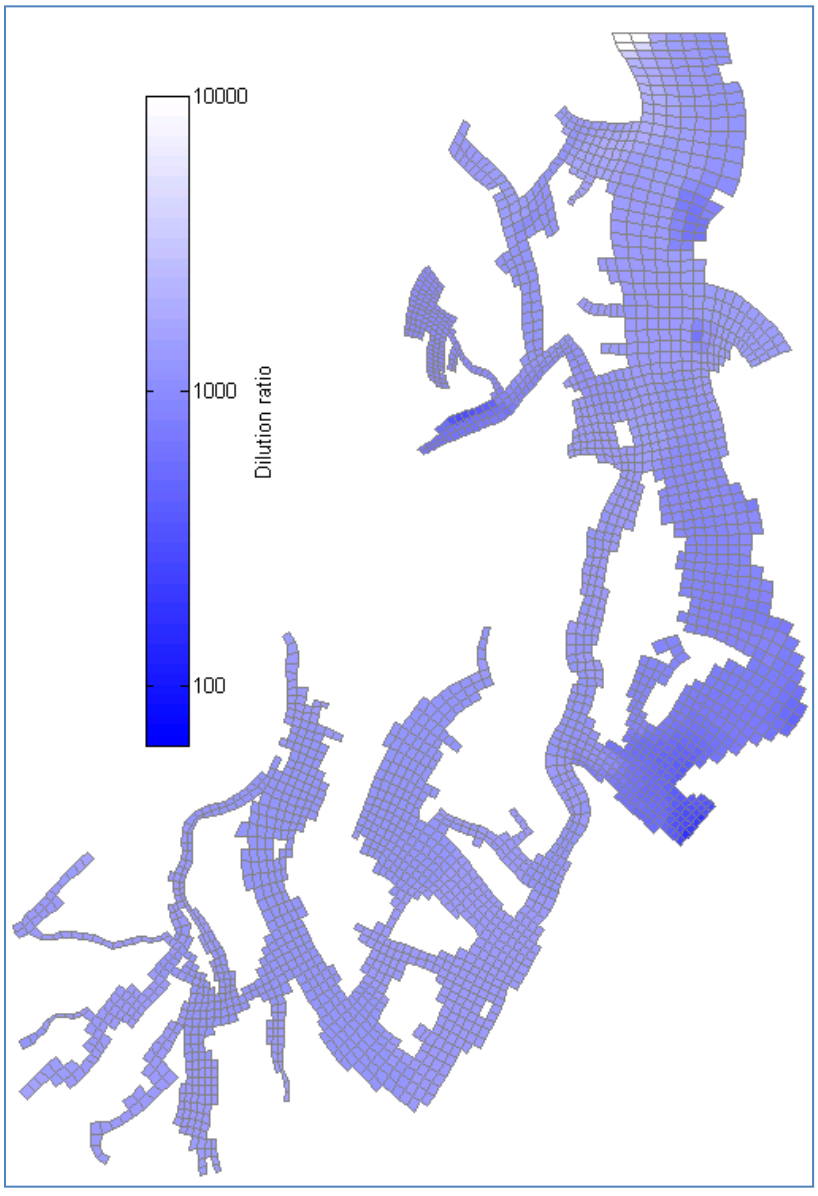


Figure 73. Dilution factors calculated from maximum water-column dye concentrations for Central Puget Sound marine point source discharge tracer simulations (September 2007).

The purpose of the tracer simulations was to determine the potential connectivity between Central Puget Sound nutrient sources and South Puget Sound water quality. Because at least some of the simulated tracer released from Central Puget Sound watershed inflows and marine point sources enters South Puget Sound during the critical period for low dissolved oxygen levels, we cannot rule out the influence of the Central Puget Sound sources.

Given the intricacies of nutrient transport and transformation within the marine environment, these results do not verify that Central Puget Sound nutrients influence South Puget Sound dissolved oxygen levels. This question is partly addressed with the detailed water quality model described in Ahmed et al. (2014). The model evaluates where nutrients from human sources spur algae growth.

# Conclusions

The South and Central Puget Sound circulation model was calibrated and confirmed using 2006 and 2007 water surface elevations, salinity and temperature data, and current velocities. The circulation model performs well and provides the basis for the water quality model described in Ahmed et al. (2014).

## Tidal Elevations

Overall, the model-predicted water surface elevations agree well with a RMSE of <16 cm (<5% of the tidal range) throughout the model domain. Hammersley Inlet/Oakland Bay had an RMSE of 40 cm (9% of the tidal range), due to subtle shape complexities that could not be represented well enough by the model grid to describe this fine-scale area. However, the effects were limited in geographic area, and a separate water quality model is available should it be needed (Ahmed and Wagner, 2011).

In addition to comparing the water surface elevations, we transformed the predicted elevations into tidal constituents represented by magnitudes and phases in the frequency domain. The model captures the magnitude and phasing of the five (O1, K1, N2, M2, and S2) major tidal constituents well. Oakland Bay had the largest errors in the tidal constituents.

## Temperature and Salinity

The complex shape and circulation patterns produce highly variable temperature and salinity patterns in the model domain, particularly in the surface layers that are influenced by both the meteorological and river boundary conditions. The model reproduces the spatial and temporal patterns in both the surface and near-bottom layers.

The model replicates salinity and temperature throughout the model domain well, although some sharp gradients could not be represented. The overall RMSE for temperature was 0.78 °C with a mean bias of -0.14 °C. However the bias for temperature is not statistically significant because it lies within 2 standard deviations of zero difference (i.e., at the 95% confidence interval). The overall RMSE for salinity was 0.75 ppt with a mean bias of -0.32 ppt. Again, within the 95% confidence interval, the bias is not significant.

Limited boundary condition (temperature and salinity) sensitivity analyses were performed as part of model calibration. Additional analyses may be performed as needed.

## Current Velocities

The model reproduces the cross-sectional averaged instantaneous current velocities recorded at key transects well, including relative magnitudes and phasing. However, several transect aspects were very different from model grid cell orientation, and the direction change likely contributed to differences between the data and model. Bottom-mounted current velocity data confirmed

that the model predicts the phasing correctly in Carr, Case, and Budd Inlet. Some fine-scale phenomenon could not be reproduced, such as the east-west variations in Budd Inlet, likely due to the resolution of the model. However, these do not limit the applicability of the model.

Surface current velocities are predicted well by the model for strong and weak ebb- and flood-tide conditions, including the relative magnitude and direction, compared with Tide Prints (McGary and Lincoln, 1977). Known features, such as quiescent waters and fast-moving passages, are reproduced by the model.

## Flushing Times

We applied the model to estimate flushing time for portions of South Puget Sound. Flushing time varied with location within South Puget Sound and estimates were strongly influenced by the methods used to calculate it. Flushing time is fastest near the Tacoma Narrows and decreases with distance away. However, flushing times for individual inlets relative to the rest of South Puget Sound are shorter.

## Simulated Dye Studies

We simulated the circulation of virtual dye released from watershed inflows and marine point sources within South and Central Puget Sound. Based on predicted dilution levels derived from water-column maximum dye concentrations, water from these sources exchanges through the Tacoma Narrows. We cannot rule out the influence of Central Puget Sound sources on South Puget Sound water quality. However, the results are not sufficient to rule in an influence either, given the complexity of nutrient transport and transformation within marine environments. Ahmed et al. (2014) addresses the link between sources throughout South and Central Puget Sound and water quality responses.

# Recommendations

While not necessary for the current effort, we recommend that future detailed model applications in other regions of Puget Sound consider the following:

- Continuous monitoring for temperature and salinity profiles at the model boundary would eliminate any questions of short-term phenomena such as upwelling that could affect water masses entering the model domain. Future Puget Sound-wide networks should consider potential model boundaries in the sampling design.
- Verifying water surface elevations against measured data that include the effect of wind is very useful. In future modeling where no nearby station provides in-situ data, short-term installations of pressure transducers in key locations could verify that wind is parameterized appropriately.
- Particularly in systems where wind plays a strong role, such as Hood Canal, a more extensive network of meteorological stations would be helpful. Our initial study design included the installation of meteorological stations to record wind and other variables near the marine waters. However, the data were not of sufficient quality to use, and we relied on National Weather Service stations in South and Central Puget Sound to drive the model.
- Complex local mixing processes around Tacoma Narrows and Hope Island may be improved by site-specific studies. We considered using a finer grid cell in these areas. However, given the long computer runtime, a more detailed model grid would produce runtimes that would not be suitable to water quality scenario simulations.

## Next Steps

Ahmed et al. (2014) describe the accompanying water quality model development. We estimated dissolved oxygen impacts with water quality model, and we identified areas with the greatest declines in oxygen due to human sources. However, we recommend further water quality model development, focused on sediment-water exchanges.

# References


Ahmed, A. and L.C. Wagner, 2011. Oakland Bay, Hammersley Inlet, & Selected Tributaries Fecal Coliform Bacteria Total Maximum Daily Load: Water Quality Improvement Report (WQIR)/Implementation Plan (WQIP). Washington State Department of Ecology, Olympia, WA. Publication No. 11-10-039. https://fortress.wa.gov/ecy/publications/SummaryPages/1110039.html.

Ahmed, A., G. Pelletier, M. Roberts, and A. Kolosseus, 2014. South Puget Sound Dissolved Oxygen Study: Water Quality Model Calibration and Scenarios. Washington State Department of Ecology, Olympia, WA. Publication No. 14-03-004. https://fortress.wa.gov/ecy/publications/SummaryPages/1403004.html.

Albertson, S.L., K. Erickson, J.A. Newton, G. Pelletier, R.A. Reynolds, and M.L. Roberts, 2002a. Summary of South Puget Sound Water Quality Study, Washington State Department of Ecology, Olympia, WA. Publication No. 02-03-020. https://fortress.wa.gov/ecy/publications/summarypages/0203020.html.

Albertson, S.L., K. Erickson, J.A. Newton, G. Pelletier, R.A. Reynolds, and M.L. Roberts, 2002b. South Puget Sound Water Quality Study, Phase 1. Washington State Department of Ecology, Olympia, WA. Publication No. 02-03-021. https://fortress.wa.gov/ecy/publications/summarypages/0203021.html.

Albertson, S.L., J.K. Bos, G. Pelletier, and M.L. Roberts, 2007a. Circulation and Residual Flow in the South Basin of Puget Sound, and its Effects on Near Bottom Dissolved Oxygen. Georgia Basin and Puget Sound Research Conference. March 2007. Vancouver, BC.

Albertson, S., J. Bos, K. Erickson, C. Maloy, G. Pelletier, and M.L. Roberts, 2007b. Quality Assurance Project Plan: South Puget Sound Water Quality Study Phase 2: Dissolved Oxygen. Washington State Department of Ecology, Olympia, WA. Publication No. 07-03-101. https://fortress.wa.gov/ecy/publications/summarypages/0703101.html.

Aura Nova Consultants, Brown and Caldwell, Evans-Hamilton, J. E. Edinger and Associates, Washington State Department of Ecology, and the University of Washington Department of Oceanography, 1998. Budd Inlet Scientific Study Final Report. Prepared for the LOTT Partnership, Olympia, WA.

Babson, A.L., M. Kawase, and P. MacCready, 2006. Seasonal and interannual variability in the circulation of Puget Sound, Washington: A box model study. Atmosphere-Ocean 44(1):29-45.

Barnes, C. A. and C. C. Ebbesmeyer, 1978. Some aspects of Puget Sound's circulation and water properties. In: Estuarine Transport Processes. B. Kjerfve (ed.), University of South Carolina Press, Columbia, South Carolina. pp. 209-228.

Bos, J.K., R.A. Reynolds, J. Newton, and S.L. Albertson, 2001. Assessing sensitivity to eutrophication of the southern Puget Sound basin: Spatial and seasonal perspectives. Proceedings of Puget Sound Research Conference, Seattle, WA.

Bretschneider, D.E., G.A. Cannon, J.R. Holbrook and D.J. Pashinski, 1985. Variability of subtidal current structure in a fjord estuary: Puget Sound, Washington. J. Geophys. Res. 90(C6):11,949–11,958.

Cannon, G.A.,1983. An overview of circulation in the Puget Sound estuarine system. NOAA Technical Memorandum. ERL PMEL-48.

Cannon, G.A. and C.C. Ebbesmeyer, 1978. Winter replacement of bottom water in Puget Sound, in Estuarine Transport Processes, edited by B. Kjerfve, p. 229-238, University of South Carolina Press, Columbia, SC.

Cokelet, E.D., R.J. Stewart, and C.C. Ebbesmeyer, 1990. The annual mean transport in Puget Sound. NOAA Technical Memorandum, ERL-PMEL-92.

Cole, T.M. and E.M. Buchak, 1995. CE-QUAL-W2: A Two-Dimensional, Laterally Averaged, Hydrodynamic and Water Quality Model, Version 2.0: Users Manual, Instruction Report EL-95-1, US Army Engineer Waterways Experiment Station, Vicksburg, MS.

Collias, E., N. McGary, and C. Barnes, 1974. Atlas of Physical and Chemical Properties of Puget Sound and its Approaches. University of Washington Press, Seattle, WA. 235 pp.

Ebbesmeyer, C.C., C.A. Coomes, J.M. Cox, J.M. Helseth, L.R. Hinchey, G.A. Cannon, and C.A. Barnes, 1984. Synthesis of current measurements in Puget Sound, Washington – Volume 3: Circulation in Puget Sound: An interpretation based on historical records of currents. NOAA Technical Memorandum NOS OMS 5.

Edinger, J.E. and E.M. Buchak, 1980. Numerical Hydrodynamics of Estuaries *in* Estuarine and Wetland Processes with Emphasis on Modeling.

Edinger J.E. and E.M. Buchak, 1995. Numerical Intermediate and Far Field Dilution Modeling. Journal of Water, Air and Soil Pollution 83: 147-160, 1995.

Edwards, K.A., M. Kawase, and C.P. Sarason, 2007. Circulation in Carr Inlet, Puget Sound, During Spring 2003. Estuaries and Coasts Vol. 30, No. 6, p. 945–958. December 2007.

Finlayson, D.P., 2003. Combined bathymetry and topography of the Puget Lowland, Washington State. University of Washington, Seattle, WA. www.ocean.washington.edu/data/pugetsound.

Finlayson, D.P., 2004. Puget Sound Tide Model (PSTides). www.ocean.washington.edu/data/pugetsound/.

Finlayson, D.P., 2005. Coastal Geomorphology in Puget Sound. Shoreline and Coastal Planners Group, Padilla Bay National Estuarine Research Reserve, Mount Vernon, WA. June 23, 2005.

Friebertshauser, M.A. and A.C. Duxbury, 1972. A water budget study of Puget Sound and its subregions. Limnology and Oceanography 17(2) 237-247.

Gill, A.E., 1982. Atmosphere-ocean dynamics. International Geophysics Series. Vol. 30. Academic Press, New York.

Hicks, S.D., 2006. Understanding Tides. U.S. Department of Commerce, National Oceanic and Atmospheric Administration, National Ocean Service Publication. Chapter 8, Tidal Harmonic Constituents. Available from: tidesandcurrents.noaa.gov/publications/Understanding_Tides_by_Steacy_finalFINAL11_30.pdf.

Hoffman, Charles, 2010. Personal communication. Water Quality Program, Southwest Regional Office, Washington State Department of Ecology, Olympia, WA. March 2010.

Kolluru,V.S., E.M. Buchak, and J.E. Edinger, 1998. Integrated Model to Simulate the Transport and Fate of Mine Tailings in Deep Waters. In Proceedings of Tailings and Mine Waste '98. 1998. Balkema, Rotterdam, ISBN 905410922.

Lavelle, J.W., H.O. Mofjeld, E. Lempriere-Doggett, G.A. Cannon, D.J. Pashinski, E.D. Cokelet, L. Lytle, and S. Gill, 1988. A Multiply-Connected Channel Model of Tides and Tidal Currents in Puget Sound, Washington and a Comparison with Updated Observations. NOAA Technical Memorandum ERL PMEL-84.

McGary, N. and J.H. Lincoln, 1977. Tide prints: Surface currents in Puget Sound. Washington Sea Grant Publication Number WSG 77-1.

Mofjeld, H.O., A J. Venturato, V.V. Titov, F.I. González, and J.C. Newman, 2002. Tidal Datum Distributions in Puget Sound, Washington, Based on a Tidal Model. NOAA Technical Memorandum OAR PMEL-122 (PB2003102259). NOAA/Pacific Marine Environmental Laboratory, Seattle, WA. 35 pp.

Mohamedali, T., M. Roberts, B. Sackmann, A. Whiley, and A. Kolosseus, 2011. South Puget Sound Dissolved Oxygen Study: Interim Nutrient Load Summary for 2006-2007. Washington State Department of Ecology, Olympia, WA. Publication No. 11-03-001. https://fortress.wa.gov/ecy/publications/SummaryPages/1103001.html

Monsen, N.E., J.E. Cloern, L.V. Lucas, and S.G. Monismith, 2002. A comment on the use of flushing time, residence time, and age as transport time scales. Limnology and Oceanography 47(5):1545-153.

Nairn, Bruce, 2009. Personal communication. King County Wastewater Treatment Division, Seattle, WA.

Roberts, M., J. Bos, and S. Albertson, 2008. South Puget Sound Dissolved Oxygen Study – Interim Data Report. December 2008. Washington State Department of Ecology, Olympia, WA. Publication No. 08-03-037. https://fortress.wa.gov/ecy/publications/summarypages/0803037.html.

Roberts, M., A. Ahmed, G. Pelletier, and D. Osterberg, 2012. Deschutes River, Capitol Lake, and Budd Inlet Temperature, Fecal Coliform Bacteria, Dissolved Oxygen, pH, and Fine Sediment Total Maximum Daily Load: Water Quality Study Findings. Washington State Department of Ecology, Olympia WA. Publication No. 12-03-008. https://fortress.wa.gov/ecy/publications/summarypages/1203008.html.

Sackmann, B., 2009. Quality Assurance Project Plan: Puget Sound Dissolved Oxygen Modeling Study: Large-scale Model Development. Washington State Department of Ecology, Olympia, WA. Publication No. 09-03-103. https://fortress.wa.gov/ecy/publications/summarypages/0903103.html.

Seim, H.E. and M.C. Gregg, 1997. The importance of aspiration and channel curvature in producing strong vertical mixing over a sill. Journal of Geophysical Research, Vol. 102, No. C2. p. 3451–3472.

Thomson, R.E., 1981. Oceanography of the British Columbia Coast. Canadian Special Publication of Fisheries and Aquatic Sciences 56. 291 pp.

University of Washington, 1971. Puget Sound and Approaches Seasonal Variations of Oceanographic Parameters in its Near-surface Waters. Department of Oceanography. Washington Sea Grant Report Contract No. RD-NE4.

URS Company, 1986. Southern Puget Sound Water Quality Assessment Study: Circulation and Flushing in South Puget Sound. Prepared for the Washington State Department of Ecology, Olympia, WA. Publication No. 86-e36. https://fortress.wa.gov/ecy/publications/summarypages/86e36.html.

Wu, J., 1982. Wind-stress coefficients over sea surface from breeze to hurricane. Journal of Geophysical Research. Vol. 87. No. C12. p. 9704-9706.

# Appendices

*This page is purposely left blank*

# Appendix A. Procedure for establishing model grid bathymetry

1. Depths for each model grid cell were determined by sampling the Finlayson (2005) digital elevation model. While preserving the vertical NAVD88 referenced depths, the horizontal projection of the data set (psdem05.lyr ) was converted from NAD_1983_HARN_WA_stateplane_south-ft **to** NAD-1927_UTM_zone10N_m using GIS9.2 as follows:

   Use "Project Raster" tool from ArcToolbox\Data Management Tools\Projections and Transformations\Raster and input all the required fields as shown below:

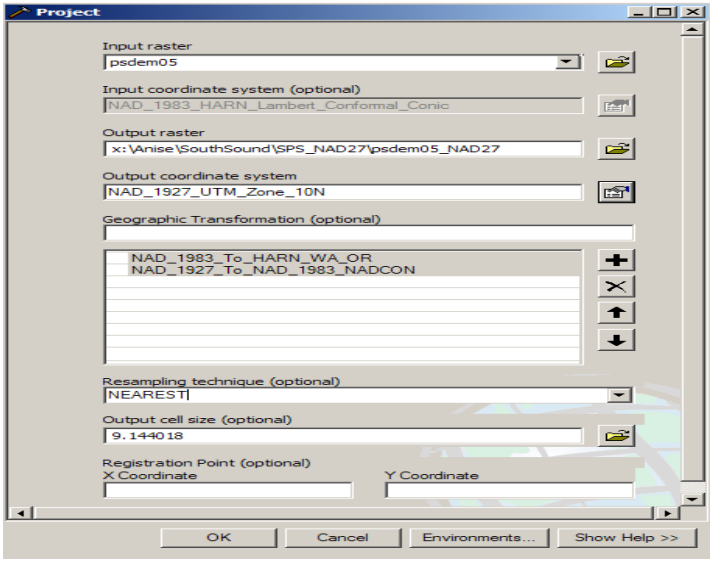


2. Close GIS9.2. You do not need to save anything, since the new psdem05_NAD27 is already saved.

3. Restart GIS9.2 and add psdem05_NAD27. Build the pyramids when you display the file.

4. Turn on the extensions "Spatial Analyst."

5. Add southpugetsound3_shoreline.shp (= waterbody shape file, NAD-1927_UTM_zone10N_m). Use it to clip psdem05_NAD27 using the tool "Extract by Mask" in ArcToolBox\Spatial Analyst Tools\Extraction\Extract by Mask. The new file is psdemextract.

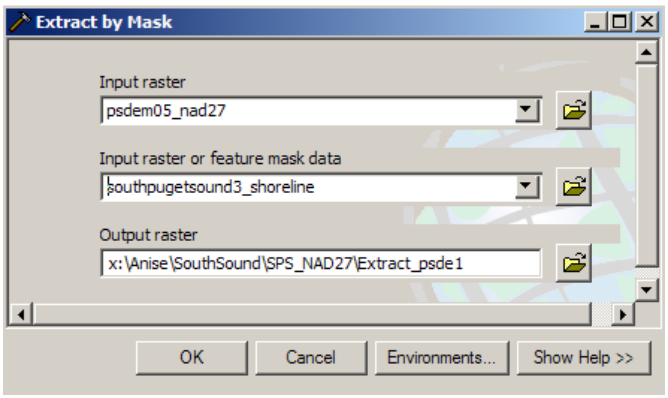


6. Also convert the g3g file (Edmonds_g3g.shp = South Puget Sound grid shape file, NAD-1927_UTM_zone10N_m) to grid centroids using: XTools Pro/Feature Conversions/shapes to centroids. The file is named grid_center. Export the data as a dbf file: grid_centroids.dbf.

7. Bring the DEM file psdemextract into ArcView 3.3 and the g3g-grid, using the extension surface_areas. Include the extension "surface areas from elevation grids" and spatial analyst, and click the "grid statistics by polygon" icon (the sigma symbol). Highlight the columns as shown below. This will create a table with statistics (including max depth) for each grid cell. The file is named Gid_Maxdepth. This table should be exported as a dbf file and saved as grid_maxdepth .dbf.

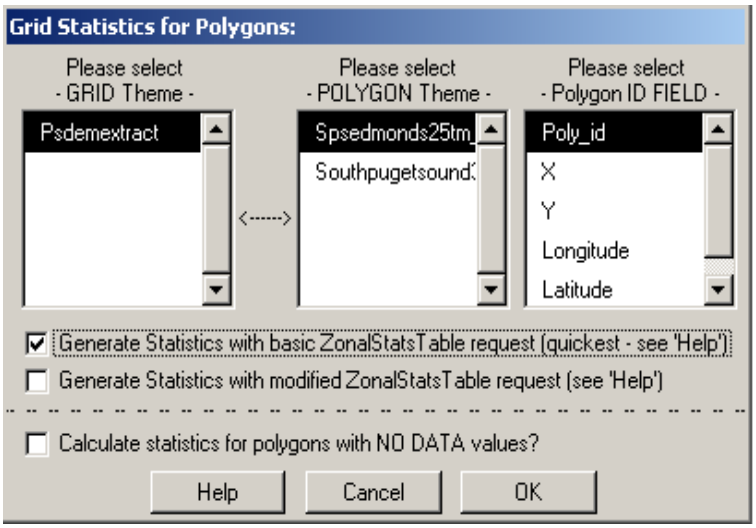


8. Bring both the centroid dbf as well as grid_maxdepth dbfs into Excel and add the minimum depth (i.e., max value) to the centroid tab. Save as Excel.xls (1997) version. Using Arc Catalogue in GIS 9.3, convert the xls file to a dbf file. Add the dbf file as an xy file. Save it as a shape file. This is the new bathymetry file with the centroid of grid cells associated with the maximum depth in the cell.

9. Bring this into GEMSS when creating a new bathymetry file.

Creating smoothed grid depths in GEMSS:

1. In GEMSS load the waterbody shape file: southpugetsound3_shoreline.shp.
2. Load the depth shape file.
3. Load GridGen from Tools Menu.
4. Load the grid file.
5. Click Scan depth and select the appropriate file and depth attribute.

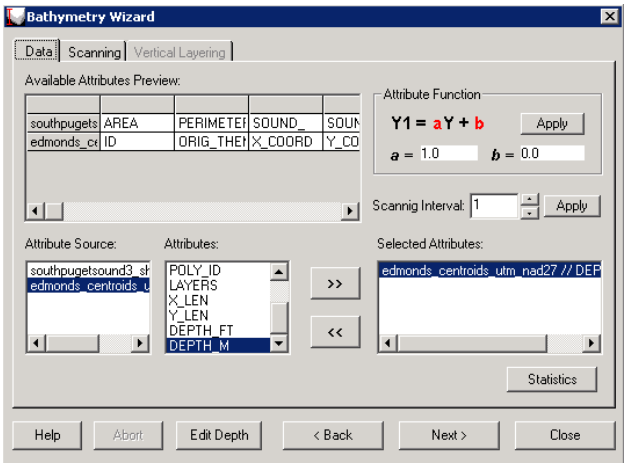


6. Click next and **do not** select the bathymetry smoothing box.

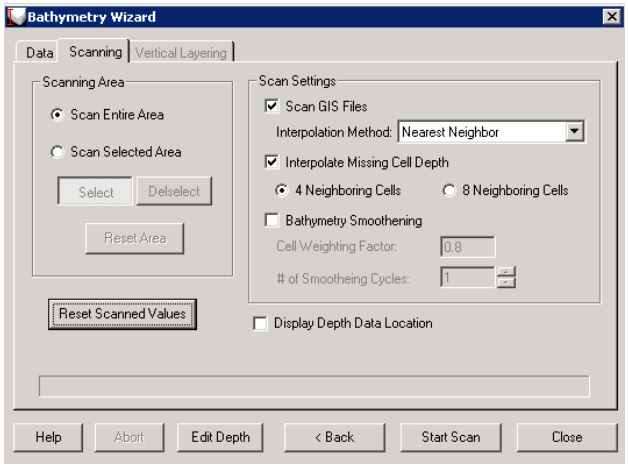


7. Click “Reset Scanned Values” (this will clear old depth values) and then click “Start Scan.”
8. Proceed with non-uniform vertical layering as per L1-Scheme.

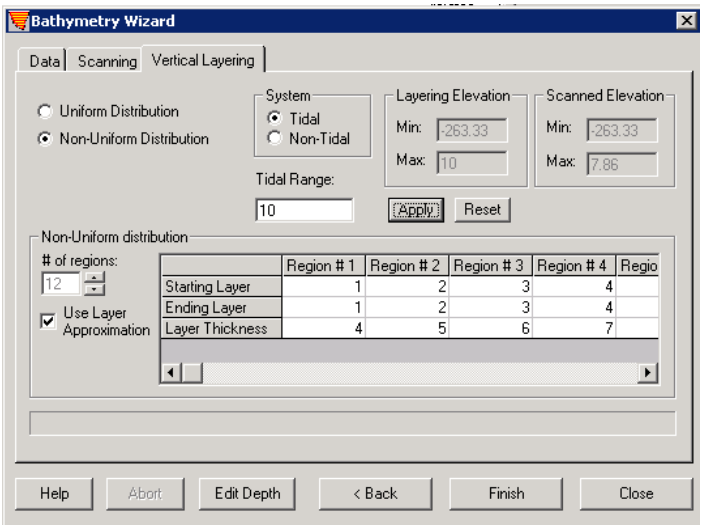


Table 1. Layering with L1-Scheme.

| Layer | Thickness, m | Upper depth, m | Lower depth, m |
|---|---|---|---|
| 1 | 4 | 10 | 6 |
| 2 | 5 | 6 | 1 |
| 3 | 6 | 1 | -5 |
| 4 | 7 | -5 | -12 |
| 5 | 8 | -12 | -20 |
| 6 | 9 | -20 | -29 |
| 7 | 10 | -29 | -39 |
| 8 | 12 | -39 | -51 |
| 9 | 14 | -51 | -65 |
| 10 | 16 | -65 | -81 |
| 11 | 18 | -81 | -99 |
| 12 | 20 | -99 | -119 |
| 13 | 25 | -119 | -144 |
| 14 | 25 | -144 | -169 |
| 15 | 25 | -169 | -194 |
| 16 | 25 | -194 | -219 |
| 17 | 25 | -219 | -244 |

9. Click “yes” to bathymetric smoothing to avoid “holes.”

10. Manually set the last three rows of cells at open boundary to the same depth along the thalweg with a value equal to the average of the last three cells.

11. In addition, the areas of Oakland Bay/Hammersley Inlet, Budd Inlet, and Tacoma Narrows were deepened to match actual bathymetry and to improve calibration of water surface elevations. The total volume of the model grid (nominal size 500m x 500m) was within 4% of the volume estimated using Finlayson’s bathymetry depths (9m x 9m gird) as available in Ecology’s GIS database psdem05.

# Appendix B. Estimating time varying trapping levels for point source discharges

Freshwater point sources to marine waters in Central and South Puget Sound include municipal wastewater treatment plants (WWTP) and industrial discharges. These are typically discharged below the water surface. Since the density of freshwater is less than the saline marine waters, it rises and either reaches the surface or gets trapped at depth where density differences are low or zero. In either case, different flows from the point sources would exist in the different vertical grid layers depending upon the diameter of the trapped plume. For any given point source, the fraction of plume flow in a layer would be equal to the ratio of the layer depth (where part of the plume is trapped) to the plume diameter times the total flow.

To estimate the plume trapping level (whether surface or below), EPA's mixing zone model Visual Plumes (www.epa.gov/ceampubl/swater/vplume/) was used. The model requires outfall characteristics, effluent flow, temperature, ambient current velocity, ambient temperature, and ambient salinity.

The monthly average flows for each of the point sources were obtained from Ecology's database. Effluent temperature data specific to each individual WWTP were not available so the monthly temperature data from the Chambers Creek WWTP was applied to all the municipal WWTP discharges except for the Tacoma Central WWTP, which had temperature data available. Outfall information such as location, diffuser and port configuration, and depth were obtained from engineering reports, plan drawings, or NPDES permit fact sheets.

Ambient data (salinity, temperature, and depth) for the specific month and year were obtained from the Puget Sound Regional Synthesis Model (PRISM) cruises, or from Ecology's EAP routine ambient monitoring. Fiftieth percentile ambient current velocities were obtained from mixing studies for the individual outfalls. The $50^{th}$ percentile ambient current velocities are typically used (www.ecy.wa.gov/programs/eap/mixzone/mixzone.html) to estimate a steady state dilution factor at the edge of designated mixing zone (in the order of 250 feet or more from the diffuser depending upon the depth of diffuser). The discharge plume typically traps within this zone (nearfield mixing), beyond which the plume spreads due to farfield dispersion (predominantly horizontal) and there is no significant vertical movement within short distances. The model grid dimension is much larger than the size of the nearfield mixing zone. As such the discharge trapping levels within the nearfield mixing is used for the grid cell containing the diffuser.

The output from the Visual Plume model shows the elevation of the plume center from the sea floor, the plume diameter and whether the top of the plume reached surface or not. West Point and South King WWTPs were evaluated by Bruce Nairn of King County. Ecology's Southwest Region (SWRO) conducted the mixing zone analysis for the rest of the WWTPs and Industrial discharges. Table B-1 provides this information for each of the WWTPs and Industrial point sources. Similar information was provided by King County for West Point and South King County WWTPs (Bruce Nairn, 2009).

The next step is to convert the diffuser depth (MLLW), diffuser height from bottom, plume center elevations from bottom into NAVD88 vertical datum reference and bringing the diffuser

into the model grid domain. Knowing the plume diameter, plume center location above bottom and the grid bottom elevation in NAVD88, the location of the bottom and top of the plume can be calculated in terms of NAVD88. These elevations are then compared with the grid layer elevations to determine in which layer the bottom and top of the plume resides (see Figure B-1). This may be different for different months of the year depending upon whether the trapping levels are different or not. Once this is established, the fraction of flow in a layer is equal to the depth of plume within a layer divided by the plume diameter.

The top and bottom layers would be partially full whereas the intermediate layers would be completely filled by the effluent. Once the fraction of flow in the layers where effluent is trapped is established for a given monthly average flow, daily flows within a given month are parsed according to the fractions in the respective layers. This generates a time-series of flow for each of the layers where the effluent is trapped.

Table B-1. Elevations of plume centerline and size of the plume at the trapping level (August 2006 – July 2007).

| WWTP | Outfall Depth (m, MLLW) | Outfall Height from Sea Floor (m) | Plume | Aug | Sept | Oct | Nov | Dec | Jan | Feb | Mar | Apr | May | June | July |
|---|---|---|---|---|---|---|---|---|---|---|---|---|---|---|---|
| | | | | Plume center elevation with respect to sea floor, meters | | | | | | | | | | | |
| Midway | 47.6 | 0.5 | center | 32.9 | 29.8 | 44.9 | 37 | 38 | 34.4 | 43.9 | 42.9 | 34.7 | 39.3 | 33 | 41.8 |
| | | | dia | 43.3 | 45.3 | 22.4 | 46.4 | 46.9 | 49.9 | 30.7 | 33.5 | 45.2 | 35.2 | 44.2 | 31.3 |
| | | | top | surface | surface | surface | surface | surface | surface | surface | surface | surface | surface | surface | surface |
| Miller | 60.5 | 0.4 | center | 28 | 31.1 | 56.3 | 44 | 44.2 | 30 | 53.8 | 35.2 | 34.7 | 43.1 | 33.6 | 33.5 |
| | | | dia | 10.1 | 11.8 | 21.8 | 16.1 | 17.2 | 10.5 | 32.2 | 12.3 | 13.3 | 16.5 | 13 | 11.9 |
| | | | top | trap | trap | surface | trap | trap | trap | trap | trap | trap | trap | trap | trap |
| Salmon Creek | 59.7 | 0.6 | center | 19.6 | 54.9 | 27.6 | 25.2 | 24.8 | 32.4 | 39.6 | 30.6 | 25.5 | 39.5 | 20 | 29.6 |
| | | | dia | 16.3 | 37.8 | 21 | 28.8 | 27.6 | 39 | 46.4 | 29.7 | 24.3 | 33.4 | 15.8 | 21.4 |
| | | | top | trap | surface | trap | trap | trap | trap | trap | trap | trap | trap | trap | trap |
| Redondo | 14.3 | 0.8 | center | 14 | 14.3 | 14.6 | 14.3 | 14.8 | 14.6 | 14.6 | 11.3 | 13 | 13.5 | 11.2 | 10.4 |
| | | | dia | 6.2 | 5.9 | 4.9 | 5.3 | 5.1 | 5.1 | 5.5 | 4.2 | 5.2 | 5.4 | 4.5 | 4.1 |
| | | | top | trap | trap | surface | trap | surface | surface | surface | trap | trap | trap | trap | trap |
| Lakota | 56.1 | 0.3 | center | 30.7 | 32.5 | 33.3 | 32.2 | 33.7 | 38.9 | 33.7 | 31.1 | 30.7 | 33.1 | 38.4 | 29.8 |
| | | | dia | 15.5 | 16.4 | 17.3 | 16.4 | 17.8 | 17.4 | 17.5 | 15.9 | 15.5 | 17.3 | 22 | 15.1 |
| | | | top | trap | trap | trap | trap | trap | trap | trap | trap | trap | trap | trap | trap |
| Tacoma Central | 35.1 | 3.1 | center | 37.4 | 37.7 | 37 | 31.5 | 37.6 | 24.6 | 37.2 | 30.9 | 37.5 | 38.1 | 37.3 | 37.6 |
| | | | dia | 16.9 | 14.8 | 14.8 | 9.4 | 12.2 | 8.1 | 13.3 | 9.1 | 14.5 | 13 | 16.1 | 14.3 |
| | | | top | surface | surface | surface | trap | surface | trap | surface | trap | surface | surface | surface | surface |
| Simpson | 15.5 | 1.7 | center | 12.7 | 13.2 | 13.1 | 10.2 | 10.6 | 10.6 | 10.8 | 10.1 | 10.9 | 11.9 | 11 | 11 |
| | | | dia | 7.2 | 7.6 | 8 | 6 | 6.3 | 7.8 | 6.7 | 6.3 | 6.2 | 6.1 | 6.1 | 6 |
| | | | top | trap | trap | trap | trap | trap | trap | trap | trap | trap | trap | trap | trap |
| Tacoma North End | 38.1 | 1 | center | 35.5 | 37.4 | 36.7 | 33.4 | 36.6 | 27.8 | 36.5 | 33.5 | 36.5 | 37.5 | 36.8 | 37.2 |
| | | | dia | 25.6 | 20.9 | 21.4 | 38.1 | 21.5 | 31.8 | 27.7 | 28.8 | 25.5 | 19.9 | 23.5 | 21.1 |
| | | | top | surface | surface | surface | trap | surface | trap | surface | trap | surface | surface | surface | surface |
| Chambers Creek | 31.1 | 2.4 | center | 31.5 | 31.3 | 30.7 | 30.5 | 30.7 | 29.3 | 30.9 | 28.6 | 31.3 | 30.9 | 29.9 | 30.2 |
| | | | dia | 21.4 | 22.8 | 23.2 | 21.3 | 18 | 18.5 | 20.7 | 19.7 | 21.9 | 23.8 | 25 | 25.6 |
| | | | top | surface | surface | surface | surface | trap | trap | surface | trap | surface | surface | surface | surface |
| Fort Lewis | 20.7 | 0.6 | center | 19.2 | 18.8 | 19.3 | 18.5 | 19 | 18.6 | 18.3 | 15.3 | 18 | 18.5 | 18.8 | 19.1 |
| | | | dia | 11.8 | 12.3 | 11.2 | 13.3 | 13.3 | 16 | 14.3 | 11.9 | 13.3 | 12.1 | 11.7 | 11.7 |
| | | | top | surface | surface | surface | surface | surface | surface | surface | trap | trap | trap | trap | surface |
| Shelton | 9.8 | 0.3 | center | 5.2 | 5.2 | 5.2 | 3.2 | 3.2 | 3 | 3.8 | 3.3 | 4.1 | 4.5 | 4.6 | 4.5 |
| | | | dia | 10.4 | 10.4 | 10.3 | 14.6 | 14.1 | 15.4 | 11.4 | 11.7 | 10.4 | 10.1 | 9.5 | 9.9 |
| | | | top | surface | surface | surface | surface | trap | trap | trap | trap | trap | trap | trap | surface |
| Central Kitsap | 12.5 | 1.3 | center | 12.2 | 12 | 12.4 | 12.2 | 10.2 | 12.2 | 11.9 | 12.2 | 12 | 12.4 | 11.8 | 12.1 |
| | | | dia | 8.6 | 9.4 | 8.4 | 9.9 | 9.5 | 9.7 | 9.5 | 9.6 | 8.8 | 8.7 | 9.6 | 8.8 |
| | | | top | surface | surface | surface | surface | trap | surface | surface | surface | surface | surface | surface | surface |
| Port Orchard | 14.8 | 1.1 | center | 15.9 | 15.7 | 15.8 | 15.6 | 15.8 | 15.8 | 15.6 | 15.7 | 15.8 | 15.9 | 15.6 | 15.6 |
| | | | dia | 4.4 | 4.3 | 4.2 | 5.2 | 5.2 | 5 | 4.4 | 4.7 | 4.5 | 4.5 | 4.4 | 4.5 |
| | | | top | surface | surface | surface | surface | surface | surface | surface | surface | surface | surface | surface | surface |
| Bremerton | 8.4 | 0.8 | center | 9.1 | 9.1 | 8.9 | 9 | 8.8 | 8.9 | 8.9 | 9 | 9 | 8.9 | 8.9 | 9 |
| | | | dia | 3.6 | 3.6 | 3.5 | 6.7 | 6.2 | 3.5 | 3.5 | 3.7 | 3.8 | 3.6 | 3.7 | 3.6 |
| | | | top | surface | surface | surface | surface | surface | surface | surface | surface | surface | surface | surface | surface |

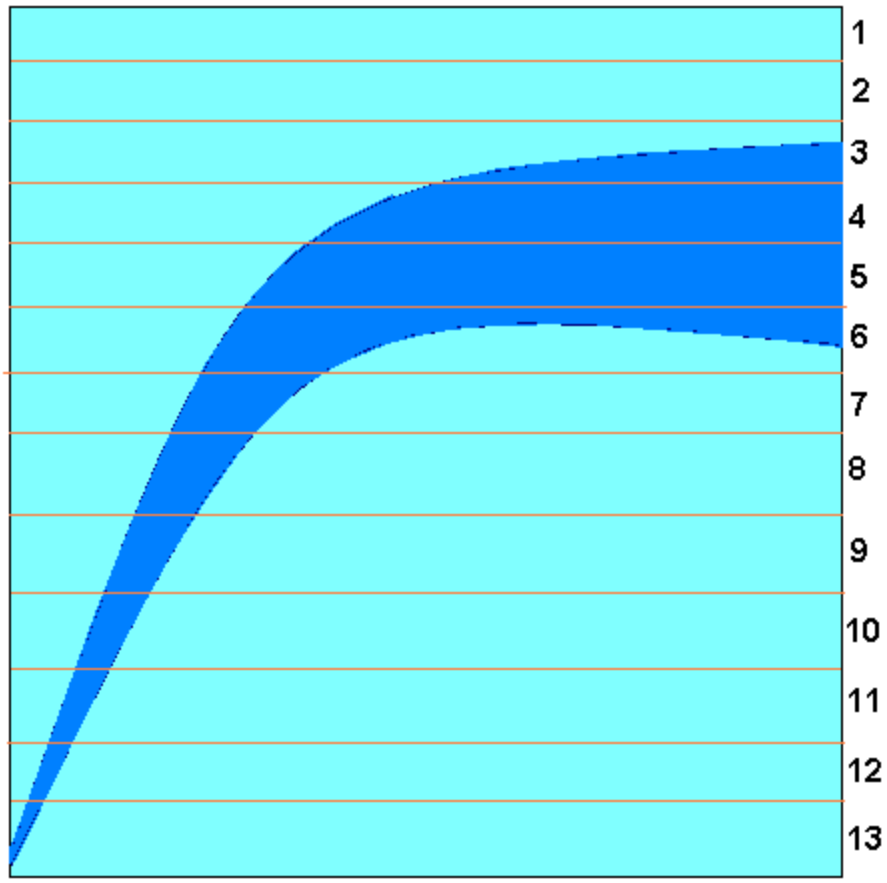


Figure B-1. Marine point source trapped within the water column.

# Appendix C. Hydrodynamic and meteorological rates and constants

| Parameter | Description | Value |
|---|---|---|
| Hydrodynamics/Transport | | |
| Coriolis Force Terms | Reference Latitude (degrees) | 47.5 |
| Wind Stress Coefficient | Method | Wu (1982) |
| Bottom Friction | Method | Chezy |
| | Chezy Coefficient | Constant |
| | Limiting Chezy Selector | 0 |
| | Czo = (units m^1/2/sec) | 40 (20 for shallow inlets) |
| Transport Modeling Scheme | Scheme | Quickest with Ultimate |
| | Advection Theta in Z-Direction | 0 |
| | Diffusion Theta in Z-Direction | 0 |
| | HOTS Initiation Time Period (days) | 1 |
| Wetting and Drying of Layers | Wetting Limiting Thickness Factor | 0.8 |
| | Drying Limiting Thickness Factor | 0.8 |
| Density | Density Fuction | Gill (1982) |
| Vertical Momentum Dispersion | Scheme | 1-Equation |
| | Mixing Length | Von Karman |
| Momentum Dispersion Coef. (m^2/sec) | X-Direction | Smagorinsky |
| | Axo = | 0.1 |
| | n(x) = | |
| | Y-Direction | Smagorinsky |
| | Ayo = | 0.1 |
| | n(y) = | |
| Transport Diffusion Coef. (m^2/sec) | X-Direction | Prandtl |
| | Y-Direction | Prandtl |
| | Prandtl Number | 10 |

| Parameter | Description | Value |
|---|---|---|
| Meteorology | | |
| | Input Data Type for Meteorology | 2 : Time Varying Data |
| | TVD Input File Name for Meteorology | North_06_07_15min_wCorrSolar.met Shelton_06_07_15min_wCorrSolar.met |
| | Time Varying Input Data Interpolation Scheme for M | 1 : Linear Interpolation Between Time t1 and t2 |
| ta_v | Air Temperature (°C) | 0 : From TVD File |
| td_v | Dew Point Temperature (°C) | 0 : From TVD File |
| cc_v | Cloud Coverage (tenths) | 0 : From TVD File |
| sp_v | Atmospheric Pressue (mm Hg) | 0 : From TVD File |
| phi_v | Wind Direction (degrees) | 0 : From TVD File |
| wa_v | Wind Speed (m/s) | 0 : From TVD File |
| rs_v | Solar Radiation (w/m^2) | 0 : From TVD File |
| wsc_v | Wind Sheltering Coefficient (constant) | 1 |
| sd_v | Secchi Depth (m) | 0 : From TVD File |
| rh_v | Relative Humidity (%) | 0 : From TVD File |
| ishe | Surface Heat Exchange Method | 2 : Term by Term |
| KEMethod | Compute K & E in the Model | 0 |
| cshe_v | Surface Heat Exchange Coefficient (w/m2/C) | 30 |
| te_v | Equilibrium Temperature (°C) | 21 |
| PAR | Fraction of Solar Radiation in the Range of 400 to 700 nm | 0.43 |
| Albedo | Fraction of Solar Radiation Reflected from the Water Surface | 0.07 |
| iwsf | Wind Speed Function | 1 : Brady |
| BetaMethod | Method to Compute Fraction of Solar Energy Absorbed at Sfc | 1 : Linear Relation |
| Beta | Fraction of Solar Energy Absorbed at the Surface | 0.43 |
| Gamma_A | Light Attenuation Parameter a | 1.2 |
| Gamma_B | Light Attenuation Parameter b | 0.6 |

# Appendix D. Excerpts from Tide Prints for strong and weak ebb and flood conditions (McGary and Lincoln, 1977)

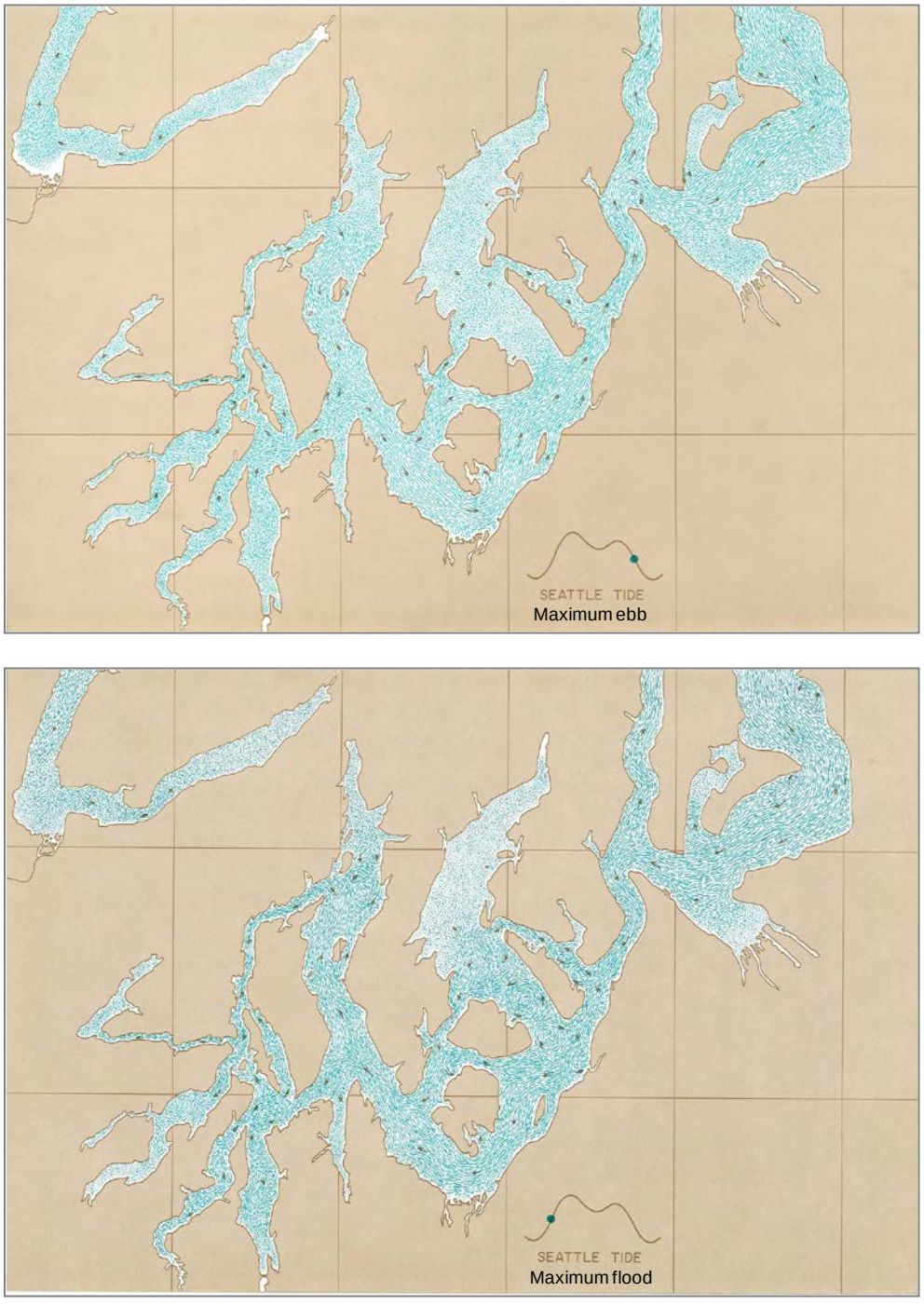


Figure D-1. Tide prints for maximum ebb and flood conditions in South Puget Sound.

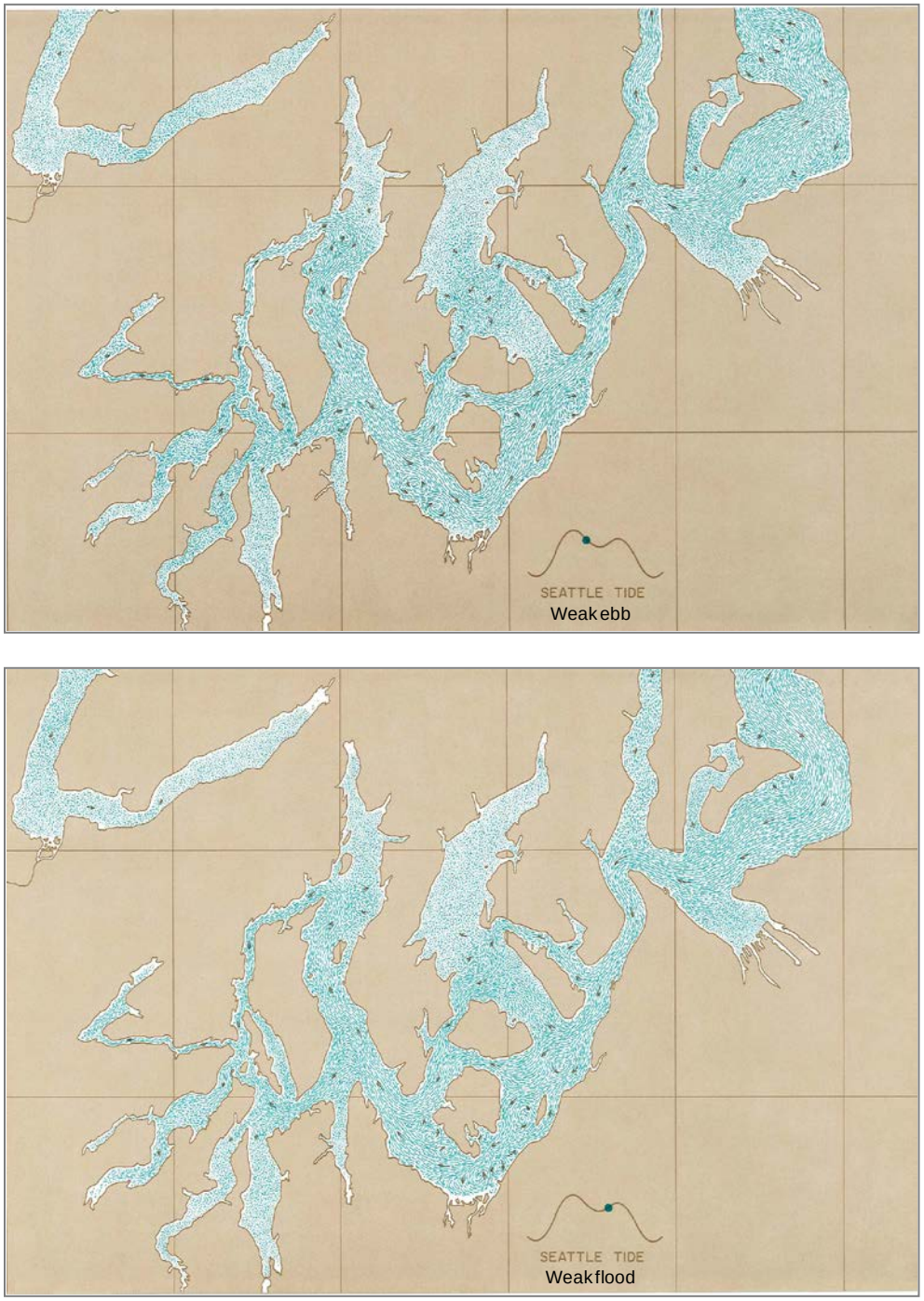


Figure D-2. Tide prints for weak ebb and flood conditions in South Puget Sound.

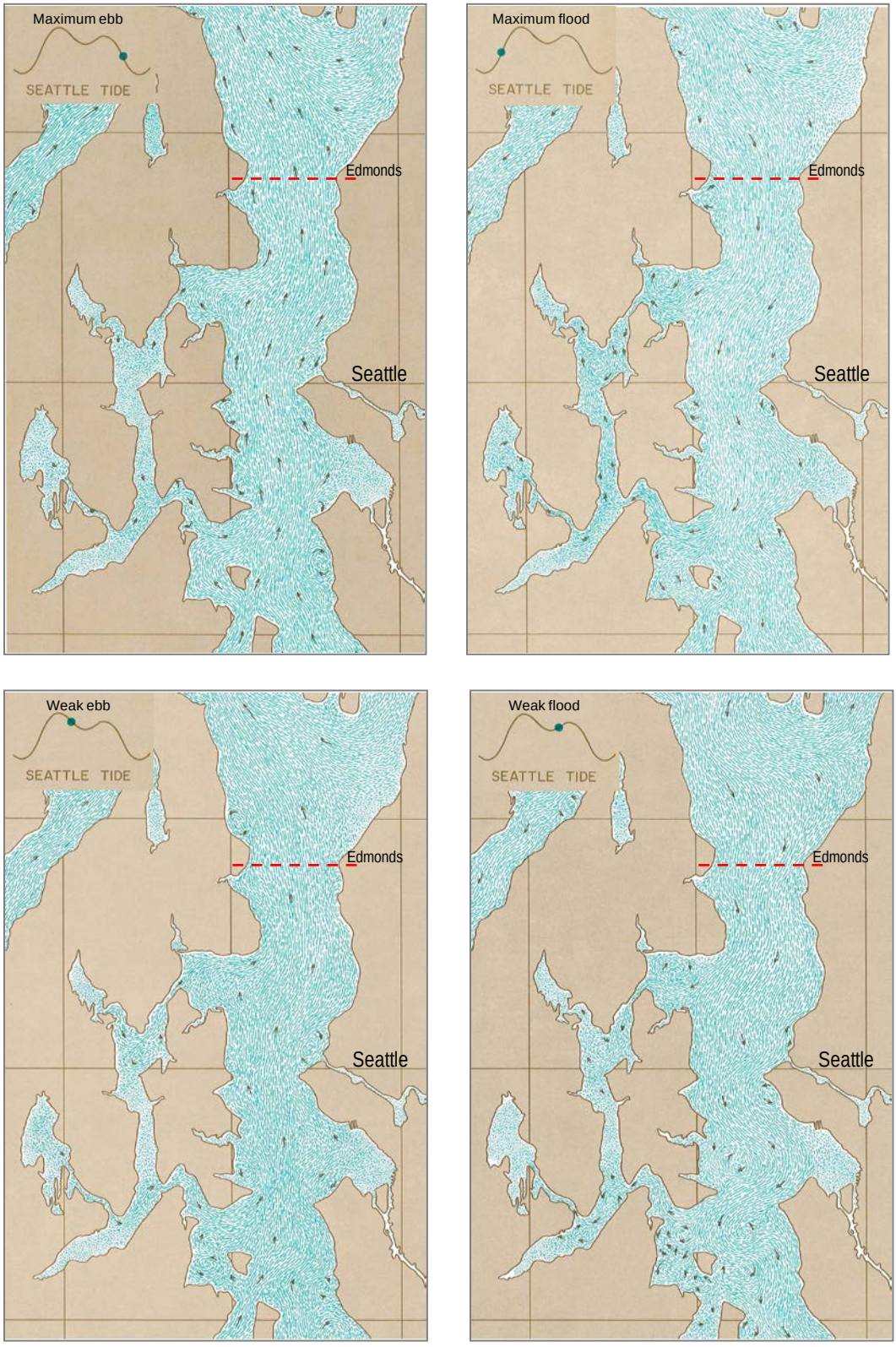


Figure D-3. Tide prints for strong (top) and weak (bottom) ebb and flood conditions in Central Puget Sound.

# Appendix E. Glossary, Acronyms, and Abbreviations

## Glossary

**Acoustic Doppler Current Profiler** (**ADCP):** A device that measures three-dimensional water velocity as a function of depth from near-bottom to near-surface.

**Advection:** The transfer of a property such as heat, cold, or salinity, by the horizontal movement of fluid.

**Bathymetry:** Measure of underwater depth of a waterbody.

**Boundary conditions:** External inputs to a model, or a set of mathematical conditions to be satisfied along the edges or physical boundaries of the region in which the solution is sought.

**Calibration period:** In this study, the calibration period is between July 2006 and October 2007

**Constituent:** In this study constituents are temperature and salinity

**Critical period:** In this study, the critical period is late summer early fall period.

**Curvilinear grid:** A uniform model grid composed of shoreline fitting trapezoidal elements.

**Diel:** Of, or pertaining to, a 24-hour period.

**Dissolved oxygen (DO):** The amount of oxygen gas ($O_2$) dissolved in a volume of water (e.g., mg/l).

**Domain:** the spatial extent of the model grid

**e-folding time:** The time required for a simulated dye tracer to decrease to 37% (1/e) dye of the original concentration at a specific location.

**Estuarine flow:** Water circulation that results from the combined effect of tides and density differences causing net transport seaward at the surface and landward at depth. When the flow pattern is reversed (e.g., landward at the surface) it is said to be inverse.

**Forcing:** Information used as input to models.

**Initial conditions:** The starting values for the model at all depths and locations for all state variables (e.g., temperature, salinity, velocity).

**Mean Lower Low Water** (**MLLW):** The mean of only the lower low tides (does not include the higher low tides).

**Model:** In this report model is the South and Central Puget Sound hydrodynamic model which is based on Generalized Environmental Model for Surfacewater Systems (GEMSS)

**Morphology:** Shape (e.g., channel morphology).

**Nonpoint source:** Pollution that enters any waters from any dispersed activities including atmospheric deposition, surface water runoff from agricultural lands, urban areas, forest lands, subsurface or underground sources, or discharges from boats or vessels not otherwise regulated under the National Pollutant Discharge Elimination System Program. Generally, any unconfined and diffuse source of contamination. Legally, any source of water pollution that does not meet the legal definition of "point source" in Section 502(14) of the Clean Water Act.

**Nutrient:** Substance such as carbon, nitrogen, and phosphorus used by organisms to live and grow. Too many nutrients in the water can promote algal blooms and rob the water of oxygen vital to aquatic organisms.

**Parameter:** Water quality constituent being measured (analyte). A physical, chemical, or biological property whose values determine environmental characteristics or behavior.

**Point Source:** Sources of pollution that discharges at a specific location from pipes, outfalls, and conveyance channels to surface water. Examples of point sources include municipal wastewater treatment plants, municipal stormwater systems, industrial waste treatment facilities, and construction sites that clear more than 5 acres of land.

**Pycnocline:** Depth at which the maximum change in density occurs.

**Reflux:** The amount of outflow from an area that returns when the tide changes. Reflux increases the flushing time of an estuary.

**Residence time:** The average time it takes for a substance (salinity, water) to move through a known volume.

**Root mean square error** (**RMSE**)**:** The square-root of the sum of the squared differences between the observed data and model results divided by the sample size.

**Spatial:** How concentrations differ among various parts of the river.

**Temporal trends:** Characterize trends over time.

**Thalweg:** The deepest along-channel path down an estuary.

**Tidal amplitude:** The height of the sea surface.

**Tidal phase:** The time variability of the sea surface. Phase is generally represented as 0 to 360° or 0 to 2Π radians.

**Total Maximum Daily Load (TMDL):** A TMDL is a value of the maximum amount of a pollutant that a body of water can receive while still meeting water quality standards; alternatively TMDL is an allocation of that pollutant deemed acceptable to the subject receiving waters.

**Watershed:** A drainage area or basin in which all land and water areas drain or flow toward a central collector such as a stream, river, or lake at a lower elevation.

**Water surface elevation:** Elevation of the water surface as measured from the North American Vertical Datum (NAVD88).

## Acronyms and Abbreviations

| | |
|---|---|
| ADCP | (See Glossary above) |
| Ecology | Washington State Department of Ecology |
| EPA | U.S. Environmental Protection Agency |
| ERM | Environmental Resources Management |
| GEMSS | Generalized Environmental Modeling System for Surface Waters |
| GIS | Geographical Information System |
| K1 | Luni-solar declinational diurnal tidal constituent |
| M2 | Principal lunar semidiurnal tidal constituent |
| MLLW | Mean lower low water |
| N2 | Larger lunar elliptic semidiurnal tidal constituent |
| NAVD88 | North American Vertical Datum of 1988 |
| NOAA | National Oceanic and Atmospheric Administration |
| NOS | National Ocean Survey |
| O1 | Lunar declinational diurnal tidal constituent |
| ORCA | Oceanic Remote Chemical-optical Analyzer (monitoring buoy) |
| POM | Princeton Ocean Model |
| PRISM | Puget Sound Regional Synthesis Model |
| PSTides | Puget Sound Tide Model |
| RMSE | (See Glossary above) |
| S2 | Principal solar semidiurnal tidal constituent |
| USGS | U.S. Geological Survey |
| UTM | Universal Trans-Mercator |
| vs | Versus |
| WRIA | Water Resource Inventory Area |
| WWTP | Wastewater treatment plant |

*Units of Measurement*

| | |
|---|---|
| °C | degrees centigrade |
| cfs | cubic feet per second |
| cm | centimeter |
| cms | cubic meters per second, a unit of flow (also here as cm/sec in Figures 61 & 62) |
| ft | feet |
| hrs | hours |
| Hz | Hertz |
| km | kilometer, a unit of length equal to 1,000 meters |
| m | meter |
| $m^2$ | meters squared |
| $m^3/s$ | cubic meters per second |

| | |
|---|---|
| mgd | million gallons per day |
| mg/L | milligrams per liter (parts per million) |
| mm | millimeter |
| m/s | meters per second |
| ppt | practical salinity units |